NNT : 2024AIXM0033

THÈSE DE DOCTORAT

Soutenue à Aix-Marseille Université
le 22 février 2024 par

Justine LAOUÉ

Physico-chemical leaf defenses of *Quercus pubescens* in response to amplified drought: A long-term study in the Mediterranean region

Discipline
Sciences de l'Environnement

Spécialité
Écologie

École doctorale
ED 251 – Sciences de l'Environnement

Laboratoire/Partenaires de recherche
IMBE UMR CNRS 7263 – IRD 237 – Institut Méditerranéen de Biodiversité et d'Écologie marine et continentale

Composition du jury

Cecilia BRUNETTI National Research Council	Rapportrice
Joan LLUSIÀ BENET Center de Recerca Ecològica I Aplicacions Forestals	Rapporteur
Sylvie BAUDINO Université Jean Monnet, Saint-Étienne	Présidente de jury
Sylvain DELZON Institut national de recherche pour l'agriculture, l'alimentation et l'environnement	Examinateur
Elena ORMEÑO Centre national de la recherche scientifique	Directrice de thèse
Catherine FERNANDEZ Aix-Marseille Université	Co-directrice de thèse

Affidavit

I, undersigned, Justine Laoué, hereby declare that the work presented in this manuscript is my own work, carried out under the scientific supervision of Elena Ormeño Lafuente and Catherine Fernandez, in accordance with the principles of honesty, integrity and responsibility inherent to the research mission. The research work and the writing of this manuscript have been carried out in compliance with both the French national charter for Research Integrity and the Aix-Marseille University charter on the fight against plagiarism.

This work has not been submitted previously either in this country or in another country in the same or in a similar version to any other examination body.

Marseille, December 15th, 2023



Cette œuvre est mise à disposition selon les termes de la Licence Creative Commons Attribution - Pas d'Utilisation Commerciale - Pas de Modification 4.0 International.

List of publications and/or patent and conference participation

1) List of publications and/or patents [1] related to the thesis project:

1. **Laoué, J.**, Havaux, M., Ksas, B., Tuccio, B., Lecareux, C., Fernandez, C., & Ormeño, E. (2023). Long-term rain exclusion in a Mediterranean forest: response of physiological and physico-chemical traits of *Quercus pubescens* across seasons. *The Plant Journal*, 116(5), 1293-1308. doi.org/10.1111/tpj.16424

2. **Laoué, J.**, Fernandez C., & Ormeño E. (2022). Plant Flavonoids in Mediterranean Species: A Focus on Flavonols as Protective Metabolites under Climate Stress. *Plants*, 11(2), 172. doi.org/10.3390/plants11020172

3. **Laoué, J.**, Gea-Izquierdo, G., Dupouyet, S., Conde, M., Fernandez, C., & Ormeño, E. (2024). Leaf morpho-anatomical adjustments in a *Quercus pubescens* forest after ten years of partial rain exclusion in the field. *Tree physiology*, tpae047. doi.org/10.1093/treephys/tpae047

4. **Laoué, J.**, Havaux, M., Ksas, B., G., Orts, J-P., M. Reiter, I., Fernandez, C., & Ormeño, E. (2024). A decade of rain exclusion in a Mediterranean forest reveals long memory and trade-offs of leaf chemical defenses. Submitted in: *Scientific reports*. Manuscript ID: c5bbe3d4-9036-424d-850c-b63dbb3e9011

2) Participation in conferences[2] and summer schools during the thesis period:

International conferences:

1. **Laoué, J.**, Havaux, M., Ksas, B., Gea Izquierdo, I., Reiter, G., Dupouyet, S., Orts, J.P., Tonetto, A., Fernandez, C., Ormeño. Chemical and morphological leaf defenses of *Quercus pubescens* after 10 years of amplified and recurrent drought. British Ecological Society annual meeting (December 2022, Edinburgh, SCOTLAND) – *Poster.*

[1] This list includes published articles, articles submitted for publication and articles in preparation, as well as books, book chapters and/or any form of valorization of the results of work specific to the thesis project discipline. References to publications must follow standard bibliography rules and comply with AMU's publications charter.

[2] The term "conference" is generic. It includes "conference", "congress", "workshop", "colloquium", "national and/or international meetings", etc.

2. **Laoué, J.**, Havaux, M., Ksas, B., Gea Izquierdo, G., Leduc, G., Dupouyet, S., Orts, J.P., Tonetto, A., Boularand, S., Fernandez, C., Ormeño. Défenses physico-chimiques du chêne pubescent face à la sécheresse en région méditerranéenne. Colloque 204 du 89ème congrès de l'Acfas : « La forêt face aux changements climatiques : des solutions innovantes pour une gestion durable », colloque virtuel (May 2022, Québec, CANADA) – *Poster.*

National conferences:

1. **Laoué, J.**, Havaux, M., Ksas, B., Lecareux, C., Dupouyet, S., Orts, Fernandez, C., & Ormeño, E. Fonctionnement de la forêt méditerranéenne sous contrainte hydrique : exemple du chêne pubescent. SANTECOFOR, « Santé des écosystèmes forestiers : Enjeux de société » (March 2023, Paris) – *Oral communication.*

2. **Laoué, J.**, Havaux, M., Ksas, B., Dupouyet, S., Orts, J.P., Fernandez, C., & Ormeño, E. Défenses physico-chimiques du chêne pubescent face aux restrictions des précipitations en milieu naturel. Journée des doctorants Institut Méditerranéen de Biodiversité et d' Écologie (July 2022, Marseille) – *Oral communication.*

3. **Laoué, J.**, Havaux, M., Ksas, B., Dupouyet, S., Orts, J.P., Tonetto, A., Boularand, S., Fernandez, C., & Ormeño, E. Physico-chemical defenses of *Quercus pubescens* to recurrent drought conditions *in natura*. Journée du GDR MediatEC en écologie chimique (October 2021, Toulouse) – *Oral communication.*

4. **Laoué, J.**, Havaux, M., Ksas, B., Dupouyet, S., Orts, J.P., Tonetto, A., Boularand, S., Fernandez, C., & Ormeño, E. Physico-chemical defenses of *Quercus pubescens* to recurrent drought conditions *in natura*. 28ème congrès des doctorants de l'ED Sciences de l'Environnement (April 2021, Marseille) – *Poster.*

Résumé

Les changements climatiques dans la région méditerranéenne se traduisent par des étés de plus en plus chauds et secs mais aussi plus longs, marqués par une diminution des précipitations annuelles d'environ 30% d'ici la fin du XXIème siècle. Ces changements rapides pourraient fortement modifier la physiologie des arbres et impacter leur croissance ainsi que leur survie. Dans un tel contexte, il est donc important d'évaluer les stratégies d'adaptation des forêts face à la contrainte hydrique sur le long-terme. Afin de limiter les pertes en eau tout en luttant contre le stress oxydatif, les végétaux déploient un grand nombre de défenses au niveau des feuilles. Ces défenses sont, soit chimiques, avec l'accumulation de métabolites antioxydants centraux et spécialisés qui réduisent le stress oxydant, soit physiques (e.g. épaississement des feuilles, augmentation de la densité de trichomes ou diminution de la densité stomatique) afin de limiter les pertes en eau. Si de nombreuses études ont illustré la modulation des défenses chimiques et les ajustements morpho-anatomiques des feuilles sous déficit hydrique en laboratoire ou en pépinière, les études effectuées *in natura* sont plus rares. Ce projet de doctorat vise à étudier si une sécheresse amplifiée et récurrente à long terme (> 10 ans) sous climat méditerranéen augmente le niveau de stress physiologique du chêne pubescent (*Quercus pubescens* Willd.) au niveau des feuilles et entraîne une modulation des traits chimiques et morpho-anatomiques foliaires afin de lutter contre le déficit hydrique et le stress oxydant associé. Ce travail a été effectué sur le site de l'O_3HP (Oak Observatory at Observatoire de Haute Provence) labellisé *AnaEE-France*, *AnaEE-ERIC* et *Suivis à long terme du vivant d'INEE-CNRS*. Il s'agit d'un site d'expérimentation *in natura* à long terme au sein d'une chênaie pubescente équipé depuis avril 2012 d'un système dynamique d'exclusion des pluies au-dessus de la canopée. Ce système permet de réduire de ~30 % les précipitations annuelles sur une partie de cette forêt et de comparer le fonctionnement des arbres situés sur cette parcelle à celui des arbres adjacents soumis au régime naturel de précipitations. Ces travaux de thèse ont permis de mettre en évidence un impact négatif de la sécheresse sur le fonctionnement physiologique du chêne pubescent induisant des changements dans les défenses chimiques et physiques des feuilles. Les changements observés pourraient permettre au chêne pubescent de (1) protéger son appareil photosynthétique en augmentant la production de métabolites antioxydants centraux (chlorophylles, lutéine, β-carotène, and néoxanthine), (2) minimiser la perte d'eau au niveau des feuilles en augmentant la densité des trichomes non glandulaires, et (3) réduire les coûts de production en diminuant la densité des trichomes glandulaires et en réduisant la taille et l'épaisseur des feuilles. Ces résultats révèlent une grande capacité du chêne pubescent à faire face à la sécheresse dans un contexte de changements climatiques. Toutefois, un autre résultat clé de ce travail est la diminution de la concentration en flavonols pendant la saison estivale ce qui pourrait favoriser la pression biotique subie par le chêne pubescent sur le très long-terme compte tenu du rôle toxique de ces composés pour les herbivores. En perspectives, de futures études devraient être menées pour évaluer cet aspect et prendre en compte les effets conjoints de la sécheresse et la hausse des températures qui seront exacerbées pour la fin du siècle dans la région méditerranéenne.

Mots clés : changements climatiques, chêne pubescent, écophysiologie, exclusion des pluies, métabolismes central et spécialisé, sécheresse à long-terme, traits chimiques, traits physiques des feuilles

Abstract

Climate change in the Mediterranean region is resulting in increasingly hot and dry summers, as well as longer durations marked by a decrease in annual precipitation of about 30% by the end of the XXIst century. These rapid changes could significantly alter the physiology of trees, impacting their growth and survival. In such a context, it is crucial to assess the adaptation strategies of forests to long-term water stress. In order to minimize water loss while countering oxidative stress, plants deploy numerous defenses at the leaf level. These defenses are either chemical, involving the accumulation of central and specialized antioxidant metabolites that reduce oxidative stress, or physical (e.g. thickening of leaves, increased trichome density, or decreased stomatal density) to limit water loss. While many studies have illustrated the modulation of chemical defenses and morpho-anatomical adjustments of leaves under water deficit in laboratories or plant nurseries, *in situ* studies are less common. This PhD project aims to investigate whether amplified and recurrent long-term drought (> 10 years) under a Mediterranean climate increases the physiological stress level of Downy oak (*Quercus pubescens* Willd.) leaves and leads to modulation of chemical and morpho-anatomical leaf traits to cope with water deficit and associated oxidative stress. This work was conducted at the O_3HP site (Oak Observatory at Observatoire de Haute Provence), labeled *AnaEE-France, AnaEE-ERIC*, and *Long-Term Monitoring of Living Systems* by INEE-CNRS. It is a long-term, *in natura* experimental site within a Downy oak forest, equipped since April 2012 with a dynamic rain exclusion system above the canopy. This system reduces annual precipitation by ~30% in part of the forest, allowing a comparison of tree functioning on this plot with that of adjacent trees subjected to the natural precipitation regime. The thesis work revealed a negative impact of drought on the physiological functioning of *Q. pubescens*, inducing changes in chemical and physical leaf defenses. The observed changes could enable Downy oak to (1) protect its photosynthetic apparatus by increasing the production of central antioxidant metabolites (chlorophylls, lutein, β-carotene, and neoxanthin), (2) minimize leaf water loss by increasing the density of non-glandular trichomes, and (3) reduce production costs by decreasing glandular trichome density and reducing leaf size and thickness. These results highlight the Downy oak's significant ability to withstand drought in the context of climate change. However, another key finding is the reduction in flavonol concentrations during the summer, which could promote biotic pressure on Downy oak in the very long term due to the toxic role of these compounds for herbivores. In perspective, future studies should evaluate this aspect and consider the combined effects of drought and rising temperatures, which will be exacerbated by the end of the century in the Mediterranean region.

Keywords: central and specialized metabolism, climate change, Downy oak, ecophysiology, long-term drought, leaf chemical traits, leaf physical traits, rain exclusion

Preface

This doctoral thesis is affiliated to the doctoral school “Environmental Sciences” (Ecole Doctorale "Sciences de l’ Environnement", ED 251) of Aix-Marseille University (AMU) and was conducted under the supervision of Dr. Elena Ormeño Lafuente and Dr. Catherine Fernandez. The doctoral research took place within the Mediterranean Institute of Biodiversity and Ecology of Marine and Continental Environments (IMBE, UMR CNRS 7263, IRD 237) in the team "Diversity and Functioning: from Molecules to Ecosystems" (DFME).

My doctoral scholarship was funded by “Direction Générale Déléguée à la Science (DGDS) from CNRS (Centre National de la Recherche Scientifique) as part of the project METAPHORES (METAbolomic and MorPHOlogical adaptations of a Downy oak forest to long-term rain REStriction) funded by the CNRS call MITI (Mission pour les initiatives transverses et interdisciplinaires).

The present thesis work is presented in the form of an introduction (Chapter I), materials and methods section (Chapter II), four articles (Chapters III, IV, V and VI), and a general discussion (Chapter VII) and conclusion (Chapter VIII).

The first article (Chapter III) is a review paper published in the journal *Plants*: **Laoué J, Fernandez C, Ormeño E. 2022.** Plant Flavonoids in Mediterranean Species: A Focus on Flavonols as Protective Metabolites under Climate Stress. *Plants* **11:** 172. doi.org/10.3390/plants11020172

The second article (Chapter IV) has been published in the journal *The Plant Journal:* **Laoué J, Havaux M, Ksas B, Tuccio B, Lecareux C, Fernandez C, Ormeño E. 2023.** Long-term rain exclusion in a Mediterranean forest: response of physiological and physico-chemical traits of *Quercus pubescens* across seasons. *The Plant Journal* **116:** 1293-1308. doi.org/10.1111/tpj.16424

The third article (Chapter V) has been published in the journal *Tree Physiology*: **Laoué J, Gea-Izquierdo G, Dupouyet S, Conde M, Fernandez C, & Ormeño E. 2024**. Leaf morpho-anatomical adjustments in a *Quercus pubescens* forest after ten years of partial rain exclusion in the field. *Tree physiology*, tpae047. doi.org/10.1093/treephys/tpae047

The fourth article (Chapter VI) has been submitted to the journal "*Scientific reports*".

Acknowledgments

En premier lieu, je tiens à remercier mes directrices de thèse Elena Ormeño Lafuente et Catherine Fernandez. Je vous remercie de m'avoir donné cette immense opportunité de réaliser ce projet de thèse qui m'a passionnée du début à la fin. Merci pour votre soutien, pour la confiance que vous m'avez accordée et pour tous vos conseils qui ont rendu ce projet encore plus passionnant. Elena, je te remercie pour ton aide, ta grande disponibilité, ton écoute et tes conseils à la fois scientifiques et humains. J'ai beaucoup appris à tes côtés et je te remercie de m'avoir transmis tes connaissances mais également ta rigueur scientifique. Cathy, je te remercie pour tous tes conseils et pour les fois où tu as su me rassurer. Je vous remercie toutes les deux pour m'avoir donné les clés pour réussir dans le monde de la recherche.

Je souhaite remercier chaleureusement Cécilia Brunetti, Joan Llusià, Sylvie Baudino et Sylvain Delzon de m'avoir fait l'honneur d'être les rapporteurs et examinateurs de ma thèse.

Je remercie également les membres de mon comité de thèse : Michel Havaux, Magali Proffit, Béatrice Tuccio et Henri Wortham pour leurs conseils scientifiques.

Un énorme merci général à toute l'équipe DFME : Virginie Baldy, Christine Ballini, Anne Bousquet-Mélou, Emmanuel Corket, Sylvie Dupouyet, Caroline Lecareux, Hélène Folzer, Thierry Gauquelin, Mathieu Santonja, Stéphane Greff, Raphaël Gros, Véronique Masotti, Jean-Philippe Mévy, Marie-Dominique Salducci et Irene Teixidor-Toneu. Merci pour vos partages de connaissances et d'expériences.

Je tiens à remercier plus particulièrement Jean-Philippe Orts pour son aide sur le terrain, bien évidemment. Aussi, je te remercie pour toutes tes histoires, et pour toutes nos discussions durant ces multiples campagnes de terrain. Merci d'avoir partagé tes nombreuses connaissances et merci pour les visites guidées de la partie « astronomie » de l'OHP. Et pour finir, le plus important, je retiendrai surtout nos grands échanges sur nos compagnons à quatre pattes, on ne s'en lassera jamais !

Un merci également à Caroline Lecareux. Caro, c'est grâce à toi que j'ai appris toutes (ou presque) les facettes de la GC-MS ! Je te remercie de m'avoir guidée, même à distance le pied dans le plâtre ! Je te remercie également pour tous les moments que nous avons passés à rire (fort) dans ton bureau.

Je remercie également Sylvie Dupouyet pour son aide si précieuse sur le terrain ! Merci pour tous tes conseils et astuces mais surtout pour ta gentillesse et ton humour !

Je tiens également à remercier chaleureusement toutes les personnes avec qui j'ai eu la chance de collaborer au cours de cette thèse : Michel Havaux, Brigitte Ksas, Guillaume Leduc, Béatrice Tuccio, Guillermo Gea-Izquierdo, Sophie Brasselet et Paulina Gasecka. Je vous remercie de m'avoir permis d'acquérir tant de nouvelles connaissances, dans des domaines très variés qui m'ont passionnée !

Je remercie en particulier Guillermo Gea-Izquierdo pour son accueil au sein de son équipe à Madrid. Un merci également aux doctorants de l'équipe, David Almagro Fernández-Tostado et Macarena Férriz, ainsi qu'à María Conde et María Del Rey. Merci pour votre gentillesse et votre accueil !

Et puis aussi, et pas des moindres… un énorme merci à tous.tes les doctorant.es (et docteur.es !!) avec qui j'ai partagé le bureau, les pauses du midi et bien d'autres moments ! Charlotte Biryol, Thomas Bourgeois, Solène Brasseur, Salomé Coquin, Lola Czuckermand, Dounia Dhaou, Quentin Lambert, Arnaud Lec'hvien, Thibaud Legros, Claire Ménival, Elodie Quer, Eliane Schermer. J'aimerais vous faire un paragraphe à chacun pour vous exprimer tout mon amour mais c'est un peu « too much », alors… Juste un gros gros gros merci à vous tous.tes. Merci pour ce noyau fort que nous nous sommes créé, alimenté par plein d'entraide, d'écoute, de conseils, de confidences et surtout beaucoup de rires ! Vous êtes tous.tes des personnes incroyables. Vous allez tellement me manquer !

Je remercie également tous les stagiaires que j'ai pu croiser lors de ma thèse et qui ont contribué à mettre de la bonne humeur lors des pauses du midi ! Pour leur aide sur le terrain, merci à Julie Gouinguenet et Alexis Balembois.

Un grand merci également à tous mes amis, pour la plupart éparpillés aux quatre coins du globe ! Les « bordelais » et les « québécois », merci d'être une constante dans ma vie, merci de me soutenir, pour certains depuis de nombreuses années… Merci pour toutes les solides amitiés que j'ai créées à l'Université de Bordeaux et à l'Université Laval au Québec, merci pour tous ces beaux souvenirs et même si on est loin, je n'oublie rien !

Je remercie aussi tous mes proches. Mes parents, pour leur éternel soutien dans tous les choix que je fais. Bien sûr, mes grands-parents, Giliane et Jean-Bernard, pour lesquels quelques lignes ne suffiront jamais à leur exprimer toute ma reconnaissance. Merci de m'avoir soutenue, depuis toujours, dans tous mes choix. Merci d'avoir toujours su me remonter le moral quand je doutais de moi. C'est en partie grâce à vous que je suis arrivée si loin et que je suis devenue la personne que je suis aujourd'hui.

Alexandre, je te remercie pour ton soutien sans faille depuis notre rencontre. Nous avons tous les deux vécu en même temps cette grande expérience qu'est la thèse et nous voilà arrivés au bout… Je suis si fière de toi, de tout ce que tu as accompli et ce n'est que le début… Docteur Raimbault !!! Merci d'être toujours là pour moi, merci pour ces 9 belles années d'aventures passées à tes côtés…

Et je finis mes remerciements par un merci très spécial, pour un petit être très spécial, qui ne lira jamais ces quelques lignes car oui, Marcel ne sait pas lire… ! Mais quand même, merci mon petit Marcel de m'avoir accompagnée chaque jour dans cette thèse ! Je n'ai pas eu meilleur soutien que le regard attendrissant et les câlins de mon merveilleux petit chien !



Merci pour tout !

À mes grands-parents

Contents

Affidavit **3**
Preface **8**
List of publications and/or patent and conference participation **4**
Résumé **6**
Abstract **7**
Acknowledgments **8**
Contents **13**
CHAPTER I: Introduction **17**
1. Mediterranean forests under climate change 18
2. Modulation of physiological traits under drought stress 20
3. Modulation of physical traits under drought stress 21
3.1. Modulation of leaf morphological traits under drought stress 21
3.1.1. Functional leaf traits 21
3.1.2. Leaf surface traits 22
3.2. Modulation of anatomical leaf traits under drought stress 26
4. Modulation of chemical traits under drought stress 27
4.1. Plant central metabolites 29
4.1.1. Photosynthetic pigments 29
4.1.2. Plastoquinones 32
4.2. Plant specialized metabolites 33
4.2.1. Phenolic compounds 34
4.2.2. Terpenoids/isoprenoids 35
4.2.3. Fatty acid derivatives and other compounds within cuticular waxes 36
4.2.4. Plant specialized metabolites under drought stress: expected changes according to ecophysiological theories 38
5. *In natura* impact of amplified drought on *Quercus pubescens*: state of the art 40
6. Objectives of the thesis 42
7. Personal contribution to the thesis and collaborators 44
7.1. Personal contribution to chapters IV, V and VI 44
7.2. Personal contribution to exploratory experiments not valorized during my thesis 45
7.2.1. Physiological stress: oxidative pressure technique development 45
7.2.2. Raman spectra and localization of metabolites 47
CHAPTER II: Materials and methods **50**
1. The study model: *Quercus pubescens* Willd. 51
2. Experimental site 52
3. Ecophysiological trait analyses 56
3.1. Gas exchange 56

3.2. Water potential 56
4. Physical trait analyses 56
4.1. Morphological traits 56
4.1.1. Functional leaf traits 56
4.1.2. Leaf surface traits 57
4.2. Anatomical traits 57
5. Chemical analyses 57
5.1. Photosynthetic pigments and tocochromanols 58
5.2. Phenolic compounds 58
5.3. Cuticular waxes 59
6. Statistical analyses 59
CHAPTER III: Bibliographic review on plant flavonols in Mediterranean species 61
1. Introduction 63
2. Chemical and physical properties of flavonols: relationship with their function 66
3. Biosynthesis and storage of flavonols: relationship with their function 68
4. Flavonols in plants: an important polyphenol to cope with rapid climate change 72
4.1. Drought 76
4.2. Warming 76
4.3. UV Radiation 77
4.4. Salinity 78
5. Flavonols as antioxidants: a unifying mode of action against climate stresses 79
6. Flavonols as indirect growth regulators 81
7. Conclusions 83
CHAPTER IV: Impact of seasonal cycle and long-term amplified drought on central and specialized leaf metabolites in 2021 85
Abstract 86
1. Introduction 87
2. Experimental procedures 89
2.1. Experimental site and species 89
2.2. Physiological and physical traits 91
2.3. Chemical traits 91
2.4. Statistical analysis 93
3. Results 93
3.1. Physiological and physical traits: seasonality and drought responses 93
3.2. Chemical traits: seasonality and drought responses 95
4. Discussion 101
4.1. Physiological traits 102
4.2. Physical traits 103
4.3. Chemical traits 103
5. Conclusion 107
6. Acknowledgements 107

CHAPTER V: Impact of long-term amplified drought on morphological and anatomical leaf traits after 10 years of rain exclusion: a focus on the summer 2021 108
Abstract 109
1. Introduction 110
2. Materials and methods 112
2.1. Study site and species 112
2.2. Physiological leaf traits 114
2.3. Morphological and anatomical leaf traits 114
2.4. Statistical analyses 115
3. Results 115
3.1. Changes in leaf functional traits after 10 years of amplified drought 115
3.2. Adjustments in leaf gas exchange after 10 years of amplified drought 116
3.3. Adjustments of morphological traits after 10 years of amplified drought 118
3.4. Adjustments of anatomical traits after 10 years of amplified drought 121
3.5. Concomitant morpho-anatomical and physiological adjustments in response to 10 years of amplified drought 122
4. Discussion 125
5. Conclusion 128
6. Acknowledgements 129
CHAPTER VI: Impact of long-term amplified drought on central and specialized leaf metabolites over 2016-2022 period 130
Abstract 131
1. Introduction 132
2. Materials and Methods 134
2.1. Study site, sampling design and campaigns 134
2.2. Physiological traits 135
2.3. Analysis of central (photosynthetic pigments) and specialized metabolites (flavonols) 136
2.4. Statistical analysis 137
3. Results 137
3.1. Climatic conditions across years and drought conditions 137
3.2. Physiological traits across years and drought conditions 139
3.3. Variation in photosynthetic pigments and flavonols across years and drought conditions 142
3.4. Correlations between metabolite concentration and precipitation 147
4. Discussion 148
5. Conclusion 151
6. Acknowledgements 152
CHAPTER VII: Discussion 153
CHAPTER VIII: Conclusion and perspectives 162
References 167
List of figures 206

List of tables **213**
ANNEXES **214**
A. Supplementary information for analyses of chapter IV 214
B. Supplementary information for analyses of chapter V 223
C. Supplementary information for analyses of chapter VI 227

CHAPTER I: Introduction



Saint-Michel- l'Observatoire, Alpes-de-Haute-Provence, France

1. Mediterranean forests under climate change

The Mediterranean region is one of the major climate change 'hot spots' representing a critical area which is affected by increasing warming and precipitation decline (Cos *et al.*, 2022). It is exposed to hot and dry summer seasons, which are projected to become even more severe in the future (Lionello & Scarascia, 2018; Cramer *et al.*, 2018) own to a likely warming rate 20% larger than global average (Lionello & Scarascia, 2018) (**Figure 1**).

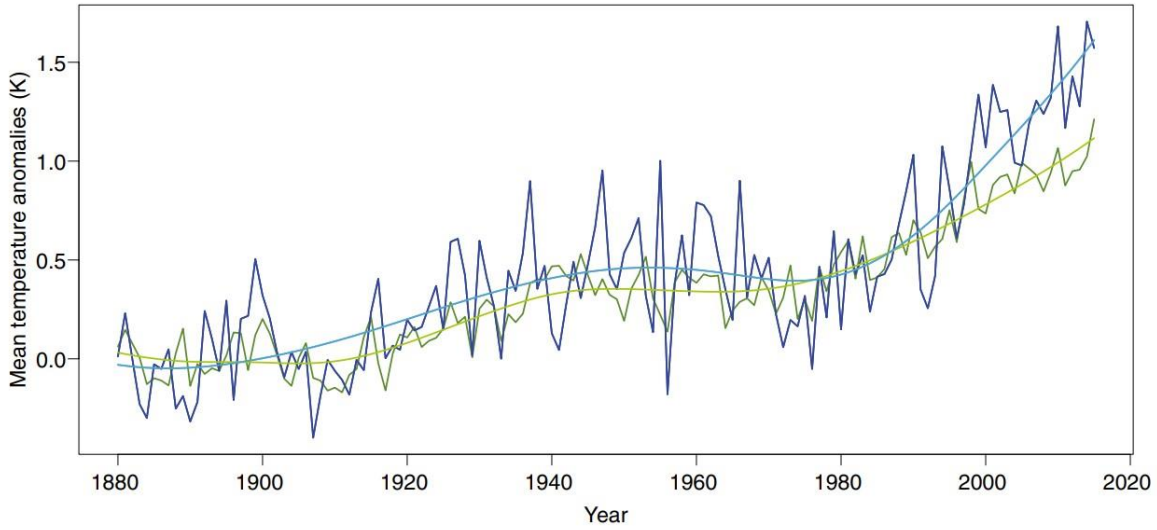

Figure 1: Historic warming of the atmosphere globally and in the Mediterranean Basin. Annual mean air temperature anomalies are shown with respect to the period 1880–1899, with the Mediterranean Basin (blue) and the globe (green) presented with (light curves) and without (dark curves) smoothing (Cramer *et al.*, 2018).

According to the RCP[3] 8.5 scenario – which corresponds to a high greenhouse gas emissions pathway, where emissions of carbon dioxide (CO_2) and other greenhouse gases continue to rise throughout the XXIst century – it is expected that average surface temperatures increase up to 3.5 – 4 °C for the period 2046–2065 and between 3.5 and 5.5 °C for the period 2080–2100 in most Mediterranean areas (Riahi *et al.*, 2011) (**Figure 2**). Summer warming is expected to be especially pronounced in comparison to annual temperature changes increasing up to 7 °C by the end of the century (Zittis *et al.*, 2019). In terms of precipitation, the RCP 8.5 scenario assesses that annual precipitation will decrease up to 30 % by the end of the century, or even 40 % in certain parts of the southern Mediterranean area, particularly during the dry summer seasons (Zittis *et al.*, 2019, 2021). This dryness will be more pronounced in parts of the Iberian Peninsula,

[3] Representative Concentration Pathway

Southern France, Italy, Western Greece, and central/Northern Turkey while over the already semi-arid Southern Mediterranean, accentuation of summer drought is projected to be much smaller in comparison with the wet season (Zittis *et al.*, 2019).

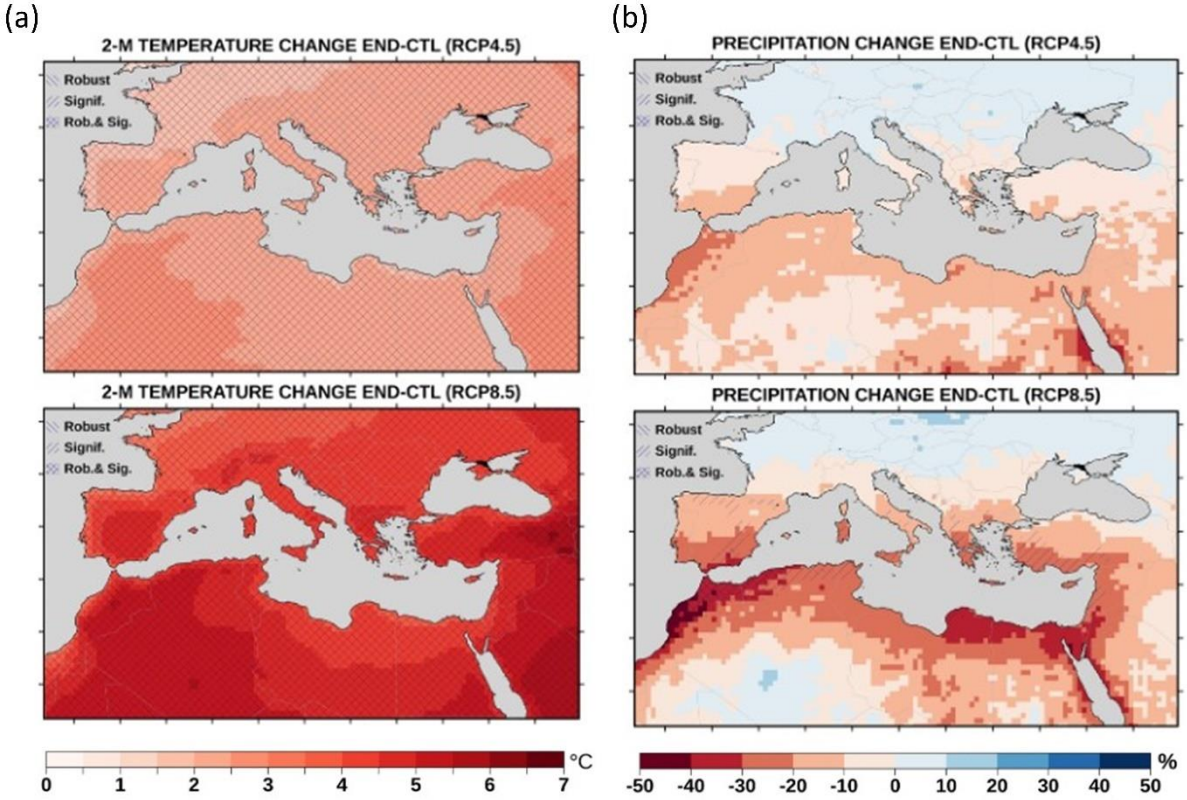

Figure 2: Projected changes of (a) mean annual temperature and (b) mean annual precipitation for the end (END 2081-2100) of the 21st century with respect to the reference period (CTL 1986–2005), for two Representative Concentration Pathways (RCP4.5: top row and RCP8.5: bottom row) in the Mediterranean region. Modified from Zittis *et al.* (2019).

Although Mediterranean forests are naturally adapted to relatively dry and warm summer, the rapid, intense and severe expected climate changes will dramatically lead to reduced soil moisture and evapotranspiration. Because of their long lifespan, trees are more frequently exposed to recurrent drought events (McDowell *et al.*, 2008; Anderegg *et al.*, 2015). As a result, physiological functioning of trees will be negatively impacted by climate changes, thus threatening plant functioning (growth, reproduction, defense) and leading to potential irreversible damage or even mortality during severe drought periods (McDowell, 2011; Klein, 2015). Therefore, one of the foremost challenges in ecology is to predict how plants will respond to a rapid increase in relative aridity.

Episodes of unexpected tree mortality due to climate warming and long drought periods have been intensively reported over the last decades, notably in the Mediterranean region. For example, several events of particularly hot and dry summers such as those observed in Spain have led to tree mortality from 2012 to 2020, affecting

3.3 % of the total forested area in Catalonia (especially during summers 2012 and 2016) and mostly impacting *Fagus sylvatica* L. (23 %), deciduous oaks (*Quercus pubescens* Willd. and *Quercus faginea* Lam., 22 % in total), and the evergreen *Quercus ilex* L. (12 %) (Hartmann *et al.*, 2022). In Southern France, unusual hot and dry climate the past decades has induced the decline and mortality of *Abies alba* Mill. (Cailleret *et al.*, 2014), and negatively impacted *Pinus halepensis* Mill. growth, including crown development, fruiting and radial growth (Girard *et al.*, 2012).

Under increasing aridity and thus reduction in soil water availability, tree functioning is impacted through slow-down of physiological processes, such as photosynthesis or water transport (McDowell *et al.*, 2008; Anderegg *et al.*, 2015). To limit drought-related physiological impact, species acclimate through modulation of their physico-chemical traits. Common physical traits related to species acclimation to water stress include changes in stomatal and trichome density, specific leaf area (SLA) and leaf thickness (De Micco & Aronne, 2012). Chemical traits include central and specialized metabolites which are produced in response to water stress and account for plant defenses (Hussain *et al.*, 2019; Kapoor *et al.*, 2020).

2. Modulation of physiological traits under drought stress

To cope with drought stress, one of the most prompt response of plants is modulation of stomatal conductivity where water-saving species exhibit total stomatal closure to rapidly prevent evapotranspiration (isohydric regulation of water status) and water-expending species present partial stomatal closure to partially maintain the entrance of CO_2 and thus net photosynthesis (anisohydric regulation of water status) (Damesin & Rambal, 1995; Tardieu & Simonneau, 1998). Isohydric regulation refers to a strict control mechanism where plants maintain a relatively constant leaf water potential (Ψ_{leaf}) by closing stomata and thus reducing stomatal conductance to water (g_s) even under mild soil water potential decreases (McDowell *et al.*, 2008). This conservative approach prevents excessive water loss but limits CO_2 uptake, so species are more prone to die from carbon starvation during drought. By contrast, species that feature anisohydric regulation of water maintain higher stomatal conductance for a given water potential compared to isohydric plants thus prioritizing CO_2 uptake. Anisohydric plants do not maintain a constant Ψ_{leaf} and may keep their stomata partially open even under water stress conditions (Tardieu & Simonneau, 1998; Chen *et al.*, 2022a). Although anisohydric trees are considered to be better suited to drought-prone habitats since they maintain photosynthesis (McDowell *et al.*, 2008), this strategy also results in higher water loss and species survival could be endangered under long-term drought.

Stomatal behavior is influenced not only by water potential but also by leaf physical adaptations which are critical for leaf gas exchange (H_2O and CO_2) and allow plants to adjust their leaf physiological parameters such as net CO_2 assimilation (A_n), stomatal conductance to water (g_s), transpiration (E) and water use efficiency (WUE) (Franks & Farquhar, 2007; Franks *et al.*, 2009).

3. Modulation of physical traits under drought stress

Plant resistance to drought is linked to adaptive strategies influenced by the timing of phenological events and physical traits, which are primarily associated with increasing water uptake and storage, reducing water loss, and mechanical reinforcement of tissues, especially in Mediterranean-type ecosystems (De Micco & Aronne, 2012). Various morphological and anatomical adaptations to dry conditions occur at the leaf level enabling plants to thrive in drought-prone environments by conserving and making efficient use of limited water resources (Read & Sanson, 2003; Paula & Pausas, 2006; Wang *et al.*, 2021).

3.1. Modulation of leaf morphological traits under drought stress

3.1.1. Functional leaf traits

One key morphological change to limit drought stress is the reduction in **leaf size**, since it reduces the area for transpiration, thus minimizing water loss. This response has been described in deciduous species *Quercus robur* L. and *Quercus petraea* (Matt.) Liebl. where total leaf area was reduced by 18 and 55 %, respectively (Ponton *et al.*, 2002), as well as in the evergreen *Q. ilex* (Ogaya & Penuelas, 2006).

The **specific leaf area** (SLA) refers to the leaf area relative to its dry mass and is an important trait providing insights into plant investment in leaf tissue for photosynthesis and other functions. The SLA negatively correlates with leaf thickness (Wilson *et al.*, 1999; Gouveia & Freitas, 2009; Marenco *et al.*, 2009) and it is the most commonly regarded physical trait for plant performance under drought stress (Wellstein *et al.*, 2017). Several studies have reported that leaves with low SLA (and thus high thickness since both are

negatively correlated, Vile *et al.*, 2005) – allow plants to cope with dry conditions by reducing water loss through transpiration (Ramírez-Valiente *et al.*, 2017, 2020), while higher SLA (and thus thinner leaves) coupled with larger leaves can reflect an acquisition resource-use strategy where light capture, photosynthesis, and resource assimilation are maximized (Pérez-Ramos *et al.*, 2013; Reich, 2014).

3.1.2. Leaf surface traits

Stomatal traits also play a crucial role in plant response to drought, as they directly impact leaf gas exchange and thus plant physiological performance. They are responsible for allowing air containing oxygen and carbon dioxide to enter within the plant for respiration and photosynthesis, while also releasing water vapor into the atmosphere through transpiration. Stomatal density is typically higher on the lower leaf surface (or abaxial surface). The pores are bordered by a pair of specialized cells known as "guard cells" that regulate stomatal opening. Stomata is also used to refer to an entire stomatal complex, both the pore itself and the guard cells (Pirasteh-Anosheh *et al.*, 2016). In the context of drought stress, stomata play a major role as their closure is the first line response to prevent the water loss via transpiration. Drought can lead to changes in stomatal size, density, and distribution, which may strongly affect gas exchange and thus relationships with plant water status (Xu & Zhou, 2008; Anjum *et al.*, 2011). In some cases, plants may reduce the number of stomata to conserve water by decreasing the overall surface area where transpiration occurs as observed in crop species with reduced stomatal density under drought stress (Hughes *et al.*, 2017; Morales-Navarro *et al.*, 2018). Alternatively, some plants increase the stomatal density but develop stomata with a smaller size and apertures to balance both gas exchange and water saving as reported in maize (Zhao *et al.*, 2015). Additionally, smaller stomata can limit water loss during transpiration and also have the ability to close more rapidly (Franks *et al.*, 2009; Drake *et al.*, 2013).

Plant trichomes are appendages that derive from aerial epidermal cells in leaves, stems and floral organs and act as a direct barrier against transpiration but also as a protection against herbivores and UV-radiation (Wang *et al.*, 2021). Trichomes represent small, hair-like structures with various forms and functions. They can be unicellular or multicellular and come in different shapes and sizes, depending on the plant species (**Figure 3**). They are classified as glandular or non-glandular trichomes (Bickford, 2016). Glandular trichomes store and secrete large quantities of specialized metabolites including terpenoids (Mahmoud *et al.*, 2021), flavonoids (Tattini *et al.*, 2000) and phenolic acids (Zhou *et al.*, 2021) which are involved in plant defense against environmental stresses such as drought (Haberstroh *et al.*, 2018) or herbivory (Peiffer *et al.*, 2009). By contrast, non-glandular trichomes do not secrete specialized metabolites but act as a direct physical protection against high light and temperatures, and play a key role in limiting transpiration (Santos Tozin *et al.*, 2016).

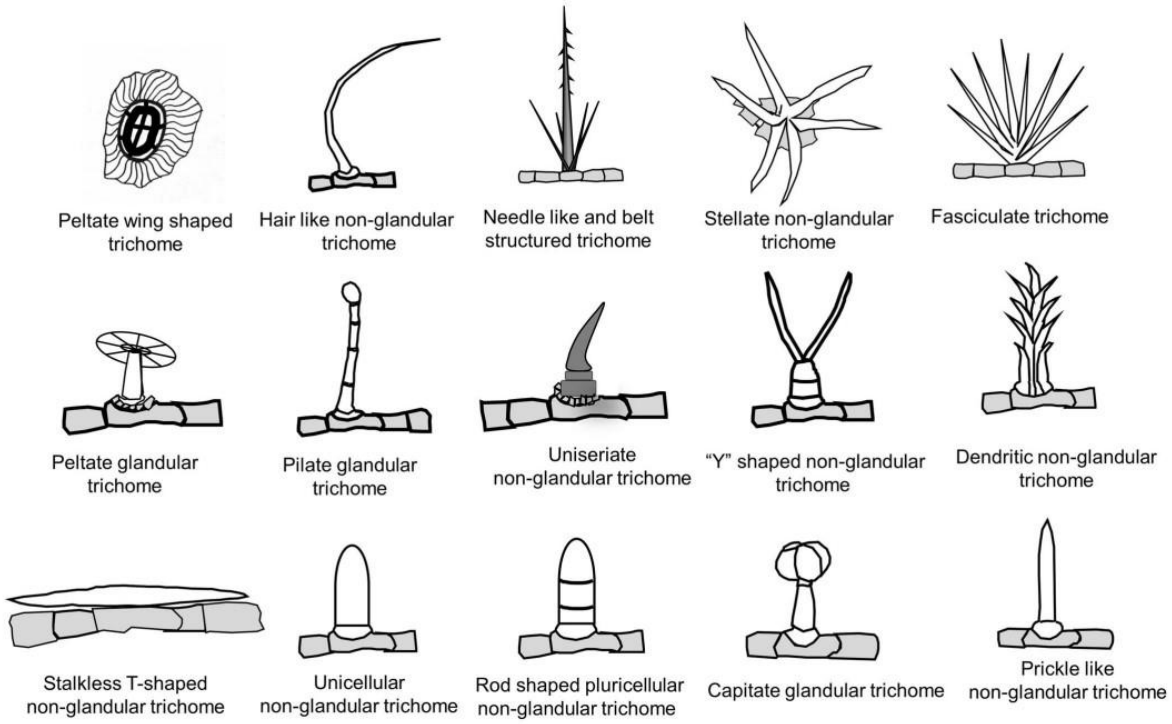

Figure 3: Examples of morphology of different trichome types found in different plant species (Li *et al.*, 2023b).

Leaf trichome types have been used as analytical traits in the taxonomy of *Quercus* species (Dyal, 1936; Hardin, 1976) and also to detect hybridization and introgression among oaks (Hardin, 1975; Kissling, 1977). Dyal (1936) recognized two fundamental types of trichomes in *Quercus* leaves, namely "glandular" and "non-glandular" trichomes based upon the trichomes glistening or viscid appearance. In *Quercus* species, glandular trichomes are smaller – compared to non-glandular trichomes – (see picture of simple uniseriate type in **Table 1**), collapse upon drying, and should not be confused with the capitate type of glandular trichomes found in other plant species (see **Figure 3**). The second type is the "non-glandular" trichome which shows more variability between oak species (Thomson & Mohlenbrock, 1979) and is generally branched and thick-walled. With the use of scanning electron microscopy (SEM), Hardin (1976) provided a more precise description of trichome types in oak species and recognized ten different types (**Figure 4**). A description and example of images of the different trichome types found in various *Quercus* species are given in **Table 1** (Hardin, 1976, 1979; Engel *et al.*, 1993; Fortini *et al.*, 2009, 2013).

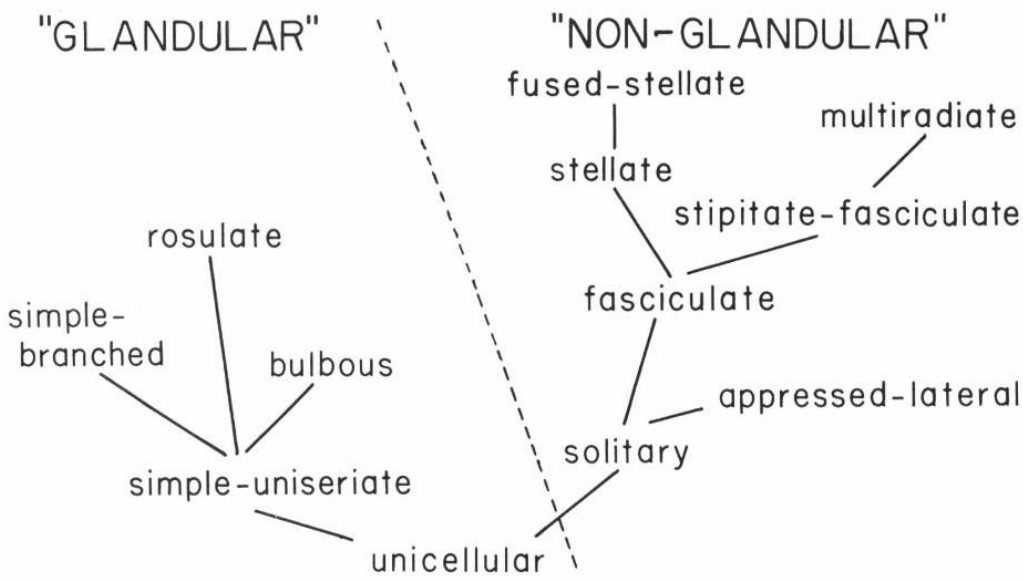

Figure 4: Different types of glandular and non-glandular trichomes found in *Quercus* species (Hardin, 1976).

The **density of the leaf trichome** varies according to plant species and is influenced by both, genetic and environmental factors. Environmental factors like soil water deficit, high air temperature, and vapor pressure deficit often lead to an increase in the density of the leaf trichome (Shibuya *et al.*, 2016; Chen *et al.*, 2022b). The presence of leaf trichomes can directly influence various physiological processes, including transpiration rate, stomatal conductance, and water use efficiency (WUE) (Konrad *et al.*, 2015). A recent study of Buckley *et al.* (2022) proved that leaf trichomes reduce the boundary layer conductance for heat transfer between leaves and the air, thus reducing exchange rates, though to a greater extent for transpiration than for CO_2 assimilation. Additionally, a denser trichome layer can also collect and retain mist or dew droplets above the stomatal pores, thus reducing the water potential gradient between the leaf and the air, increasing WUE (Brewer *et al.*, 1991). In *Quercus* species, trichomes are mainly present in the abaxial leaf surface, but some species (e.g. *Q. ilex*, *Q. robur*, *Q. pubescens* and *Q. virgiliana*) may present a few trichomes in the adaxial side of their leaves, although to a less extent compared to abaxial surface (Hardin, 1979; Fortini *et al.*, 2009; Fernández *et al.*, 2014). In *Q. ilex*, adaxial trichomes can also contribute to water absorption thanks to their high hydrophilicity and play an essential role in both, protecting against the excess of light energy and enhancing foliar water uptake in sites with scarce precipitations such as Mediterranean arid regions (Fernández *et al.*, 2014).

Table 1: The ten types of trichomes found in *Quercus* species as described by Hardin (1976).

Trichome type	Description (Hardin, 1976)	Images (SEM)
I. Glandular		
1. Simple-uniseriate	Thin-walled, unicellular or multicellular and uniseriate.	 *Quercus robur* (Hardin, 1976)
2. Simple-branched	Thin-walled, multicellular, uniseriate, with a few branches. Not a common type in oaks.	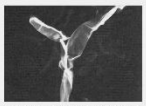 *Quercus velutina* (Hardin, 1976)
3. Bulbous	Thin-walled, multicellular, uniseriate (or irregularly multiseriate) with a bulbous portion (apical, central or basal).	 *Quercus petraea* (Fortini *et al.*, 2009)
4. Rosulate	Rosette or tuft of glandular thin-walled trichome.	 *Quercus incana* (Hardin, 1976)
II. Non-glandular		
5. Solitary	Single, long, straight or slightly wavy, generally tick-walled.	 *Quercus frainetto* (Fortini *et al.*, 2013)
6. Appressed-lateral	Solitary, more or less tihck-walled trichome, generally appressed with a lateral point of attachment.	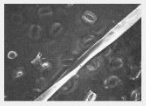 *Quercus gilva* (Hardin, 1976)
7. Fasciculate	Thick-walled cells clustered and fused at least at the base. The number of cells (arms or rays) varies from 2 to 12.	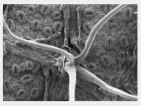 *Quercus pubescens* (Fortini *et al.*, 2013)
8. Multiradiate	Thick-walled, clustered or tufted type with rays radiating rom more than one level.	 *Quercus myrtifolia* (Hardin, 1979)
9. Stellate	Thick-walled, radiate form with rays fused only at the base and all diverge from one point.	 *Quercus petraea* (Fortini *et al.*, 2013)
10. Fused-stellate	Trichome with fusion of the rays beyond the base to a maximum of two-thirds the length of the rays.	 *Quercus minima* (Hardin, 1976)

3.2. Modulation of anatomical leaf traits under drought stress

Leaf anatomical traits refer to the structural features of the internal and external leaf anatomy. These traits are responsive to environmental factors and thus highly plastic in their development and biochemical function (Ni *et al.*, 2022). They are essential for understanding how plants respond to their environment, as well as their photosynthetic performance, and their overall growth and functioning. Leaf anatomical traits include epidermis, mesophyll (palisade and spongy tissue), and vascular tissue characteristics (**Figure 5**).

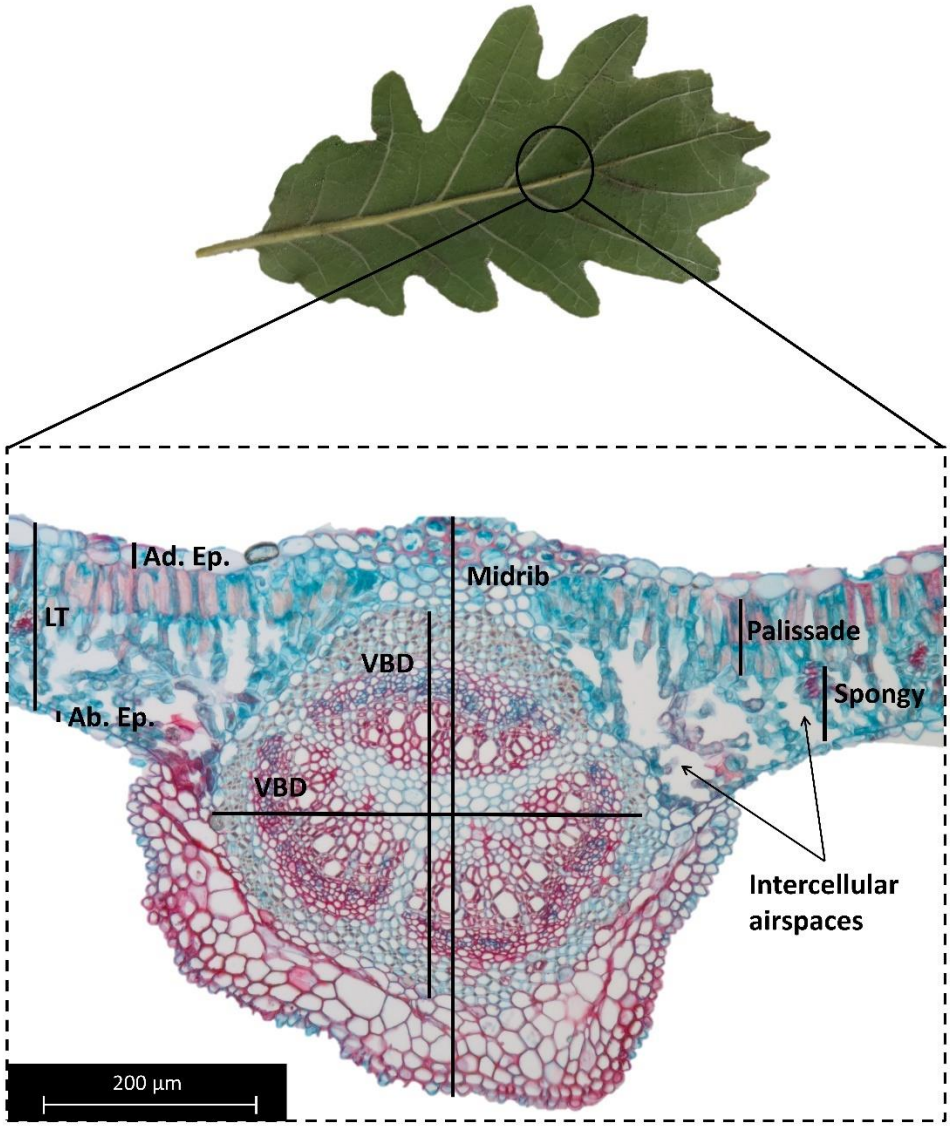

Figure 5: Leaf anatomical traits of *Q. pubescens* leaf. Leaf cross-sections were stained with safranin (lignified tissues) and astra blue (non-lignified tissues). Ab. Ep., abaxial epidermis; Ad Ep., adaxial epidermis; LT, leaf thickness; and VBD, midrib vascular bundle diameter.

Leaf anatomical traits are responsible for distinct functions but collaborate closely. For example, the composition and structure of **mesophyll tissues** affect light absorption and gas exchange, thus influencing photosynthesis efficiency while the epidermal tissues are vital for regulating leaf water balance and providing protection against both, water loss and mechanical injury (Javelle *et al.*, 2011). More precisely, the **palisade tissue** is the main site of photosynthesis and modulates leaf photosynthetic efficiency through changes in tissue-porosity (Kumar *et al.*, 2012). The **spongy tissue** possesses larger intercellular spaces than the palisade tissue which could improve gas transportation, especially CO_2 for photosynthesis. Increasing evidence demonstrates that palisade and spongy tissues are the main limiting factors for optimizing photosynthesis (Terashima *et al.*, 2011).

4. Modulation of chemical traits under drought stress

Drought stress can lead to partial or total stomatal closure allowing plants to reduce evapotranspiration but also limiting the entrance of CO_2 and thus net photosynthesis as described above. The restriction of CO_2 entrance due to stomatal closure can disrupt the normal flow of the electron transport chain in chloroplasts since chloroplasts continue to capture light energy, but the reduction in photosynthesis creates an imbalance in the electron flow. This imbalance can result in the leakage of electrons and the subsequent excess of cell energy leading to generation of reactive oxygen species (ROS) (Sierla *et al.*, 2016) (**Figure 6**). When reaching a certain level, ROS become extremely deleterious and can damage cellular membranes and other cellular components resulting in oxidative stress and eventually cell death (Cruz De Carvalho, 2008). For limiting cell oxidation when photosynthesis is limited, getting rid of cell energy excess (through fluorescence and heat dissipation processes) and synthesizing antioxidant metabolites becomes fundamental for plant survival.

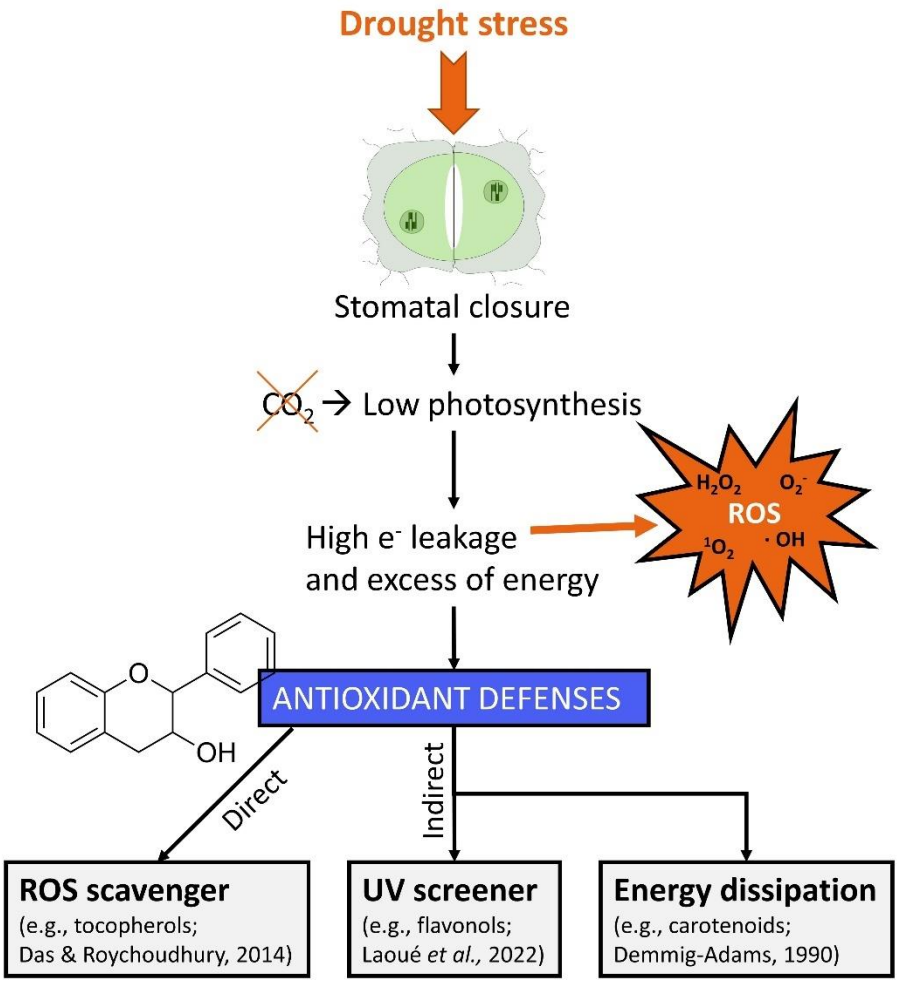

Figure 6: Simplified schema of the response of plants to drought stress and the mechanisms (ROS scavenger, UV screener, energy dissipation) whereby plant defenses reduce cell oxidation.

As a whole, carbon allocation for the production of defense metabolites is crucial for survival under severe environmental stress. Plant chemical defenses can be classified as central or specialized metabolites. Although distinction between these two categories is the object of debate, **central metabolites** - also referred to as primary or universal – are involved in the primary metabolic pathways and are ubiquitously produced by all plant species. Asides from providing essential protection for all plants against environmental stressors, they are more largely required for plant functioning as they are necessary for photosynthesis, growth and reproduction (Fang *et al.*, 2019). **Specialized metabolites** are structurally very diverse and are synthesized from precursors issued from central metabolism. They are present in specific plant species or taxa where they account for supplementary plant defenses against biotic and abiotic stresses and mediate plant interaction with its environment (Bennett & Wallsgrove, 1994; Moghe & Kruse, 2018; Yadav *et al.*, 2021). Production and diversity of specialized metabolites are therefore considered by some authors as an indicator of plant fitness, defense and therefore

survival (Moghe *et al.*, 2017; Moghe & Kruse, 2018) and an adaptive plant characteristic subjected to natural selection during evolution (Wang *et al.*, 2019). A decline in the production of either, central or specialized metabolites under stress conditions can thus be considered as a loss of competitive ability for a given species.

As an example, carotenoids (central metabolite) or tocopherols (specialized metabolites) play a direct protective role against drought-related oxidative stress since they are antioxidant metabolites acting as ROS scavengers (Das & Roychoudhury, 2014; Rastogi *et al.*, 2014). Others may indirectly protect against cell oxidation. For example, some flavonoids act as UV screener (Ferreyra *et al.*, 2021; Laoué *et al.*, 2022), carotenoids from the xanthophyll cycle allow for dissipating excess energy (Demmig-Adams, 1990; Havaux & Kloppstech, 2001; Demmig-Adams *et al.*, 2020) (**Figure 6**) and waxy specialized metabolites located in the most external cuticular waxy layer of leaves limit non-stomatal water loss by making up a physical barrier for water diffusion (Simões *et al.*, 2020). A higher production of central and specialized defense metabolites can therefore promote plant acclimation to drought.

4.1. Plant central metabolites

Leaf central metabolites fulfill many essential functions in plants and include both, high molecular weight metabolites (not considered in this thesis) like sugars, amino acids, nucleotides, lipids, and energy sources and metabolites with relatively low molecular weight required for photosynthesis such as photosynthetic pigments and plastoquinones.

4.1.1. Photosynthetic pigments

Photosynthetic pigments are mainly found in the chloroplasts of plant cells where they are essential for capturing and absorbing light energy during the process of photosynthesis (Maoka, 2020; Stirbet *et al.*, 2020). These pigments play a major role in converting light energy into chemical energy, which is essential for the synthesis of glucose and other organic molecules from carbon dioxide and water. The most important photosynthetic pigments in plants (described hereafter) are carotenoids derived from the methyl-D-erythritol phosphate (or non-mevalonate) pathway and chlorophylls (chlorophyll *a*, chlorophyll *b*) (**Figure 7**).

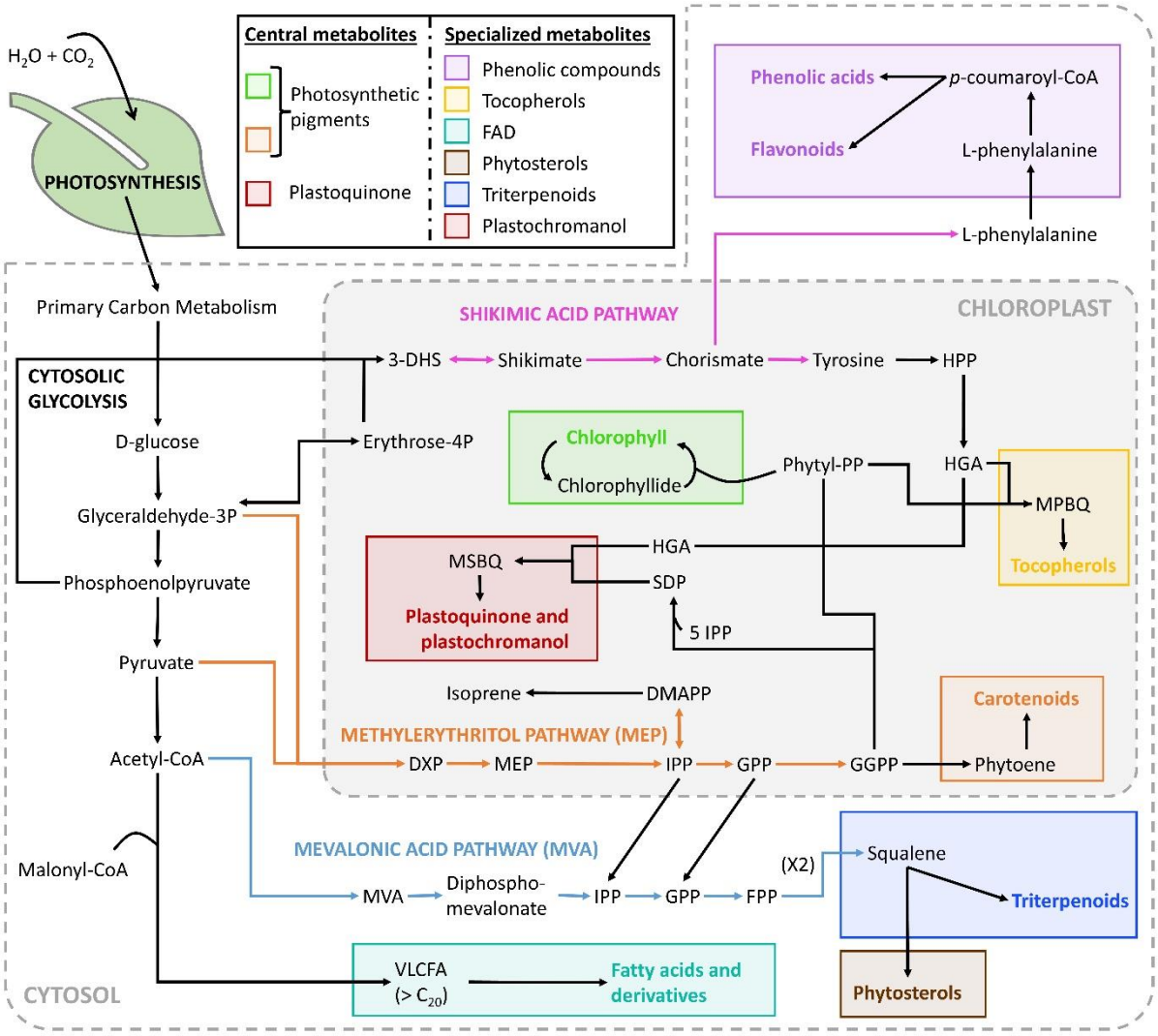

Figure 7: Simplified biosynthetic pathways of metabolites targeted in this study. Compounds forming cuticular waxes are indicated with a star although they are not exclusive to waxes. Abbreviations are as follows: 3-DHS, 3-dehydroshikimate; 5 IPP, 5 Isopentenyl diphosphate; CoA, coenzyme A; DMAPP, dimethylallyl-diphosphate; DXP, 1-deoxy-D-xylulose-5-phosphate; FAD, fatty acids and derivatives; FPP, farnesyl pyrophosphate; GGPP, geranylgeranyl pyrophosphate; GPP, Geranyl pyrophosphate; HGA, homogentisic acid or homogentisate (phenolic acid); HPP, hydroxyphenylpyruvate; IPP, isopentenyl diphosphate; MEP, 2-C-methyl-D-Erythritol-4-phosphate; MPBQ, methylphytylbenzoquinol; MVA, (R)-mevalonate; Phytyl-PP, phytyl-diphosphate; MSBQ, methyl-solanesyl-enzoquinone; SDP, solanesyl diphosphate; VLCFA, Very Long Chain Fatty Acid. Modified from Laoué *et al.* (2023).

Chlorophylls are green pigments that absorb light from both the ends of the visible electromagnetic spectrum (i.e. from blue region as well as red region), while carotenoids absorb light in the blue and green regions (Mandal & Dutta, 2020). These pigments work in tandem to capture light energy and initiate the complex biochemical reactions of photosynthesis, providing the basis for essential biological processes by which solar energy is transformed into organic matter in all photosynthetic organisms (A. Lal, 2018). Chemically, both chlorophyll *a* and *b* possess a hetero polycyclic planer structure with a central Mg^{2+} ion. Chlorophyll *b* differs from chlorophyll *a* and contains an aldehydic group

(-CHO) in the second ring instead of a methyl group (-CH3) present in chlorophyll *a* (**Figure 8a**). This modification gives chlorophyll *b* a slight difference in its ability to absorb light: chlorophyll *a* mostly absorbs violet and orange light while chlorophyll *b* mostly absorbs blue and yellow light. Chlorophylls can be strongly affected by water deficit (Mohawesh, 2016; Noori *et al.*, 2018). Numerous studies have reported that prolonged and severe drought stress degrade chlorophyll leading to lower chlorophyll content in plant cells (Moran *et al.*, 1994; Guerfel *et al.*, 2009). Such degradation implies a loss of green pigmentation in leaves, a phenomenon known as leaf senescence or chlorosis.

Carotenoids are yellow-orange pigments grouping together ca. 1200 compounds (Polyakov *et al.*, 2023) which take their name from carrot (*Daucus carota*), a plant that accumulates high levels of these pigments in the root. Mainly contained in chloroplasts within the plant kingdom, they account for a typical example illustrating how complex can be classifying plant metabolites as central or specialized. From an ecological perspective, carotenoids are rather considered as central metabolites since they are essential for photosynthesis and act as precursors of phytohormones and other signaling compounds (this classification of carotenoids as "central" metabolites is used in this thesis) (Roca & Pérez-Gálvez, 2021; Sytiuk *et al.*, 2023). Nevertheless, from a biochemical perspective, carotenoids can be considered specialized metabolites since most of them are tetraterpenoids (40-carbon skeleton or C_{40}) synthesized through the terpenoid biosynthetic pathway (MEP; **Figure 7**). Moreover, secondary taxon-specific carotenoids in chromoplasts (not considered in this thesis) are clear specialized metabolites since they are not required for photosynthesis but rather intervene as intermediates in plant-animal interactions by furnishing flowers and fruits with fragrances and colors (Ruiz-Sola & Rodríguez-Concepción, 2012; Serra, 2015).

The general structure of carotenoids commonly consists of a polyene chain with nine conjugated double bonds and an end group at both ends of the polyene chain (**Figure 8b**). Due to their extensive conjugated double-bond system, they are able to absorb light between 400 and 550 nm and then transfer this energy to chlorophylls through singlet–singlet excitation transfer, thus increasing the photosynthetic capacity of plants (Maoka, 2020; Crupi *et al.*, 2023). Besides their role on light harvesting to transfer excitation energy to reaction centers, carotenoids play a crucial role in photoprotection, and they are of capital importance in response to water stress (Esteban *et al.*, 2015). This photoprotection can be attributed to both (i) their capacity to dissipate the excess of absorbed energy (Demmig-Adams, 1990) and (ii) their antioxidant activity due to their capacity to quench $^1O_2$ and scavenge free radicals (Krinsky, 1989). In particular, carotenoids from the xanthophyll cycle (violaxanthin, antheraxanthin, and zeaxanthin) contribute to dissipate the excitation energy within the antenna of photosystem II, which accumulates in excess when stomatal closure limits photosynthesis (Demmig-Adams, 1990).

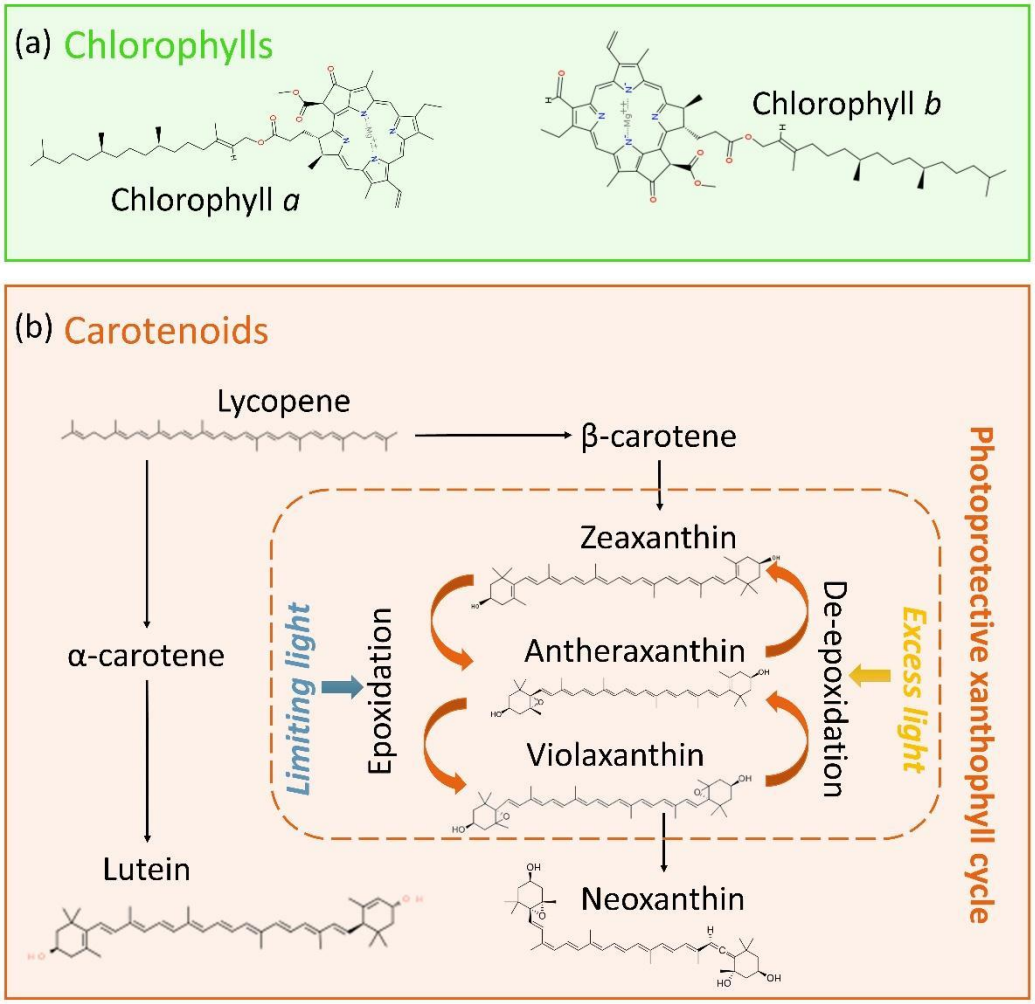

Figure 8: Photosynthetic pigments found in plants. (a) Structure of chlorophyll *a* and *b*. (b) Biosynthesis of carotenoids from lycopene as well as interconversions of zeaxanthin, antheraxanthin and violaxanthin in the xanthophyl cycle. Modified from Demmig-Adams *et al.* (2020).

4.1.2. Plastoquinones

Plastoquinones (PQ) – issued from both the MEP and shikimate pathway (**Figure 7**) – are essential metabolites in plants acting as photosynthetic electron carrier during the electron transport phase of photosynthesis occurring in the thylakoid membrane of chloroplasts. They can be classified as central metabolites since they play an essential role in photosynthesis, and plants deficient in PQ are not viable (Havaux, 2020). Plastoquinones have an antioxidant function (Hundal *et al.*, 1995) and their accumulation confers enhanced resistance to light-induced stress as shown in *Arabidopsis* mutants (Ksas *et al.*, 2018).

4.2. Plant specialized metabolites

During their evolution, trees have developed a battery of chemical defenses referred to as specialized (or secondary) metabolites in response to biotic and abiotic stresses. Specialized metabolites can be classified into four main groups according to their biosynthetic origin: (1) **phenolic compounds** including polyphenols (phenolic acids, lignin, coumarins, stilbenes, lignans, flavonoids, tannins and tocochromanols) and, simple phenolics; (2) **terpenoids** (also referred to as isoprenoids) including a myriad of oxygenated and non-oxygenated terpenes, (3) **fatty acid derivatives** including short-chain and long-chain compounds, and (4) **nitrogen and sulfur-containing compounds** (named alkaloids and glucosinolates, respectively and not studied in this thesis) (Yadav *et al.*, 2021) (**Figure 9**).

Specialized metabolites play a crucial role for coping with antioxidant pressure, both directly (i.e. they act as ROS scavenging) and indirectly through the dissipation of excess absorbed energy (Demmig-Adams, 1990; Osmond *et al.*, 2000). Furthermore, drought-induced volatile specialized metabolites (not tackled in this thesis) serve as signals to activate plant tissue defense mechanisms, thereby helping to alleviate the effects of drought stress (Yadav *et al.*, 2021).

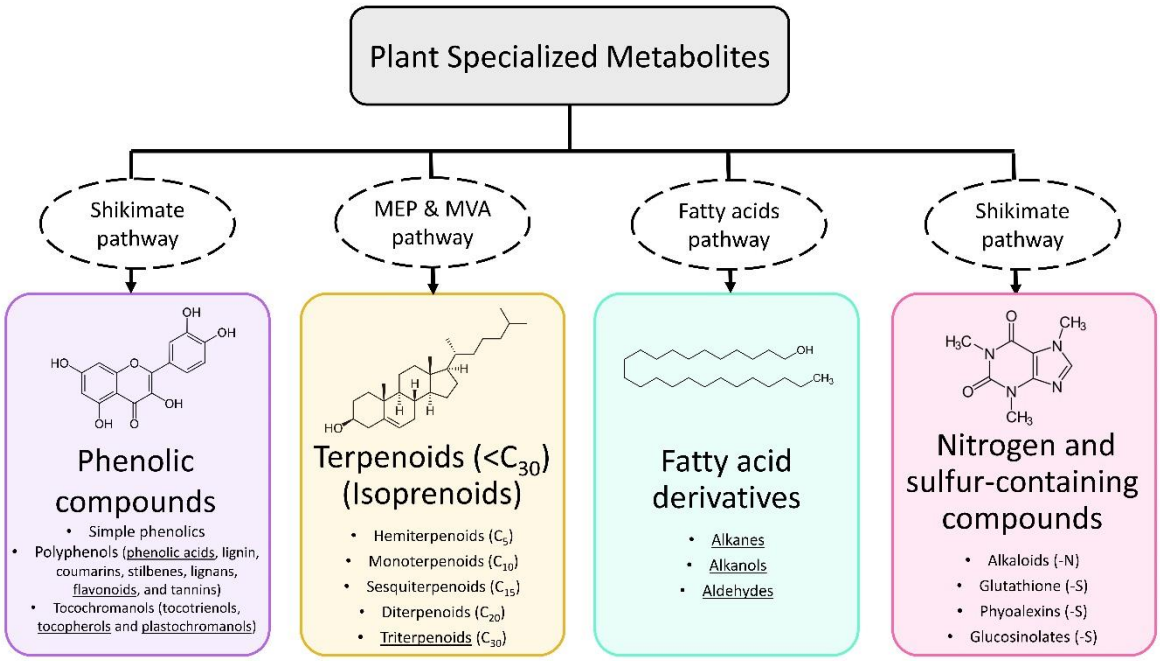

Figure 9: The four main groups of specialized metabolites in plants and their biosynthetic pathways, modified from figures in Yadav *et al.* (2021). The underlined groups of compounds denote targeted/detected metabolites in the present thesis. Abbreviations are as follows: MEP, methylerythritol phosphate pathway; MVA, mevalonate pathway.

4.2.1. Phenolic compounds

Phenolic compounds are synthesized through the shikimate pathway, or phenylpropanoid pathway (**Figure 7**). Based on their chemical structure, phenolic compounds can be divided into different subgroups including simple phenolics (one phenol unit alone) and polyphenols (with more than one phenolic unit) which include phenolic acids, flavonoids, tannins, coumarins, lignans, quinones, stilbenes, and curcuminoids (Saltveit, 2010). They are among the most widespread specialized metabolites in the plant kingdom (Lattanzio *et al.*, 2006) and are notably involved in the synthesis of lignin, a molecule common in all higher plants (Bourgaud *et al.*, 2001). They are characterized by the presence of one or more phenol rings (also known as aromatic rings) in their chemical structure. Phenol itself is a benzene ring that is substituted with a hydroxyl group (-OH) (Mamari, 2021). Phenolic compounds such as flavonoids may be present in plants in free form but are more commonly derivatives by processes such as glycosylation, prenylation, acetylation, methylation, and polymerization, thus affecting their bioactivity (Ibrahim *et al.*, 1987; Le Roy *et al.*, 2016).

Numerous studies on plant species highlighted higher accumulation of phenolic compounds under drought conditions thus providing plant resistance as reviewed by Kumar *et al.* (2023). Their biological functions are due to their wide array of structures. For example, the antioxidant capacity of phenolic acids and their derivatives is mainly related to the number of hydroxyl groups and usually glycosylation of flavonoids decreases their antioxidant activity (Šamec *et al.*, 2021). In addition, some flavonoids possess great ability to absorb UV wavelengths even if their role as 'UV-screening' is possibly not their most important function (Agati & Tattini, 2010; Ferreyra *et al.*, 2021).

In the present manuscript, the case of flavonoids will be further discussed in **Chapter III** (p. 61) in the form of a review published in *Plants* in which their role as protective metabolites under abiotic stress is mainly described, with a focus on Mediterranean species. Flavonoids are a major group of polyphenols largely widespread in plants where they play numerous roles including defense and signaling under stress conditions. These compounds encompass several chemical subgroups such as flavonols which are one the most represented classes. The most studied flavonols are kaempferol, quercetin and myricetin well known for their antioxidant properties and a potential role in UV-defense through UV-screening mechanisms making them critical for plant adaptation to climate change (Laoué *et al.*, 2022).

Tocochromanols are lipid-soluble molecules that belong to the group of vitamin E, which includes tocopherols, tocotrienols and plastochromanol-8 (PC-8) (Falk & Munné-Bosch, 2010; Kruk *et al.*, 2014). Tocochromanols have a chromanol ring with a hydroxyl group, making them phenolic compounds (Szewczyk *et al.*, 2021). These compounds are important antioxidants found in plants, and they play a significant role in protecting cells and tissues from oxidative damage caused by ROS. Both tocochromanol subgroups can be

classified into different homologues, that is the α-, β- or γ-, and δ-forms according to the number and position of the methyl groups at the chromanol ring system (Kamal-Eldin & Appelqvist, 1996). They derive from both the MEP and shikimate pathways (DellaPenna & Last, 2006) (**Figure 7**). **Tocopherols** are ubiquitous in all plant species and are particularly concentrated in photosynthetic tissues, while tocotrienols are only found in some plant species and are almost exclusively found in seeds and fruits, particularly in monocots (Falk & Munné-Bosch, 2010). **PC-8** has a structure similar to that of tocopherols and tocotrienols, consisting of a chromanol ring (responsible for their antioxidant properties) and a hydrophobic side chain. **Hydroxy-plastochromanol (PC-OH)** has been identified *in vitro* as the main non-enzymatic product of the singlet oxygen ($^1O_2$) scavenging activity of PC-8 (Gruszka *et al.*, 2008). Therefore, PC-OH is considered as a specific product of $^1O_2$ in stressed plants (Szymańska *et al.*, 2014) and can be used as indicator of the leaf oxidative stress (Laoué *et al.*, 2023).

During drought stress, the primary function of these compounds is related to their antioxidant properties (Munné-Bosch & Alegre, 2002). In addition, tocopherols can help to protect cellular membranes by scavenging lipid peroxyl radicals for example in thylakoid membranes which is essential for maintaining membrane integrity and function during water stress (Munné-Bosch, 2005). Tocopherols may also interact with signaling pathways involved in the plant response to drought stress and their accumulation has been associated to increasing drought tolerance in many plant species (Munné-Bosch *et al.*, 1999; García-Plazaola & Becerril, 2000; Munné-Bosch & Alegre, 2001).

4.2.2. Terpenoids/isoprenoids

Terpenoids, also known as isoprenoids, are a large and diverse class of compounds which are produced from isopentenyl diphosphate (IPP) and dimethylallyl diphosphate (DMAPP). Both precursors, IPP and DMAPP, are synthesized through two biosynthetic pathways namely (1) the MEP (2-C-methyl-D-Erythritol-4-phosphate) pathway occurring in the plastid which gives most monoterpenoids, diterpenoids and tetraterpenoids (carotenoids) and (2) the MVA (mevalonate) pathway for the production of most sesquiterpenoids and triterpenoids in the cytosol (Vranová *et al.*, 2013; Sun *et al.*, 2016; Henry *et al.*, 2018) (**Figure 7**). Terpenoids are differentiated from one another by their basic skeleton and functional groups. Volatile and semi-volatile isoprenoids (C_5-C_{20}) may play a direct antioxidant function by scavenging ROS and an indirect protective effect by altering ROS signaling, and/or membrane stabilization, thus conferring protection under thermal and oxidative stress conditions, even though the mechanism of volatile isoprenoid action is difficult to test directly *in planta* (Vickers *et al.*, 2009). In this thesis, a focus is done on non-volatile triterpenoids (C_{30}) present in cuticular waxes (see p. 36).

4.2.3. Fatty acid derivatives and other compounds within cuticular waxes

Cuticular waxes is a term largely used to refer to compounds present in the cuticle of plant organs (leaves, stems and fruits). The plant cuticle is a waxy and hydrophobic layer developed by plants to colonize lands (Edwards, 1996) and can be divided in two domains, namely the 'cuticular layer' (cutin-rich domain with integrated polysaccharides) and the 'cuticle proper' (rich in waxes) (**Figure 10a,b**). These waxes are either deposited within the cutin matrix (referred as intracuticular wax) or accumulate on the most external cuticular layer, the epicuticular wax layer (**Figure 10b**). In some species, such as *Q. pubescens* and *Q. faginea*, these epicuticular waxes present a crystalline structure in the abaxial leaf surface (Tschan & Denk, 2012) (**Figure 10c**).

The chemical composition of leaf cuticular waxes vary according to species. **Fatty-acids** (e.g. tetracosanoic acid) **and their derivatives** (alkanes, alkanols, aldehyde) represent the major group of cuticular waxes. Fatty acid derivatives mainly comprise long-chain fatty acid derivatives (alkanes, alkanols and aldehydes) and, to a lesser extent, short-chain (C_6) volatile compounds (not considered in this thesis). Other metabolites can however be found in the leaf cuticle, the composition varying according to plant species (Shepherd & Wynne Griffiths, 2006; Jetter & Riederer, 2016). **Polyphenols** (e.g. flavonols) and **triterpenoids** (e.g. lupeol) can thus be present in the leaf cuticle (Haas *et al.*, 2003; Simões *et al.*, 2020). *Quercus* species contain high significant amounts of triterpenoids within leaf cuticle as well as sterols and tocopherols (Simões *et al.*, 2020; Bueno *et al.*, 2020; Laoué *et al.*, 2023).

Triterpenoids – synthesized from IPP and DMAPP (**Figure 7**) and composed of 30 carbon atoms – confer mechanical stability to aliphatic waxes, especially at elevated temperature, and thereby reduce thermal stress (Schuster *et al.*, 2016). This enhancement of the leaf mechanical resistance reduces the thermal stress on the layer of aliphatic cuticular waxes thus maintaining its barrier properties even at elevated temperature (Schuster *et al.*, 2016) (**Figure 10b**).

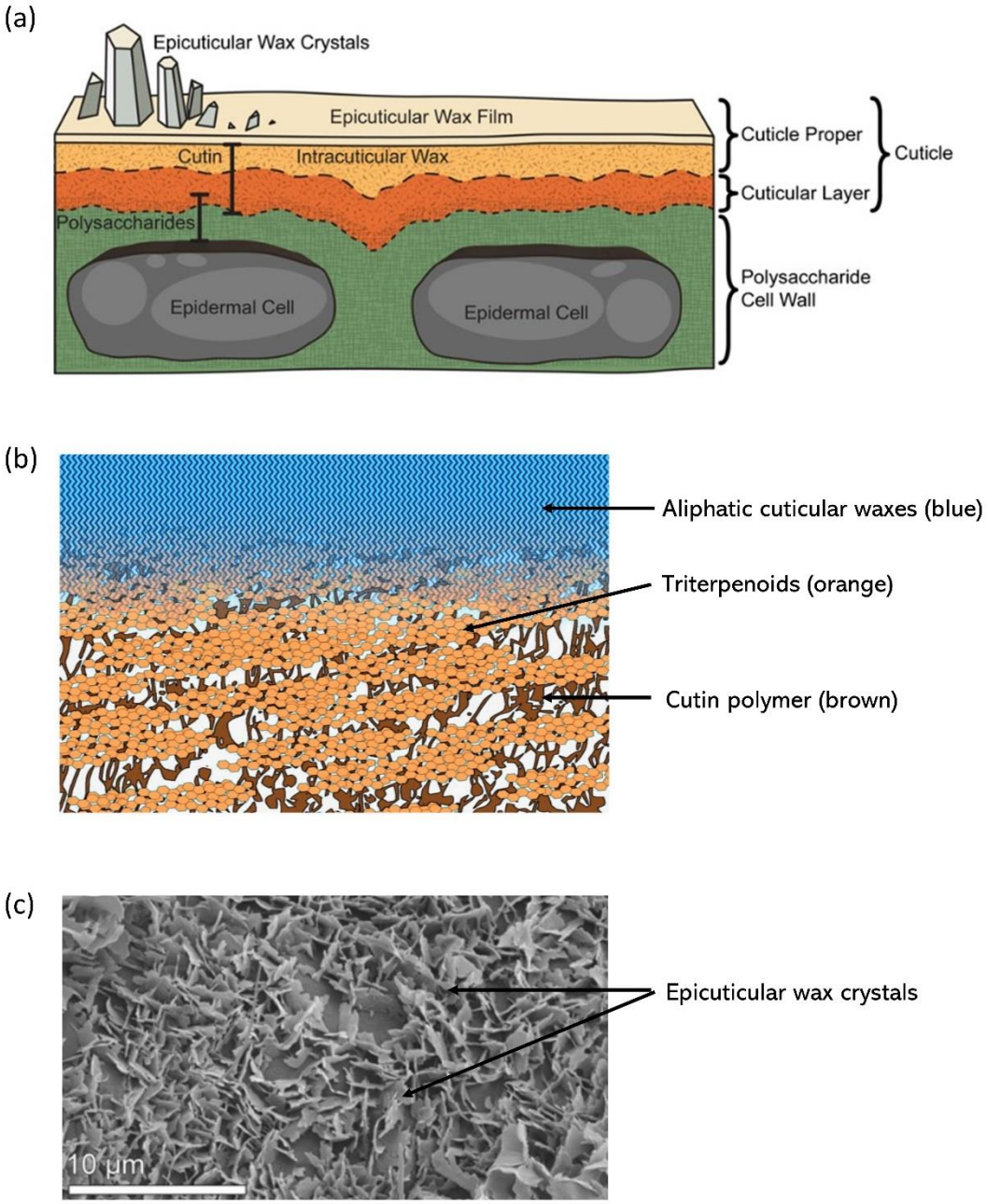

Figure 10: Plant cuticle structure. (a) Schematic representation of a leaf transversal cut showing the major structural features of the cuticle. Extracted from Yeats & Rose (2013). (b) Schematic model of triterpenoid localization. Triterpenoids (orange) form extended deposits within the cutin polymer (brown) which fixate the polymer strands. Extracted from Schuster *et al.* (2016). (c) Scanning electron microscopy (SEM) images of *Quercus pubescens* abaxial leaf surface. Extracted from Tschan & Denk (2012).

Cuticular wax quantity and composition are also indicators of plant responses to drought (Simões *et al.*, 2020). Several studies under controlled conditions reported that drought enhances the accumulation of cuticular waxes in the model plant *Arabidopsis* and in various crop species (Kosma *et al.*, 2009; Xue *et al.*, 2017). In general, long-chain alkanes

(C_{29}, C_{31}, and C_{33}), accounted for the observed 93% increases in total wax amount in plants under water deficit (Kosma *et al.*, 2009). A recent study of Simões *et al.* (2022) on the Mediterranean Cork oak (*Quercus suber* L.) – a species well adapted to the long dry summer conditions occurring in the Mediterranean region – showed that cuticular wax content displayed a seasonal pattern which increased from spring to reach its peak in summer. Moreover, the authors found that triterpenoids were the dominant wax components in this species, with lupeol making up about 70% of the cuticular wax fraction reinforcing the idea that these compounds are critical for mechanical and thermal stability, especially during summer season.

Q. suber, an evergreen sclerophyllous oak species, displayed a higher amount (i.e., 189-125 $\mu g.cm^{-2}$) of leaf cuticular waxes compared to other *Quercus* species. For instance, young leaves of *Q. ilex* (another evergreen oak) have 71 $\mu g/cm^2$ of cuticular wax (Martins *et al.*, 1999), *Q. robur* (deciduous oak growing in cooler climates) has 59 $\mu g.cm^{-2}$ (Prasad & Gülz, 1990) and *Q. petraea* (deciduous oak) has 101–134 $\mu g.cm^{-2}$ (Bahamonde *et al.*, 2018). These results reinforce the idea that both, cuticular wax qualitative and quantitative composition is a major trait to cope with drought conditions.

4.2.4. Plant specialized metabolites under drought stress: expected changes according to ecophysiological theories

Plant cellular activity can be divided into two main processes: **growth**, which encompasses cell division and enlargement, and **differentiation**, involving chemical and morphological changes leading to cell maturation and specialization. Plants have to strike a balance between growing rapidly to cope with competition and maintaining the necessary defenses against environmental stresses. This is the **growth-differentiation balance** (GDB) framework, a crucial challenge for plant survival (Herms & Mattson, 1992). Examples of cellular differentiation processes include the thickening of leaf cuticle and secondary cell walls, production of wax and cellular inclusions, and specialized metabolism (Herms & Mattson, 1992).

In stress conditions, plants are faced to a dilemma between growth and defense processes (Herms & Mattson, 1992). This trade-off is mainly conditioned by available C and N resources. Net CO_2 assimilation is intimately linked to growth and thus to primary metabolism but also can fuel the rate of specialized metabolism. Central and specialized metabolisms are well known to have the same chemical precursors. For example, phenylalanine is a precursor of the phenolic compound's biosynthesis pathway, and it is also an essential amino acid for protein production in central metabolism. Phenolic compound biosynthesis is then in competition with growth mechanisms.

According to the growth–differentiation balance hypothesis (GDBH) (Herms & Mattson, 1992), in resource-rich environments (i.e. with high water and nutrients availability), growth processes (primary metabolism) receive allocation priority for resources (Bazzaz *et al.*, 1987), decreasing the relative availability of carbon for the support of specialized metabolism and structural reinforcement. However, when these resources decrease under moderate stress, plants prioritize the production of specialized defense metabolites to the detriment of growth. Finally, when stress is too intense, both metabolisms are reduced to a minimum. This theory assumes that growth processes are slowed considerably by even moderate shortages of nutrients or water while net photosynthesis is not as sensitive to resource limitation (**Figure 11**).

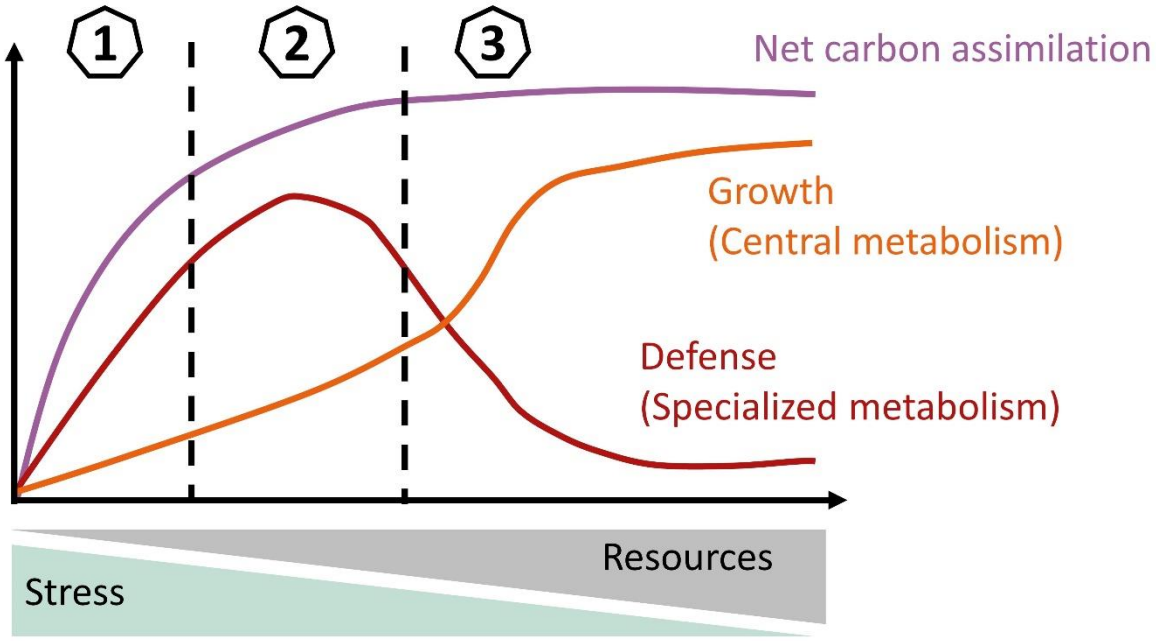

Figure 11: Schema representing the Growth-Differentiation-Balance (GDB) theory, modified from Herms & Mattson (1992). (1) Severe resource deficiency (severe stress) altering photosynthetic system and limiting the rate of CO_2 assimilation leading to both, low growth (central metabolism) and specialized defenses (specialized metabolism). (2) Moderate resource deficiency (moderate stress) does not alter net CO_2 assimilation while the growth rate is slowing, leading to a surplus of C in the plant which benefits specialized metabolism. (3) Optimal resource availability (no stress), growth is maximal favoring central metabolism at the expense of specialized metabolism.

The different response and patterns in the concentration of specialized defense metabolites can also be explained by the **oxidative pressure hypothesis** (Close & McArthur, 2002). According to this hypothesis, the distribution and abundance of phenolic compounds is a response of plants to cope with photodamage – due to excess light energy or drought stress – and the related oxidative pressure, rather than a trade-off in resource allocation when plants grow in resource-limited environments (**Figure 12**).

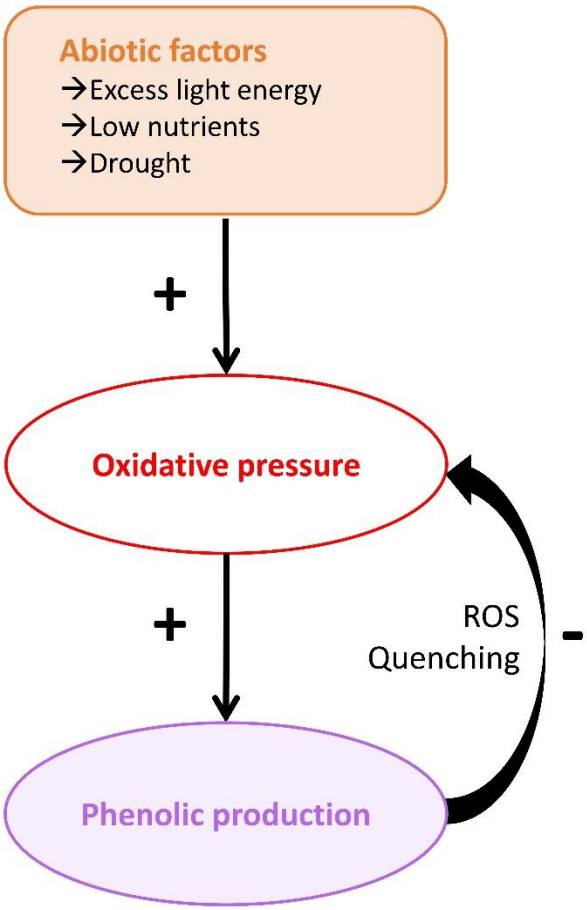

Figure 12: Schema of the oxidative pressure hypothesis after Treutter (2006). Symbols indicate positive (+) or negative (-) effects.

5. *In natura* impact of amplified drought on *Quercus pubescens*: state of the art

In Southern France, a dynamic rainfall exclusion system set-up in a *Quercus pubescens* Willd. forest allows, since April 2012, ~30% rain exclusion (more details of this experimental site are given in the "materials and methods" section). Several studies carried out in this *in natura* site from 2012 to 2015 on the physiology and defense metabolites of *Q. pubescens* leaves revealed some significant negative impacts on leaf physiology and metabolome adjustments to short or mild-term water stress (Genard-Zielinski *et al.*, 2018a; Saunier *et al.*, 2018, 2022). During these first years of partial rain exclusion, *Q. pubescens* leaves displayed a reduction in stomatal conductance (g_s) to minimize water loss through transpiration (**Table 2**) which led to a strong decrease in net carbon assimilation (A_n) but did not impact tree growth (in terms of leaf biomass production) (**Table 2**). After 4 years of amplified drought (2015), rain restriction implied

a decrease in some photosynthetic pigments (β-carotene, lutein and neoxanthin) which was not observed after 3 years of amplified drought (**Table 2**). It is worth noting that 2015 was severely dry while 2014 was a wet year. The observed decrease in those central metabolites in 2015, could be possibly due to the oxidative pressure within the leaves leading to carotenoid oxidation. Notably, antioxidants such as α-tocopherol and plastochromanol accumulated significantly in *Q. pubescens* across the seasonal cycle in 2015, particularly during summer and autumn, suggesting their crucial role in protecting chloroplast membranes, although they did not accumulate more under rain exclusion compared to adjacent trees growing under natural raining conditions. Despite flavonoids are well known to have a role in photoprotection (Ferreyra *et al.*, 2021) and are of major importance for drought resistance (Nakabayashi *et al.*, 2014b), flavonoids did not over accumulate from 2012 to 2015 under rain restriction as often reported in various plant species in response to drought conditions (Fini *et al.*, 2012; Rivas-Ubach *et al.*, 2014; Nichols *et al.*, 2015; Popović *et al.*, 2016). On the contrary, a decrease in some flavonols (a major class of flavonoids) was observed after 3 to 4 years of amplified drought (**Table 2**). Additionally, an increase in specialized defense (isoprene, not studied in the present thesis) was only identified after only one year of amplified drought (**Table 2**).

Table 2: Summary of studies on the impact of short and mid-term amplified drought *in natura* (at O_3HP) on physiological, metabolic and growth traits of *Quercus pubescens.* The three cited studies were performed on the same experimental forest (*in natura*).

Reference	Year and season of measurements	Duration of amplified drought	Physiological traits and effect of amplified drought	Effect of amplified drought on central metabolites	Effect of amplified drought on specialized metabolites	Effect of amplified drought on growth traits
Genard-Zielinski *et al.* (2018)	2012 (summer)	Short-term	A_n =; g_s ↘	Not measured	Isoprene emission ↗	Not measured
Genard-Zielinski *et al.* (2018)	2013 (summer)	Short-term	A_n ↘; g_s =	Not measured	Isoprene emission =	Not measured
Saunier *et al.* (2018; 2022)	2014 (summer)	Mild-term	A_n ↘; g_s ↘; WUE =; Ψ_{md} =; Ψ_{pd} ↘	β-carotene = Lutein = Neoxanthin = VAZ = Chlorophyll =	Plastochromanol ↗ α-tocopherol = Isoprene emission ↘ Quercetin derivatives ↘ Myricitrin ↘	LMA = Leaf biomass production =
Saunier *et al.* (2018; 2022)	2015 (summer)	Mild-term	A_n ↘; g_s ↘; WUE ↗; Ψ_{md} =; Ψ_{pd} ↘	β-carotene ↘ Lutein ↘ Neoxanthin ↘ VAZ = Chlorophyll =	Plastochromanol = α-tocopherol = Isoprene emission = Kaempferol hexose ↗ Myricitrin ↘	LMA = Leaf biomass production =

In light of these previous results, the aim of the present thesis was to continue investigating the responses of leaf defenses issued from central and specialized metabolism after long-term amplified drought (> 10 years). Since previous studies showed limited changes in chemical leaf traits (especially phenolic compounds) under rain restriction, morpho-anatomical leaf traits were taken into account in this thesis – as they represent key adaptive changes, particularly in response to long-term drought (Della Torre *et al.*, 2021).

6. Objectives of the thesis

Based on previous research synthesized in the previous section, the goal of this thesis is to track the long-term effects of reduced precipitation on *Q. pubescens* with a focus on leaf chemical traits already analyzed in previous studies (mainly the flavonoid family belonging to polyphenol group and photosynthetic pigments from central metabolism), but also include new chemical traits not tackled in previous research (i.e. cuticular specialized metabolites) as well as a deep analysis of morphological and anatomical leaf traits.

For achieving these goals, the thesis is structured within 4 chapters as follows (**Figure 13**):

(1) A literature review on the importance of flavonols belonging to the large family of flavonoids, in the context of climate change, especially in the Mediterranean region where plants are particularly exposed to water deficit (**Chapter III**, p. 61).

(2) Study of leaf chemical traits in response to long-term amplified drought and across the seasonal cycle through analyses of both central (chlorophylls, carotenoids, plastoquinone) and specialized (polyphenols, tocochromanols, triterpenoids, fatty acid derivatives) metabolites. Metabolites were analyzed by distinguishing those present in the leaf as a whole, and those present in the cuticular layer only, the later never characterized in *Q. pubescens* leaves before (**Chapter IV**, p. 85).

(3) Investigating leaf morphological (e.g. surface traits such as trichome and stomatal density, and functional traits such as leaf size and SLA) and anatomical (e.g. tissue thickness) adjustments in response to recurrent and long-term amplified drought with a focus on summer tree response as well as studying the relationship between morpho-anatomical and physiological traits (A_n, g_s, E, WUE) (**Chapter V**, p. 108).

(4) Exploring the long-term (> 10 years) effects of rain restriction through a seven-year summer monitoring of both, central and specialized metabolites of *Q. pubescens* leaves. This chapter contributes to understand the trade-offs between leaf defenses and the memory effects of different precipitation patterns occurring through years (**Chapter VI**, p. 130).

Our main hypotheses are that:

- Concentration in phenolic compounds drops after ten years of amplified drought, as previously observed after 3-4 years contrasting with the ecophysiological theories previously described (GDBH, Herms & Mattson, 1992; and oxidative pressure, Close & McArthur, 2002).

- Concentration in cuticular waxes increase under amplified drought as a mean to limit water loss (Kosma *et al.*, 2009; Xue *et al.*, 2017; Seufert *et al.*, 2022).
- Morphological and anatomical adjustments take place to maintain physiological functioning of trees by limiting water loss (De Micco & Aronne, 2012).

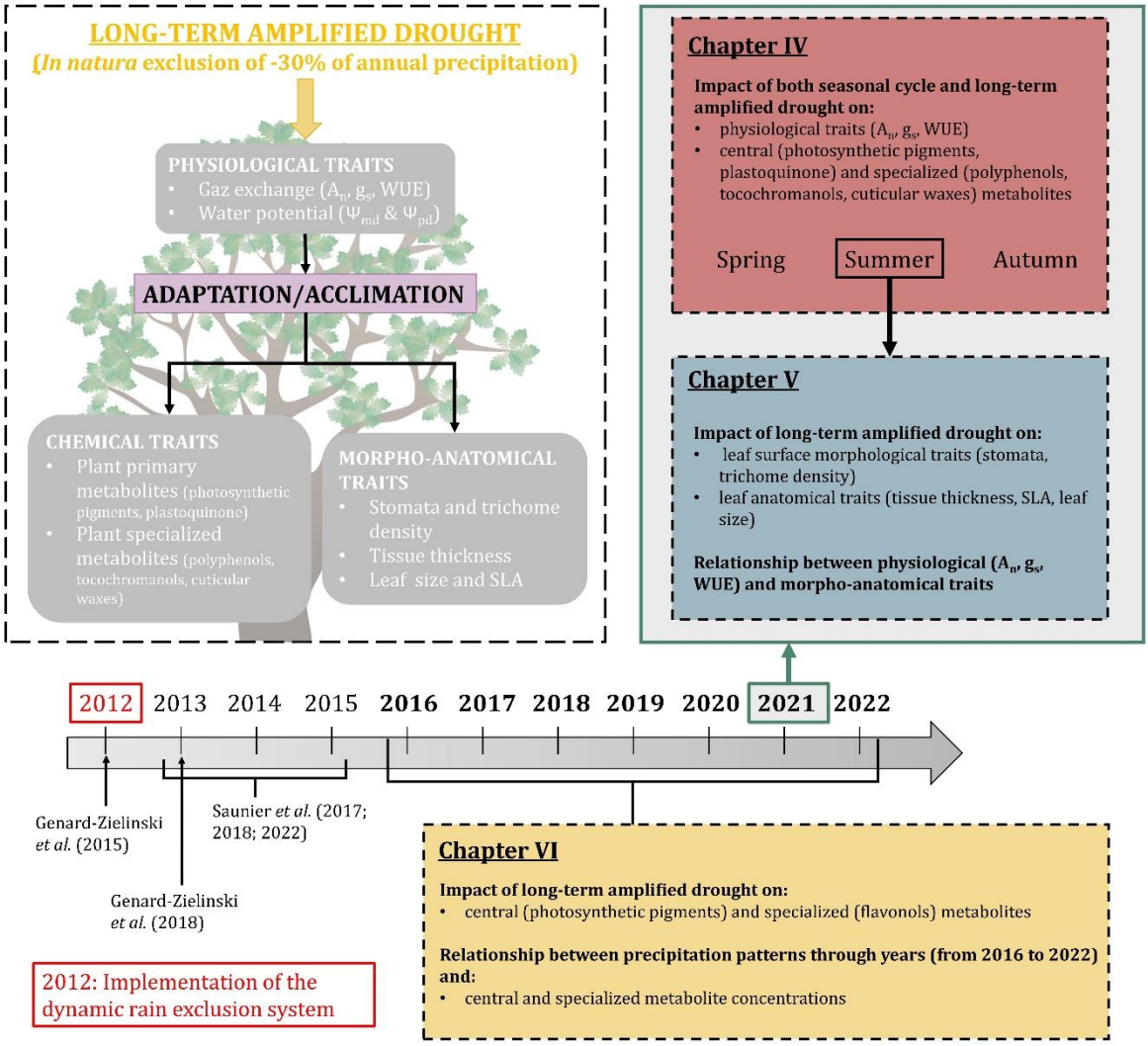

Figure 13: Summary of the different chapters of this thesis. A_n, net CO_2 assimilation; g_s, stomatal conductance to water; SLA, Specific Leaf Area; WUE, water-use efficiency; Ψ_{md}, midday water potential; Ψ_{pd}, predawn water potential.

7. Personal contribution to the thesis and collaborators

7.1. Personal contribution to chapters IV, V and VI

For this thesis work, I carried out 5 field campaigns for *in situ* gas exchange and water potential measurements (in October 2020, May, July, and October 2021, and in July 2022) with the assistance of Jean-Philippe Orts, Sylvie Dupouyet, and Elena Ormeño (IMBE). During these campaigns, leaf samples were also collected for further laboratory analyses with the help of Michel Havaux and Brigitte Ksas (CEA).

The project design for the thesis and the development of the various chapters were conducted with the guidance of my two thesis supervisors, Elena Ormeño and Catherine Fernandez. The measurement monitoring and results analysis were supervised by Elena Ormeño and approval by the PhD committee that took place every year and also by collaborators/co-authors.

In **Chapter IV**, the quantification of photosynthetic pigments, plastoquinones, and tocochromanols were carried out at the Institute of Biosciences and Biotechnologies of Aix-Marseille (BIAM) at CEA Cadarache, in PEPPS team ("Plant Environmental Physiology and Stress Signaling"), with the assistance of Michel Havaux (research director) and Brigitte Ksas (engineer). Phenolic compounds were analyzed in the Metabolomics and Metabolomic Platform (P2M2) in Rennes. Regarding cuticular waxes, I established the wax extraction protocol, developed the GC-MS analysis method, and conducted all laboratory work at IMBE, including chromatography analysis with the assistance of Caroline Lecareux (engineer). I performed statistical analysis of all physiological data and metabolite quantification with advice from Elena Ormeño.

For **Chapter V**, I received training in scanning electron microscopy (SEM) with the assistance of Alain Tonetto from the Analytical Research and Technological Imaging Platform (PRATIM) at Aix-Marseille University. I independently acquired numerous images of oak leaf surfaces and analyzed all images using image processing software (Image J). I also had the opportunity to spend a 3-month stay in Madrid at the Forest Research Center of INIA-CSIC (Instituto Nacional de Investigación y Tecnología Agraria y Alimentaria) (as part of the European label acquisition) hosted by Guillermo Gea-Izquierdo (researcher) to study anatomical leaf traits. I learned how to perform anatomical sections and histological staining of leaves with the help of María Conde (engineer technician). For all the data derived from different imaging techniques, I conducted all statistical analyses under the supervision of Elena Ormeño.

For **Chapter VI**, metabolite quantifications were carried out on leaves collected in summer before the start of my thesis (2016 to 2020) and on leaves collected during my thesis (2021 and 2022). Similar to Chapter IV, the quantification of photosynthetic pigments, plastoquinones, and tocochromanols was conducted at CEA in Cadarache, and flavonol quantifications were performed at the Metabolomics and Metabolomic Platform (P2M2) in Rennes.

For the three experimental chapters (IV, V, and VI) of this thesis, I compiled all climate data (temperature and precipitation) from the experimental site for the period 2016 - 2022) with assistance of Ilja Reiter and Jean-Philippe Orts (IMBE). I wrote the literature review (**Chapter III**) published in 2022 in the "*Plants*" journal. I also wrote the three scientific articles included in this manuscript (Chapters IV, V, and VI) by interpreting the results and comparing them to previous studies through bibliographic work. Chapter IV was published in 2023 in "*The Plant Journal*," Chapter V has been submitted to "*Tree Physiology*," and Chapter VI has been submitted to "*Scientific reports*".

7.2. Personal contribution to exploratory experiments not valorized during my thesis

During my thesis, I also performed supplementary and preliminary/exploratory experiments (shortly described below) through collaborations with specialists in other disciplines (chemists and physicians). These experiments could only be initiated and could not be further developed in the frame of my thesis. A synthesis of these experiments is described hereafter but will not be further referred to.

7.2.1. Physiological stress: oxidative pressure technique development

I collaborated with Dr. Béatrice Tuccio, chemists from the Institute of radical chemistry (Institut de chimie radicalaire, UMR 7273) to develop a method for assessing physiological stress in trees through measurements of **oxidative markers**. These initial experiments aimed to verify whether **electron paramagnetic resonance (EPR) spectroscopy** could be a tool for studying oxidative stress in oak leaf thylakoids. As part of this collaboration, I conducted the thylakoid extractions in our laboratory (through different steps of grinding, filtration and centrifugation). I was then trained by Béatrice to learn the technique of EPR spectroscopy, which is a method for detecting low concentrations of paramagnetic species (i.e. with unpaired electrons).

After inconclusive spin-trapping tests (involving the use of a diamagnetic molecule to trap a free radical in the form of a more stable paramagnetic adduct detectable by EPR),

we chose to focus on the overall redox status of the plant material (thylakoid extracts) under irradiation (blue and red light absorbed by chlorophyll) in a green-lit room (kindly installed by Patrick Bernasconi, engineer assistant) (**Figure 14a**). For this purpose, we conducted several experimental campaigns by introducing a stable radical with a known initial concentration into the medium containing the thylakoid extracts and monitoring the evolution of its EPR signal over time under different conditions (with or without irradiation) (**Figure 14b**). In a biological environment (i.e. in the presence of reducers), the nitroxide TEMPOL is easily reduced to hydroxylamine TEMPOL-H, which is invisible in EPR. The presence of oxidants such as reactive oxygen species (ROS) allows the reoxidation of TEMPOL-H to TEMPOL (**Figure 14c**). An increase in the signal corresponds to the reoxidation of hydroxylamine TEMPOL-H under irradiation, confirming the production of oxidative species under irradiation (**Figure 14b**). Analyzing the evolution of the EPR signal over time allowed us to obtain valuable information about the redox status of the system under study.

These results are preliminary and thus exploratory, but results obtained suggest it is worth the effort to develop this technique, since it could be a very interesting tool for measuring oxidative stress in plant material. In our experiments, we did not study a sufficient number of trees to produce statistically exploitable results and achieve an optimal experiment repeatability.

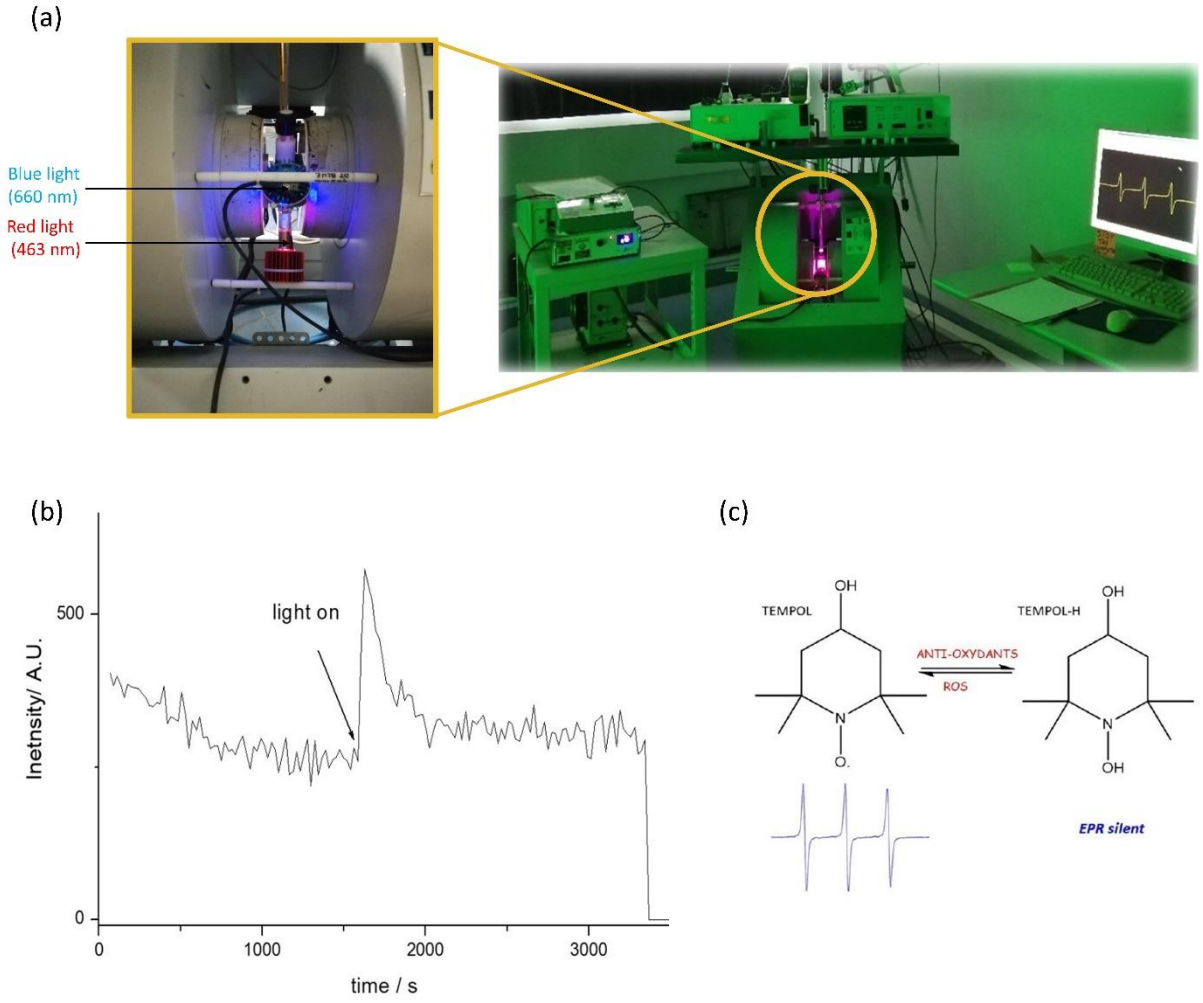

Figure 14: EPR spectrometry study on *Q. pubescens* leaf thylakoids. (a) Spectrometer BRUKER EMX with light (blue and red) installation. (b) TEMPOL EPR signal variation before and after irradiation. (c) redox balance between TEMPOL and TEMPOL-H.

7.2.2. Raman spectra and localization of metabolites

A second collaboration was carried out with Dr. Sophie Brasselet and Dr. Paulina Gasecka from the Institute of Optical Physics (Fresnel, UMR CNRS AMU) in order to **localize metabolites** in leaves of *Q. pubescens* through **Stimulated Raman Spectroscopy (SRS) microscopy imaging**.

Raman technology has the potential to bring a new approach in the study of metabolite localization which can be related to specific function of plant metabolites. Moreover, the Raman signal of central and specialized metabolites could be used to investigate changes in plant metabolite localization according to different organs (leaf, stem, root) and/or

specific structures such as stomata or trichomes. Additionally, this technique can be used to evaluate the degree of stress by comparing the peak heights of the spectra for given samples under different environmental conditions (Altangerel *et al.*, 2017). This method is based on the inelastic scattering of light, where scattered photons experience a frequency shift due to molecular vibrations (Park *et al.*, 2023). When this technique is applied to plant leaves, it allows for the identification and relative quantification of various metabolites such as pigments, flavonoids, and lipids. By using a laser to excite the molecules present in the leaves (**Figure 15a**), Raman spectroscopy provides a non-destructive and fast approach for metabolite analysis.

During our experiments, we were able to characterize the Raman spectra of eight metabolites of interest (chlorophyll *a*, phenylalanine, gallic acid, quercetin-glucoside, β-carotene, kaempferol-glucoside, lutein, and lupeol) using standard molecules (**Figure 15b**). Once these spectra were measured, we were able to target specific wavelengths of targeted metabolites to study their distribution on the abaxial leaf surface through Stimulated Raman Spectroscopy (SRS) microscopy imaging (**Figure 15c**). A semi-quantitative approach could have been further developed to quantify the target metabolites with an accuracy comparable to conventional quantification methods such as HPLC, without the need for sample pre-treatment. Such an approach is currently being refined (Park *et al.*, 2023).

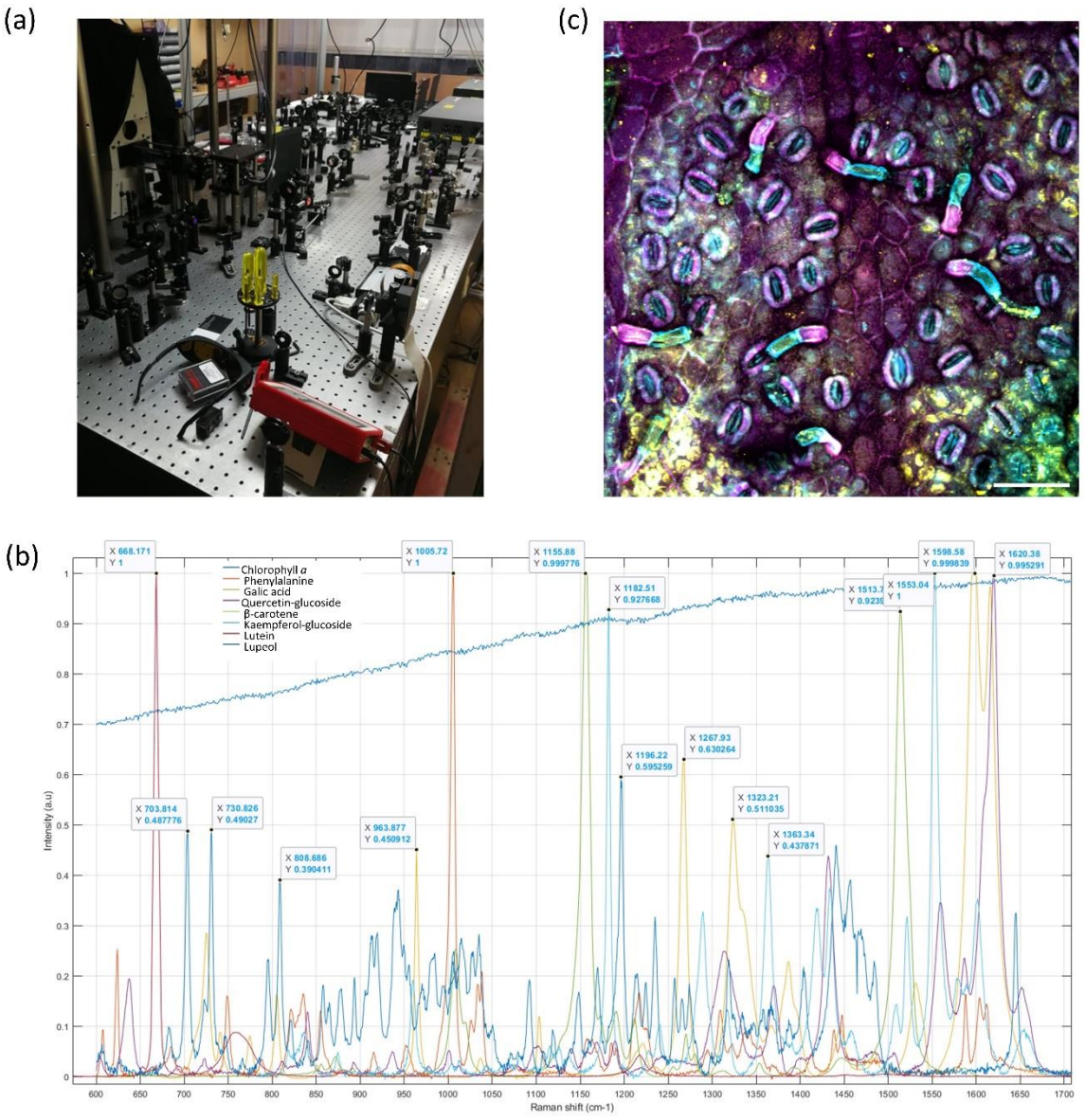

Figure 15: Raman imaging and spectra on *Q. pubescens* leaf surface. (a) Experimental laser device. (b) Raman spectrum of metabolites of interest (chlorophyll *a*, phenylalanine, galic acid, quercetin-glucoside, β-carotene, kaempferol-glucoside, lutein, and lupeol). (c) Stimulated Raman Spectroscopy (SRS) microscopy imaging showing β-carotene (yellow), acid galic/quercetin-glucoside (purple) and fluorescence (blue).

CHAPTER II: Materials and methods



Oak Observatory at Observatoire de Haute-Provence (O3HP), Saint-Michel-l'Observatoire

1. The study model: *Quercus pubescens* Willd.

Downy oak (*Quercus pubescens* Willd.) is a deciduous medium-sized oak (15-20m) growing in southern Europe, at low and middle altitudes, under sub-Mediterranean and temperate climatic conditions. It distributed from the Atlantic coast of France (South of Bretagne and Normandie) to the shores of the Mediterranean Sea, and across peninsular Italy, the Balkan Peninsula and the Aegean regions, to the coasts of the Black Sea and most of Anatolia (**Figure 16**). In the Northern Mediterranean basin, this species covers over 2 million ha (Saunier *et al.*, 2017b). Downy oak is the dominant forest species in the sud-PACA (Provence-Alpes-Côte d'Azur) region in South France, covering 307,000 hectares (IGN, results from five annual inventory campaigns from 2018 to 2022). Its abundance has made it a favored study model to assess the impact of climate change in the Mediterranean, with a focus on the decomposition of its litter (Santonja *et al.*, 2015) and canopy central and specialized metabolites Biogenic volatile organic compounds (BVOC) emissions (Genard-Zielinski *et al.*, 2014, 2018a; Saunier *et al.*, 2017b, 2020). It is characterized by very high isoprene emission rates with daily mean isoprene emission rate (ERd) fluctuated between 23 and 98 µgC g_{DM}^{-1} h^{-1}, which account for ~99% of the BVOC carbon mass (Genard-Zielinski *et al.*, 2015). In the context of climate change, studies on the impact of drought have revealed a decrease in isoprene emissions after 3-4 years (mid-term drought; Saunier *et al.*, 2017a, 2018) of amplified drought condition in a *Q. pubescens* forest, which can be interpreted as a putative loss of defenses since isoprene confers protection against oxidative stress in plants (Velikova *et al.*, 2011).

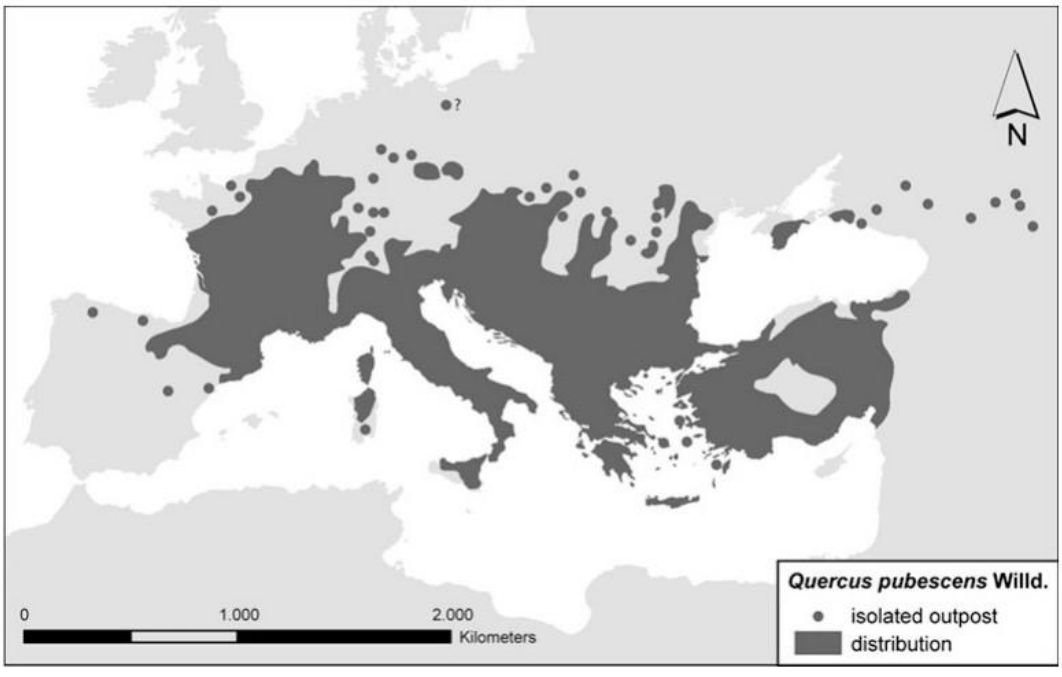

Figure 16: Distribution of *Quercus pubescens* Willd. in Europe from Wellstein *et al.,* (2017).

Downy oak behaves as a heliophilous and thermophilous species and is perfectly adapted to withstand both moderate summer drought stress and low winter temperatures (Pasta *et al.*, 2016). It is described as a drought-resistant species (Levitt, 1980; Struve *et al.*, 2009) since this species has developed adaptive mechanisms that enable it to withstand the increased summer drought periods typical of the Mediterranean region. These adaptations involve, prior to the water stress period in spring, rapid radial growth when water is not yet limiting (Zweifel *et al.*, 2006). Subsequently, this species avoids leaf dehydration under water stress through the development of a deep root system and high hydraulic conductivity that allows subsurface soil moisture uptake to leaves thus maintaining high relative leaf moisture (Nardini & Pitt, 1999; Tognetti *et al.*, 2007; Struve *et al.*, 2009). Fotelli *et al.* (2000) showed that among other Mediterranean oak species (i.e. *Quercus frainetto* Ten., *Quercus macrolepis* Kotschy., *Quercus ilex* L.), *Q. pubescens* maintained the highest water potential under drought conditions, reinforcing the idea that Downy oak has a greater efficiency in hydraulic transport compared to other *Quercus* species (Tognetti *et al.*, 1998b). Additionally, *Q. pubescens* typically behaves as anisohydric plant species meaning that despite increasing water shortage, stomata can remain partially opened (Poyatos *et al.*, 2008).

2. Experimental site

This study was conducted at the O_3HP (Oak Observatory at the "Observatoire de Haute Provence"), an experimental forest site *in natura* mainly populated by *Q. pubescens,* (~90%) and to a less extent by *Acer monspessulanum* L. (~10%). This site allows long-term monitoring of the impact of restricted precipitation on a deciduous Mediterranean forest. It is located 60 km north of Marseille in Southern France (5°42′44″E, 43°55′54″N) at an elevation of 650 m above sea level. Annual rainfall is 784 mm and annual mean temperature 13.1 °C (calculated for the period 1993-2022) which corresponds to a sub-humid (600 – 800 mm) and supra-Mediterranean bioclimate where trees are submitted to 2-3 dry months (Quézel & Médail, 2003). It is worth to note that according to the previous climate series (1967-2000) (Santonja *et al.*, 2015), average annual precipitation and temperature for the site were 830 mm and 11.9 °C respectively, indicating precipitation reduction and warming already naturally occur in the field site.

This experimental site is equipped since April 2012 with a dynamic rainfall exclusion device (**Figure 17a,b**) which is deployed during some rain events from April to October to exclude between 30 and 40 % of annual precipitation (which corresponds, on average to 20 days of rain exclusion) thus simulating future climate predictions in the Mediterranean region (Lionello & Scarascia, 2018; Zittis *et al.*, 2019). This system allows

to increase the number of dry months from 2-3 to 4-5 dry months with an annual rainfall of about 500 mm (calculated for the period 2012-2022) which corresponds to a semi-arid climate (400 – 600 mm). Excluded water is drained off-site via gutters. Two plots are monitored, namely the amplified drought (AD) plot of 300 m^2 where trees are subjected to partial rain exclusion and the natural drought (ND) adjacent plot (300 m^2) without rain exclusion where trees grow under natural drought conditions occurring in this Mediterranean forest (**Figure 17c**). Between 5 and 10 Downy oak trees were selected within each plots (ND and AD) to study their leaf physiological, metabolic and morpho-anatomical traits (**Figure 17c**).

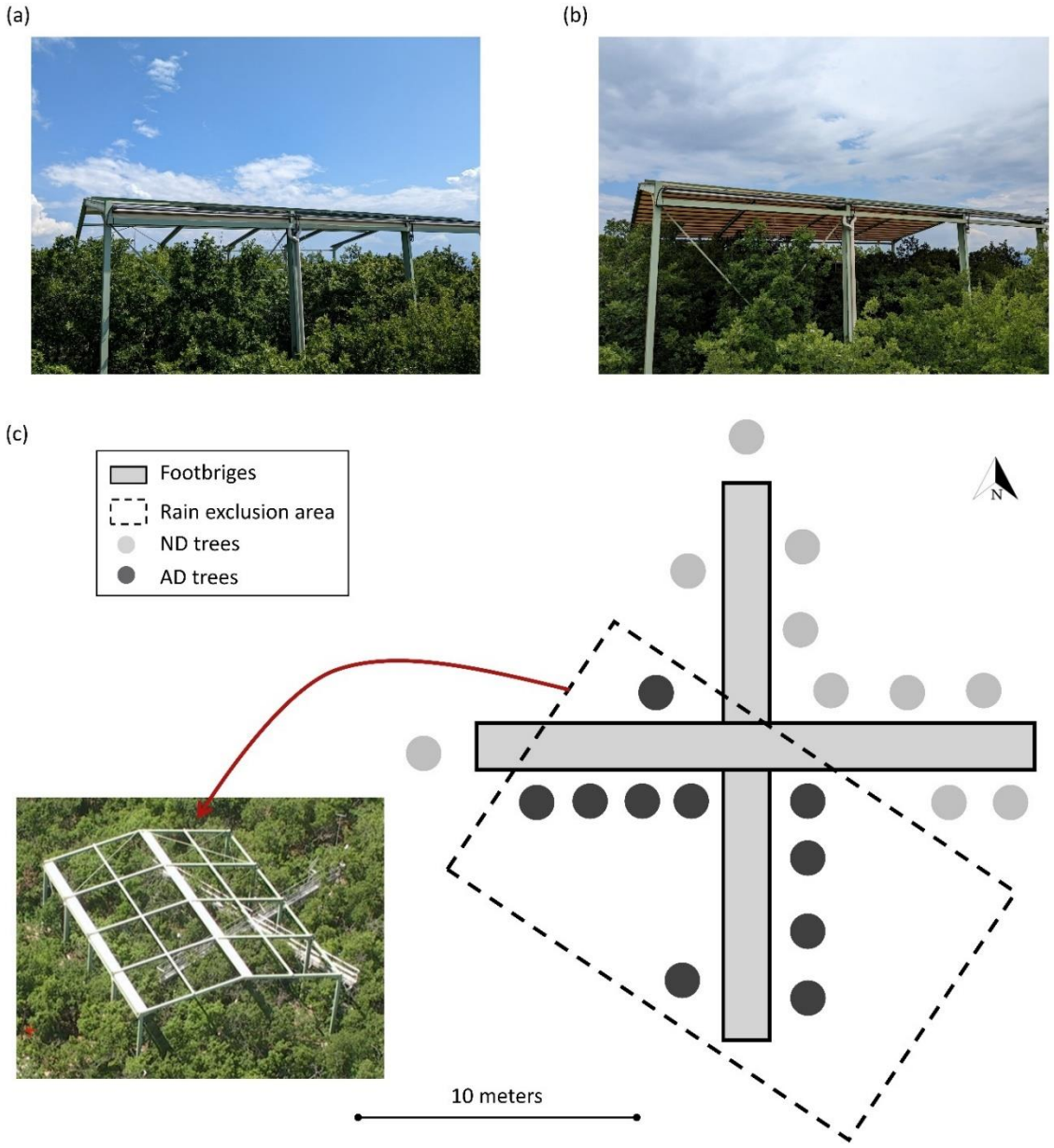

Figure 17: Experimental site at the Oak Observatory at Observatoire de Haute Provence (O_3HP). Photo of the experimental site at the O_3HP with the exclusion device (a) opened and (b) closed. (c) Scheme of the experimental site showing the distribution of the 20 sampled trees. Trees

under natural drought (ND) are shown in light grey and under amplified drought (AD) in dark grey.

During the period 2014-2022, ombrothermic diagrams revealed (i) six dry years (2015, 2016, 2017, 2020, 2021 and 2022) with two to five dry months, 2017 and 2020 being the driest years and (ii) three wet years (2014, 2018 and 2019) where the total annual precipitation was above 784 mm (**Figure 18**). Between 2014 and 2022, from 24% to 48% of annual precipitation were excluded every year (**Figure 18**).

Annual mean temperatures were quite similar through years excepting 2022 where it was 14.7 °C, that is, 1.6 °C above the annual mean temperature recorded in this site (i.e. 13.1 °C, over the 1993-2022 period) (**Table 3**). Both, 2017 and 2022 were naturally highly dry displaying a high number of dry months (three-five dry months under ND) and accordingly, trees under AD were also exposed to a high number of dry months (seven) while in 2018 trees were exposed to only two months of natural drought (**Figure 18**).

Table 3: Climatic data (cumulative annual precipitation and annual mean temperature) for 2014-2022 period. Cumulative annual precipitation is presented under natural drought (ND) and amplified drought (AD).

Year	Cumulative annual precipitation (mm) under ND	Cumulative annual precipitation (mm) under AD	Annual mean temperature (°C)
2014	1233	819	13.3
2015	596	423	13.8
2016	804	479	13.4
2017	484	294	13.7
2018	1075	567	13.7
2019	1092	604	13.7
2020	499	300	13.7
2021	728	426	12.9
2022	665	581	14.7

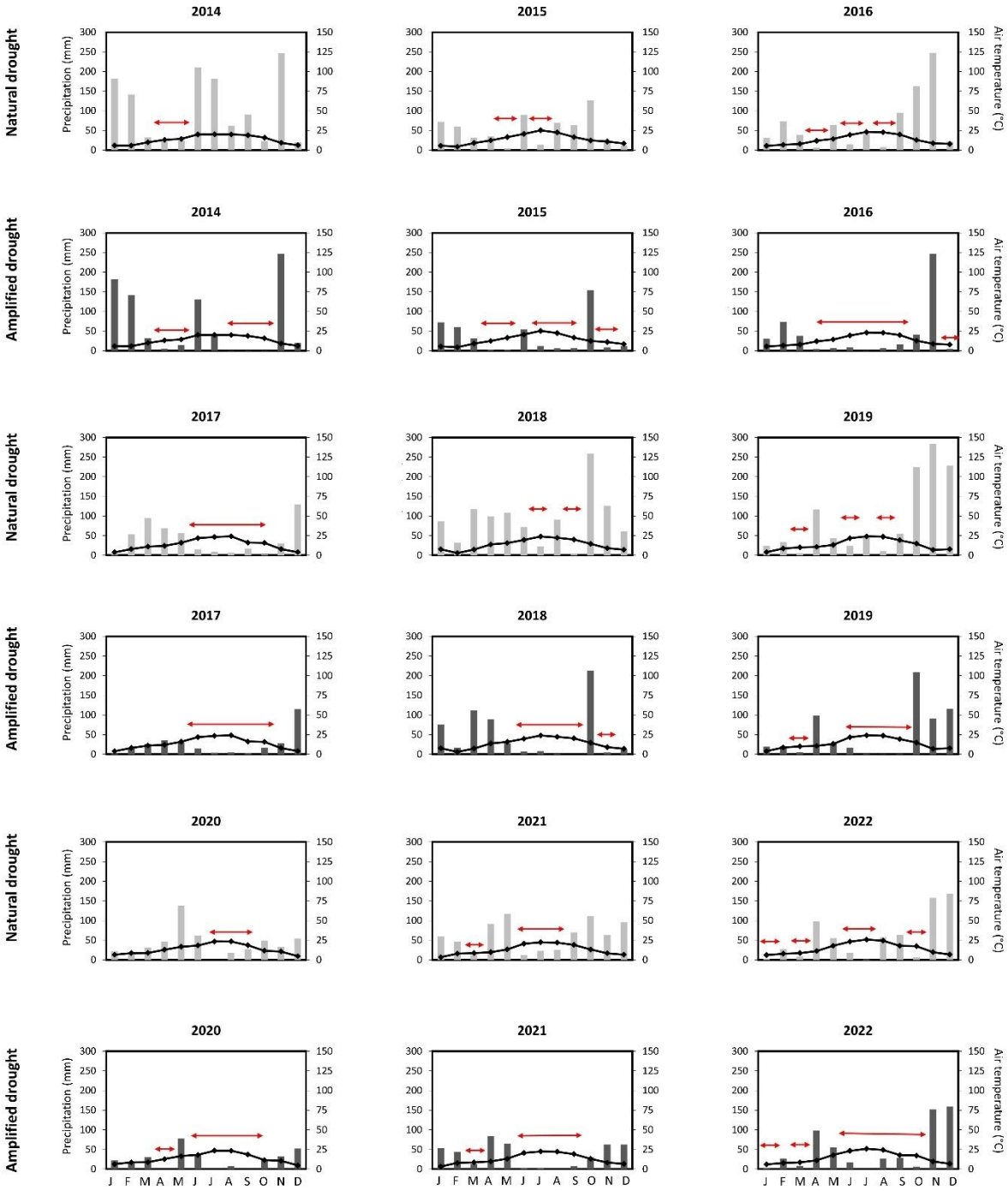

Figure 18: Ombrothermic diagrams for natural (light gray) and amplified (dark gray) drought plots on the experimental site O_3HP (Oak Observatory at Observatoire de Haute Provence) from 2014 to 2022. Bars represent monthly cumulative precipitation (P, mm) and curves represent mean monthly temperature (T, °C) with P = 2 T. When temperature curves are above precipitation bars, it corresponds to dry periods indicated by red horizontal arrows.

3. Ecophysiological trait analyses

3.1. Gas exchange

Gas exchanges were measured on three leaves from a sun exposed branch at the top of the canopy of each tree using an open-system gas analyzer for high-precision detection of CO_2 and H_2O gasses (CIRAS-3, PP Systems, Amesbury, MA, USA). The reference CO_2 concentration was set to 400 µmol mol^{-1}, temperature of the leaf chamber was set to 27°C, and photosynthetically active radiation (PAR) was set to 1000 µmol m^{-2} sec^{-1}. Traits measured were the net CO_2 assimilation (A_n, µmol CO_2 m^{-2} sec^{-1}), stomatal conductance (g_s, mmol H_2O m^{-2} sec^{-1}), internal CO_2 concentration (C_i, µmol mol^{-1}), and WUE (mmol CO_2 mol^{-1} H_2O).

3.2. Water potential

Stem water potential was measured using stems containing three to five leaves. Both water potential at midday (Ψ_{md}) and predawn (Ψ_{pd}) were measured with a Scholander pressure chamber (PMS Instrument Co. USA; range 0–7 MPa).

4. Physical trait analyses

For the morphological and anatomical analyses, leaves were collected from the twenty monitored trees (ND and AD; **Figure 17c**) at the top of the canopy, during the field campaign in July 2021 (**108**). Leaves were collected and immersed in liquid nitrogen, and then stored in a freezer at -80°C until analyses.

4.1. Morphological traits

4.1.1. Functional leaf traits

The specific leaf area (SLA, cm^2 g^{-1}) was calculated as the ratio of leaf surface (cm^2) – measured using ImageJ software – to dry mass calculated on 10-15 leaves by tree.

4.1.2. Leaf surface traits

The stomatal size, stomatal density and trichome density of *Q. pubescens* leaves were measured using 3 leaves/tree and 10 trees/condition and 3 different areas/leaf (totaling 180 analyses). Measurements were performed on the abaxial surface since the adaxial surface possessed a very low density of non-glandular trichomes and no glandular trichome (Safou & Saint-Martin, 1989; Fortini *et al.*, 2009). The leaf abaxial surfaces were observed through scanning electron microscope (Zeiss Evo 15 VP EP -SEM, Germany, 20 kV accelerating potential, 10 mm working distance) at 100X magnification to calculate the density of trichomes and 500X magnification for stomatal size and density. Before microscopic observations, leaf sections were sputtered with gold. Stomatal size was calculated as an ellipse from the measured guard cell length. Images were analyzed using ImageJ software (National Institutes of Health, Bethesda, MD, USA).

4.2. Anatomical traits

Leaf anatomical traits were characterized through leaf tissue thickness, measured on 3 leaves/tree and 3 segments/leaf (1 x 0.5 cm) on either side of the main vein. Each segment was progressively dehydrated in ethanol series (70 % to 100 %, 7 times) followed by xylene and then embedded with warm paraffin. Leaf transverse sections (9 µm) were then cut using a rotary microtome (Leica biosystem RM235, Nussloch Germany), then stained with safranin (lignified tissues) and astra blue (non-lignified tissues) and finally assembled in slides and sealed with neutral glue (Férriz *et al.*, 2023). The thickness of both, adaxial and abaxial epidermis as well as palisade parenchyma and spongy parenchyma were determined using a light microscope (Leica DM2500, Germany) at a magnification of 100X.

5. Chemical analyses

For the chemical analyses, leaves were collected from the twenty monitored trees (n=10 under ND and n=10 under AD; **Figure 17c**) at the top of the canopy, during each field campaign. According to each chapter the number of monitored trees changes as follows:

- **Chapter IV**: seven trees by drought condition
- **Chapter VI**: five trees by drought condition

During sampling campaigns, 10-15 leaves were collected and immersed in liquid nitrogen, and then stored in a freezer at -80°C until being analyzed. For the analysis of central and specialized metabolites, leaves were freeze-dried and then ground to obtain a powder.

5.1. Photosynthetic pigments and tocochromanols

Photosynthetic pigments were extracted from leaf powder (20 to 50 mg) using 2 ml of methanol and were quantified by high-performance liquid chromatography (HPLC) in collaboration with the CEA in Cadarache. Chlorophylls and several carotenoids were analyzed, including those from the xanthophyll cycle (violaxanthin + antheraxanthin + zeaxanthin, referred as VAZ) as well as neoxanthin, lutein, and β-carotene. Their concentrations (µg g_{DM}^{-1}) were calculated from calibration curves performed using carotenoid pigment standards (Extrasynthèse, France) and chlorophyll *a* and *b* standards (Sigma-Aldrich, USA). More details of the method are given in Havaux *et al.* (2007).

Plastoquinones (PQ) and tocochromanols, including α-tocopherol, plastochromanol-8 (PC-8), and hydroxy-plastochromanol (PC-OH), were extracted from leaf powder (20 to 50 mg) mixed in 2 mL of ethyl acetate. After centrifugation, the supernatant was filtered and evaporated on ice under a stream of N_2. The residue was recovered in methanol/hexane (17:1 vol) and analyzed by HPLC (see Ksas *et al.*, 2015, 2018) with UV absorbance and fluorescence detection. The column was a Macherey-Nagel Nucleosil 100–5 C18. PC-8 was detected by fluorescence at 330 nm with an excitation at 290 nm. Plastoquinones consisted of the pool of reduced and oxidized forms of Plastoquinone-9, referred to as plastoquinones (PQ). Quantification was achieved using PQ and PC-8 standards, which were a kind gift from Dr. J. Kruk (Krakow, Poland) and α-tocopherol standard was purchased from Sigma.

5.2. Phenolic compounds

Phenolic compounds were extracted using 10 mg of leaf powder and 1 mL of methanol containing 1 % formic acid. The extract was homogenized for 5 min in an ultrasonic bath and centrifuged at 12000 tr min 1 for 5 min. Analyses were performed with an Acquity UPLCDAD- ESI-TQD system (Waters, USA) in collaboration with the Metabolomics and Metabolome Platform (P2M2) in Rennes. UPLC separation was carried out using a C18 BEH column (2.1 mm 9 150 mm, 1.7 lm, Waters, USA). Elution rate was set to 0.4 ml min-1 at a constant temperature of 30 °C. Injection volume was set to 2 µl. Chromatographic solvents are composed of solvent A water with 0.1% formic acid and solvent B acetonitrile with 0.1% formic acid. The chromatographic gradient was 3% of solvent B for 3 min and then 17 min linear gradient until 90% solvent B, followed by column cleaning at 90% solvent B for 3 min and then 6 min equilibration at 3% solvent B giving a 25 min total runtime. Photodiode array was set from 190 to 600 nm, and phenolic compounds' wavelength detection was chosen depending on compound characteristic spectra (350 nm, 320 nm, or 280 nm). Their identity or structure was confirmed with the triple quadrupole mass detector in negative ionization mode. Parameters of the electrospray source were as follows: capillary voltage 2.9 kV, cone voltage 35 V, cone temperature was

maintained at 150°C, and desolvatation temperature at 400°C. External quantification with mono glycosylated flavonols (quercetin and myricitrin) and hydroxycinnamic acid standards (caffeoyl acid, chlorogenic acid, and coumaric acid) was applied.

5.3. Cuticular waxes

Cuticular waxes were extracted and quantified using Gas-Chromatography/Mass-Spectrometry (GC-MS) in our laboratory at IMBE in Marseille. Cuticular waxes were extracted by immersing precisely defined leaf circles (9.54 cm^2) – obtained from three to five leaves – into 3 ml of cyclohexane and chloroform (70:30 vol) under constant shaking for 2 min using a vortex. Cuticular wax removal was checked through scanning electron microscopy as shown in **Figure S2**. Then, 2.5 ml of the extract was recovered. Tetracosane D50 (C_{24}; 98%; Sigma-Aldrich) was added as an internal standard, and the total solvent was evaporated. Those cuticular wax extractions were then resuspended into 250 µl of acetonitrile and derivatized with 20 µl of N,O-Bis(trimethylsilyl)trifluoroacetamide (BSTFA, Sigma-Aldrich) and 20 µl of pyridine (Sigma-Aldrich) to improve the separation of metabolites. The extract was filtered with a PTFE syringe filter (0.2 µm, 30 mm diameter). To allow derivatization, the mixture was heated for 30 min at 70°C. Each derivatized sample was analyzed by injecting 1 µl in an Agilent 7890 GC–MS equipped with an ALS7693 automatic injector, a MSD5977A Network mass detector (70 eV), and an HP5-MS apolar column (30 m x 0.25 mm x 0.25 µm; J&W Agilent Technologies). Cuticular waxes were identified through the Agilent ChemStation software by comparing their mass spectra, retention times, and Kovats retention index with libraries (NIST 2020 and ADAMS 2008), published data, and experimental data for some available standards (alkanes C8-40, lupeol, α-amyrin, β-amyrin, α-tocopherol, and δ-tocopherol). Identified compounds were quantified against the internal standard (tetracosane D50). Results were expressed by dry matter (µg g_{DM}^{-1}) by oven-drying leaf circles (used for extractions) at 65°C for 48 h.

6. Statistical analyses

All the statistical analyses were conducted using the software R v.4.0.3 (R Core Team, 2020). Before analyses, normality and homoscedasticity were checked and data were log-transformed if necessary.

To test our hypothesis we used 4 types of statistical analyses: **(1)** a principal component analysis (PCA) to evaluate how physiological, chemical and morpho-anatomical traits were associated according to seasons (**Chapter IV**), years (**Chapter VI**) and drought conditions (**Chapter IV, V and VI**); **(2)** two-way ANOVA analyses to highlight differences in physiological and metabolic traits according to seasons, years and drought conditions; **(3)** student tests to evaluate differences between drought condition for

morpho-anatomical traits; and **(4)** a correlation analysis to identify positives and/or negatives correlations between the different traits and to highlight trade-offs.

(1) For the PCA, we used the first two principal components to show the dispersion of the data. When two factors were used (seasons and drought or years and drought), a two-way PERMANOVA was performed with 9999 permutations to highlight the effect of the two factors separately, and their interaction.

(2) A two-way ANOVA was conducted to reveal any significant changes in physiological traits and metabolic concentrations according to both season and drought conditions (**Chapter IV**) or year and drought conditions (**Chapter VI**). Two-way ANOVAs were followed by post hoc Tukey tests to evaluate the differences between the two factors. When significant interactions occurred between the two factors, we performed a one-way ANOVA followed by Tukey tests to evaluate differences between season/year and Student tests to evaluate differences between drought conditions (ND and AD) for each season/year.

(3) A Student test was used to test for morpho-anatomical trait adjustments between drought conditions (ND and AD) (**Chapter V**).

(4) Relationships between physiological and morpho-anatomical traits (**Chapter V**), as well as between metabolite concentrations and precipitation (**Chapter VI**) were determined by Pearson correlation coefficients (*r*). Additionally, Pearson's correlation matrices were performed to assess the relationship between physiological traits and between anatomical traits (**Chapter V**).

CHAPTER III: Bibliographic review on plant flavonols in Mediterranean species

Plant Flavonoids in Mediterranean Species: A Focus on Flavonols as Protective Metabolites under Climate Stress

Justine Laoué[1], Catherine Fernandez[1] and Elena Ormeño[1]

[1]Aix Marseille University, Avignon University, CNRS, IRD, IMBE, 13003 Marseille, France

This chapter refers to an article published in January 2022 in the international scientific open access journal *Plants*.

Plants 2022, 11(2), 172; https://doi.org/10.3390/plants11020172

Abstract

Flavonoids are specialized metabolites largely widespread in plants where they play numerous roles including defense and signaling under stress conditions. These compounds encompass several chemical subgroups such as flavonols which are one the most represented classes. The most studied flavonols are kaempferol, quercetin and myricetin to which research attributes antioxidative properties and a potential role in UV-defense through UV-screening mechanisms making them critical for plant adaptation to climate change. Despite the great interest in flavonol functions in the last decades, some functional aspects remain under debate. This review summarizes the importance of flavonoids in plant defense against climate stressors and as signal molecules with a focus on flavonols in Mediterranean plant species. The review emphasizes the relationship between flavonol location (at the organ, tissue and cellular scales) and their function as defense metabolites against climate-related stresses. It also provides evidence that biosynthesis of flavonols, or flavonoids as a whole, could be a crucial process allowing plants to adapt to climate change, especially in the Mediterranean area which is considered as one of the most sensitive regions to climate change over the globe.

Keywords: biological function; secondary metabolism; biosynthesis; localization; stress response; defense mechanism; antioxidant; leaves; reactive oxygen species

1. Introduction

Plants possess thousands of plant secondary or specialized metabolites (PSMs) whose chemical diversity is species-specific. These chemicals play crucial ecophysiological roles as they are implicated in plant interactions with its environment and plant defense against environmental stress conditions (Yang *et al.*, 2018). Most of them can be classified within five chemical families: terpenes, phenolic compounds, benzenoids, fatty acid derivatives and alkaloids. Based on their chemical structure, phenolic compounds can be divided into different subgroups including simple phenolics (one phenol unit alone) and polyphenols (with more than one phenolic unit) comprising phenolic acids, flavonoids, tannins, coumarins, lignans, quinones, stilbenes, and curcuminoids (Crozier *et al.*, 2006). Flavonoids, a major class of polyphenols, widely present in the plant kingdom, represent a large group of PSMs which are either produced constitutively or induced by environmental stresses (Treutter, 2006).

The role of flavonoids in protection against UV and drought stress in Mediterranean endemic species has been suggested by recent studies which show a monthly variation in the polyphenol concentrations with the highest levels occurring in summer at midday when drought, temperature and UV radiations are the highest (Gori *et al.*, 2019, 2020). It is also known that geographical factors such as latitude and altitude influence the composition of defensive chemicals including phenolic compound levels (Moreira *et al.*, 2014, 2018). Mediterranean species display contrasting polyphenol compositions and concentrations (Tattini *et al.*, 2000, 2004, 2006, 2007) which strongly respond to abiotic stresses. This suggests a key role of phenolic compounds and species-specific functions in plants living in constraining environments such as the Mediterranean region (Di Ferdinando *et al.*, 2014). Accordingly, accumulation of flavonoid concentrations in response to drought have also been reported in some Mediterranean species (Hernández *et al.*, 2004; Rivas-Ubach *et al.*, 2014; de Miguel *et al.*, 2016). In this context, it is particularly pertinent to understand the role of flavonoids in the adaptation of Mediterranean plant species to rapid climate change.

Flavonoids feature a 15-carbon atom basic skeleton, arranged in the form C6-C3-C6 and present two aromatic rings (A and B) linked by a unit of three carbon atoms (C ring), which may or may not give rise to a third aromatic ring (Santos *et al.*, 2017). There are several classes of flavonoids including chalcones, aurones, flavanonols, flavones, isoflavones, flavanols, flavonols, anthocyanins, proanthocyanidins and leucoanthocyanidins. Flavonoids can occur as aglycones, glycosides, and methylated derivatives. More than 6000 different flavonoids have been identified (Panche *et al.*, 2016) which differ in the number and position of the hydroxyl groups, and their extent of alkylation and/or glycosylation (Pandey & Rizvi, 2009). For example, the flavonols (e.g., quercetin and kaempferol), have a 3-hydroxy pyran-4-one group on the C ring whereas

the flavanols catechins have only a 3-hydoxyl group on the C ring (Kumar & Pandey, 2013).

Flavonoids feature a broad spectrum of biological activities in plants which has been related to their chemical diversity and can be linked to their localization within leaf tissues as addressed later in this review. They participate in many cellular activities such as signaling, auxin transport and pigmentation (Taylor & Grotewold, 2005; Peer & Murphy, 2007; Morita *et al.*, 2014; Gayomba *et al.*, 2016). One of the most highlighted functions of flavonoids is plant protection against abiotic (e.g., drought, salinity, UV radiation and heat) and biotic (e.g., insects and pathogens attack) stresses (Lattanzio *et al.*, 2006; Naikoo *et al.*, 2019; Sharma *et al.*, 2019). Most commonly, investigations have reported that flavonoids play a role in the modulation of reactive oxygen species (ROS) and possess UV-screening mechanisms (Tattini *et al.*, 2004; Agati & Tattini, 2010; Agati *et al.*, 2012; Barnes *et al.*, 2016; Davies *et al.*, 2018) as described later in this review. Their action as antioxidant is based on (i) their direct capacity to scavenge ROS (Rice-Evans *et al.*, 1997), (ii) their role in inhibition of ROS formation by chelating ion of metals (Brown *et al.*, 1998; Leopoldini *et al.*, 2006) and (iii) their ability to activate antioxidant enzymes (Agrawal, 2011; Kumar & Pandey, 2013). They also act as indirect plant growth regulators as explained in the last section of this review (Peer & Murphy, 2007; Brunetti *et al.*, 2018).

One of the most important flavonoid sub-groups are flavonols which include kaempferol, quercetin and myricetin, the most studied flavonols (Ferrer *et al.*, 2008). Numerous functional roles have been attributed to flavonols, especially their role as antioxidant molecules and UV-screening pigments since they have long been considered as the most effective UV-B absorbers thus conferring strong photo-protection (Pollastri & Tattini, 2011). The catechol group in the B-ring (**Figure 19**), as observed in the flavonol quercetin and its derivates, makes flavonols the most effective antioxidant compounds and therefore key compounds in the plant responses to changing climate. Flavonols seem particularly important in Mediterranean plant species as studies usually report a high concentration of flavonols such as quercetin under excess light and drought stress (Tattini *et al.*, 2000, 2004; Fini *et al.*, 2012). The higher distribution of quercetin in Mediterranean plants may explain their ability to cope with a dry climate and high solar irradiance as this flavonol is an excellent antioxidant (Rice-Evans *et al.*, 1997).

This review resumes the chemical and physical properties, biosynthesis, storage localization, and biological functions of plant flavonoids, and relationships among these five features with a deeper focus on flavonols. We finally focus on the response and protection conferred by flavonols under climate stress in Mediterranean plants species. All these sections are described by reviewing a number of interdisciplinary studies (biochemistry, ecology and ecophysiology studies) that have used genomic, transcriptomic, metabolomic and imaging approaches.

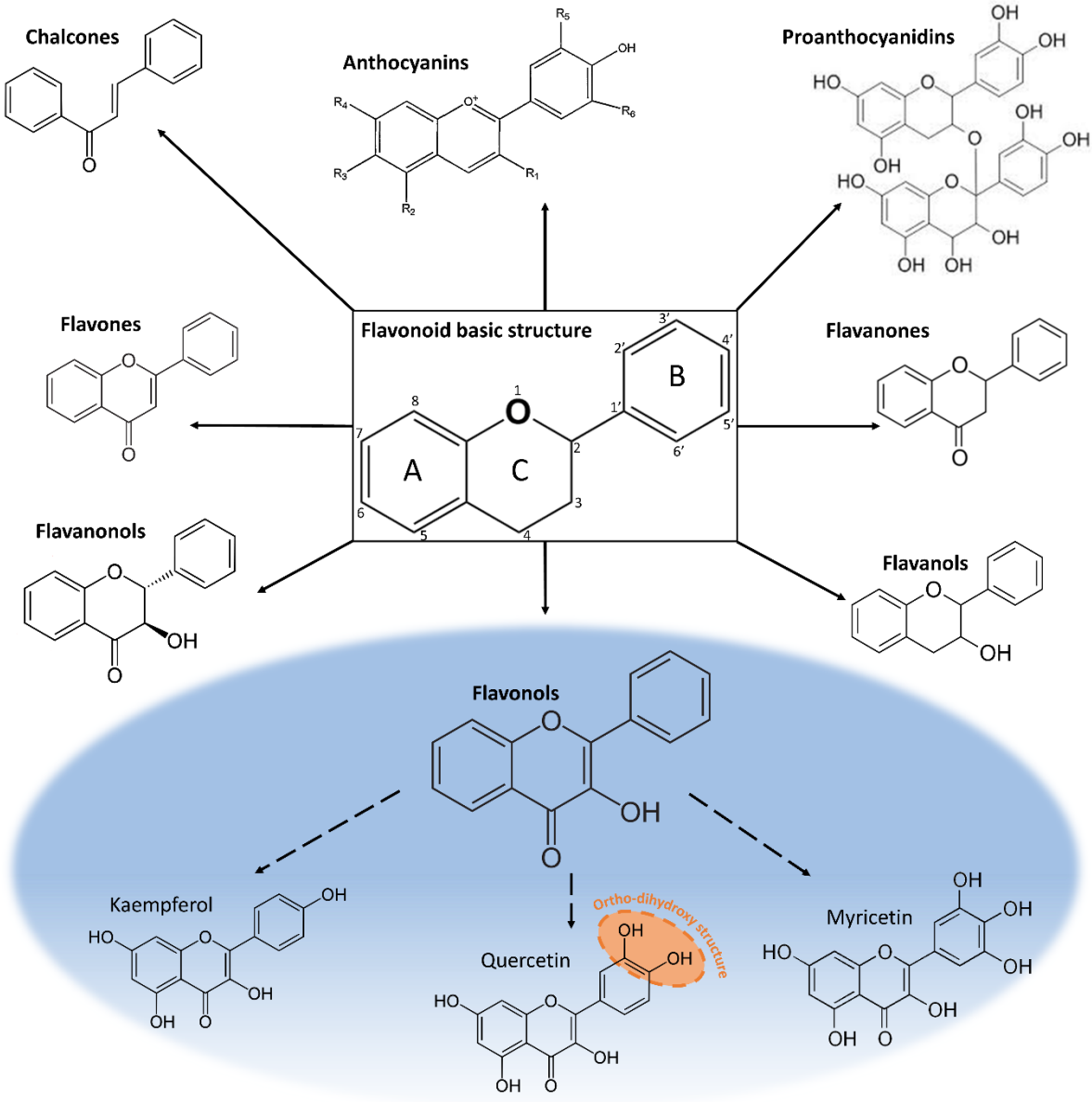

Figure 19: Structure and classification of flavonoids. The main subclasses of major flavonols are circled in blue. The difference between flavonoid groups depends on the chemical structure, the degree of oxidation, and the unsaturation of the linking chain (C3). Flavonols differ from each other in the number and position of the hydroxyl groups (-OH). The *ortho*-dihydroxy structure of quercetin circled in orange.

2. Chemical and physical properties of flavonols: relationship with their function

Flavonols, and flavonoids as a whole, have historically been studied for their functions in UV-B protection in plants because they display strong absorption in the UV spectral region and exhibit fluorescence with excitation maxima about 350–370 nm (Caldwell *et al.*, 1983; Smith & Markham, 1998). Their biological activity in plants remains to be elucidated and some of them are still under debate (Pollastri & Tattini, 2011). Overall, it has been proved that their functions depend on their chemical and physical properties (Wang *et al.*, 2018a).

Flavonols, closely related in structure to flavones, are characterized by the presence of a hydroxyl group (-OH) at the C3 position and a carbonyl function (C=O) at the C4 position, both on the C ring (Narayana *et al.*, 2001) (**Figure 19**). In the structure of flavonoids, the C ring may be a heterocyclic pyran—which yields flavanols (e.g., catechin) and anthocyanidins, or pyrone—which yields flavonols (e.g., kaempferol, quercetin, myricetin), flavones (e.g., luteolin, apigenin), and flavanones (e.g., naringenin, eriodyctiol) (Aherne & O'Brien, 2002) (**Figure 19**). Flavonol diversity is due to the aglycone structure and its oxidation or reduction state, the position of the hydroxyl group and the degree of hydroxylation (Heim *et al.*, 2002).

Chemical structure and physical properties of flavonols are intimately linked to their biological functions. Several studies have shown that their antioxidant activity increases with the number of hydroxyl groups and depends on the -OH position within the molecule (Rice-evans *et al.*, 1995; Rice-Evans *et al.*, 1996) (**Table 4**). Differences in the chemical structure and the relationship to their antioxidant activities are summarized in **Table 4**. The substitution patterns in kaempferol, quercetin and myricetin are 3,5,7,4'-OH, 3,5,7,3',4'-OH and 3,5,7,3',4',5'-OH, respectively (**Figure 19**). The presence of a third -OH group in the B ring in myricetin does not enhance the effectiveness against aqueous phase radicals compared to quercetin (Rice-Evans *et al.*, 1996) (**Table 4**), highlighting the importance of the *ortho*-dihydroxy structure in the B ring of quercetin which allows electron delocalization and thus increases their antioxidant activity (Soufi *et al.*, 2014) (**Figure 19**).

Table 4: Comparative physico-chemical properties of some of the main flavonols, flavones and flavanones. The higher the number of hydroxyl groups, the higher the antioxidant activity. An exception is made for quercetin for which the higher antioxidant activity is due to the *ortho*-dihydroxy structure in the B ring (see **Figure 19**).

Flavonoid class	Compound subclass	Number of hydroxyl groups	TEAC [3] value (mM)		Maximum absorption wavelength (nm) [4]
			[1]	[2]	
Flavonols	Kaempferol	4	1.34 ± 0.08	1.98 ± 0.13	367
Flavonols	Quercetin	5	4.7 ± 0.1	4.30 ± 0.16	371
Flavonols	Myricetin	6	3.1 ± 0.30	2.45 ± 0.35	374
Flavones	Chrysin	2	1.43 ± 0.07	0.98 ± 0.04	313
Flavones	Apigenin	3	1.45 ± 0.08	1.04 ± 0.06	337
Flavanones	Naringenin	3	1.53 ± 0.05	0.59 ± 0.08	289
Flavanonols	Taxifolin	5	1.9 ± 0.03	2.43 ± 0.12	290

[1] Data extracted from Rice-Evans *et al.* (1996); [2] Data extracted from Melidou *et al.*, (2005); [3] TEAC (Trolox equivalent antioxidant activity) is defined as the concentration of Trolox solution with equivalent antioxidant potential to a 1 mM concentration of the compound under investigation.; [4] Maximum absorption wavelength extracted from Rice-Evans et al. (1996) and measured by spectroscopy.

Similar to other PSMs, flavonols often exist in glycosylated forms (also referred to as glycoside conjugates) which are formed by an aglycone core bound to glycosidic sugars through oxygen or more rarely carbon atoms (Le Roy *et al.*, 2016; Shah & Smith, 2020). The glycosidic sugar is generally glucose, but also frequently galactose and rhamnose. The most common flavonol glycosides containing glucose are astragalin (kaempferol 3-*O*-glucoside) and isoquercetin (quercetin 3-*O*-glucoside) which have as aglycone cores kaempferol and quercetin, respectively. Myricetin can be coupled with rhamnose giving myricitrin (myricetin 3-*O*-rhamnoside) (Markham & Porter, 1979; Iwashina, 2000). Glycosylation of flavonols is of high biological importance since it tends to decrease their antioxidant activity (Williamson *et al.*, 1999; Vogt & Jones, 2000; Gachon *et al.*, 2005). For example, Rice-Evans *et al.* (1996) have demonstrated that glycosylation of quercetin blocks the -OH at the C3 position in the C ring thus reducing its antioxidant capacity. Glycosylation also preserves the reactive -OH groups from auto-oxidation (Brunetti *et al.*, 2013). Glycoside forms of flavonols is an important structural modification which influences their physical properties by increasing their solubility, stability and bioavailability (Behr *et al.*, 2020). Glycosylation modifies their cellular and tissular repartition too (Le Roy *et al.*, 2016) (see section “68”). Overall, the functional diversity and biological activities of flavonols are due to the modification of the aglycone core. The attachment of functional groups such as sugars, hydroxyl and methyl groups gives flavonols their ability to have different biological roles and storage sites in the plant.

Most flavonols (as well as flavones) exhibit two major absorption bands: Band I (320–385 nm) own to the B ring absorption, and Band II (250–285 nm) which refers to the A ring absorption. Increase in the numbers of hydroxyl groups in flavonoids induces an adsorption shift towards the red band such as 367 nm in kaempferol, 371 nm in quercetin and 374 nm in myricetin (Cook & Samman, 1996) (**Table 4**). The structure of flavanones leads to different UV absorption wavelengths (e.g., lower maximum absorption wavelength) compared to flavones and flavonols as well as a lowered antioxidant activity (**Table 4**). These differences can lead to various and different biological functions. In fact, dihydroxy B ring-substituted flavonoids have a greater antioxidant capacity, while their monohydroxy B ring-substituted counterparts have greater ability to absorb UV wavelengths (Agati *et al.*, 2012).

3. Biosynthesis and storage of flavonols: relationship with their function

The precursor of flavonoids is the amino acid phenylalanine which is the intermediate in the biosynthetic transformations leading from shikimic acid to phenylpropanoids (Swain & Williams, 1970) (**Figure 20**). Phenylalanine, derived from the shikimate pathway, is synthetized in chloroplasts and then transported into cytosol by a phenylalanine plastidial cationic amino acid transporter (PhpCAT) identified in *petunia* flowers by Widhalm *et al.* (2015) (**Figure 20**) (Qian *et al.*, 2019). Flavonoids are synthesized through the phenylpropanoid pathway with a step transforming the phenylalanine into cinnamic acid and then into *p*-coumaric acid (**Figure 20**). These two compounds are synthesized via the phenylalanine ammonia-lyase (PAL) and cinnamate 4-hydroxylase (C4H), respectively. The first enzyme involved is the chalcone synthase (CHS) producing naringenin chalcone through p-coumaric acid and three malonyl-CoA. Then chalcone isomerase (CHI) leads to naringenin from which all flavonoids derive. Flavanonols (or dihydroflavonols) arise from flavanones by the intervention of flavanone 3-hydrolxylase (F3H) a key enzyme in the flavonoid pathway. F3H catalyzes the oxidation of naringenin into dihydrokaempferol (colorless dihydroflavonol) that subsequently can be hydroxylated on the 3’ or 5’ position of the B ring, by flavonoid 3’-hydroxylase (F3’H) or flavonoid 3’,5’-hydroxylase (F3’5’H), producing dihydroquercetin (taxifolin) and dihydromyricetin, respectively. In addition, naringenin may be directly hydroxylated by F3’H or F3’5’H to give, respectively, eriodictyol and pentahydroxy-flavanone, which are again hydroxylated by F3H into dihydroquercetin (taxifolin) and dihydromyricetin (Petrussa *et al.*, 2013) (**Figure 20**).

A set of enzymes involved in flavonol biosynthesis (CHS, CHI, F3H, FLS, and F3'H) has been detected (for a review see Ferrer *et al.* (2008)). Their biosynthesis is triggered in response to light and ROS stress occurring in photosystems. The three main flavonols—quercetin, kaempferol and myricetin—are formed from dihydroflavonols by the action of flavonol synthase (FLS). FLS is the most important enzyme in the biosynthesis of flavonols and it is in competition with dihydroflavonol 4-reductase (DFR) involved in the synthesis of leucoanthocyanidins (Davies *et al.*, 2003) (**Figure 20**). The basic structure of flavonols (see **Figure 19**) is obtained by oxidation of dihydroflavonols by FLS (Owens *et al.*, 2008).

Flavonoid biosynthesis is first regulated at genetic and transcriptional levels (Quattrocchio *et al.*, 2006). Such regulations have been described in various model plant species thanks to the availability of many mutants affecting the expression of several flavonoid biosynthetic genes (Abrahams *et al.*, 2002; Pang *et al.*, 2009). MYB (myeloblastosis) and basic helix–loop–helix (bHLH) transcription factors, together with WD40 proteins are the main transcriptional regulators of the flavonoid biosynthetic pathway genes (Hichri *et al.*, 2011; Xu *et al.*, 2015). Flavonol biosynthesis is more specifically regulated by different MYBs transcription factors as identified in *Arabidopsis thaliana*, *Prunus persica* and grapevine (Stracke *et al.*, 2007; Czemmel *et al.*, 2009; Ravaglia *et al.*, 2013; Tirumalai *et al.*, 2019). In *Arabidopsis*, AtMYB11, AtMYB12, and AtMYB111 from the R2R3- MYB gene family activate on their own the CHS, CHI, F3H, and FLS promoters (Stracke *et al.*, 2007). Interestingly, the authors identified additional genes including UDP-glycosyltransferases (UGTs) and demonstrated that the accumulation of flavonol glycosides correlates with the expression domains of the different MYB factors.

Biosynthesis of flavonoids mainly occurs in the cytoplasm, more precisely in the cytosolic face of the endoplasmic reticulum as shown in many different species (Wagner & Hrazdina, 1984; Winkel-Shirley, 1999; Winkel, 2004) (**Figure 20**). Furthermore, some of the enzymes involved in flavonol biosynthesis have been shown to co-localize in the nucleus, consistent with the idea that some flavonols are directly or indirectly involved in the protection of DNA against ROS oxidative damages in particular by suppressing the Fenton reaction (i.e. sequestration of metal ions Fe(II); **Figure 20**) (Imlay *et al.*, 1988; Saslowsky *et al.*, 2005; Melidou *et al.*, 2005). Flavonols have also been detected in chloroplasts, and a study from Zaprometov & Nikolaeva (2003) concluded that chloroplasts are capable of flavonoid biosynthesis but this hypothesis needs to be confirmed by other experimental support (Zaprometov & Nikolaeva, 2003; Hernández *et al.*, 2009). The presence of antioxidant flavonols in chloroplasts could be explained because chloroplasts are a major source of ROS. Overall, the presence of flavonols in various cell compartments can be mainly explained by their antioxidant activities (for a review see Hernández *et al.* (2009)), but their subcellular transport needs to be better elucidated.

Once synthesized, the end-products of the flavonoid pathway such as flavonols are transported towards various cellular organelles (i.e. vacuole, chloroplasts and nucleus; **Figure 20**). Intracellular transport in leaf tissues occurs primarily to the vacuoles of different cells (stomata guard cells, epidermal and subepidermal cells). Their transportation from the biosynthesis site to the storage site is driven by different transporters such as multidrug and toxic compound extrusion (MATE) (Debeaujon *et al.*, 2001). In vacuoles, flavonols are mainly stored in glycosylated forms—since glycosylation increases their solubility in the aqueous cellular compartment (Lepiniec *et al.*, 2006)—where they have been suggested to reduce the H_2O_2 concentration (Yamasaki *et al.*, 1997). Although vacuoles from epidermal cells are their main flavonol reservoirs, flavonols are also transported and stored in the cell walls of the epidermal cells as methylated flavonol glucosides (Ibrahim *et al.*, 1987) and within the leaf cuticle (Heredia-Guerrero *et al.*, 2016). Flavonoids (including flavonols) are also synthesized and then accumulated in glandular trichomes of leaves, with higher concentrations in leaves exposed to high levels of light (as shown in the Mediterranean species *Phillyrea latifolia*; Agati *et al.*, (2020)). All these studies illustrate that flavonoids are mainly stored in the outer leaf tissues (epidermis, cuticle and outer storage structures) which optimizes their role as UV-screeners or ROS scavengers. In addition, quercetin-glycosides have been detected in the mesophyll of leaves subjected to drought stress which is consistent with their potential function as H_2O_2 scavengers (Fini *et al.*, 2012). Likewise, flavonoids reach the highest concentrations in leaves compared to other plant organs (Herrmann, 1988), which is related to their protective role under excess light (see Section **4**.). Imaging techniques, such as confocal microscopy, are used to precisely locate flavonoids within leaf tissue (Hutzler *et al.*, 1998).

The transport mechanisms of flavonoids from the biosynthetic site to the storage site (within cellular organelles and tissues) but also between plant organs, remain poorly understood. The transport of flavonoids to the chloroplast is not known. Some hypotheses have been proposed for flavonoid transport including membrane vesicle-mediated transport and membrane transporter-mediated transport (Zhao & Dixon, 2010; Zhao, 2015). Several transporters are known to be involved in flavonoid transport such as MATE (multidrug and toxic compound extrusion) transporters cited above (for transport of flavonoids between the cytosol to the vacuole) (Debeaujon *et al.*, 2001; Marinova *et al.*, 2007) and the ATP binding cassette (ABC) (**Figure 20**) (Rea, 2007). The later participate in long-distance unidirectional transport of flavonoids (e.g. naringenin, dihydrokaempferol and dihydroquercetin) between roots and shoots (Buer *et al.*, 2007). The transport of flavonoids between different plant organs seems crucial to respond to the various stresses undergone by the plant.

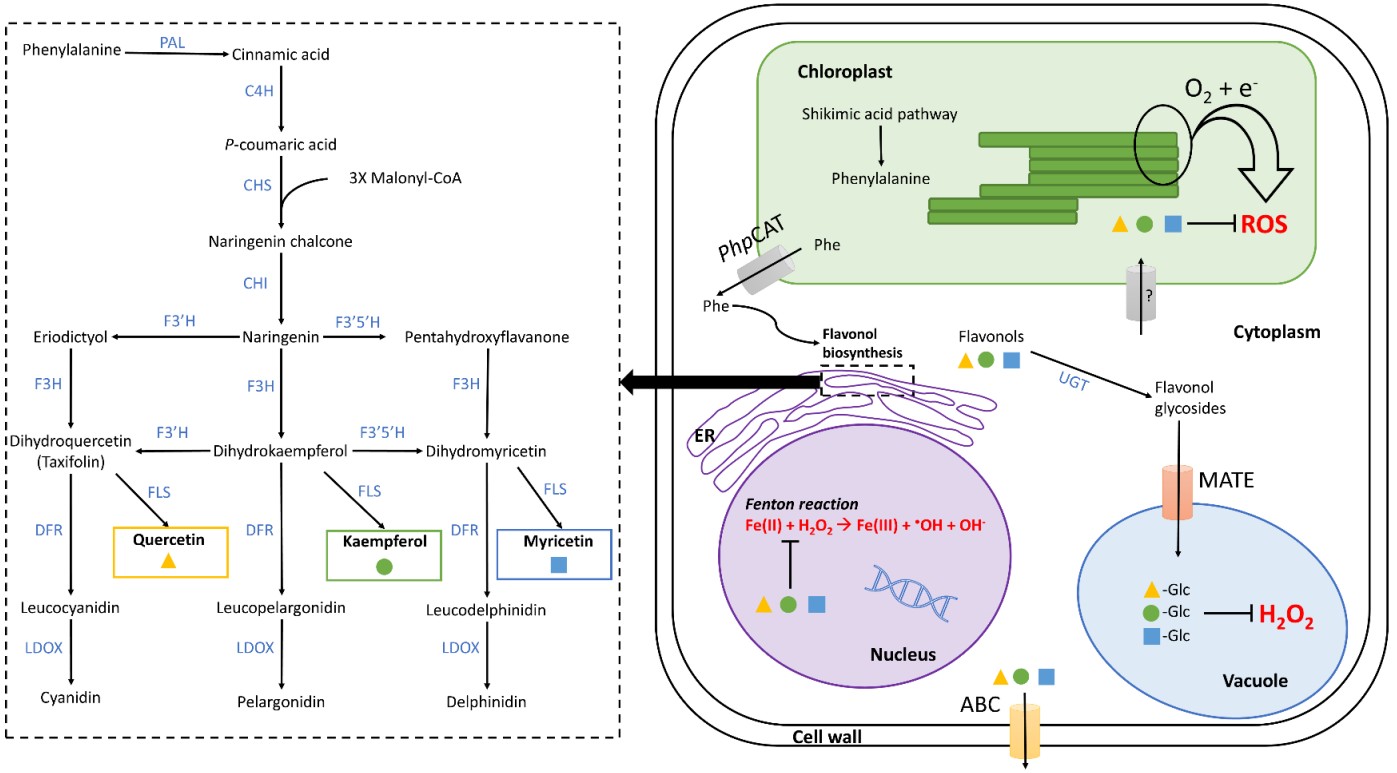

Figure 20: Biosynthesis and subcellular localization of flavonols in leave tissues. Flavonols are synthesized in the cytoplasm, on the cytosolic face of the endoplasmic reticulum (ER) (right picture). The different enzymes involved in their biosynthesis (left box) are shown in blue and flavonols are indicated and framed by different colors. The pathway shown represents the general pathway found in model plants such as Arabidopsis thaliana. The first step begins with the synthesis of phenylalanine in the chloroplasts which is then transported to the cytosol via the phenylalanine plasticial cationic amino acid transporter (PhpCAT), identified in petunia. Abbreviations are as follows: C4H, cinnamate 4-hydroxylase; CHI, chalcone isomerase; CHS, naringenin-chalcone synthase; DFR, bifunctional dihydroflavonol 4 reductase/flavanone 4-reductase; F3H, flavanone 3-hydroxylase; F3′H, flavonoid 3′-hydroxylase; F3′5′H, flavonoid 3′5′-hydroxylase; FLS, flavonol synthase; LDOX, leucoanthocyanidin dioxygenase; PAL, phenylalanine ammonia-lyase; Phe, phenylalanine; UGT, UDP-dependent glucosyl transferase. Once synthetized, flavonols can be subjected to various modifications (glycosylation, methylation, etc.) and be stocked into vacuoles. They are transported into different compartments and through cells by MATE (multidrug and toxic compound extrusion) and ABC (ATP binding cassette) transporters families. In nucleus, vacuole, and chloroplast, flavonols will inhibit ROS accumulation.

4. Flavonols in plants: an important polyphenol to cope with rapid climate change

In the context of climate change, the increasing CO_2 concentration in the atmosphere implies global warming (Shukla *et al.*, 2019) and depletion of the stratospheric ozone layer, resulting in UV-B radiation increases (Caldwell & Flint, 1994). At the regional scale, the Mediterranean is a critical hot spot in the context of climate change due to the expected increase in surface temperatures, drought episodes and solar radiation exposure (Giorgi & Lionello, 2008; Lionello *et al.*, 2014; Lionello & Scarascia, 2018). By the end of the twenty-first century, precipitation will decrease at a rate of around -20 mm/K (or -4%/K) in this region and temperature will warm 20% more than the global average, especially in summer (i.e. 50% larger than global warming) (Lionello & Scarascia, 2018). A warmer climate in the Mediterranean area will also cause variations in the hydrological cycle consisting of a rise in both sea level and soil salinity (Daliakopoulos *et al.*, 2016). Arid regions are the most prone to salinization due to the precipitation scarcity leading to low drainage of salts in soil (Corwin, 2021). Ultraviolet (UV) radiation, drought, warming and salinity expected in the Mediterranean region threaten plant development as they negatively impact physiological and biochemical processes, resulting in reductions in plant growth and reproduction success (fitness) (Sharma *et al.*, 2019). To counterbalance such climatic stresses, plants develop physical and chemical defenses (Davis, 2001), the latter being partly represented by PSMs, including polyphenols (Sardans & Peñuelas, 2013; Di Ferdinando *et al.*, 2014).

To a certain extent, Mediterranean plants are able to tolerate warming, increased drought and UV radiation excess (Matesanz & Valladares, 2014). Morphological and physiological plasticity have been observed in Mediterranean trees, shrubs and herb species (for a review see Matesanz & Valladares (2014)). Plasticity differs not only among species and populations but also among traits and environmental factors. Species with high phenotypic plasticity, and in particular those able to evolve rapidly, have an evolutionary advantage, especially under rapid climate change. Among the plasticity traits, plant metabolic plasticity is crucial for resistance and adaptation to various abiotic stresses and has thus been used as an indicator of plant survival in a changing environment. Mediterranean species display very contrasting flavonoid composition and concentration (Di Ferdinando *et al.*, 2014), thus suggesting a species-specific response to climate stressors. A study of Sosa *et al.* (2005) highlighted the diversification in composition and content of flavonoids in a same species (*Cistus ladanifer*) from different populations and locations (different climatic conditions). This result suggests that flavonoids could have various ecological functions strongly linked to environmental conditions. All these studies illustrate the fact that the metabolic plasticity can be an

important asset for Mediterranean plants to cope with changing climate. In recent decades, various studies have demonstrated the effect of climate-related stresses on flavonoid metabolism. Some of them reveal an enhancement of flavonol production under drought, heat, UV radiation and salinity, as well as their protective role under these stress conditions as described hereafter (**Table 5**). These studies strongly suggest an important role of flavonols to cope with unfavorable Mediterranean environmental conditions, especially with climate change.

Table 5: Increasing of flavonol concentration under different abiotic stresses reported in literature for different species and experimental conditions. All studies are performed on harvested leaves or roots.

Abiotic stress	Flavonol type	Species	Plant organ	Tissue localization	Growth conditions	Measurement technique	Conclusion/Function	References
Drought	Kaempferol, quercetin	*Arabidopsis thaliana*	Not specified (all plant)	Not studied	Growth chamber	LC-PDA-MS	Scavenging radical activity (Quercetin 3-*O*-glucoside and kaempferol 3-*O*-glucoside). Quercetins had a higher antioxidant activity than kaempferols.	(Nakabayashi *et al.*, 2014b)
Drought	Myricetin, kaempferol	*Populus* spp.	Leaves and root	Not studied	Growth chamber	HPLC-PDA	Antioxidant capacity.	(Popović *et al.*, 2016)
Drought	Kaempferol, quercetin	*Trifolium repens* L.	Leaves	Not studied	Field conditions	HPLC	Under drought stress, kaempferol glycosides accumulation was related to reduced senescence and to less pronounced decreases in shoot dry weight.	(Nichols *et al.*, 2015)
Drought and UV radiation	Quercetin	*Fraxinus ornus*	Leaves	Mesophyll (in the vacuoles of cells)	Grown outsdoor in an experimental plot	Confocal microscope for flavonol localization. HPLC–MS for quantification.	Increase of quercetin 3-*O*-glucoside in severe drought and excess light stresses. Potential function as H_2O_2 scavenger.	(Fini *et al.*, 2012)
UV radiation	Kaempferol	*Picea abies*	Needles	Not studied	Field cabinet experiments	RP-HPLC	Potentially UV-B screening.	(Fischbach *et al.*, 1999)
UV radiation	Kaempferol, quercetin	*Arabidopsis thaliana*	Leaves	Not studied	Growth chamber	UPLC-TQD	Antioxidant activity.	(Csepregi *et al.*, 2017)
UV radiation	Kaempferol, quercetin	*Arabidopsis thaliana*	Leaves	Not studied	Growth chamber	UPLC-MS	Accumulation of specific flavonol glycosides, i.e., kaempferol and quercetin di- and triglycosides (rhamnosylated) in response to UV-radiation.	(Hectors *et al.*, 2014)
UV radiation	Myricetin and quercetin	*Cistus incanus* L.	Leaves	Not studied	Field conditions	HPLC–DAD	Major light-induced increases observed for myricetin and quercetin derivatives.	(Sebastiani *et al.*, 2019)
Low temperature	Quercetin, kaempferol and rhamnetin	*Quercus ilex* L.	Leaves	Not studied	Field conditions (forest)	HPLC–MS/MS	High amount of flavonol-hexosides detected in winter. They could contribute to photoprotection.	(Brossa *et al.*, 2009)
Heat and drought	Kaempferol, quercetin	*Citrus* spp. (Cleopatra and Carrizo)	Leaves	Not studied	Greenhouses	UPLC/ESI-QTOF-MS	Combination of heat and drought favours accumulation of kaempferol and quercetin derivatives in poorly-drought tolerant species.	(Zandalinas *et al.*, 2017)

Table 5. *Continue*

Abiotic stress	Flavonol type	Species	Plant organ	Tissue localization	Growth conditions	Measurement technique	Conclusion/Function	References
Heat and salinity	Kaempferol, quercetin	*Solanum lycopersicon* L.	Leaves	Not studied	*In vitro* (using aerated hydroponic systems containing a modified Hoagland solution)	UHPLC/QTOF-MS	Accumulation of kaempferol and quercetin derivatives leads to lower oxidative damage when plant grow under concomitant heat and salt stress.	(Martinez *et al.*, 2016)
Salinity and UV-radiation	Quercetin	*Ligustrum vulgare*	Leaves	Epidermal, boundary of epidermal and adaxial palisade, and in the palisade parenchyma cell layers	Greenhouses	Epifluorescence microscope and Confocal Laser Scanning Microscope (CLSM) for flavonoids localization. HPLC for quantification.	Increase of quercetin 3-O-glycoside in response to UV-radiation and salinity stress (NaCl). Potential role as antioxidant and photoprotection.	(Agati *et al.*, 2011)
Salinity	Kaempferol, quercetin	*Casuarina glauca*	Nodules, roots and branchets	Not studied	*In vitro* (using Broughton and Dillworth's medium)	LC-HRMS	Kaempferol and quercetin derivatives accumulate in case of severe salt stress and play a key role in protection against oxidative damage.	(Jorge *et al.*, 2019)
Salinity	Kaempferol, quercetin	*Apocynum venetum L.*	Leaves	Not studied	Plant culture room	HPLC	Kaempferol and quercetin accumulation under salt stress.	(Xu *et al.*, 2020b)

Abbreviations: HPLC: High-performance liquid chromatography; HPLC–DAD: High-performance liquid chromatography-diode array detection; HPLC–MS: High performance liquid chromatography-mass spectrometry; HPLC-PDA: High-performance liquid chromatography–photodiode array detection; LC-HRM: Liquid chromatography-high resolution metabolomics; LC-PDA-MS: Liquid chromatography-photodiode-array-mass spectrometry; RP-HPLC: Reverse phase-high performance liquid chromatography; UHPLC/QTOF-MS: Ultra-high performance liquid chromatography-quadrupole time-of-flight mass spectrometry. UPLC/ESI QTOF-MS: Ultra performance liquid chromatography/Electrospray-ionizationquadrupole time-of-flight mass spectrometry; UPLC-MS: Ultra Performance Liquid Chromatography-mass spectrometry; UPLC-TQD: Ultra Performance Liquid Chromatographytandem Quadrupol.

4.1. Drought

Flavonol concentrations increase under drought stress as found in several species (Sánchez-Rodríguez *et al.*, 2011; Nakabayashi *et al.*, 2014a; Griesser *et al.*, 2015; Hodaei *et al.*, 2018). A recent study on the model species *Arabidopsis thaliana* has also confirmed by transcriptomic evidence the enhancement of flavonol metabolism under drought conditions (Nakabayashi *et al.*, 2014b). In fact, drought regulates key genes coding for the enzymatic activity involved in flavonol biosynthesis such as chalcone isomerase (CHI), flavonoid 3'-hydroxylase (F3'H), flavanone 3-hydroxylase (F3H) and flavonol synthase (FLS) which results in increased flavonol concentrations (Liu *et al.*, 2013; Gharibi *et al.*, 2019) (**Figure 20**). Moreover, it has been shown that some transcription factors such as MYB and bHLH families play a role in the accumulation of flavonoids resulting in enhanced drought tolerance (Baldoni *et al.*, 2015; Wang *et al.*, 2016). It is also now known that there exists a relationship between aglycone/glycone flavonols and the oxidative stress, the glycosylated forms of flavonols being less effective antioxidants (Vogt & Jones, 2000; Gachon *et al.*, 2005). Despite their contrasting antioxidant protection, an accumulation of quercetin 3-*O*-glucosides and a decrease in the antioxidant enzyme activity have been observed under water stress in leaves of the Mediterranean species *Fraxinus ornus*, suggesting that these glycoside forms of flavonols could act as H_2O_2 scavengers during water stress (Fini *et al.*, 2012). The precise role of flavonoid glycosylation under drought remains complex to evaluate because of the signaling crosstalk between flavonoid production and stress response. Other recent studies also highlight the sensitivity of flavonol concentration in response to drought in different Mediterranean tree species such as *Pinus pinaster* Ait. and *Quercus ilex* L. (Rivas-Ubach *et al.*, 2014; de Miguel *et al.*, 2016; de Simón *et al.*, 2017). All these studies support the idea that increasing foliar concentration of flavonoids is a key defense strategy under water depletion. They also reveal the strong capacity of Mediterranean species to reinforce the flavonoid metabolism to cope with drought.

4.2. Warming

Warming, expected to be paralleled by aggravated drought in the Mediterranean region, is an important stress factor affecting plant growth and survival (Mittler, 2006). In plants, many biochemical reactions are sensitive to temperature, the stress from which varies according to the pic of temperature reached and duration (Ahuja *et al.*, 2010). As a consequence of heat, leaf water status and stomatal conductance are affected, resulting in a higher ROS production (Hasanuzzaman *et al.*, 2013). Temperature has a high influence on flavonoid metabolism, especially on anthocyanin accumulation which is reduced in response to high temperatures, as shown in grapevine and apple fruit (Lin-Wang *et al.*,

2011; Movahed *et al.*, 2016; Pastore *et al.*, 2017). In shrub and a conifer species, recent studies have reported an effect of enhanced temperature which leads to a reduction in flavonoids in stems (Zhang *et al.*, 2018) and leaves (Nissinen *et al.*, 2016, 2017), this being related to an increase in plant growth. In those studies, results support the theory that under non-limiting resources, plants exposed to a moderate elevated temperature will use carbon for growth rather than for synthesis of defense compounds (Kellomäki & Wang, 2001).

Concerning Mediterranean species, they have developed a wide range of adaptative traits to survive to summer climate conditions, including both elevated temperatures and drought (Lo Gullo & Salleo, 1988). For example, several studies have been conducted on the typically Mediterranean species, *Cistus ladanifer* L., whose leaves and stems secrete an exudate rich in secondary metabolites, in particular flavonoids (Vogt *et al.*, 1987; Chaves *et al.*, 1993). Seasonality, closely related to temperatures, influences strongly flavonols content in *C. ladanifer* L. (Chaves *et al.*, 1993, 1997). The maximum secretion of flavonoids in the exudate of this species is produced during summer when plants suffer the most from high temperatures, and also UV irradiation and water stress (Chaves *et al.*, 1997). Few recent studies reported the effect of warming on the concentration of phenolics, especially when combined with others stress such as drought (Zandalinas *et al.*, 2017; Moreira *et al.*, 2020). The study of Zandalinas *et al.*, (2017) on *Citrus* plants highlighted that the combination of water stress and heat stress lead to higher levels of flavonols (i.e., kaempferol derivates) than in heat stress only. These findings are particularly interesting as the combination of drought and heat is the most recurrent condition in Mediterranean regions. It has also been reported in a typical Mediterranean tree species (*Quercus ilex* L.) that in winter (at the lowest temperatures), flavonol contents were the highest (Brossa *et al.*, 2009). The highest amount of flavonols in this season can be explained by their contribution to photoprotection as in winter low photosynthetic activity and low excess energy dissipation can increase the risk of photodamage. Despite all this evidence about the role flavonoids play in Mediterranean plant adaptation to environmental changes, future studies need to address their efficiency when these changes operate rapidly.

4.3. UV Radiation

High solar radiation is one of the most important changes plants will have to cope with under future climate change (Bornman *et al.*, 2019). UV radiation is generally divided into three classes based on the light wavelength: UV-C (<280 nm), UV-B (280–315 nm), and UV-A (315–400 nm) (Stapleton, 1992). Flavonols have largely been considered as an important role in UV protection by inhibiting ROS generation, and ROS quenching once they are formed (Agati *et al.*, 2011, 2012; Pollastri & Tattini, 2011). In addition, as many other flavonoids, they have the capacity to absorb solar wavelengths in the range between

280 and 320 nm (UV-B) (Pollastri & Tattini, 2011). However, in the recent past, the idea of flavonols as the most effective UV-B absorbers has been questioned (Gerhardt *et al.*, 2008; Agati & Tattini, 2010; Agati *et al.*, 2011). Due to their tissue distribution, often on leaf surface (e.g. cuticle, trichomes), they could act as UV-screening, but photoprotection is possibly not their most important function (Agati & Tattini, 2010; Agati *et al.*, 2013; Csepregi *et al.*, 2017). UV-induced increases in the ratio of dihydroxy to monohydroxy B-ring substituted flavonols glycosides (such as quercetin to kaempferol ratios) as reported in different plant species exposed to various proportions of UV radiation (Ryan *et al.*, 1998, 2002; Gerhardt *et al.*, 2008; Kotilainen *et al.*, 2008). Indeed, kaempferol and quercetin are both able to absorb light in the UV-A and UV-B regions, but they present variations in their ROS scavenging properties. The dihydroxylated B-ring of quercetin provides increased antioxidant activity relative to the monohydroxylated ring of kaempferol which explains the higher accumulation of quercetin than kaempferol under oxidative stresses (Rice-Evans *et al.*, 1996; Osmond *et al.*, 2000). In addition, a screening advantage for quercetin glycosides over kaempferol glycosides could be due to the higher capacity of quercetin glycosides to dissipate UV-B excitation energy through tautomerization (Smith & Markham, 1998).

A recent study from Hectors *et al.* (2014) highlighted the role of the rhamnosylated kaempferol and quercetin glycosides during UV acclimation in *Arabidopsis thaliana.* The concentration of these compounds increased because of UV-stress and the resulting oxidative stress. However, the biological role of these flavonol derivatives remains unclear as they feature less effective antioxidant activity than their aglycone forms (Vogt & Jones, 2000; Gachon *et al.*, 2005). It has thus been suggested that accumulation of flavonol glycosides constitutes a reserve of flavonols which can be used during long-term UV acclimation and does not represent the first line response upon exposure to UV radiation (Pollastri & Tattini, 2011). Studies on Mediterranean plants species usually report a concentration of dihydroxy B-ring-substituted flavonols (quercetin) greater than that of monohydroxy-flavonols (kaempferol) under excess light and drought stress (Tattini *et al.*, 2000, 2004; Fini *et al.*, 2012). The higher concentration of quercetin in Mediterranean plants compared to kaempferol is probably related to their high adaptation to light exposure as quercetin is an excellent antioxidant (Rice-Evans *et al.*, 1997). Comparatively, the reverse is observed in shaded plants with a decrease in the quercetin: kaempferol ratio (Gerhardt *et al.*, 2008; Hectors *et al.*, 2012).

4.4. Salinity

Soil salinity may occur for two reasons: natural accumulation of salt in the soil over long periods or human-induced accumulation due to activities that change the hydrologic soil balance (Parihar *et al.*, 2015). In Mediterranean regions, increasing crop irrigation is crucial to cope with the drier climate but it often causes soil salinization because water

used for irrigation is groundwater whose high salinization is due to seawater intrusion (Libutti *et al.*, 2018). In addition, the natural accumulation of salt in the soil can be due to poor precipitation, which can be observed in Mediterranean regions, resulting in lower drainage of soil water. In plants, the excess of salt in soils reduces their ability to uptake water and competes with the mineral nutrient metabolism reducing plant growth (Grattan & Grieve, 1999; Fageria *et al.*, 2011). Under salt stress, a reduction in photosynthesis is observed due to the reduction in water potential (Romero-Aranda *et al.*, 2001; Wang *et al.*, 2018b). In fact, salt stress can lead to stomatal closure reducing CO_2 uptake by leaves thereby exposing chloroplast to an excess of energy leading to the generation of ROS and leaf oxidative damage (Miller *et al.*, 2010). Salt stress and water deficit stress show a high degree of similarity in physiological, biochemical and molecular responses, probably due to the fact that salt stress brings osmotic effects (Sairam & Tyagi, 2004). As shown in many studies, salinity stress induces flavonol accumulation to mitigate oxidative stress (Ben Abdallah *et al.*, 2016; Mrázová *et al.*, 2017). These results are also supported by genomic evidence where key genes of the flavonol pathway were upregulated under salt stress (e.g. FLS, F3'H and F3H) (Li *et al.*, 2013; Xu *et al.*, 2020b).

Salt stress' effect on flavonoid contents in Mediterranean species remains poorly documented. Tattini *et al.*, (2009) have described the response of salinity on three different evergreen Mediterranean species (*Olea europaea* L., *Phillyrea latifolia* L. and *Pistacia lentiscus* L.) which are widely distributed in dry coastal areas of the Mediterranean basin, where soil salinity concentrations accumulate especially during the warm summer season. In the two least salt stress-tolerant species (i.e. *O. europaea* and *P. latifolia*), phenylpropanoid metabolism was upregulated compared to the species that better utilizes Na^+ and Cl^- for osmotic adjustment (*P. lentiscus*). The most salinity-sensitive species reduced their growth more than the most resistant species to better devote their energy to antioxidant defenses (i.e. flavonoid biosynthesis).

5. Flavonols as antioxidants: a unifying mode of action against climate stresses

All factors previously described (light, high temperatures, water deficit and salinity), trigger ROS production under stress conditions overwhelming the scavenging mechanisms of the antioxidant system in plants and eventually leading to several cellular damages including alteration of DNA which can cause cell death (Mittler, 2006). Major sites of ROS production in plants are located in the chloroplast, mitochondria and peroxisomes (Das & Roychoudhury, 2014).

Flavonol biosynthesis is almost exclusively enhanced due to triggered ROS formation associated with oxidative stress (Agati *et al.*, 2012; Kumar & Pandey, 2013). The major source of ROS production occurs during the photosynthetic electron transport system. In case of drought stress, partial or total stomatal closure allows plants to reduce evapotranspiration but also limits the entrance of CO_2 and thus net photosynthesis leading to an excess of unused light energy and perturbation in the chloroplastic electron chain since chloroplasts continue to absorb light energy. As a result, leaf cells produce a significant rise of ROS (Cruz De Carvalho, 2008). An imbalance is created within the photosynthetic reactions because the energy supply (NADPH, ATP) exceeds the demand and electron acceptors become depleted. These electrons are transferred to oxygen, resulting in the production of ROS (Krieger-Liszkay *et al.*, 2008) which include superoxide (O_2^-), hydrogen peroxide (H_2O_2), hydroxyl radical ($^\bullet OH$), singlet oxygen ($^1O_2$) and perhydroxyl radical ($HO_2^\bullet$) (Yamasaki *et al.*, 1997).

The main explanation for flavonols acting as antioxidant relies on the high reactivity of their hydroxyl substituents as shown in the following reaction (Heim *et al.*, 2002):

$$F\text{-}OH + R^\bullet \rightarrow F\text{-}O^\bullet + RH$$

Specifically, the B-ring hydroxyl structure is the main driver of flavonoid potential to scavenge ROS (Heim *et al.*, 2002). Flavonols are greatly antioxidant because of their ability to donate electrons or hydrogen atoms. They act as antioxidants by several mechanisms. The first on is direct scavenging of ROS, as described in the reaction above. They also inhibit ROS formation through the chelation of metals. For example, quercetin present a strong capacity to chelate ions of metals such as Fe and Cu-ions thus preventing free radical formation including the damaging ROS (Brown *et al.*, 1998; Leopoldini *et al.*, 2006). Due to their specific structure, in particular the hydroxyl groups, flavonols can form metal flavonol complexes (Symonowicz & Kolanek, 2012). They also can inhibit the enzymes that participate in the generation of free radicals (e.g. glutathione S-transferase and NADH oxidase), or potentially activate some antioxidant enzymes possessing radical scavenging capacity (Agrawal, 2011; Kumar & Pandey, 2013; Dias *et al.*, 2021).

To determine the potential role of flavonols in planta, in vitro assays were first performed, showing that flavonols can directly scavenge ROS (Rice-Evans *et al.*, 1997). However, data supporting their role as ROS scavengers in living plants remain poorly documented (for a review of effective role of flavonoids as antioxidant in plants see (Agati *et al.* (2020)). More recently studies performed under controlled conditions in laboratory on the model plant *Arabidopsis thaliana* and some crop species have correlated the increase in flavonols and the decrease in ROS, suggesting an antioxidant role of flavonols under stress conditions (Popović *et al.*, 2016; Csepregi *et al.*, 2017).

6. Flavonols as indirect growth regulators

Phytohormones allow coordination of the biosynthesis of defense compounds such as flavonoids during abiotic stress response (Jogawat *et al.*, 2021) (**Figure 21**). The main phytohormones involved in abiotic stress responses are auxins, abscisic acid (ABA), salicylic acid (SA), jasmonic acid (JA) and ethylene (ET) (Ullah *et al.*, 2018). There is clear evidence showing that flavonoids, as modulators of the ROS-signaling cascade, modify in turn, the phytohormone signals such as auxins and ABA (Peer & Murphy, 2007; Brunetti *et al.*, 2018).

Auxins are well-known phytohormones involved in developmental processes like growth elongation, root formation and plant tropisms in response to gravity (gravitropism) or light (phototropism) (Zhao, 2010). An in vitro study of Jacobs & Rubery (1988) showed that flavonols (e.g. quercetin and kaempferol) compete with a synthetic auxin transporter inhibitor known as naphthylphthalamic acid (NPA) and can perturb auxin transport in a variety of plant tissues. Later, flavonoids' role as negative regulators of auxin transport was proven in vivo in *Arabidopsis thaliana* mutants (Brown *et al.*, 2001; Buer & Muday, 2004; Kuhn *et al.*, 2011). *In vivo* experiments on *Arabidopsis thaliana* shoots showed that a specific flavonol bis-glycoside (i.e. kaempferol 3-*O*-rhamnoside-7-*O*-rhamnoside) acted as an endogenous polar auxin transport inhibitor thus reducing plant stature (Yin *et al.*, 2014). The mechanism whereby flavonols regulate auxin transport has been explored in many studies and it includes several processes. For example, quercetin reduced the auxin transport capacity of ATP-binding cassette type B (ABCB) families (Peer & Murphy, 2007). Furthermore, flavonols can regulate PIN function, which are a protein family of auxin efflux transporters (Brunetti *et al.*, 2018; Teale *et al.*, 2021) (**Figure 21**). In addition, flavonols might affect auxin transport by changing the level of ROS which have been reported to modulate polar auxin transport (i.e., polar auxin transport is altered in plants with ROS accumulation) (Fernández-Marcos *et al.*, 2013). On the other hand, auxins control flavonol biosynthesis. Auxins control WRKY23 and MYB12 transcription factors thus increasing the accumulation of flavonols and proper root growth and development (Lewis *et al.*, 2011; Grunewald *et al.*, 2012). By regulating auxin flows, flavonols play a key role in responses to abiotic stresses because they influence auxin distribution and thus take part in the control of plant organ development in response to water deficit, salinity or other stress factors. For example, auxin's accumulation positively modulates root architecture especially the lateral root number (Shi *et al.*, 2014).

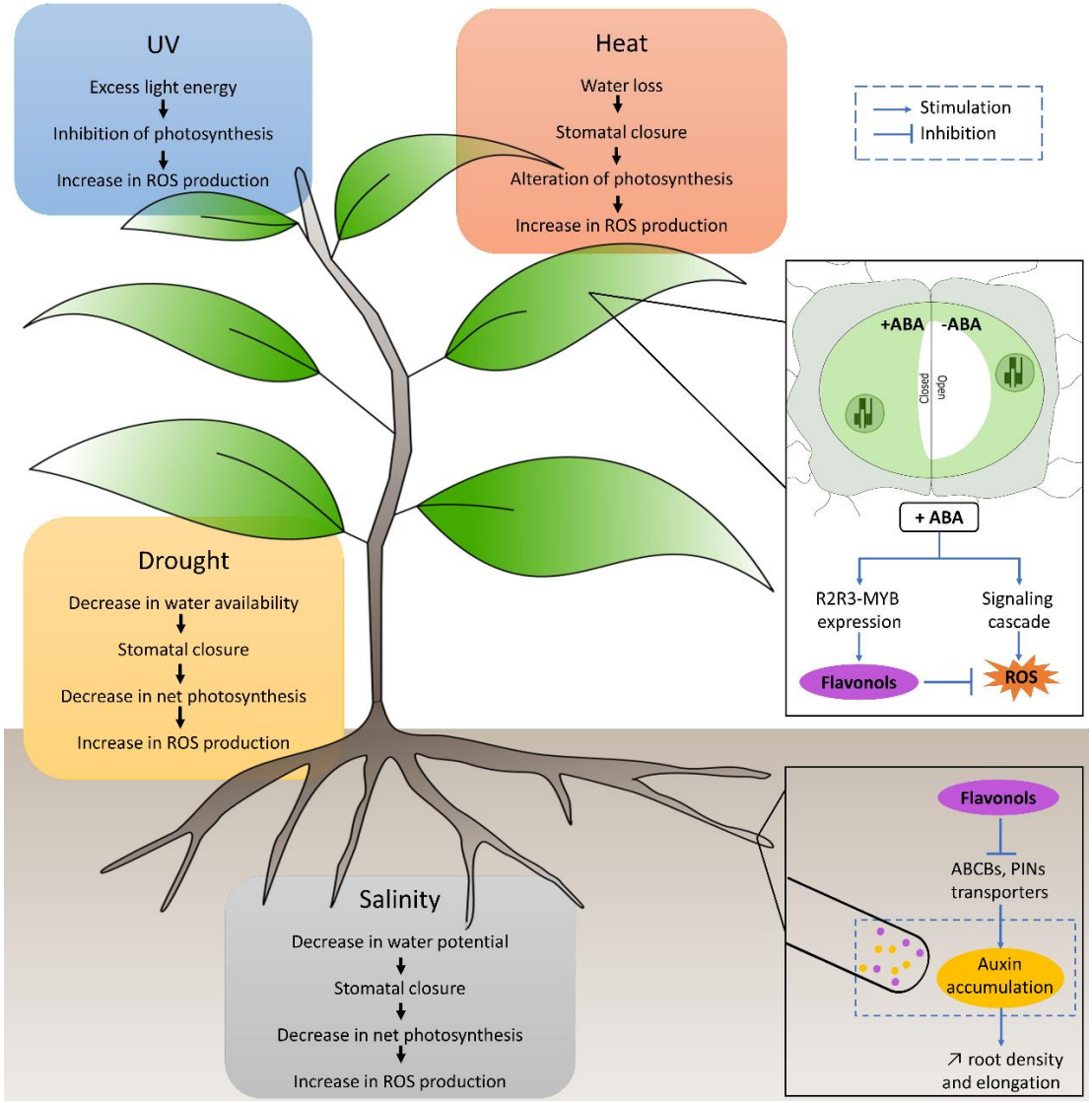

Figure 21: Plant responses to abiotic stress. The colored boxes summarize the four abiotic stresses referred to in this review and their main consequences for plant physiology. Flavonols' role as ROS scavengers and their interaction with the phytohormones ABA in leaves and auxin in roots is shown in black boxes. In leaves, the opening of stomata is allowed by the binding of ABA to membrane receptors resulting in an efflux of ions and therefore an efflux of water leading to stomata closure. ABA act on the R2R3-MYB gene by enhancing its expression thus stimulating flavonol biosynthesis. It also triggers a signaling cascade leading to ROS production. In roots, flavonols inhibit auxin transport leading to auxin accumulation and root elongation.

Various studies have found that flavonols played a role in UV acclimation by regulating auxin movement and catabolism thus leading to UV-induced morphogenic responses refs. (Jansen, 2002; Agati & Tattini, 2010; Hectors *et al.*, 2012; Brunetti *et al.*, 2013). Moreover, better tolerance to stress may also be due to the interaction of many other hormones such as abscisic acid (ABA) with auxins resulting in the maintenance of root growth (Xu *et al.*, 2013).

ABA is a phytohormone considered as a plant stress hormone because it plays an important role in integrating various stress signals and controlling downstream stress responses (Tuteja, 2007). In abiotic stress, ABA plays a crucial role by regulating various physiological processes such as stomatal closure, dormancy, germination, vegetative growth and modulation of root architecture, thus conferring adaptation to drought, salt and other osmotic stresses (Sah *et al.*, 2016). In plants, there is an ABA flavonol relationship in which ABA regulates flavonol biosynthesis and flavonols regulate the ABA-signaling network as well (Brunetti *et al.*, 2019a). At the genetic level, ABA signaling regulates the expression of the R2R3-MYB gene family which are highly responsive to light irradiance and redox-controlled (Heine *et al.*, 2004). MYB genes are also known to be the main transcriptional regulators of the flavonoid biosynthetic pathway genes (Hichri *et al.*, 2011) which highlights the link between the ABA signaling pathway and flavonoid biosynthesis. Although the regulation of flavonol biosynthesis by the ABA signaling pathway remains poorly documented, there is recent evidence showing that flavonols, especially quercetin derivates, may regulate the ABA signaling pathway (Watkins *et al.*, 2017). This later study is based on the fact that in guard cells, ABA induces a signaling cascade including the synthesis of ROS thus regulating stomatal closure (Mittler & Blumwald, 2015). However, in response to osmotic stress, ROS signaling must be rapid, but it also requires ROS scavenging by flavonols to limit cell damage. Indeed, it showed that quercetin accumulated in stomata guard cells was related to the decrease in ROS (i.e. H_2O_2) which are required to close stomata in response to ABA (Wang & Song, 2008). These signaling cascades involving complex interaction of ABA-induced ROS and flavonols is a crucial mechanism to understand the control of stomatal aperture, especially in stress conditions such as drought (**Figure 21**).

7. Conclusions

Although the precise role of polyphenols in plants remains complex to evaluate (because of the signaling crosstalk between their production and stress response) there is abundant evidence to support that flavonoids, especially flavonols, confer protection and indirectly regulate plant growth under abiotic stress. Enhancement of the flavonoid metabolism and eventually their production under climatic stress conditions can thereby be interpreted as an improvement of the chemical defense system in the plant. While flavonoid-related research studies have mostly used experimental designs integrating a single stress under controlled conditions, we suggest future research directions should consider field experiments where the response of the flavonoid metabolism is studied under a combination of abiotic stress, such as drought and warming in the Mediterranean ecosystems since such a scenario, rather than drought alone, will occur frequently in this region. Since these unprecedently rapid changes will probably affect Mediterranean terrestrial ecosystems dramatically, this type of study is necessary to anticipate the

degree of protection chemical defenses may confer to Mediterranean species. To face such conditions, plants rich in PSM such as flavonoids with antioxidant functions will likely present competitive advantages over species with little investment in these defenses.

CHAPTER IV: Impact of seasonal cycle and long-term amplified drought on central and specialized leaf metabolites in 2021

Long-term rain exclusion in a Mediterranean forest: response of physiological and physico-chemical traits of *Quercus pubescens* across seasons

Justine Laoué[1], Michel Havaux[2], Brigitte Ksas[2], Béatrice Tuccio[3], Caroline Lecareux[1], Catherine Fernandez[1], Elena Ormeño[1]

[1]Aix Marseille Univ., Univ Avignon, CNRS, IRD, IMBE, Marseille France
[2]Aix Marseille Univ., CEA, CNRS UMR 7265 BIAM, CEA/Cadarache, Saint-Paul-lès-Durance, France
[3]Aix Marseille Univ., CNRS, ICR, UMR 7273, Marseille France

This chapter refers to an article published in August 2023 in the international scientific journal *The Plant Journal*. https://doi.org/10.1111/tpj.16424

Abstract

With climate change, an aggravation in summer drought is expected in the Mediterranean region. To assess the impact of such future scenario, we compared the response of *Quercus pubescens*, a drought resistant deciduous oak species, to long-term amplified drought (AD) (partial rain exclusion *in natura* for 10 years) and natural drought (ND). We studied leaf physiological and physico-chemical trait responses to ND and AD over the seasonal cycle, with a focus on chemical traits including major groups of central (photosynthetic pigments and plastoquinones) and specialized (tocochromanols, phenolic compounds and cuticular waxes) metabolites. Seasonality was the main driver of all leaf traits including cuticular triterpenoids which were highly concentrated in summer suggesting their importance to cope with drought and thermal stress periods. Under AD, trees reduced CO_2 assimilation (-42%) in summer and leaf concentrations of some phenolic compounds and photosynthetic pigments (carotenoids from the xanthophyll cycle) but also enhanced the levels of other photosynthetic pigments (chlorophylls, lutein and neoxanthin) and plastochromanol-8, an antioxidant located in chloroplasts. Overall, the metabolomic adjustments across seasons and drought conditions reinforce the idea that *Q. pubescens* is highly resistant to drought although significant losses of antioxidant defenses and photoprotection were identified under AD.

Keywords: climate change, cuticular waxes, drought, ecophysiology, *Quercus pubescens,* rainfall exclusion, seasonality, targeted metabolomics

1. Introduction

The Mediterranean region is an important climate change "hot spot" combining dry and hot summer periods which are expected to accentuate in the future (Lionello & Scarascia, 2018). Climate models forecast a significant reduction of annual precipitation reaching -30% or even exceeding -40% in some parts of southern Mediterranean with the highest water scarcity during summer months (Zittis *et al.*, 2019). These changes occur rapidly and will increase in intensity, frequency and severity prolonging the summer drought, thereby endangering the growth and survival of Mediterranean forest ecosystems (Peñuelas *et al.*, 2018). One of the most important challenges in ecology is thus to anticipate the plant responses to drier climate.

Plant's physico-chemical leaf traits are strongly influenced by seasonal variations in temperature, light, humidity, precipitation, and phenology (Saunier *et al.*, 2018, 2022; Liebelt *et al.*, 2019). Adjustments in these traits remain crucial to cope with summer drought stress (Brunetti *et al.*, 2019b). Plants exhibit a range of physical traits which allow adaptation to dry conditions, mainly by reducing water loss (De Micco & Aronne, 2012). The most commonly regarded physical trait for plant performance under drought is the specific leaf area (SLA) (Wellstein *et al.*, 2017). Several studies have reported that leaves with low SLA imply high thickness as a mean to cope with dry conditions (Ramírez-Valiente *et al.*, 2017, 2020) while higher SLA (and thus thinner leaves) coupled with larger leaves, can reflect an acquisition resource-use strategy where light capture, photosynthesis and resource assimilation are maximized (Pérez-Ramos *et al.*, 2013; Reich, 2014).

Among chemical traits, plants synthesize and store a large variety of carbon-based metabolites classified as central (or universal) metabolites which play crucial roles for basic plant functioning, growth and survival and as specialized metabolites which mediate plant interaction with the environment and represent supplementary defenses against biotic and abiotic stresses (Fang *et al.*, 2019). One of their major roles is to get rid of Reactive Oxygen Species (ROS) overproduced upon excess of UV-radiation, temperature and water deficit (Havaux & Kloppstech, 2001; Reddy *et al.*, 2004; Shepherd & Wynne Griffiths, 2006; Hernández *et al.*, 2012; Ormeño *et al.*, 2020b). Such metabolites include carotenoids, tocochromanols, plastoquinones and phenolic compounds well known to act as ROS scavengers (Das & Roychoudhury, 2014; Ksas *et al.*, 2015; Esteban *et al.*, 2015; Muñoz & Munné-Bosch, 2019; Havaux, 2020; Laoué *et al.*, 2022). In addition to their role as direct ROS scavengers, phenolic compounds also contribute to UV protection and can act as signaling molecules (Peer & Murphy, 2006; Santos-Sánchez *et al.*, 2019; Laoué *et al.*, 2022). Leaf pigments (e.g. chlorophylls and carotenoids) are essential for photosynthesis and photoprotection by harvesting and transferring light energy (Maoka, 2020; Moreno *et al.*, 2021a). In particular, carotenoids from the xanthophyll cycle (violaxanthin, antheraxanthin and zeaxanthin) contribute to dissipate the excitation energy within the

antenna of photosystem II which accumulates in excess when stomatal closure limits photosynthesis (Demmig-Adams, 1990). Plastoquinones (PQ) are classified in this study as central metabolites since they play an essential role in photosynthesis, and plants deficient in PQ are not viable (Havaux, 2020). Moreover, PQ have also antioxidant function (Hundal *et al.*, 1995). In addition, cuticular waxes are located in the outer leaf layer and play a major role in evapotranspiration limitation through their hydrophobic properties (Holloway, 1994; Schuster *et al.*, 2016). They are thus key plant defenses against drought (Shepherd & Wynne Griffiths, 2006). In an evolutionary context, plants have developed water-resistant cuticles to colonize lands (Edwards, 1996). Cuticular waxes are predominantly formed by long chain aliphatic waxes including fatty acids and their derivatives (alkanes, alkanols and aldehydes) as well as triterpenoids, highly concentrated in some species (Shepherd & Wynne Griffiths, 2006; Simões *et al.*, 2020; Bueno *et al.*, 2020). Triterpenoids confer mechanical stability to aliphatic waxes especially at elevated temperature and thereby reduce thermal stress (Schuster *et al.*, 2016). Regarding the *Quercus* genera, the study of cuticular waxes has been documented in sclerophyllous species (Martins *et al.*, 1999; Ormeño *et al.*, 2020a; Bueno *et al.*, 2020; Simões *et al.*, 2022) while in deciduous species, only *Quercus robur* L. cuticular waxes have been characterized so far (Gülz & Müller, 1992).

Although changes of leaf metabolome can denote the capacity of plants for adaptation to climate change (Sardans *et al.*, 2011), their modulation due to chronic and long-term drought (over years) remains poorly documented in natural conditions. Rivas-Ubach et al. (2014) reported a clear over-accumulation of leaf phenolic compounds in *Quercus ilex* L. after 10 years of partial rain exclusion while Saunier et al. (2022) showed a drop of few phenolic compounds after 3 to 4 years of partial rain exclusion in *Quercus pubescens* Wild. Responses of cuticular waxes to long-term drought in the field has only been investigated in a site dominated by the sclerophyllous species *Quercus coccifera* L. (Ormeño et al., 2020), while this trait remains unexplored in deciduous *Quercus* species. Nevertheless, several studies under controlled conditions reported that drought enhances the accumulation of cuticular waxes in the model plant *Arabidopsis* and various crop species (Kosma *et al.*, 2009; Xue *et al.*, 2017).

In the present work, we studied the response of *Q. pubescens* to long-term amplified drought (i.e. after 10 years) over seasons in a Mediterranean forest with a focus on chemical, physical and physiological traits. We targeted numerous specialized metabolites, with a focus on cuticular waxes (never documented so far for *Q. pubescens*) and phenolic compounds, but also tocochromanols. Among tocochromanols, hydroxy-plastochromanol (PC-OH) was used as a proxy of the leaf oxidative stress since it is specifically formed upon the action of the singlet oxygen ($^1O_2$) (Szymańska *et al.*, 2014). We also targeted a few metabolites from the central or universal metabolism (chlorophylls, carotenoids and plastoquinones). Physical leaf traits encompassed leaf size and specific leaf area (SLA). Physiological traits were assessed through the measure of net photosynthesis, stomatal conductance, internal CO_2 concentration, water use efficiency as

well as midday and predawn water potential which are associated with plant response to water stress (Damesin & Rambal, 1995; Gallé *et al.*, 2007).

Previous studies on the same experimental site showed a strong impact of middle-term (3-4 years) amplified drought on physiological functioning of *Q. pubescens* with a slight decrease in the production of some carotenoids and phenolic compounds (Saunier *et al.*, 2018, 2022). Accordingly, we hypothesized that long-term (10 years) AD could compromise physiological functioning, and production of plant central and specialized metabolites, especially during the driest season. In line with Gallé et al. (2007) which highlighted that *Q pubescens* withstands extreme drought by preserving its photosynthetic apparatus through maintenance of photosynthetic pigments, we hypothesized that these central metabolites could at least be maintained or even be triggered during long-term summer drought allowing recovery of photosynthetic activity in autumn.

2. Experimental procedures

2.1. Experimental site and species

This study was conducted at O_3HP (Oak Observatory at the "Observatoire de Haute Provence"), a long-term experimental *in natura* forest site belonging to both AnaEE-France (Analysis and Experimentation on Ecosystems) and AnaEE-ERIC (European Research Infrastructure Consortium). The site is located at Saint-Michel-l'Observatoire at 60 km north of Marseille in southern France (5°42′44″E, 43°55′54″N) at an elevation of 650 m above sea level. The study site is characterized by a supra-Mediterranean humid bioclimate with an average annual precipitation of 830 mm and annual mean temperature of 11.9 °C for the period 1967-2000. The forest is mainly composed of *Q. pubescens* which represents ~ 90 % of the biomass, followed by ~ 10% of *Acer monspessulanum* L. trees.

The implementation of a rainfall exclusion system at O_3HP since April 2012 allows to simulate future climate predictions in the Mediterranean region by reducing precipitation and increasing the length of the dry season in an amplified drought (AD) plot of 300 m^2 which is compared to an adjacent plot (300 m^2) where trees grow under natural drought (ND) (**Figure S1**). The exclusion system runs from April-May to September-October following a rainfall prediction curve for 2100 with most exclusion between the beginning of July and the end of September. Three measurement campaigns were carried out in 2021: spring (May 17-19), summer (July 12-14) and autumn (October 11-13). During the year 2021, annual mean temperature was 12.3 °C; **Figure 22d**) and it was a naturally dry year with 4 dry months (see Ombrothermic diagram **Figure 22a**) and an

annual precipitation of 729 mm in the ND (sub-humid bioclimate; Thompson, 2020). As a whole, a total of 41% of precipitation was excluded in the AD plot (thus reaching 427 mm) simulating a semi-arid bioclimate and extending the dry period from 4 to 5 months in the AD plot (**Figure 22a**). When focusing on the previous 30 days preceding each campaign (following the approach of Sytiuk et al., 2022), it can be checked that the major rain exclusion occurred in autumn (with 94% of precipitation excluded), followed by spring (-86%) and summer (- 36%) since summer 2021 was naturally very dry (19 mm) and so rain exclusion could not be further amplified (**Figure 22c**). By contrast, spring and autumn were relatively wet with a mean precipitation of 150 and 144 mm, respectively (**Figure 22c**).

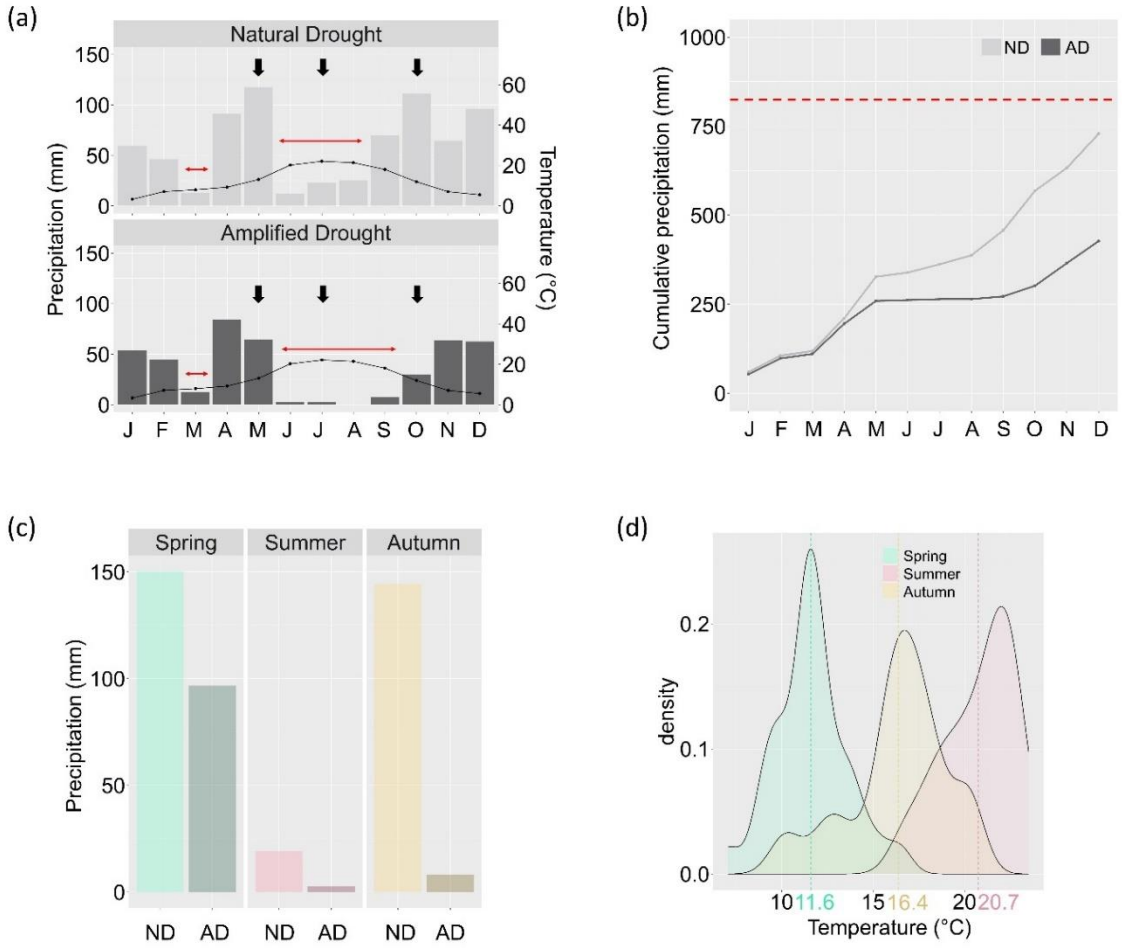

Figure 22: Climatic conditions on the experimental site in 2021. (a) Ombrothermic diagram for natural (light gray) and amplified (dark gray) drought plots where bars represent monthly cumulative precipitation (P, mm) and curves represent mean monthly temperature (T, °C) with P = 2 T. When temperature curves are above precipitation bars, it corresponds to dry periods indicated by red horizontal arrows. Vertical black arrows indicate field campaigns in May (spring), July (summer), and October (autumn). (b) Cumulative precipitation for natural (light gray) and amplified (dark gray) drought plots. The dotted red line represents the annual mean precipitation calculated for the period 1967–2000 (830 mm). (c) Sum of precipitation during the 30 days preceding each sampling campaign in spring (green), summer (pink), and autumn (yellow) under amplified drought (AD) and natural drought (ND). (d) Density of temperature values for each season where the mean temperature during the 30 days preceding each sampling campaign is highlighted in the corresponding color.

Chemical, physical and physiological traits were assessed on fourteen Downy oak trees (7 under each drought condition) over the seasonal cycle (**Figure S1**). Leaves samples came from the top of the canopy. For all chemical analyses (see below), leaf samples were collected around midday and immediately frozen in liquid nitrogen then stored at −80 °C.

2.2. Physiological and physical traits

Gas exchanges were measured on 3 leaves from a sun-exposed branch at the top of the canopy of each tree using an open-system gas analyzer for high-precision detection of CO_2 and H_2O gasses (CIRAS-3, PP Systems, Amesbury, MA, USA). The reference CO_2 concentration was set to 400 µmol mol^{-1}, temperature of the leaf chamber was set to 27 °C and photosynthetically active radiation (PAR) was set to 1000 µmol m^{-2} s^{-1}. Traits measured were the net CO_2 assimilation (A_n, µmol CO_2 m^{-2} s^{-1}), stomatal conductance (g_s, mmol H_2O m^{-2} s^{-1}), internal CO_2 concentration (C_i, µmol mol^{-1}) and water use efficiency (WUE, mmol CO_2 mol^{-1} H_2O). Stem water potential was measured using stems containing 3 to 5 leaves. Both, water potential at midday (ψ_{md}) and predawn (ψ_{pd}) were measured with a Scholander pressure chamber (PMS Instrument Co. USA; range 0-7 MPa). Regarding morphological traits, we focused on the specific leaf area (SLA, cm^2 g^{-1}) calculated as leaf size (or leaf area) per unit dry mass, and leaf size which was calculated by scanning 10-15 leaves by tree and using ImageJ software to calculate the area in cm^{-2}.

2.3. Chemical traits

Leaf powder was obtained by grinding 5-10 leaves in liquid nitrogen. Photosynthetic pigments were extracted from leaf powder (20 to 50 mg) using 2 ml of methanol and were quantified by high-performance liquid chromatography (HPLC). Chlorophylls and several carotenoids were analyzed including those from the xanthophyll cycle (violaxanthin + antheraxanthin + zeaxanthin, hereafter, also referred as VAZ), neoxanthin, lutein, and β-carotene. Their concentrations (µg g_{DM}^{-1}) were calculated from calibration curves performed using carotenoid pigment standards (Extrasynthèse, France) and chlorophyll *a* and *b* standards (Sigma-Aldrich,USA). More details of the method are given in Havaux et al. (2007).

Plastoquinones (PQ) and tocochromanols, including α-tocopherol, plastochromanol-8 (PC-8) and hydroxy-plastochromanol (PC-OH), were extracted from leaf powder (20 to 50 mg) mixed in 2 ml of ethyl acetate. After centrifugation, the supernatant was filtered and evaporated on ice under a stream of N_2. The residue was recovered in methanol/hexane (17:1 vol) and analyzed by HPLC (see Ksas et al., 2015,

2018) with UV absorbance and fluorescence detection. The column was a Macherey-Nagel Nucleosil 100-5 C18. PC-8 was detected by fluorescence at 330 nm with an excitation at 290 nm. Plastoquinones consisted of the pool of reduced and oxidized forms of Plastoquinone-9 and were referred to as plastoquinones (PQ) in the present study. Quantification was achieved using PQ and PC-8 standards which were a kind gift from Dr. J. Kruk (Krakow, Poland) and α-tocopherol standard was purchased from Sigma.

Phenolic compounds were extracted using 10 mg (DM) (from 5-10 leaves, previously lyophilized and frozen-ground) and 1 mL of methanol containing 1% formic acid. The extract was homogenized for 5 min in an ultrasonic bath and centrifuged at 12000 tr min-1 for 5 min. Analyses were performed with an Acquity UPLC-DAD-ESI-TQD system (Waters, USA). UPLC separation was carried out using a C18 BEH column (2.1 mm x 150 mm, 1.7 µm, Waters, USA). Elution rate was set to 0.4 mL min-1 at a constant temperature of 30 °C. Injection volume was set to 2 µL. Chromatographic solvents are composed of (A) water with 0.1% formic acid and (B) acetonitrile with 0.1% formic acid. The chromatographic gradient was 3% of B for 3 min, then 17 min linear gradient until 90% B, followed by column cleaning at 90% B for 3 min then 6 min equilibration at 3% B giving a 25 min total runtime. Photodiode array was set from 190 to 600 nm and phenolic compounds wavelength detection was chosen depending on compound characteristic spectra (350 nm, 320 nm or 280 nm). Their identity or structure were confirmed with the triple quadrupole mass detector in negative ionization mode. Parameters of the electrospray source were: capillary voltage 2.9 kV, cone voltage 35 V, cone temperature was maintained at 150 °C and desolvatation temperature at 400 °C. External quantification with mono glycosylated flavonols (quercetin and myricitrin) and hydroxycinnamic acid standards (caffeoyl acid, chlorogenic acid, coumaric acid) was applied.

Cuticular waxes were extracted by immersing precisely defined leaf circles (9.54 cm^2) obtained from 3-5 leaves into 3 ml of cyclohexane and chloroform (70:30 vol) under constant shaking for 2 min using a vortex. Cuticular wax removal was checked through Scanning Electron Microscopy (**Figure S2**). Then, 2.5 ml of the extract was recovered. Tetracosane D50 (C24; 98%; Sigma-Aldrich) was added as an internal standard and the total solvent was evaporated. Those cuticular wax extractions were then resuspended into 250 µl of acetonitrile and derivatized with 20 µl of N,O-Bis(trimethylsilyl)trifluoroacetamide (BSTFA, Sigma-Aldrich) and 20 µl of pyridine (Sigma-Aldrich) to improve the separation of metabolites. The extract was filtered with a PTFE syringe filter (0.2 µm, 30 mm diameter). To allow derivatization, the mixture was heated for 30 min at 70°C. Each derivatized sample was analyzed by injecting 1 µl in an Agilent 7890 gas-chromatography/mass-spectrometry (GC-MS) equipped with an ALS7693 automatic injector, a MSD5977A Network mass detector (70 eV) and an HP5-MS apolar column (30 m × 0.25 mm × 0.25 µm; J&W Agilent Technologies). Cuticular waxes were identified through the Agilent ChemStation software by comparing their mass spectra, retention times and Kovats retention index with libraries (NIST 2020 and ADAMS

2008), published data and experimental data for some available standards (alkanes C8-40, lupeol, α-amyrin, β-amyrin, α-tocopherol and δ-tocopherol). Identified compounds were quantified against the internal standard (tetracosane D50). Results were expressed by dry matter (μg g_{DM}^{-1}) by oven-drying leaf circles (used for extractions) at 65°C for 48h.

2.4. Statistical analysis

For analysis of chemical traits, we first performed a principal component analysis (PCA) followed by a two-way PERMANOVA to assess if chemical traits were modulated by seasonality and drought. Then, we used a two-way ANOVA analysis followed by post-hoc tests to highlight if leaf metabolites responded differentially according to seasons and drought conditions. All analyses were performed using groups and subgroups although detailed results on single metabolites are shown in supplementary information.

For assessing adjustments of morphological and physiological traits across seasons and drought conditions, we performed two-way ANOVAs followed by post-hoc Tukey tests. When significant interactions occurred between seasonality and drought, we performed a one-way ANOVA followed by Tukey tests to evaluate the effect of seasons on ND and AD separately, and Student tests to evaluate differences between drought conditions (ND and AD) within each season. When interaction between seasonality and drought was not significant, differences between seasons were evaluated with drought conditions pooled and the drought effects were shown separately with all seasons pooled.

Before analyses, normality and homoscedasticity were checked and data were log-transformed if necessary. All data analyses were performed using R v.4.0.3 (R Core Team, 2020) using car, agricolae and multcomp packages for two-way ANOVA analysis, Tukey and Student tests. The PCA was performed using FactoMineR and factoextra packages (Husson *et al.*, 2010; Kassambara, 2020) and the two-way PERMANOVA using vegan (Oksanen *et al.*, 2013) with 9999 permutations.

3. Results

3.1. Physiological and physical traits: seasonality and drought responses

Net CO_2 assimilation changed according to seasonality and drought (**Figure 23a**). The highest A_n was reached in spring and autumn (10.29 ± 0.68 and 9.58 ± 1.06 μmol CO_2 m^{-2}

s^{-1}, respectively) while in summer it decreased by 61% (4.06 ± 0.49 µmol CO_2 m^{-2} s^{-1}) associated to the decrease in precipitation (**Figure 23a**). Amplified drought significantly impacted the A_n leading to an overall decrease of 16% compared to ND (with a decrease up to 42% in summer) which was associated to a slight decline of g_s (R^2 = 0.39*; P* < 0.001; **Figure S3**) (**Figure 23a,b**). The internal CO_2 concentration (C_i) increased over the seasons and was marginally higher (P < 0.1) in leaves under AD, especially in summer with an increase up to 41% (**Figure 23c**). Regarding the WUE, a decrease is observed in autumn only, independently of the drought conditions (**Figure 23d**). Both, ψ_{md} and ψ_{pd} exhibited the highest values in spring (-1.39 ± 0.11 and -0.53 ± 0.03 MPa, respectively) (**Figure 23e,f**). The lowest ψ_{md} was reached in summer (-3.09 ± 0.15 MPa) with no difference between conditions since precipitation was very low in both plots (19 mm in ND and 3 mm in AD; **Figure 22c**). Water potentials were lowered under AD in autumn only: ψ_{md} tended to drop from -1.75 to -2.18 MPa and ψ_{pd} significantly decreased from –1.19 to -2.06 MPa (**Figure 23e,f**). Rain precipitation was indeed almost completely excluded (-94%) in the AD plot the month before autumn sampling (**Figure 22c**).

Regarding physical traits, leaf size remained stable across seasons and drought conditions although we noticed a non-significant larger leaf size under ND (18.58 cm^2) compared to AD (16.16 cm^2) in summer. Leaf size was the same in spring (17.45 cm^2 under ND and 17.56 cm^2 under AD) (**Figure 23g**). SLA significantly decreased through seasons with the lowest values in autumn (66.60 ± 2.56 cm^2 g^{-1} in ND plot; **Figure 23h**) and such decrease was less marked under AD in both, summer (P < 0.1) and autumn (P < 0.05).

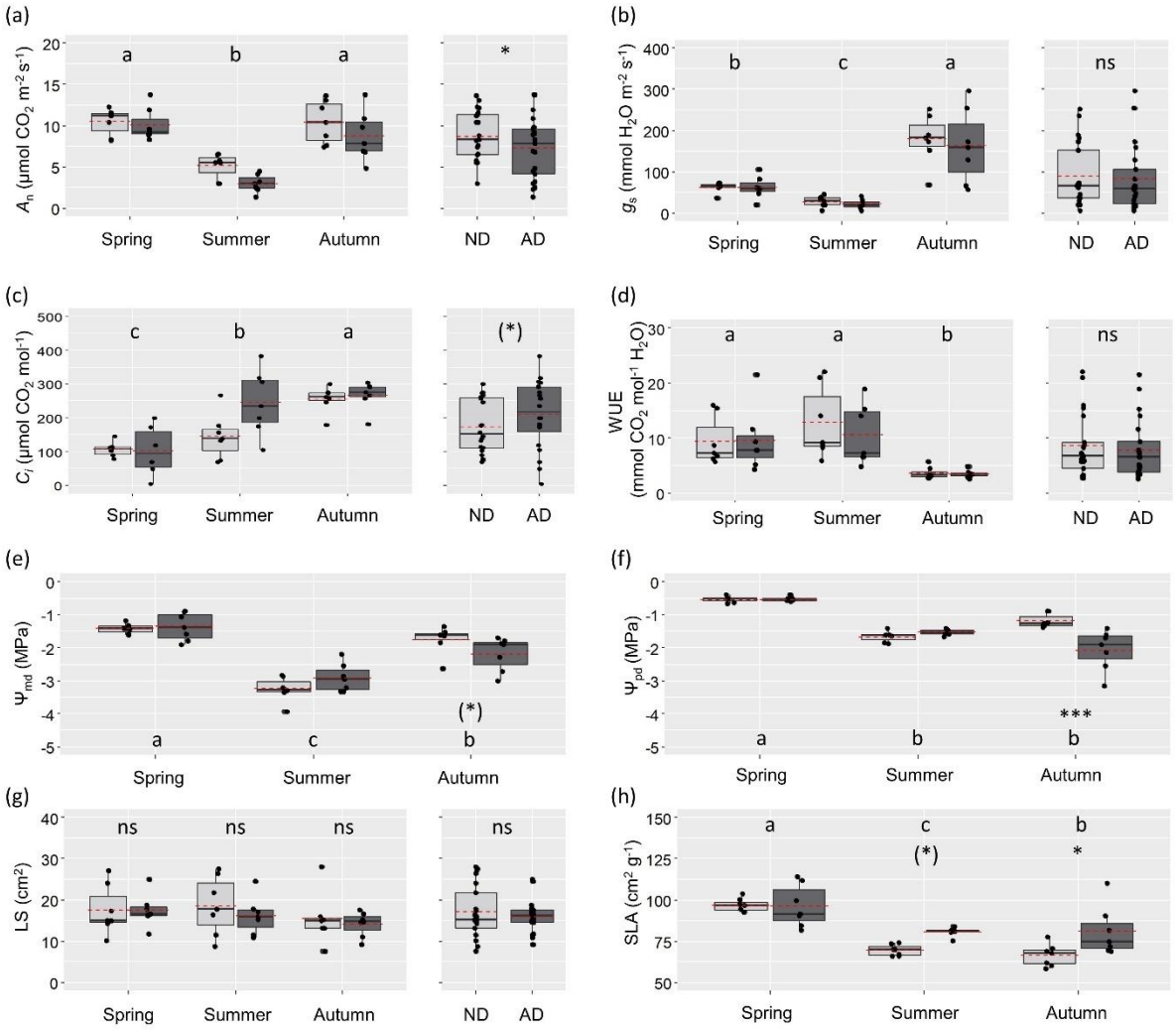

Figure 23: Physiological (a–f) and physical (g, h) leaf traits through seasons (spring, summer, and autumn) and drought conditions (natural drought (ND) in light gray and amplified drought (AD) in dark gray). When interaction between season and drought was not significant (a–d, g), significant differences across seasons and drought conditions are noted on separate graphs. When significant interactions occurred (e, f, and h), differences are highlighted in a single graph. Significant differences are denoted using letters (a > b > c) for the seasons and asterisks for drought condition: (*): $0.05 < P < 0.1$, *: $0.01 < P < 0$ 0.05, **: $0.001 < P < 0.01$, and ***$P < 0.001$. Ns is for non-significant results. The horizontal black lines inside the boxes are the medians and the horizontal red dashed lines are the means (n = 7). A_n, assimilation; C_i, internal CO_2 concentration; g_s, stomatal conductance, WUE, water-use efficiency; Ψ_{md}, midday water potential; Ψ_{pd}, predawn water potential; LS, leaf surface; and SLA, specific leaf area.

3.2. Chemical traits: seasonality and drought responses

We quantified 57 metabolites classified within five major groups including photosynthetic pigments (chlorophylls and carotenoids), plastoquinone, tocochromanols

(plastochromanol and α-tocopherol), phenolic compounds (flavonols, flavanols and phenolic acids) and cuticular waxes (alkanes, alkanols, aldehyde, fatty acids, tocopherols, phytosterol and triterpenoids) (**Table 6**) belonging to different biosynthetic pathways (**Figure S4**). Independently of the season and the drought condition, cuticular waxes were dominated by triterpenoids (37%) followed by fatty acids (28%) (**Table 7**).

The metabolic profiles across seasons and drought conditions were analyzed on 1) the five major metabolic groups, 2) subgroups within the five major metabolite groups and 3) single metabolites. PCA analysis revealed that major metabolic groups and subgroups (**Figure 24a**), but also single metabolites (**Figure 24b**) were only modulated by seasonality (PCA, PERMANOVA, $P < 0.001$). The PCA revealed two main principal components (PCs) which explained 61.3% of the metabolite concentration variations (**Figure 24a**). Carotenoids, plastoquinones, tocochromanols, fatty acids and tocopherols (from cuticular waxes) were the most contributing variables to the first axis while aldehyde (only one was detected) and triterpenoids explained the variability across the second axis. At the single compound level, PCA revealed that spring leaves were characterized by high concentrations of the photosynthetic pigment carotenoids (lutein, β-carotene and VAZ) and chlorophylls, as well as high storage of phenolic acids (feruloyl quinic acid), alkanols and to a less extent flavonols (**Figure 24**). Contrastingly, summer leaves featured high concentrations of cuticular waxes, mainly triterpenoids and aldehyde (octacosanal) (**Figure 24**). Autumn leaves were also rich in cuticular waxes, mainly tocopherols (α-tocopherol), long-chain fatty acids (pentacosanoic, hexacosanoic and octacosanoic acids) and the major triterpenoid (lupeol) (**Figure 24b**). Autumn leaves also featured high concentrations of tocochromanols (PC-8, PC-OH and α-tocopherol), plastoquinones and flavanols (catechin) (**Figure 24**).

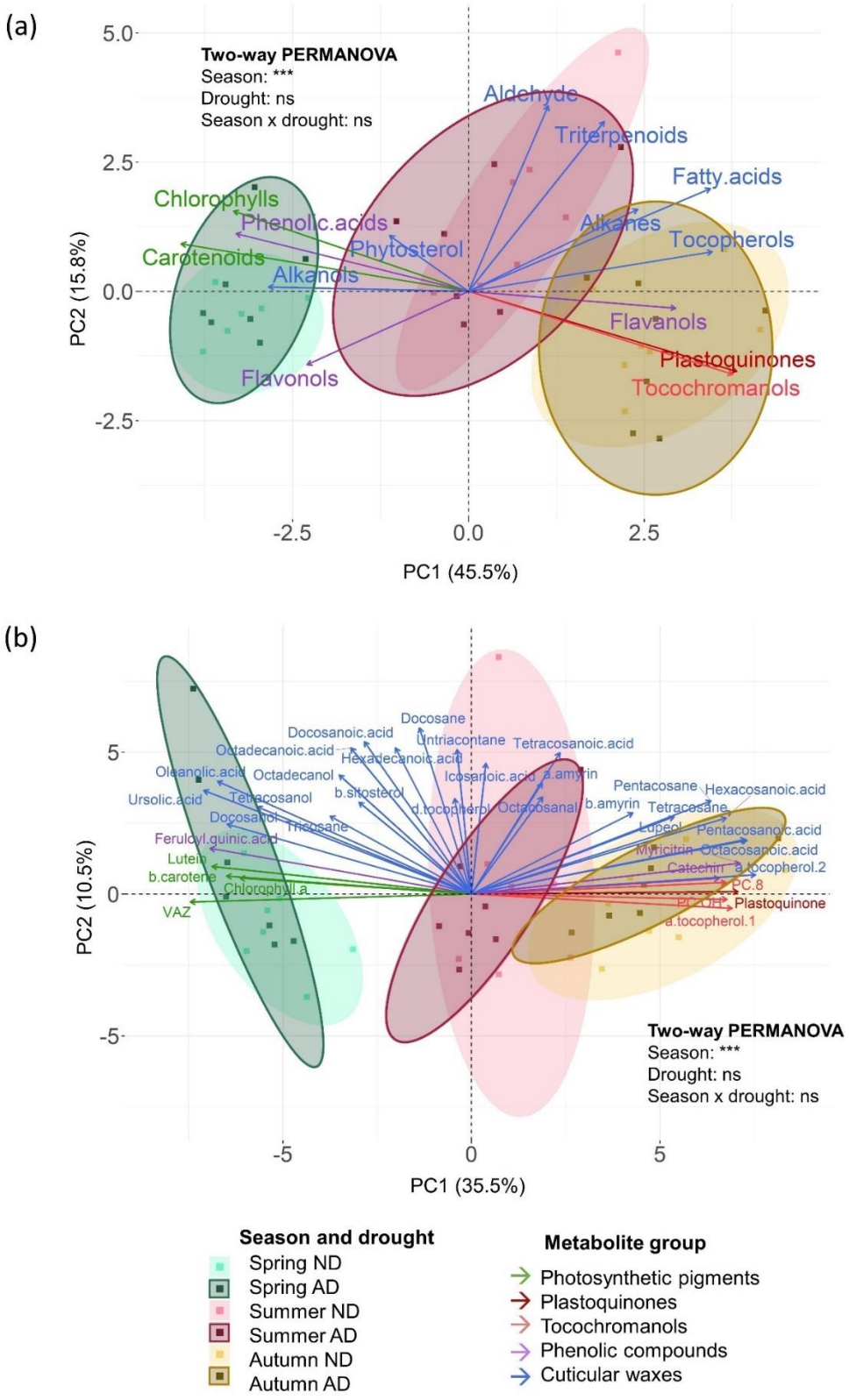

Figure 24: Principal component analysis (PCA) for the first two PCA axes of (a) the metabolite groups and subgroups, and (b) the 30 most contributive single metabolites (among the 57 single metabolites analyzed). Metabolite groups (photosynthetic pigments, plastoquinones, tocochromanols, phenolic compounds, and cuticular waxes) are indicated with arrows in different colors. Seasons are represented in green (spring), pink (summer), and yellow (autumn). Drought conditions are represented in light (ND) and dark circled colors (AD), with n = 7 for each condition.

Parametric analysis (two-way ANOVA; **Table 7**,**Table S1**,**Table S2**) revealed that storage of metabolite groups, subgroups and single metabolites was driven by seasonality but some differences between drought conditions could also be highlighted. All metabolite groups showed seasonal differences with highest concentrations of photosynthetic pigments and phenolic compounds in spring, while plastoquinones and tocochromanols were most concentrated in autumn (they also accumulated in summer but to a lesser extent compared to autumn) and cuticular waxes in both summer and autumn (**Table S1**). Among photosynthetic pigments, chlorophyll and carotenoid concentrations decreased over the seasonal cycle with the highest concentrations in spring (4263 ± 205 and 915 ± 29 µg g^{-1}_{DM}, respectively) (**Table 7**). By contrast, plastoquinones and tocochromanols were approximately 10-fold higher in autumn compared to spring. Among phenolic compounds, only flavanols increased in summer mainly due to the increase in catechin (**Table S2**) while phenolic acids exhibited the highest storage in both spring (1976 ± 161 µg g^{-1}_{DM}) and summer (1800 ± 114 µg g^{-1}_{DM}) and then dropped in autumn (1027 ± 47 µg g^{-1}_{DM}). Flavonols – the main phenolic compound subgroup (**Table 7**) – were mainly concentrated in spring (7358 ± 490 µg g^{-1}_{DM}), especially quercetin and kaempferol derivatives compared to summer and autumn where they showed similar concentrations (summer: 5650 ± 500 µg g^{-1}_{DM}; autumn: 5716 ± 400 µg g^{-1}_{DM}) (**Table 7**,**Table S2**). Total cuticular waxes reached its highest concentration in summer (4725 µg g^{-1}_{DM}) and autumn (4351 µg g^{-1}_{DM}) (**Figure S5**). Triterpenoids were the most concentrated waxes with an average of 1607 µg g^{-1}_{DM} all seasons pooled (**Figure S5**, **Table 7**) and were the only subgroup – with aldehyde – to reach the highest concentrations in summer (2182 ± 287 µg g^{-1}_{DM}) mainly attributed to the significant rise in β-amyrin and lupeol (**Table S2**). Otherwise, alkanes, fatty acids and cuticular wax tocopherols displayed the lowest concentrations in spring and were similarly concentrated in summer and autumn (**Table 7**). β-sitosterol did not show any change across seasons (**Table S2**).

Regarding metabolic changes according to drought conditions, only photosynthetic pigments tend to increase under AD (**Table S1**). Among these photosynthetic pigments, two metabolite subgroups, namely chlorophylls (chlorophyll *a* and *b*) and plastochromanols significantly increased by 12% and 8%, respectively under AD (**Table 7**, **Table S2**). The increase in plastochromanol concentrations was due to the increase in both PC-8 and PC-OH (**Table S2**). The increase in PC-8 concentrations occurred only in summer (**Table S2**). Also, AD led to a rise in two single carotenoids, namely neoxanthin (+16%) and lutein (+11%) and in cuticular waxes (docosanol, docosanoic acid and δ-tocopherol) (**Table S2**). Contrastingly, three phenolic compound concentrations (myricitrin, quercetin galloyl glucose, *p*-coumaric acid glycosylated derivative) decreased under AD from -14% to -32% as well as one cuticular wax (octacosanal; -23%) and pigments from the xanthophyll cycle (VAZ; -10%) (**Table S2**).

Table 6: Metabolite groups and subgroups targeted in this study and belonging to central and specialized metabolism in the whole leaf and leaf surface (cuticular waxes), biosynthetic pathways, main functions, and references.

Leaf part	Metabolism	Metabolite group	Metabolite subgroup	Biosynthetic pathways	Main functions	References
Whole leaf	Central	Photosynthetic pigments	Carotenoid	MEP	Light harvesting for photosynthesis Photoprotection related to xanthophyll cycle Antioxidant	Esteban *et al.* (2015), Moreno *et al.* (2021)
			Chlorophyll	MEP	Light-absorbing for photosynthesis Electron transporters in the photosynthesis	Kim *et al.* (2013)
	Central	Plastoquinones	Plastoquinones	MEP and shikimate	Electron transporters in the photosynthesis Antioxidant	Hundal *et al.* (1995), Havaux (2020)
	Specialized	Tocochromanols	Hydroxy-plastochromanol	MEP and shikimate	Oxydation marker	Szymańska (2014)
			Plastochromanol	MEP and shikimate	Antioxidant	Havaux (2020)
			Tocopherols	MEP and shikimate	Antioxidant	Muñoz & Munné-Bosch (2019)
	Specialized	Phenolic compounds	Flavonols	Shikimate	Antioxidant UV-B protection Signaling molecule	Santos-Sánchez *et al.* (2019), Laoué *et al.* (2022)
			Flavanols	Shikimate	Antioxidant UV-B protection Signaling molecule	Santos-Sánchez *et al.* (2019), Laoué *et al.* (2022)
			Phenolic acids	Shikimate	Antioxidant Signaling molecules	Santos-Sánchez *et al.* (2019)
Cuticular waxes leaf surface	Specialized	Cuticular waxes	Alkanes	Fatty acids derivatives	Cuticular transpiration barrier	Jetter & Riederer (2016), Batsale *et al.* (2021)
			Alkanols	Fatty acids derivatives	Cuticular transpiration barrier	Jetter & Riederer (2016), Batsale *et al.* (2021)
			Aldehyde	Fatty acids derivatives	Cuticular transpiration barrier	Jetter & Riederer (2016), Batsale *et al.* (2021)
			Fatty acids	Fatty acids derivatives	Cuticular transpiration barrier	Jetter & Riederer (2016), Batsale *et al.* (2021)
			Phytosterol	MVA	Maintenance of membrane homeostasis	Rogowska & Szakiel (2020)
			Triterpenoids	MVA	Cuticle stabilization during thermal stress Toxicity for herbivores	Tsubaki *et al.* (2013); Schuster *et al.* (2016)
			Tocopherols	MEP and shikimate	Antioxidant Maintenance of the integrity of long-chain fatty acids	Muñoz & Munné-Bosch (2019)

Table 7: Results of two-way ANOVA performed on metabolite subgroup concentrations (µg g^{-1}_{DM}) according to season and drought conditions (n = 7).

		Spring (Sp)				Summer (Su)				Autumn (Au)				Two-way ANOVA		
Metabolite group	**Metabolite subgroup**	**ND**		**AD**		**ND**		**AD**		**ND**		**AD**		**Season (Sp, Su, Au)**	**Drought (ND, AD)**	**S x D**
Photosynthetic pigments	Carotenoids	893.38	± 30.04	936.64	± 27.33	645.28	± 25.86	700.19	± 34.07	525.77	± 13.42	497.47	± 50.75	*** **(a, b, c)**	ns	ns
	Chlorophylls	4032.43	± 221.68	4493.39	± 188.53	3366.46	± 192.10	4034.64	± 233.46	2693.77	± 120.95	2732.86	± 361.65	*** **(a, b, c)**	* **(B, A)**	ns
Plastoquinones	Plastoquinones	192.58	± 26.80	195.17	± 11.22	713.50	± 45.29	727.99	± 35.37	1819.21	± 170.61	1909.93	± 213.64	*** **(c, b, a)**	ns	ns
Tocochromanols	Plastochromanols	3.22	± 0.37	4.01	± 0.41	9.74	± 0.68	13.76	± 0.38	46.76	± 2.63	46.54	± 5.19	*** **(c,b,a)**	* **(B, A)**	ns
	Tocopherols	75.50	± 5.92	82.16	± 5.48	308.64	± 54.88	237.51	± 13.08	580.64	± 20.57	624.90	± 73.31	*** **(c, b, a)**	ns	ns
Phenolic compounds	Flavonols	7635.31	± 309.91	7080.10	± 669.80	5387.32	± 408.91	5913.13	± 591.99	5489.95	± 379.80	5942.50	± 418.39	** **(a, b, b)**	ns	ns
	Flavanols	795.99	± 110.27	764.18	± 56.35	1358.87	± 229.86	1372.73	± 158.75	1946.73	± 404.05	1564.39	± 231.49	*** **(b, a, a)**	ns	ns
	Phenolic acids	1866.00	± 158.39	2086.64	± 163.67	1834.10	± 109.22	1765.27	± 118.00	1084.70	± 59.95	969.62	± 34.13	*** **(a, a, b)**	ns	ns
Cuticular waxes	Alkanes	109.11	± 10.52	116.71	± 14.15	138.73	± 11.33	137.87	± 16.09	159.02	± 16.90	166.14	± 20.82	* **(b,ab, a)**	ns	ns
	Alkanols	1632.35	± 220.10	1679.84	± 190.28	724.84	± 54.88	783.77	± 64.99	845.76	± 84.49	920.40	± 38.88	*** **(a, b, b)**	ns	ns
	Aldehyde	56.35	± 9.08	44.23	± 8.70	104.12	± 9.84	71.58	± 8.39	57.92	± 5.91	53.43	± 7.02	*** **(b, a, b)**	** **(A, B)**	ns
	Fatty acids	610.82	± 33.82	844.52	± 154.58	1493.33	± 163.01	1222.80	± 144.29	1458.30	± 99.26	1576.48	± 148.87	*** **(b, a, a)**	ns	ns
	Tocopherols	22.52	± 4.19	41.21	± 7.83	78.61	± 7.03	91.66	± 12.29	98.03	± 8.56	87.94	± 7.48	*** **(b, a, a)**	ns	ns
	Phytosterol	124.31	± 12.07	157.04	± 26.99	131.30	± 8.04	106.71	± 5.48	111.93	± 7.49	111.13	± 7.20	ns	ns	ns
	Triterpenoids	986.04	± 55.41	1237.42	± 158.69	2151.83	± 392.04	2212.61	± 182.77	1604.06	± 206.56	1451.93	± 156.50	*** **(c, a, b)**	ns	ns

4. Discussion

In the present study, the physiological, physical and chemical trait adjustments related to both seasonality and long-term rain exclusion were evaluated in *Q. pubescens*, a drought-resistant species (Damesin & Rambal, 1995; Struve *et al.*, 2009; Saunier *et al.*, 2018). Seasonality appeared as the main driver of all traits, but AD was also associated with some significant changes allowing to anticipate the strategies used by this species to cope with future drier climate (**Figure 25**).

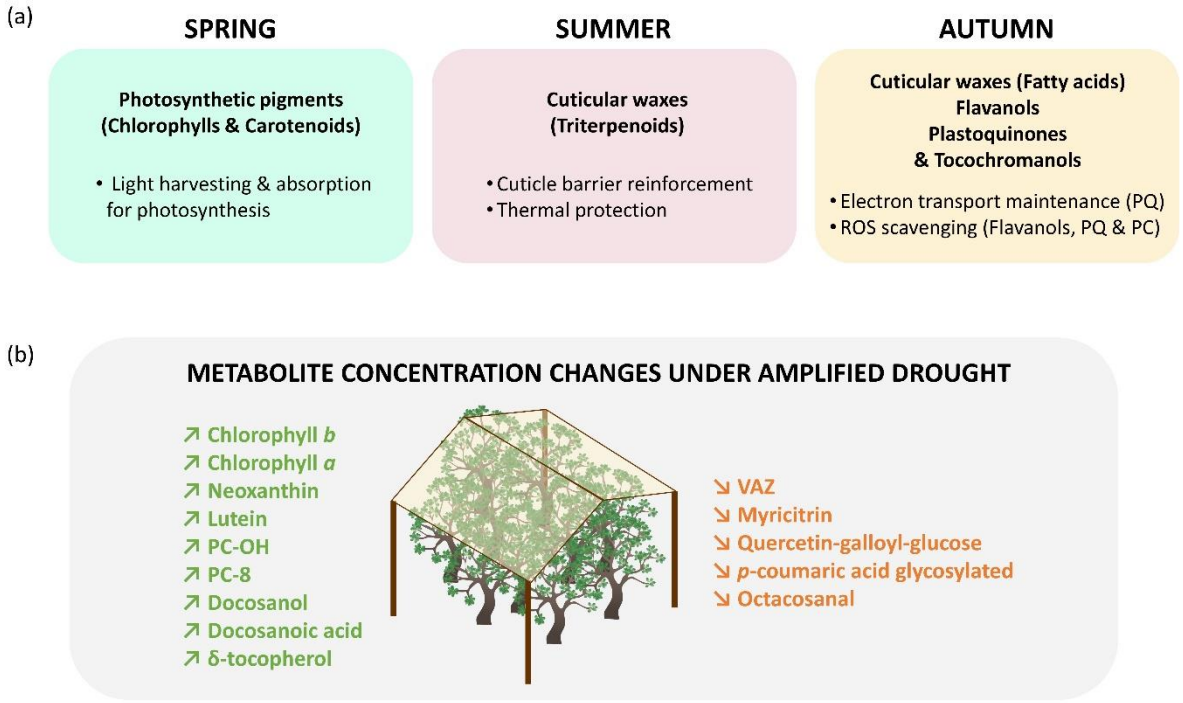

Figure 25: Overall conclusion of the main chemical trait responses of *Q. pubescens* leaves through (a) seasonality where the most concentrated groups (or subgroups) within each season are represented with their main function and (b) amplified drought (AD) where green arrows indicate a significant increase and orange arrows a significant decrease in single metabolites in comparison with natural drought (ND). PQ, Plastoquinones; PC-OH: Hydroxy plastochromanol; PC- 8, Plastochromanol-8. See **Table 6** for bibliographic references regarding metabolite functions.

4.1. Physiological traits

There was a strong effect of seasonality on physiological traits in 2021 with main stress occurring during summer as denoted by the lowest values of A_n (4 µmol CO_2 m^{-2} s^{-1}), g_s (25 mmol H_2O m^{-2} s^{-1}) and Ψ_{md} (-3 MPa). These results were also reported by Saunier et al. (2018) in 2015 in the same field site, that is, after 4 years of rain exclusion. However, 2015 was a drier year (598 mm annual precipitation) compared to 2021 (729 mm) and, accordingly, the values of all these physiological traits were slightly lower in 2015, especially in summer (A_n: 1.3 µmol CO_2 m^{-2} s^{-1}, g_s: 3.8 mmol H_2O m^{-2} s^{-1} and Ψ_{md}: -3.6 MPa; Saunier et al., 2018). The C_i was lowest in spring, intermediate in summer and highest in autumn indicating a higher CO_2 assimilation in spring through photosynthesis (denotated by higher A_n in spring) (Flexas *et al.*, 2001). During autumn, even if A_n was similar to spring, C_i was highest due to stomatal aperture (i.e. higher g_s). *Q. pubescens* is known to possess a highly efficient hydraulic system allowing to both, maintain a high relative leaf water content and display relatively high Ψ_{md} (-3 MPa) and Ψ_{pd} (-1.6 MPa) in summer compared to sclerophyllous oak Mediterranean species (e.g. *Q. ilex* with $-4 > \Psi_{pd} > -6$ MPa; Tognetti et al., 1998; Limousin et al., 2022). These physiological traits indicate that *Q. pubescens* adapts to water scarcity through a drought-avoidance strategy (Nardini & Pitt, 1999).

Amplified drought led to lower water potentials but only in autumn, while Saunier et al. (2018) reported a decrease in summer as well. Rain exclusion was indeed weak in summer 2021 since precipitation was naturally scarce thus limiting differences between the AD and ND plots. By contrast, precipitation was particularly important in autumn 2021 where 94% of precipitation was excluded in the AD plot the month before our sampling campaign, exacerbating the differences between the two plots. Stomatal conductance was not significantly limited by AD, although values tended to be lower under rain restriction (- 23% in summer). Contrastingly, g_s strongly dropped in summer during the first and fourth year of rain exclusion in the same field site (Genard-Zielinski *et al.*, 2018b; Saunier *et al.*, 2018). In the cited studies, June precipitation was higher than in 2021 which implies that the total rain exclusion in the AD plot allowed to exacerbate differences between the two plots. Amplified drought impacted A_n at any season with the main decrease occurring in summer (-42%) according to our hypothesis although such decrease was not associated to significant stomatal closure. Saunier et al. (2018) reported a higher drop in A_n during autumn (-85%) compared to summer (-60%) 2015, due to very low g_s. Along with the decline in A_n in summer 2021, the C_i was higher under AD. The change in C_i with drought is used as an indicator of stomatal or non-stomatal limitations to photosynthesis (Flexas & Medrano, 2002).With increasing stress, C_i initially declines and later undergoes an increase as drought severity intensifies (Lawlor, 1995). In our study, when trees were exposed to higher stress level in summer ($\Psi_{md} < -3$ MPa), the low values of g_s (< 22 mmol H_2O m^{-2} s^{-1} under AD) coupled with higher C_i indicates that non-

stomatal limitations to photosynthesis was predominant at this level of stress as reported in several studies (Flexas & Medrano, 2002; Medrano, 2002; Marino *et al.*, 2018).

4.2. Physical traits

SLA was the highest in spring and lowest in summer, indicating a higher leaf density in summer and probably higher leaf thickness too as a mean to limit water loss during the driest season (Wright *et al.*, 2004; Galmés *et al.*, 2013). High SLA in spring is often observed since leaves are actively growing, possess a poor leaf density, and thus display high photosynthetic rates (Shipley *et al.*, 2005; Szőllősi *et al.*, 2010). Regarding the response of trees to AD, such seasonal decreases of SLA were of a lower magnitude during both, summer and autumn, suggesting that the growth process is halted by harsher long-term drought conditions. Contrasting with our study, a previous study on *Q. pubescens* in the same field site did not report high SLA under AD after 4 years of rain exclusion (Saunier *et al.*, 2018) although the authors only measured SLA in autumn. In agreement with our study, high SLA was reported under moderate (Ψ_{md} -2.9 MPa) and severe (Ψ_{md} -4.8 MPa) drought stress in a greenhouse study (4 year-old potted plants) (Genard-Zielinski *et al.*, 2014). While low SLA under drought stress is regarded as a drought-adaptation strategy (Poorter *et al.*, 2009), such response was not observed in *Q. pubescens* in this long-term rain exclusion experiment. Moreover, contrasting with our result, increases in both, SLA and leaf surface have been associated with a resource-acquisition strategy where light capture and photosynthesis are maximized (Pérez-Ramos *et al.*, 2013; Griffin-Nolan *et al.*, 2019; Blanco-Sánchez *et al.*, 2022). *Q. pubescens* did not show this pattern since leaves did not possess higher leaf surface under AD thus limiting A_n maximization.

4.3. Chemical traits

Seasonality was the main driver of leaf metabolome as previously shown for *Q. pubescens* (Saunier *et al.*, 2018) and other Mediterranean species (Rivas-Ubach *et al.*, 2014; Gori *et al.*, 2019, 2020; Tixier *et al.*, 2020). In our study, the metabolic profile differed among seasons with a strong investment in (i) photosynthetic pigments in spring, (ii) cuticular waxes in both summer and autumn and (iii) tocochromanols, plastoquinones and flavanols in autumn (**Figure 25a**).

The highest leaf photosynthetic pigment concentrations (chlorophylls and carotenoids) in spring is in agreement with the highest A_n during favorable climatic conditions with high soil water availability (ψ_{pd} values -0.5 MPa; Epron & Dreyer, 1993)

and average temperatures of 12°C (Epron & Dreyer, 1993; Gratani *et al.*, 2000). Indeed, during spring, the main growing season, plants strongly invest in photosynthetic processes to maximize growth (Rivas-Ubach *et al.*, 2012; Rivas-Ubach *et al.*, 2014). In addition to photosynthetic pigments, a few specialized metabolites including the antioxidants phenolic acids and flavonols also accumulated in spring as shown by Saunier et al. (2018) after 3 and 4 years of rain exclusion. This observation supports the protective role of flavonols and phenolic acids to cope with strong light irradiation at the beginning of the vegetative cycle and the associated oxidative stress (Ferreyra *et al.*, 2021; Roeber *et al.*, 2021; Laoué *et al.*, 2022).

Despite the very marked effect of seasonality on leaf metabolome, some metabolite subgroups and single metabolites were sensitive to AD (**Figure 25b**). The high accumulation of PC-OH under AD indicates that trees subjected to rain exclusion displayed higher oxidative stress since this compound is specifically formed upon the action of the singlet oxygen ($^1O_2$), the main ROS in plants (Szymańska *et al.*, 2014). Such accumulation was not reported after four years of AD (**Figure S6**). Carotenoids (neoxanthin and lutein) and PC-8 were also more accumulated under AD. These metabolites confer protection against drought-related oxidative stress since they act as ROS scavengers (Rastogi *et al.*, 2014; Cazzaniga *et al.*, 2016). Saunier et al. (2018) reported opposite results with a decrease in neoxanthin and lutein in 2015, after 4 years of AD. Also, carotenoid accumulation coupled with the increase of chlorophyll *b* and chlorophyll *a* under AD, could allow to maintain efficient light-harvesting and thus prevent a drastic decline in photosynthesis (Kim *et al.*, 2013; Esteban *et al.*, 2015) as the one observed in Saunier et al. (2018) (i.e. 60% in summer and 85% in autumn). According to our hypothesis, the higher accumulation of major photosynthetic pigments and chloroplastic antioxidants confirms that *Q. pubescens* is able to resist to long-term drought by preserving its photosynthetic apparatus as suggested by Gallé et al. (2007) for extreme drought in the same species. Contrasting with these carotenoids (neoxanthin and lutein), VAZ decreased under AD. Since the xanthophyl cycle is involved in dissipating excess of energy thus limiting ROS generation (García-Plazaola *et al.*, 2008; Xu *et al.*, 2020a), a decrease of their concentration under AD indicates a loss of photoprotection which was already observed after four years of AD (Saunier *et al.*, 2018). Zeaxanthin also functions as an antioxidant supplementing the action of tocopherol (Havaux *et al.*, 2005; Havaux & García-Plazaola, 2014). The consumption of zeaxanthin and the decrease in VAZ could therefore indicate significant oxidative stress conditions in the oak leaves under AD.

Regarding phenolic compounds, a major group of plant specialized metabolites, two flavonoids (myricitrin and quercetin galloyl glucose) and one phenolic acid (*p*-coumaric acid glycosylated derivative) were less stored under AD compared to ND. Such decrease could be a consequence of their antioxidant action under AD resulting in their oxidation and thus in their consumption (Takahama, 2004; Hernandez *et al.*, 2006). These metabolites possess the highest antioxidant potential followed by carotenoids and tocopherols (Catoni *et al.*, 2008) indicating that trees under AD are likely to be more prone

to oxidant pressure. These results contrast with the evolutionary concept proposed by Close & McArthur (2002) where the abundance of phenolic compounds is expected to increase as a mean to reduce the oxidative pressure through ROS quenching. Literature shows contrasting sensitivities of phenolic compound concentrations to water scarcity. Short-term water stress (over a few weeks), often tested under controlled conditions, causes either a significant increase (Fini *et al.*, 2012; Nakabayashi *et al.*, 2014b; Nichols *et al.*, 2015) or decrease in leaf phenolic concentrations (Król *et al.*, 2014; Rahimi *et al.*, 2018). Under long-term amplified drought (over years) in the same field site, Saunier et al. (2022) also reported decreases in some phenolic compound concentrations after three and four years of rain exclusion. Contrastingly, Rivas-Ubach et al. (2014) mentioned that several phenolic compounds increased after 10 years of drought stress in *Q. ilex* thus reinforcing its antioxidant system. Notwithstanding, Rivas-Ubach et al. (2014) also noted tree mortality after only five years of AD while we did not observe mortality after 10 years since water stress is less pronounced in our experimental site. These contrasting results can be explained by the different climatic conditions between the two experimental sites. Our study was conducted in a humid/subhumid vegetation type (receiving annual mean precipitation of 830 mm) while the study on *Q. ilex* was conducted in a semi-arid/subhumid forest corresponding to a drier Mediterranean climate with an annual mean precipitation of 610 mm (Peñuelas *et al.*, 2018) where trees are exposed to higher drought-related oxidative stress. Stimulation (in *Q. iex*) or partial loss (in *Q. pubescens*) of the phenolic storage under water scarcity could also reflect a higher ability of *Q. ilex* to resist to future drought pressure in the Mediterranean basin as pointed out by Vuillemin (1982).

Regarding cuticular waxes, triterpenoids (the major cuticular waxes) exhibited the highest concentration in summer, but other subgroups (fatty acids, tocopherols and alkanes) showed the highest concentrations during both summer and autumn. According to the model of Riederer & Schneider (1990) and Riederer & Schreiber (1995), cuticular waxes consist of ordered crystalline wax domains (long-chain aliphatics) and amorphous domains (more polar and cyclic waxes) in between. Recent advances indicate that cuticular triterpenoids do not directly act as a barrier for cuticular transpiration (Jetter & Riederer, 2016; Schuster *et al.*, 2016), but rather prevent thermal damage by stabilizing the cuticle structure (Tsubaki *et al.*, 2013; Schuster *et al.*, 2016). They can contribute up to 60% of the total cuticular wax concentrations in some *Quercus* species (Bueno *et al.*, 2020) and represent 37% of the cuticular fraction of *Q. pubescens* leaves. Triterpenoids could thereby confer protection against thermal stress during hot summer thus contributing to leaf protection during concurrent periods of drought and thermal stress in *Q. pubescens*. Seasonal variation of leaf waxes has been described in other deciduous trees including *Fagus sylvatica* L. (Prasad & Giilz, 1990) and *Quercus robur* (Gülz & Müller, 1992), the latter displaying also higher cuticular wax accumulation in summer and autumn. From an ecological perspective, it is worth noting that adult individuals of *Q. robur* and sclerophyllous *Quercus* species (*Q. suber* and *Q. coccifera* L.) display leaf cuticular wax concentrations in the same range (35-200 µg cm^{-2}; Gülz & Müller, 1992;

Simões et al., 2022; Bueno et al., 2019) as *Q. pubescens* (90 µg cm^{-2}) indicating that cuticular cover is not higher in *Quercus* sclerophyllous species which possess thicker and harder leaves compared to broad-leaf deciduous *Quercus* species.

There was no clear impact of long-term drought on cuticular waxes since trees growing under AD exhibited higher concentrations of only three minor cuticular waxes (docosanol, docosanoic acid and δ-tocopherol) compared to ND while octacosanal storage decreased. Unlike natural species, the effect of drought on cuticular wax concentrations has been widely studied on the model plant *Arabidopsis thaliana* (Aharoni *et al.*, 2004; Kosma *et al.*, 2009; Yang *et al.*, 2011) and on crop species for which an increase of wax content is associated with water shortage and enhancement of drought tolerance (for a review see Xue et al., 2017). For natural species, the study of leaf cuticular wax concentrations under different drought conditions has only been documented for *Pinus pinaster* under greenhouse conditions (Le Provost *et al.*, 2013) and in leaf litter of *Q. coccifera* in the field (Ormeño et al., 2020). Unlike our study, these two latter studies revealed an increase of cuticular wax concentrations with rising water deficit. Despite *Q. pubescens* did not exhibit overaccumulation of cuticular wax concentrations under rain exclusion in our study, the fact that the major cuticular waxes (triterpenoids) exhibited the highest concentrations in summer still supports the importance of triterpenoids to stabilize the cuticle during thermal stress in summer (Shepherd & Wynne Griffiths, 2006; Jetter & Riederer, 2016; Schuster *et al.*, 2016). Besides cuticle-based strategies, plants possess many other adaptations to limit water loss (Jenks *et al.*, 2007). For example, *Q. pubescens* features a deep root system which allows to maintain hydraulic conductivity, leaf water content, relatively high assimilation rates and stomatal conductance (Damesin & Rambal, 1995; Nardini & Pitt, 1999; Struve *et al.*, 2009; Genard-Zielinski *et al.*, 2014).

Autumn leaves exhibited higher concentrations of several antioxidants such as plastoquinones, tocochromanols and flavanols. In addition to their role as photosynthetic electron carriers, plastoquinones also play important functions in various processes, such as light acclimation and act as potent antioxidants by scavenging ROS (Ksas *et al.*, 2018; Havaux, 2020). Plastoquinones, which were strongly accumulated in autumn, can scavenge superoxide and hydrogen peroxide (Khorobrykh & Tyystjärvi, 2018). The accumulation of plastoquinones and three other antioxidants (PC-8 , α-tocopherol and the flavanol catechin) suggests a strong antioxidant activity to both, limit oxidative stress still present in autumn and maintain protection of the photosynthetic apparatus in spite of the decline in photosynthetic pigment concentrations (Bernatoniene & Kopustinskiene, 2018; Muñoz & Munné-Bosch, 2019; Kumar *et al.*, 2020b).

5. Conclusion

To conclude, our study provides information about the response of physiological and physico-chemical traits of *Q. pubescens* across seasons and under a long-term rain exclusion simulating future drought in the Mediterranean region. *Q. pubescens* leaf chemical traits, especially tackled in this work, were mainly driven by the seasonality with the highest investment in (i) photosynthetic pigments in spring, (ii) cuticular wax compounds in both summer and autumn and (iii) tocochromanols, plastoquinones and flavanols in autumn. *Q. pubescens* also displayed some metabolomic adjustments in response to AD consisting of higher concentrations of pigments and chloroplastic antioxidants (PC-8) which could allow to preserve the photosynthetic apparatus from oxidative stress during drought stress. However, AD also led to lower concentrations of antioxidant defenses (i.e., flavonoids and phenolic acids) as well as a loss of photoprotection own to the decrease in xanthophyll cycle-related pigments. Although cuticular wax concentrations did not clearly change over long-term rain exclusion, the high concentration of triterpenoids in summer under both ND and AD confirms that these metabolites confer thermal protection of the leaf cuticle. Further research should be conducted to evaluate whether leaf physical traits, such as stomatal and trichome density, and anatomical features, could contribute to drought resistance in *Q. pubescens*.

6. Acknowledgements

This study was supported by the METAPHORES project funded by the 'Centre national de la recherche scientifique (CNRS)' (Grant agreement No. 250892; MITI and DGDS). We are grateful to AnaEE-France and AnaEE-ERIC for the O_3HP facilities (https://www.anaee-france.fr/service/experimentation-in-natura/ecosystemes-forestier/ecosystemes-forestiers-mediterraneens/o3hp). We thank the P2M2 platform of the University of Rennes for the metabolic profiling of phenolic compounds and Ilja Reiter for providing climatic data. We thank Jean-Philippe Orts, Sylvie Dupouyet, Salomé Coquin and Alexis Balembois for the assistance in lab work and fieldwork.

CHAPTER V: Impact of long-term amplified drought on morphological and anatomical leaf traits after 10 years of rain exclusion: a focus on the summer 2021

Leaf morpho-anatomical adjustments in a *Quercus pubescens* forest after ten years of partial rain exclusion in the field

Justine Laoué[1], Guillermo Gea-Izquierdo[2], Sylvie Dupouyet[1], María Conde[2], Catherine Fernandez[1], Elena Ormeño[1]

[1]CNRS, Aix Marseille Univ, Univ Avignon, IRD, IMBE, Marseille, France
[2]CIFOR-INIA, CSIC. Madrid, Spain

This chapter refers to an article published in April 2024 in the international scientific journal *Tree Physiology.* https://doi.org/10.1093/treephys/tpae047

Abstract

In the Mediterranean region, a reduction of annual precipitation and a longer and drier summer season are expected with climate change by the end of the century eventually endangering forest survival. To cope with such rapid change, trees may modulate their morpho-anatomical and physiological traits. In the present study, we focused on the variation in leaf gas exchange and different leaf morpho-anatomical functional traits of *Quercus pubescens* Willd. in summer using a long-term drought experiment *in natura* consisting of a dynamic rainfall exclusion system where trees have been submitted to amplified drought (AD) (~ -30% of annual precipitation) since April 2012 and compared to trees under natural drought (ND) in a Mediterranean forest. During the study, we analyzed net CO_2 assimilation (A_n), stomatal conductance (g_s), transpiration (E), water use efficiency (WUE), stomatal size and density, density of glandular trichomes and non-glandular trichomes, thickness of the different leaf tissues, specific leaf area (SLA) and leaf surface. Under AD, tree functioning was slightly impacted, since only A_n exhibited a 49% drop, while g_s, E and WUE remained stable. The decrease in A_n under AD was regulated by concomitant lower stomatal density and reduced leaf thickness. Trees under AD also featured leaves with a higher non-glandular trichome density and a lower glandular trichome density compared to ND, which simultaneously limits transpiration and production costs. This study points out that *Q. pubescens* exhibits adjustments of leaf morpho-anatomical traits which can help trees to acclimate to amplified drought scenarios as those expected in the future in the Mediterranean region.

Keywords: acclimation, climate change, functional traits, long-term drought, Mediterranean forests, photosynthesis, stomata density, stomata size, trichomes

1. Introduction

Climatic models forecast for the Mediterranean region a general warming between 1 and 5 °C by the end of the century reaching up to 7 °C during summer, as well as a reduction in annual precipitation of about 30% (Guiot & Cramer, 2016; Lionello & Scarascia, 2018; Cramer *et al.*, 2018; Zittis *et al.*, 2019). Such changes will lead to longer and more frequent summer drought periods in Mediterranean climate areas (Lionello & Scarascia, 2018), that should have a negative impact on forest productivity, health and regeneration (Peñuelas *et al.*, 2018; Cramer *et al.*, 2018).

To cope with water deficit, plants modulate their physiological as well as their morphological and anatomical traits (Basu *et al.*, 2016; Li *et al.*, 2023a). For the former, rapid stomatal closure is well known to allow water saving during drought stress. Such response implies however a reduction in carbon assimilation through photosynthesis eventually constraining plant growth (Farquhar & Sharkey, 1982; Chaves, 2002; Pirasteh-Anosheh *et al.*, 2016; Saunier *et al.*, 2018). Regarding morphological traits, stomatal density (SD) and stomatal size (SS) are involved in water loss regulation and thus, in plant adaptation to drought (Bertolino *et al.*, 2019). Another important morphological adaptation to limit water loss is the development of leaf trichomes (Bickford, 2016). Trichomes are appendages derived from aerial epidermal cells in leaves, stems and floral organs which act as a direct barrier against transpiration but also as a protection against herbivores and UV-radiation (Wang *et al.*, 2021). Drought stress increases leaf trichome density in many plant species (Shahzad *et al.*, 2021; Chen *et al.*, 2022b) including *Quercus* species (Hernandez & Park, 2022). Trichomes are classified as glandular trichomes (GT) and non-glandular trichomes (NGT) (Xiao *et al.*, 2016). Glandular trichomes store and secrete large quantities of specialized metabolites including terpenoids (Mahmoud *et al.*, 2021), flavonoids (Tattini *et al.*, 2000) and phenolic acids (Zhou *et al.*, 2021) which are involved in plant defense against environmental stresses such as drought (Haberstroh *et al.*, 2018; Laoué *et al.*, 2022) or herbivory (Peiffer *et al.*, 2009). By contrast, non-glandular trichomes do not secrete specialized metabolites but act as a physical protection against high light and temperatures, playing a key role to limit transpiration (Karabourniotis *et al.*, 2020). Finally, regarding anatomical traits, leaf thickness plays an important role in plant adaptation to withstand drought stress (Flexas *et al.*, 2014; Niinemets, 2015; Afzal *et al.*, 2017) and more specifically, variation in mesophyll anatomy is of a great importance for photosynthetic capacity (Marchi *et al.*, 2008; Somavilla *et al.*, 2014). Usually, thicker leaves possess a better tolerance against water scarcity due to enlarged palisade mesophyll cells or increase in total leaf thickness which allows the leaf to store more water (Wright *et al.*, 2004; Galmés *et al.*, 2013). Moreover, a low specific leaf area (SLA) – own to high tissue thickness – in evergreen sclerophyllous species, favors adaptation to arid and semi-arid climates (Vaz *et al.*, 2010; Ramírez-Valiente *et al.*, 2020) while large leaves with high SLA - and thus thinner leaves - in non-sclerophyllous broad-leaf deciduous species reflects an acquisition resource-use strategy where light capture,

photosynthesis and resource assimilation are maximized (Pérez-Ramos *et al.*, 2013; Reich, 2014).

Morpho-anatomical leaf traits are thus critical for leaf gas exchange since they permit plants to adjust their net CO_2 assimilation (A_n), stomatal conductance to water (g_s), transpiration (E) and water use efficiency (WUE) (Franks & Farquhar, 2007; Franks *et al.*, 2009). Studies on morpho-anatomical adjustments in response to water scarcity are well documented in deciduous oak species (Thomas & Gausling, 2000; Peguero-Pina *et al.*, 2016b; Robakowski *et al.*, 2020; Hernandez & Park, 2022). In the study of Peguero-Pina et al. (2016), significant morphological and physiological differences in response to water deficit according to oak species where trees reducing the transpiring area appear to be an example of adaptation to water deficit as observed in *Quercus faginea* Lam..

Some tree species are more vulnerable than others to water deficit. *Quercus pubescens* Willd. is a widespread deciduous species in the North-Western part of the Mediterranean basin. It is a drought-resistant species (Levitt, 1980; Struve *et al.*, 2009) using a strategy to avoid leaf dehydration under water stress which is to develop a deep root system and high hydraulic conductivity that allows subsurface soil moisture uptake to leaves thus maintaining high relative leaf moisture (Nardini & Pitt, 1999; Tognetti *et al.*, 2007; Struve *et al.*, 2009). Fotelli et al. (2000) showed that among other Mediterranean oak species (i.e. *Quercus frainetto* Ten., *Quercus macrolepis* Kotschy., *Quercus ilex* L.), *Q. pubescens* maintained the highest water potential under drought conditions, reinforcing the idea that *Q. pubescens* has a greater efficiency in hydraulic transport compared to other *Quercus* species (Tognetti *et al.*, 1998b).

Our previous studies simulating future drought conditions in a *Q. pubescens* forest revealed that canopy capacity to fix CO_2 was limited in response to short, middle and long-term amplified drought (1 y, 3-4 y and 10 y after installation of a rain exclusion system, respectively) (Saunier *et al.*, 2017b, 2018; Genard-Zielinski *et al.*, 2018a; Laoué *et al.*, 2023). Such limitation in net photosynthesis in response to long-term amplified drought (>10 y) was accompanied by a higher accumulation of leaf central antioxidant defenses (i.e. carotenoids) to preserve *Q. pubescens* photosynthetic apparatus (Laoué *et al.*, 2023) at the expense of specialized antioxidant defenses (i.e. phenolic compounds) whose production imposes an energetic cost to the plant since resources are diverted away from growth processes and related central metabolism (Paul-Victor *et al.*, 2010; Agrawal, 2011).

Although morpho-anatomical adjustments are crucial for plant acclimation to drought stress (Thomas & Gausling, 2000; Peguero-Pina *et al.*, 2016b; Robakowski *et al.*, 2020; Hernandez & Park, 2022), no study has investigated such changes in *Q. pubescens* after recurrent and long-term amplified drought. In order to fill this gap, this *in natura* study analyzed whether *Q. pubescens* deploys morpho-anatomical changes (i.e. high trichome density, low stomatal density, thicker leaves) after 10 years of amplified drought allowing

the species to acclimate to future drier climatic conditions. Additionally, the present investigation explores the relationship between these morpho-anatomical adjustments and the limited net photosynthesis in trees submitted to amplified drought (Saunier *et al.*, 2018; Laoué *et al.*, 2023) and highlights if such changes could avoid water loss allowing *Q. pubescens* to withstand the increasing limited precipitation expected in the Mediterranean area.

2. Materials and methods

2.1. Study site and species

This study was conducted at O_3HP (Oak Observatory at the "Observatoire de Haute Provence"), an experimental forest site *in natura* mainly populated by ~85-100 years old *Q. pubescens*. This experimental siteallows long-term monitoring of drought impact on a Mediterranean forest. It belongs to both AnaEE-France (Analysis and Experimentation on Ecosystems) and AnaEE-ERIC (European Research Infrastructure Consortium). It is located at 60 km north of Marseille in Southern France (5°42′44″E, 43°55′54″N) at an elevation of 650 m above sea level. Annual rainfall is 830 mm and annual mean temperature 11.9 °C (Laoué *et al.*, 2023) which corresponds to a humid supra-Mediterranean bioclimate (Quézel & Médail, 2003).

This experimental site is equipped since April 2012 with a dynamic rainfall exclusion device which is deployed during some rain events from April to October to exclude between 30 and 40 % of annual precipitation (which corresponds, on average to 20 days of rain exclusion) thus simulating future climate predictions in the Mediterranean region (Lionello & Scarascia, 2018; Zittis *et al.*, 2019). Two plots are monitored, namely the amplified drought (AD) plot of 300 m^2 where trees are subjected to partial rain exclusion and the natural drought (ND) adjacent plot (300 m^2) without rain exclusion where trees grow under natural drought conditions occurring in this Mediterranean forest, i.e. they suffer seasonal water deficit under summer drought conditions (**Figure S7**). Twenty Downy oak (*Q. pubescens*) trees (10 trees under ND and 10 trees under AD; **Figure S7**) were selected within the plots to study their leaf physiological and morpho-anatomical traits in July 2021. Regarding climatic data, the year preceding leaf sampling (2020) was considered as a dry year since the annual cumulative precipitation was 499 mm which is well below the annual mean precipitation of 830 mm (**Figure 26a**). Before our sampling dates in July 2021, the studied forest was exposed to 3 months of natural drought (in May, June and July) since temperature curves were above precipitation bars in the ombrothermic diagram. Such natural drought in 2021 was intensified in the AD plot since 27% of precipitation was excluded from April to July (**Figure 26b, c**).

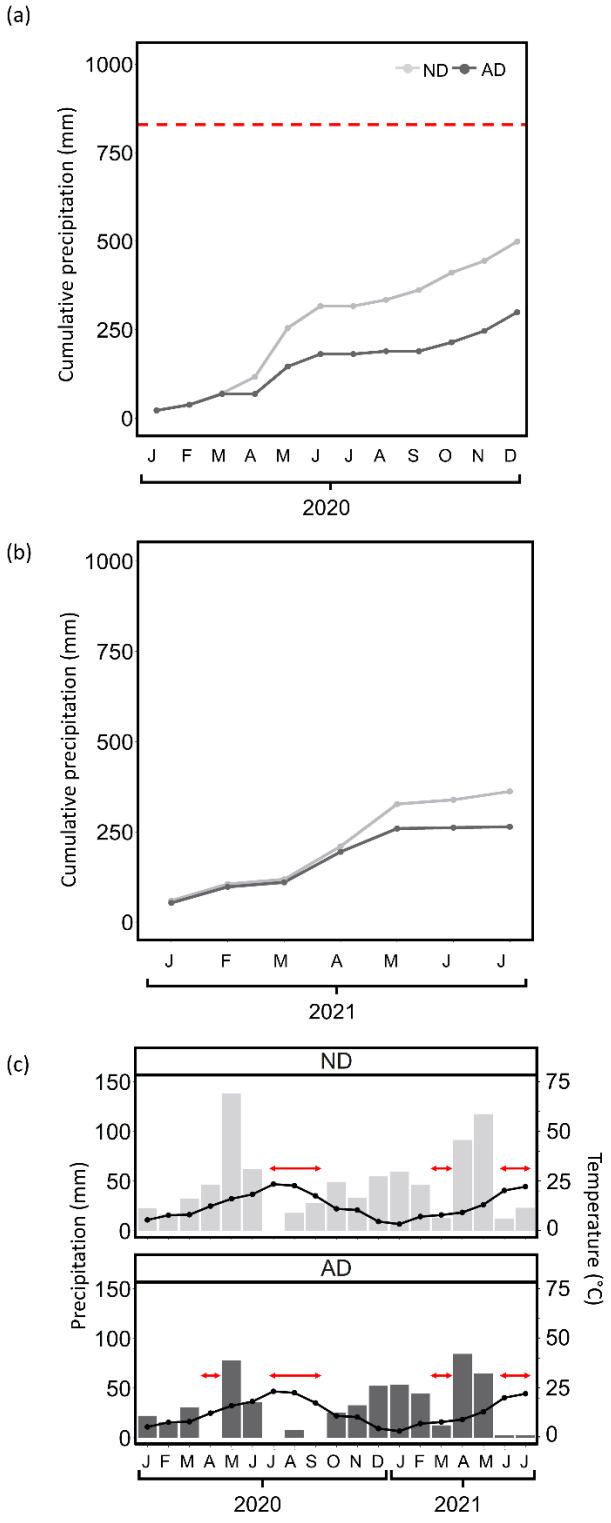

Figure 26: Climatic conditions at O_3HP. (a) Cumulative precipitation in the natural (ND, light grey) and amplified (AD, dark grey) drought plots in 2020. The dotted red line represents the annual mean precipitation calculated for the period 1967-2000 (830 mm). (b) Cumulative precipitation under ND and AD plots in 2021 (from January to July). (c) Ombrothermic diagram under natural ND and AD plots in 2020 and 2021 (until July) where bars represent monthly cumulative precipitation (P, mm) and curves represent mean monthly temperature (T, °C) with

P=2T. When temperature curves are above precipitation bars (indicated by red horizontal arrows) it corresponds to dry periods.

2.2. Physiological leaf traits

Leaf gas exchanges of CO_2 and H_2O were measured with an infrared open-gas analyzer (IRGA, CIRAS-3, PP Systems, Amesbury, MA, USA). Measurements were performed between 10 a.m. and 1 p.m. from 12-14 of July 2021 on three full sun leaves from the top of each canopy (ND and AD) accessible using an elevated footbridge (**Figure S7**). Within the leaf chamber, photosynthetically active radiation (PAR) was set to 1000 µmol m^{-2} s^{-1}, leaf chamber temperature at 27°C and CO_2 concentration at 400 µmol mol^{-1}. Physiological traits measured were the net CO_2 assimilation (A_n, µmol CO_2 m^{-2} s^{-1}), stomatal conductance to water (g_s, mmol H_2O m^{-2} s^{-1}), transpiration (E, mmol H_2O m^{-2} s^{-1}) and water use efficiency (WUE; mmol CO_2 mol^{-1} H_2O) calculated as the ratio A_n/E.

2.3. Morphological and anatomical leaf traits

Leaves were collected from the top of the canopy of each tree around midday and immediately frozen in liquid nitrogen then stored at −80 °C until use. The stomatal size, stomatal density and trichome density of *Q. pubescens* leaves were measured from 30 leaves (3 leaves/tree, 10 trees/condition) and 3 different areas/leaf (totaling 180 analyses). Measurements were performed on the abaxial surface since the adaxial surface possessed a very low density of non-glandular trichomes (NGT) and no glandular trichome (GT) (Safou & Saint-Martin, 1989; Fortini *et al.*, 2009) (also see **Figure S8**). In *Quercus pubescens*, glandular trichomes are referred as simple seriate trichomes composed of a single column of two or more thin-walled cells. Their exact function (Fortini *et al.*, 2013) and content have not been clarified but it is likely they store terpene-like compounds as in *Quercus robur* (Engel *et al.*, 1993). The leaf abaxial surfaces were observed through scanning electron microscope (Zeiss Evo 15 VP EP -SEM, Germany, 20 kV accelerating potential, 10 mm working distance) at 100X magnification to calculate the density of NGT and GT and 500X magnification for stomatal size and density. Before microscopic observations, leaf sections were sputtered with gold. Stomatal size was calculated as an ellipse from the measured guard cells length. Images were analyzed using ImageJ software (National Institutes of Health, Bethesda, MD, USA).

Leaf anatomical traits were characterized through leaf tissue thickness, leaf surface and SLA measured on 3 leaves/tree and 3 segments/leaf (1 x 0.5 cm) on either side of the main vein. Each segment was progressively dehydrated in ethanol series (70 % to 100 %, 7 times) followed by xylene and then embedded with warm paraffin. Leaf transverse sections (9 µm) were then cut using a rotary microtome (Leica biosystem

RM235, Nussloch Germany), then stained with safranin (lignified tissues) and astra blue (non-lignified tissues) and finally assembled in slides and sealed with neutral glue (Férriz *et al.*, 2023). The thickness of both, adaxial and abaxial epidermis as well as palisade parenchyma and spongy parenchyma were determined using a light microscope (Leica DM2500, Germany) at a magnification of 100X. The specific leaf area (SLA, $cm^2\ g^{-1}$) was calculated as the ratio of leaf surface (cm^2) – measured using ImageJ software – to dry mass calculated on 10-15 leaves by tree.

2.4. Statistical analyses

Differences in morpho-anatomical and physiological traits between drought conditions (ND and AD) were tested with principal component analysis (PCA), using FactoMineR and factoextra packages (Husson *et al.*, 2010; Kassambara, 2020), followed by PERMANOVA using vegan package (Oksanen *et al.*, 2013) with 9999 permutations as well as with Student tests ($P < 0.05$). The relationship between physiological and morpho-anatomical traits within each drought condition was determined by Pearson correlation coefficients (r) using the "cor.test" function. Pearson's correlation matrices (Hmisc package with "rcorr" function; Harrell Jr 2014) were performed to assess relationship between physiological traits and between leaf thickness traits with drought conditions pooled together. Data were log-transformed when necessary to reach normality and homoscedasticity. All statistical analyses were performed using R software v.4.0.3 (R Core Team, 2020).

3. Results

3.1. Changes in leaf functional traits after 10 years of amplified drought

When all traits (physiological and morpho-anatomical) were considered together, trees growing under ND and AD significantly differed in terms of morpho-anatomical traits, as explained by the first PCA component (PC1) (PERMANOVA, $P < 0.05$) which explained 35.2% of the variability (**Figure 27**). The second PCA component (PC2) was more correlated with physiological traits (g_s, E and WUE) and explained 18 % of the variation (**Figure 27**). According to PC1, trees under long-term amplified drought (AD) featured higher values of SLA and non-glandular trichome density (NGTD), whereas they exhibited lower leaf surface, stomatal density (SD) and glandular trichome density (GTD) as well as lower leaf thickness-related traits (mesophyll, palisade, spongy and total leaf

thickness) than trees under ND. The most discriminant traits in PC1 were total leaf thickness and leaf thickness-related traits (i.e., mesophyll, palisade and spongy thickness), indicating a remarkable dichotomy between AD and ND conditions according to these traits. Correlation values of each variable with the two principal components are shown in **Table S3**.

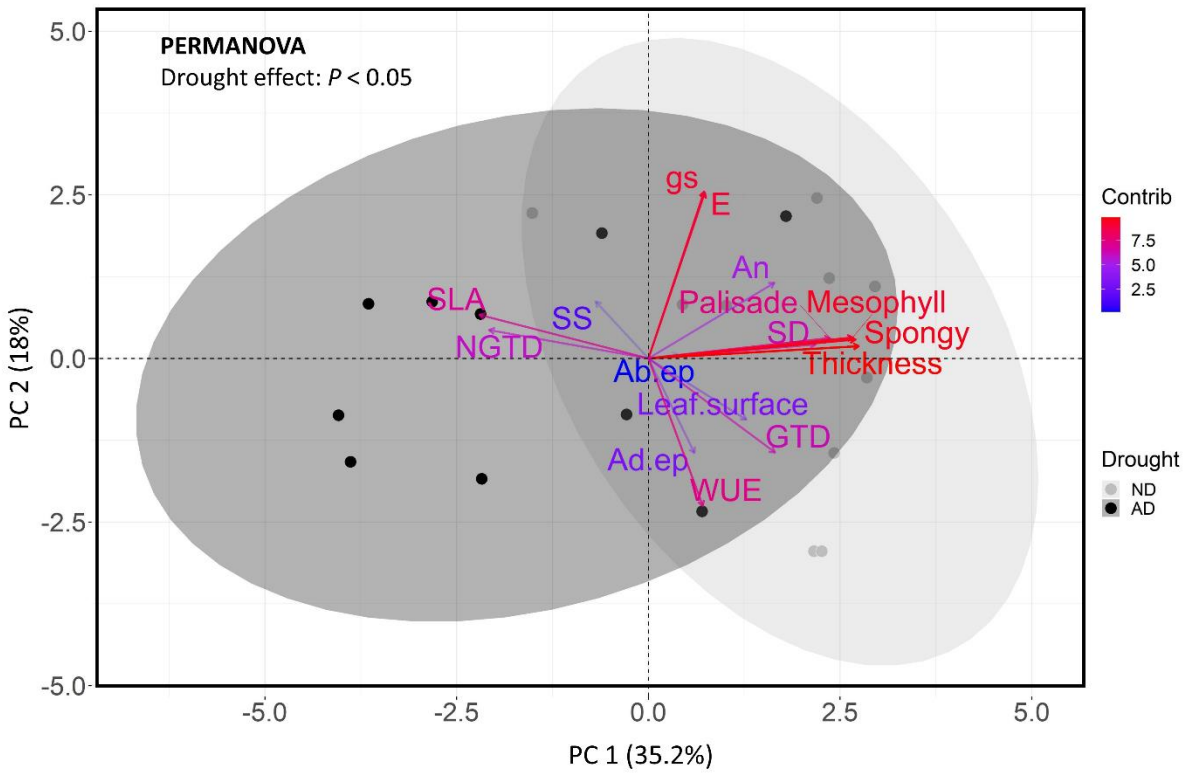

Figure 27: Principal component analysis (PCA) for the first two PCA axes including all physiological and morpho-anatomical traits measured in this study. Color scale indicate the contribution of each variable with red indicating high contribution and blue low contribution. Drought conditions are represented in light grey (ND) and dark grey (AD), with n=10 for each condition and differences were tested with a PERMANOVA (permutational multivariate ANOVA). Ab. ep, abaxial epidermis; Ad. ep, adaxial epidermis; A_n, net CO_2 assimilation; E, transpiration; GTD, glandular trichome density; g_s, stomatal conductance to water; NGTD, non-glandular trichome density; SD stomatal density; SLA, specific leaf area; SS, stomatal size; Thickness, total leaf thickness; WUE, water use efficiency.

3.2. Adjustments in leaf gas exchange after 10 years of amplified drought

Among the physiological traits measured in July 2021, A_n was the only trait significantly reduced under AD ($P < 0.001$), dropping from 5.78 under ND to 2.96 μmol CO_2 m^{-2} s^{-1} under AD. The decreases also recorded in g_s, E and WUE under AD were not significant **Table 8**.

Table 8: Physiological leaf traits measured in July 2021 under natural drought (ND) and amplified drought (AD). Significant differences are tested with Student tests and are denoted using asterisks (***: $P < 0.001$). Ns: not significant. Values are mean ± se (n=10).

Physiological traits	**ND**	**AD**	
Net Assimilation (A_n; µmol CO_2 m^{-2} s^{-1})	5.78 ± 0.56	2.96 ± 0.36	***
Stomatal conductance to water (g_s; mmol H_2O m^{-2} s^{-1})	28.27 ± 4.89	19.13 ± 3.46	Ns
Transpiration (E; mmol H_2O m^{-2} s^{-1})	0.50 ± 0.10	0.32 ± 0.07	Ns
Water Use Efficiency (WUE; mmol CO_2 mol^{-1} H_2O)	15.63 ± 2.85	13.07 ± 2.14	Ns

3.3. Adjustments of morphological traits after 10 years of amplified drought

Stomata, only present on the abaxial side of *Q. pubescens* leaves (**Figure 28a, Figure S8**), occurred in lower density under AD (510 stomata mm^{-2}) than in trees under ND (601 stomata mm^{-2}) ($P < 0.01$; **Figure 28b**). Stomatal size (SS) ranged from 88 to 481 μm^2 with no difference between the two drought conditions compared (**Figure 28c**). Stomatal density and stomatal size were not significantly correlated either under AD or ND (**Figure 30a**).

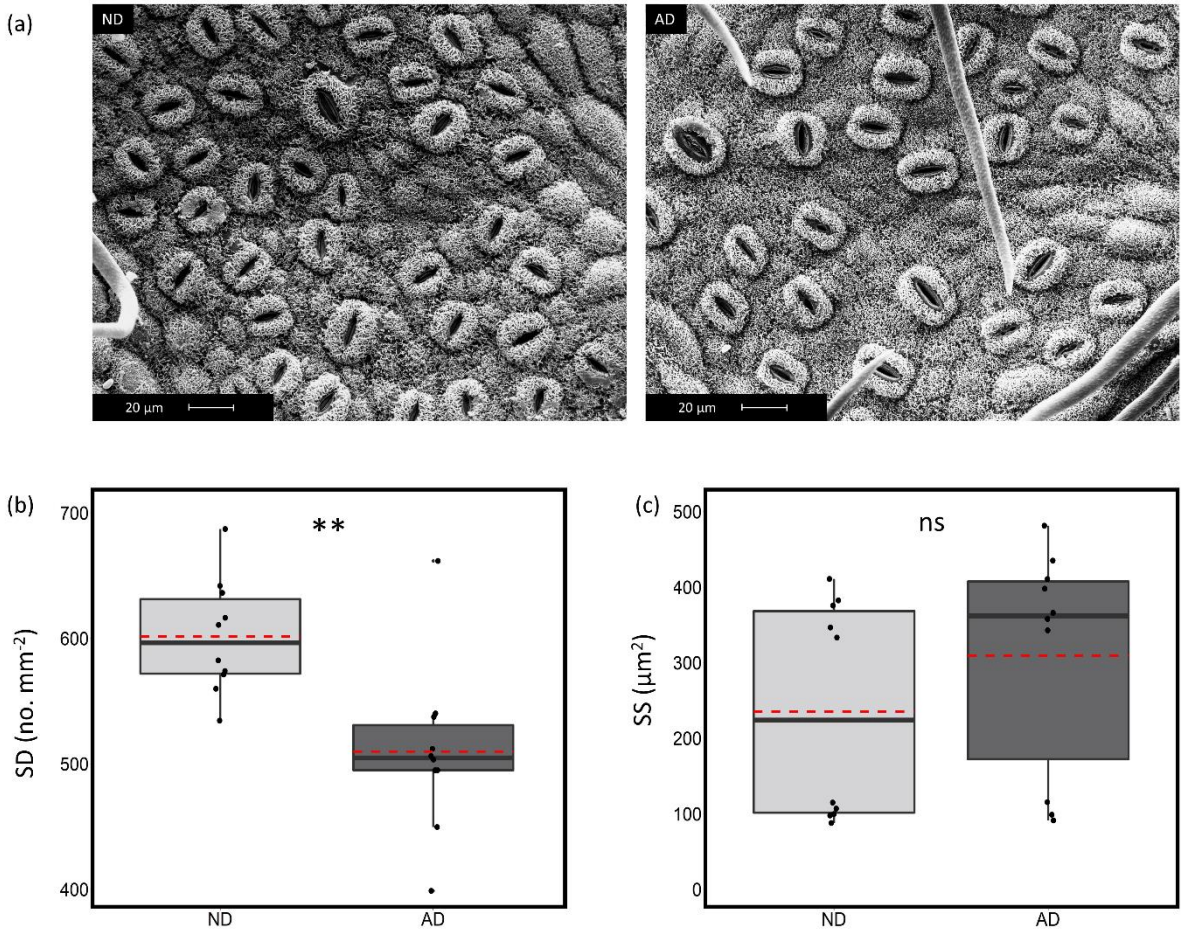

Figure 28: Leaf morphological traits of *Q. pubescens* including stomatal density and size on the abaxial leaf surface according to natural drought (ND) and amplified drought (AD) conditions. (a) Scanning electron microscopy (SEM) images of the abaxial leaf surface under ND (left) and AD (right). (b) Stomatal density (SD). (c) Stomatal size (SS). The horizontal black lines inside the boxes are the medians and the horizontal red dashed lines are the means (n=10 trees). Differences between ND and AD were tested with Student tests with asterisk denoting significant differences between conditions (**: 0.001 < *P* < 0.01; ns: not significant).

Q. pubescens abaxial leaf surfaces were covered by a crystal wax layer and presented two types of trichomes namely the non-glandular trichomes (NGT) and the glandular trichomes (GT) (**Figure 29a**). NGT were unicellular while GT were multicellular and uniseriate (i.e., they possessed a single vertical row of cells) (**Figure 29a**). NGT density (NGTD) was on average 3 and 7 trichomes mm^{-2} under ND and AD, respectively, therefore increased under AD (P = 0.05; **Figure 29b**). By contrast, GT density (GTD) significantly dropped from 33 (under ND) to 18 trichomes mm^{-2} under AD (P < 0.05; **Figure 29c**). Interestingly, we observed a negative correlation between GTD and NGTD, reflecting a trade-off between the trichomes secreting specialized metabolites and those that do not (**Figure 30b**).

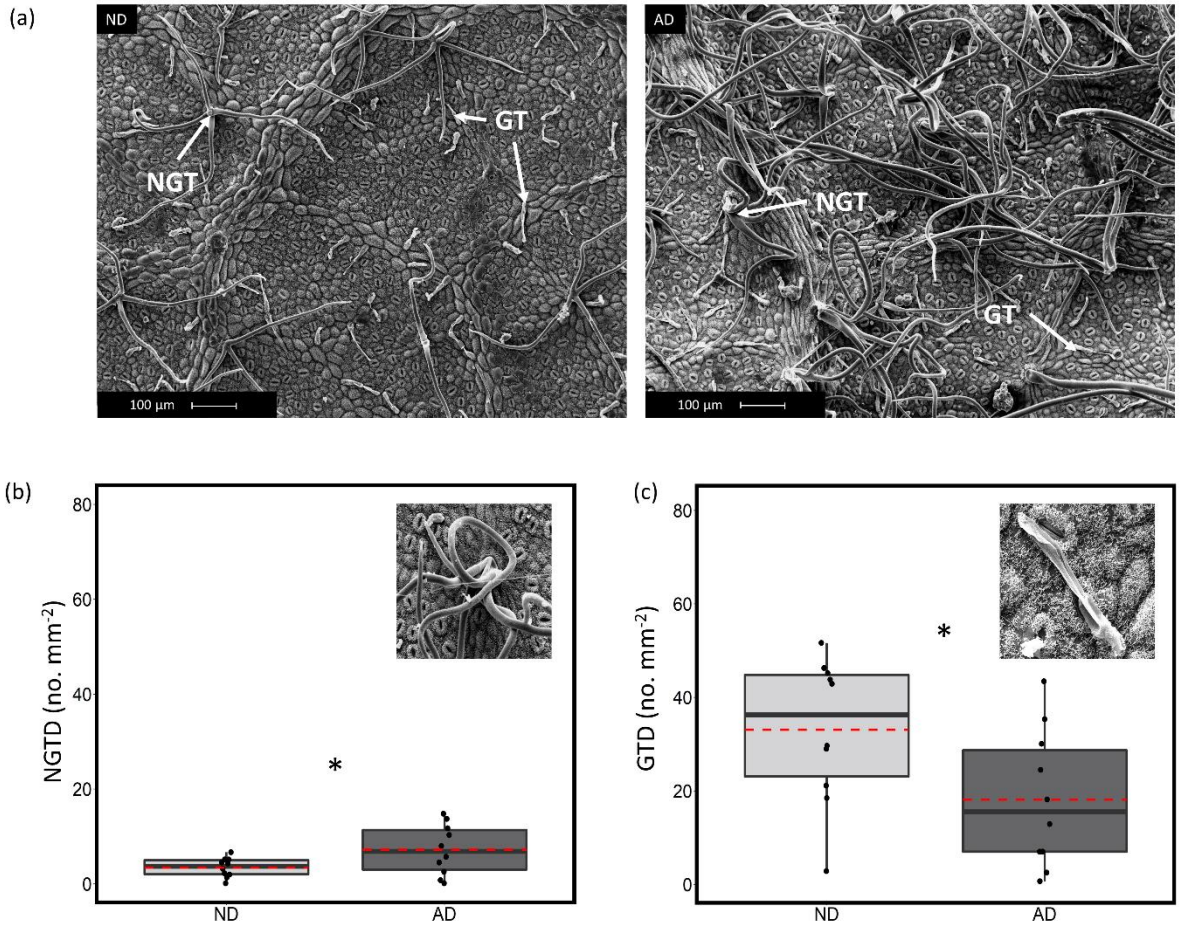

Figure 29: Leaf morphological traits of *Q. pubescens* including trichome density on the abaxial leaf surface under natural drought (ND) and amplified drought (AD) conditions. (a) Scanning electron microscopy (SEM) images of the abaxial leaf surface under ND (left) and AD (right). The arrows indicate non-glandular trichomes (NGT) and glandular trichomes (GT). (b) Non-glandular trichome density (NGTD). (c) Glandular trichome density (GTD). The horizontal black lines inside the boxes are the median and the horizontal red dashed lines are the mean (n=10 trees). Differences between ND and AD were tested with Student tests with asterisk denoting significant differences between conditions (*: $0.01 < P < 0.05$).

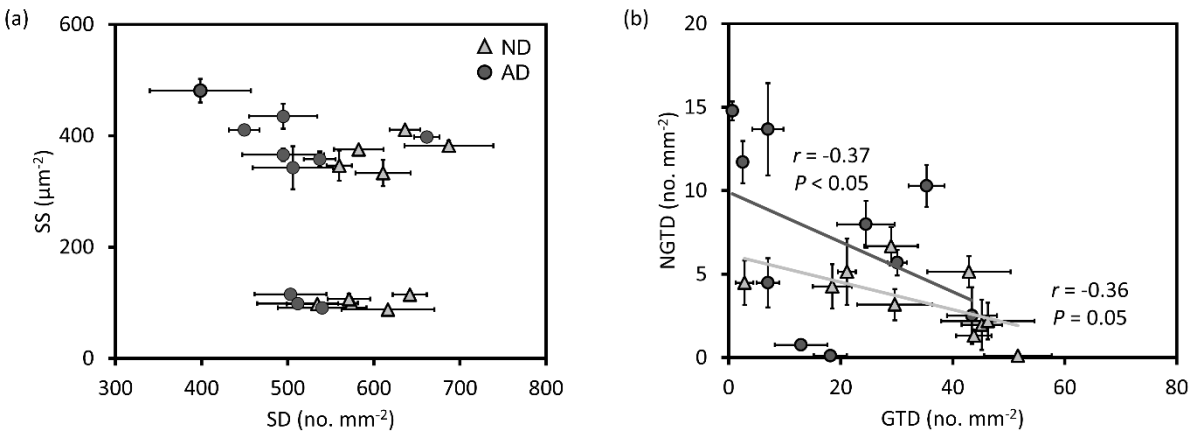

Figure 30: Linear Pearson correlations between leaf surface morphological traits. (a) Correlation between stomatal density (SD) and stomatal size (SS) under both drought conditions. (b) Correlation between glandular trichome density (GTD) and non-glandular trichome density (NGTD) under both drought conditions. In figure (b), solid light grey and dark grey lines represent the regression line for natural drought (ND) and amplified drought (AD), respectively. Pearson coefficient of determination (*r*) and P-values are indicated. Each point represents the means ± se (n=10 trees).

3.4. Adjustments of anatomical traits after 10 years of amplified drought

Leaf thickness ranged from 157 to 205 µm, and leaves were significantly thinner (-7 %) in trees growing under long-term amplified drought ($P < 0.05$; **Figure 31a, b**) because leaves had thinner mesophylls ($P < 0.05$; **Figure 31a, b**). The change in mesophyll thickness was due to a thinner spongy parenchyma thickness which significantly dropped from an average of 154 µm under ND to 141 µm under AD ($P < 0.05$; **Figure 31a, b**). Thickness of most tissues positively correlated with each other (**Figure S9**). For example, spongy and palisade parenchyma were highly correlated ($r = 0.73$, $P < 0.001$; **Figure S9**). In addition, trees under AD possessed a higher SLA in line with thinner leaves since both traits (SLA and leaf thickness) were negatively correlated ($r = 0.41$, $P < 0.01$). The leaf surface did not differ according to drought conditions, although it was slightly lower under AD (**Figure 31c**).

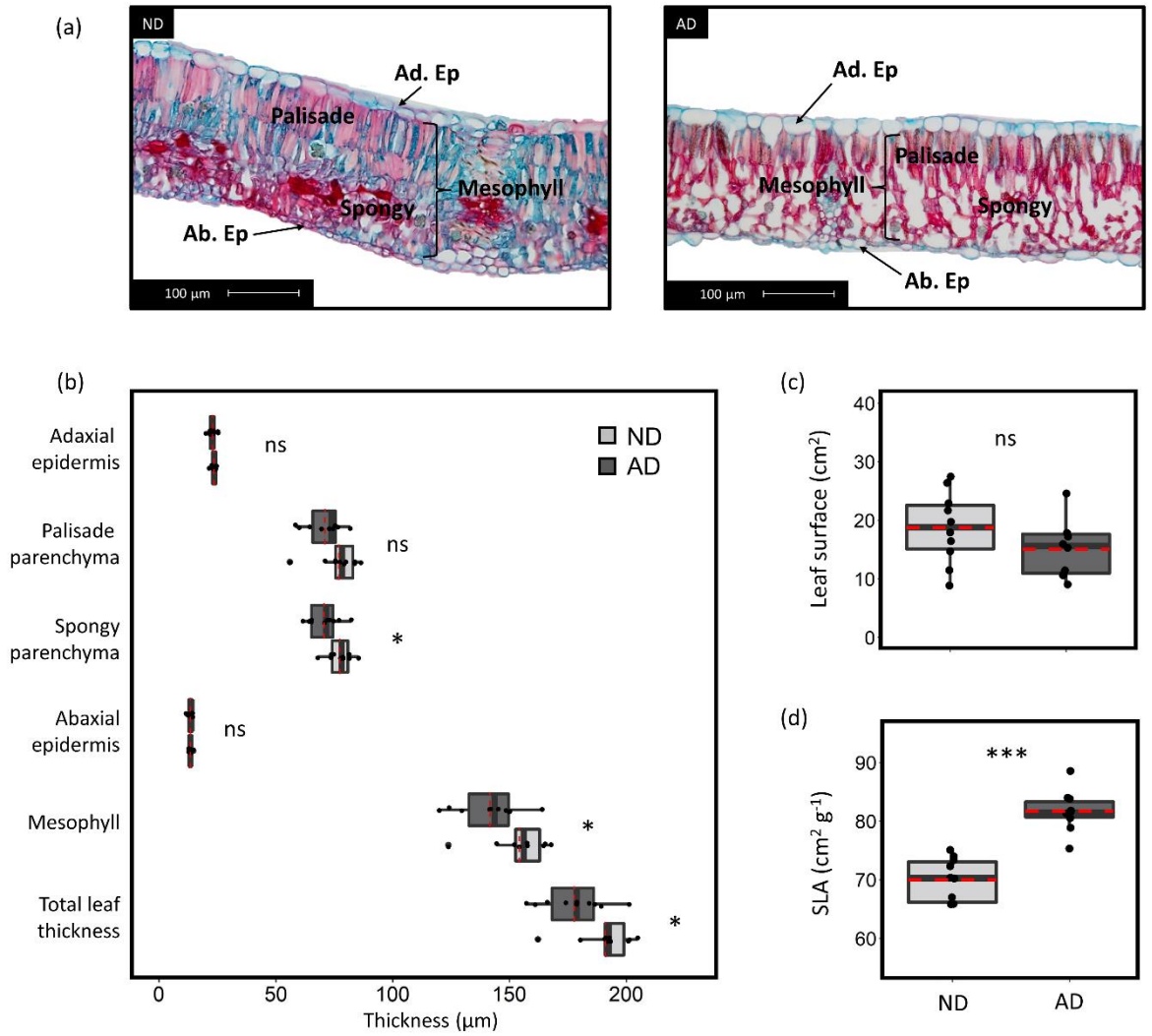

Figure 31: Leaf anatomical traits of *Q. pubescens* according to natural drought (ND) and amplified drought (AD). (a) Optical microscopy images of leaf cross sections under ND (left) and AD (right). Ad. Ep, adaxial epidermis; Ab. Ep, abaxial epidermis. (b) Leaf thickness of the different tissues. (c) Leaf surface. (d) Specific leaf area (SLA). The horizontal black lines inside the boxes represent the median and the horizontal red dashed lines represent the mean (n=10 trees). Differences between ND and AD were tested with Student tests. Asterisks denote significant differences between drought conditions (*: 0.01 < *P* < 0 .05, ***: *P* < 0.001; ns: not significant).

3.5. Concomitant morpho-anatomical and physiological adjustments in response to 10 years of amplified drought

Regarding morphological traits related to the leaf surface, higher stomatal density was associated to lower A_n under ND ($P < 0.05$) while lower stomatal density was associated to lower A_n under AD ($P = 0.06$) (**Figure 32a**). Additionally, higher NGTD under AD was

associated with low E (r = 0.43, P < 0.05; **Figure 32c**) and high WUE (r = 0.39, P < 0.05; **Figure 32d**) but was not associated with g_s (**Figure 32b**).

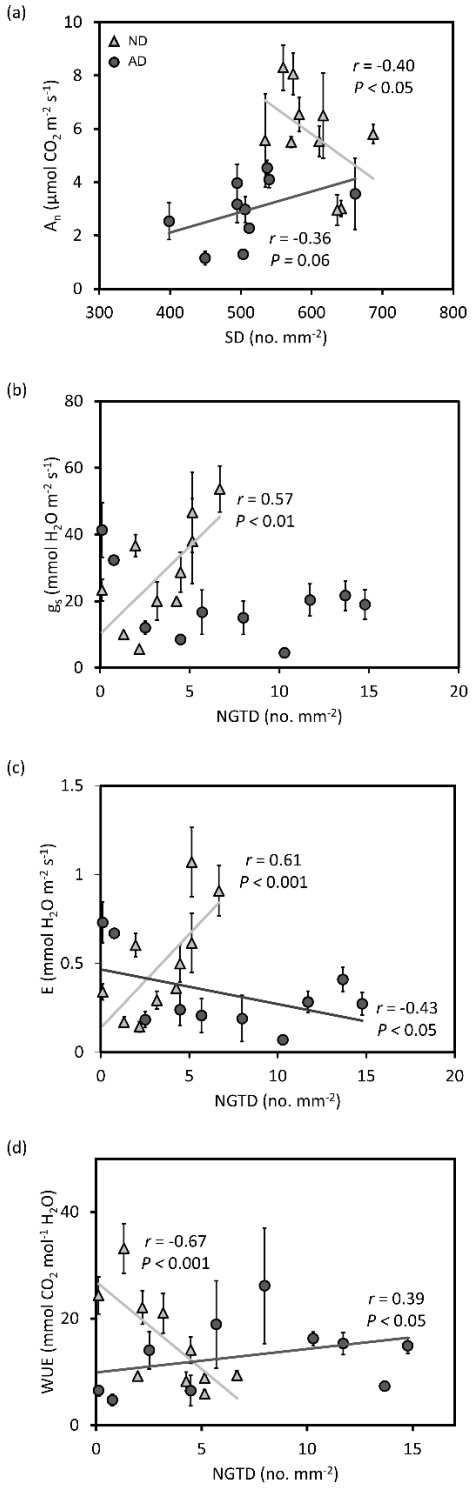

Figure 32: Linear Pearson correlations between physiological and morphological traits. A_n, net CO_2 assimilation; E, transpiration; g_s, stomatal conductance to water; NGTD, non-glandular trichome density; SD, stomatal density and WUE, water use efficiency. Solid light grey and dark grey lines represent the regression line for natural drought (ND) and amplified drought (AD), respectively. Pearson coefficient of determination (r) and P-values are indicated. Values are means ± se (n=10 trees).

The total leaf thickness was positively associated with physiological traits (A_n, g_s and E) under AD (**Figure 33a,b,c**). Especially, the decrease in A_n under AD was correlated with a decrease in the spongy parenchyma thickness (r = 0.56, P < 0.01; **Figure 33d**). Also, the spongy parenchyma thickness positively correlated with g_s (r = 0.54, P < 0.01; **Figure 33e**) and E (r = 0.48, P < 0.05; **Figure 33f**). However, the palisade thickness was not associated to physiological traits (**Figure 33g,h,i**). Lower leaf surface under AD was associated to higher WUE (r = 0.39, P < 0.05;**Figure 34**).

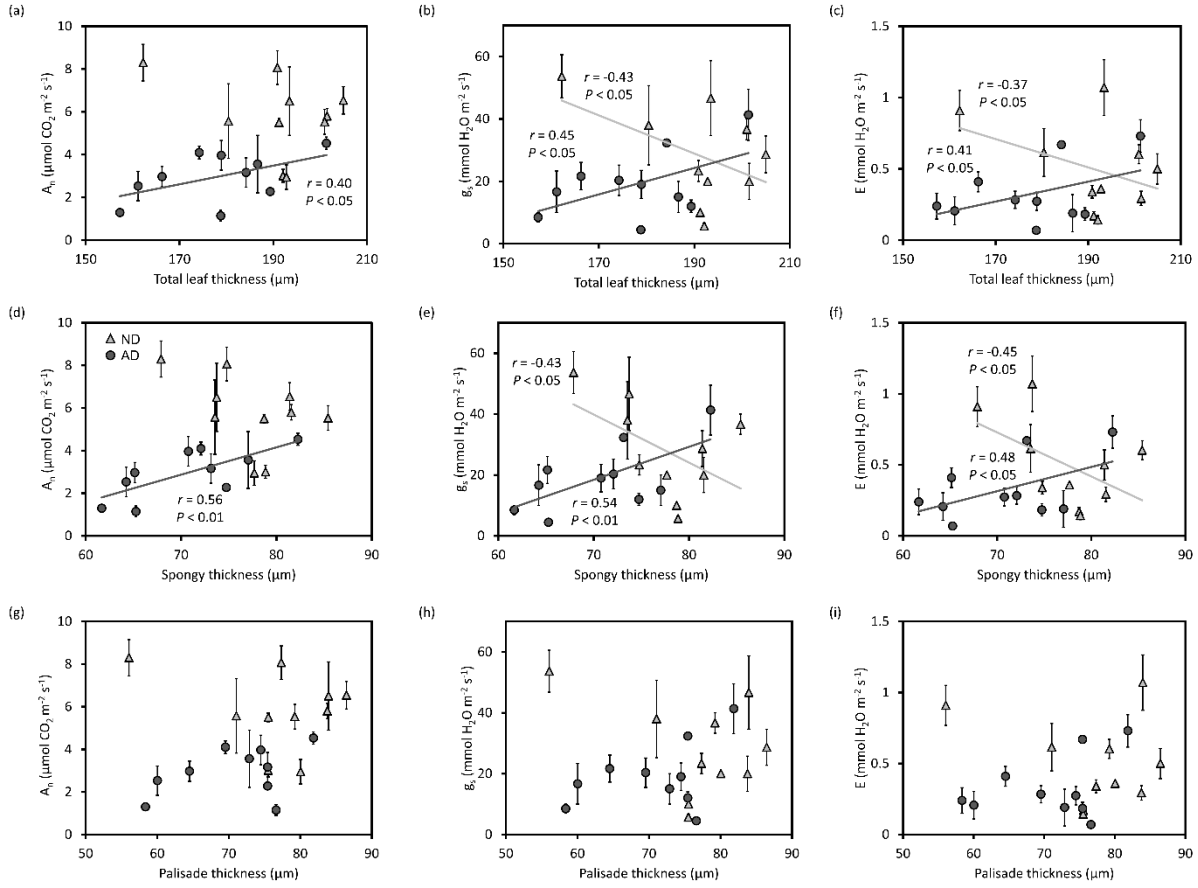

Figure 33: Linear Pearson correlations between physiological and anatomical traits. A_n, net CO_2 assimilation; E, transpiration; g_s, stomatal conductance to water and WUE, water use efficiency. Solid light grey and dark grey lines represent the regression line for natural drought (ND) and amplified drought (AD), respectively. Pearson coefficient of determination (r) and P-values are indicated. Values are means ± se (n=10 trees).

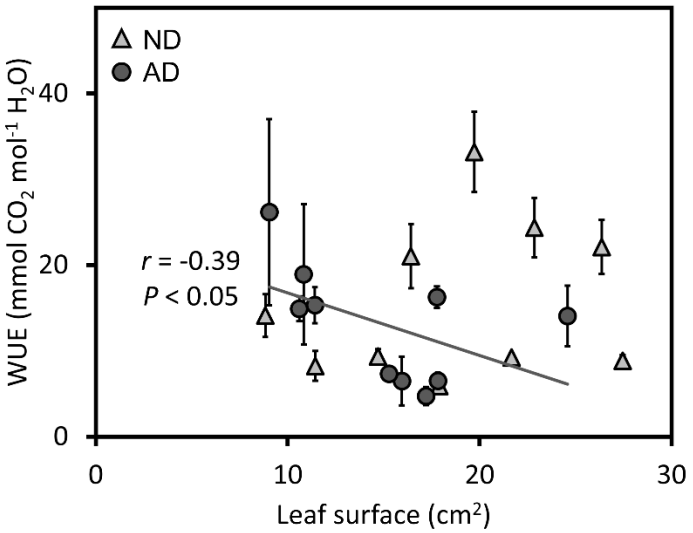

Figure 34: Linear Pearson correlations between water use efficiency (WUE) and leaf surface. Solid dark grey lines represent the regression line for amplified drought (AD). Pearson coefficient of determination (*r*) and *P*-values are indicated. Values are means ± se (n=10 trees).

4. Discussion

Previous studies on the same site indicated that production of leaf specialized chemical defenses in *Q. pubescens* was slightly reduced (e.g. some phenolic compounds) or remained stable in response to long-term (10 y) amplified drought (Laoué *et al.*, 2023). Only some central metabolites (plastochromanol-8, lutein and neoxanthin), were more accumulated after 10 years of rain withholding indicating some capacity of *Q. pubescens* to cope with increasing drought-related oxidative pressure. In order to understand the physical strategies deployed in response to prolonged rainfall deficit, we investigated whether *Q. pubescens* exhibited morpho-anatomical adjustments and how they could contribute to tree acclimation to drought.

After 10 years of partial rain exclusion, trees exhibited signs of physiological slow down through a 49% decrease of A_n measured in summer indicating a significant impact on the capacity of *Q. pubescens* to fix CO_2. This result confirms results from Saunier et al. (2018) after 3 and 4 years of partial rain exclusion on the same experimental site. Stomatal conductance remained stable under amplified long-term drought which is explained by the capacity of *Q. pubescens* to maintain the hydraulic conductivity and relative leaf moisture content (Nardini & Pitt, 1999; Tognetti *et al.*, 2007; Struve *et al.*, 2009). In addition, the decline in net photosynthesis while stomatal conductance was stable under amplified drought, revealed that non-stomatal limitations to photosynthesis were predominant at this level of stress, as highlighted in our previous study (higher

internal CO_2 concentration in summer under amplified drought) (Laoué *et al.*, 2023). In addition, the decoupling between photosynthesis and stomatal conductance has also been reported under both water and heat stress combined for other deciduous trees and partially for *Q. pubescens* (Haldimann *et al.*, 2008; Marchin *et al.*, 2023). It is worth noting that stomatal conductance stability despite increasing aridity is also typical in anisohydric plant species such as *Q. pubescens* where stomata remain partially opened even under severe water stress conditions (Damesin & Rambal, 1995; Poyatos *et al.*, 2008). This strategy can be considered advantageous since it allows stomata to stay partially opened thus maintaining a certain CO_2 assimilation (Levitt, 1980; Genard-Zielinski *et al.*, 2014). Deciduous oak species (*Q. faginea* Lam. and *Q. pyrenaica* Willd.) do not usually show a conservative water-use strategy and tend to maintain photosynthetically active leaves during most of the summer (Mediavilla & Escudero, 2003). Such characteristic allows these species to compensate for the shorter leaf longevity compared to evergreen oak species (*Q. ilex* and *Q. suber*), which avoid irreversible leaf damage during summer drought through extremely conservative water use (Mediavilla & Escudero, 2003).

Two morpho-anatomical traits (spongy parenchyma thickness and stomatal density) were positively correlated with photosynthesis in trees submitted to amplified drought. Given that spongy parenchyma and stomata provide the physical basis for CO_2 conduction for photosynthesis and could modulate the entry and diffusion of CO_2 to fixation sites (Flexas *et al.*, 2012; Borsuk *et al.*, 2022), poor spongy parenchyma thickness and stomatal density under amplified drought could have resulted in limited photosynthesis rates. Although reducing stomatal density has been described as an advantageous strategy allowing to limit both g_s and E (Liu *et al.*, 2015; Hughes *et al.*, 2017; Morales-Navarro *et al.*, 2018), stomatal density did not correlate with these physiological traits in our study. It is worth noting that only stomatal density changes do not necessarily limit gas exchange, but rather the combination with stomatal size. Indeed, smaller and denser stomata are associated with higher maximal stomatal conductance (Henry *et al.*, 2019). In our study, the absence of changes in stomatal size could explain that stomatal traits did not influence either stomatal conductance or transpiration. Unexpectedly, stomatal density negatively correlated with A_n under natural drought (**Figure 32a**) which differs from several previous studies (Xu & Zhou, 2008; Tanaka *et al.*, 2013; Zhang *et al.*, 2014). Also, the relationship between photosynthesis and stomatal traits is not only determined by mechanical process but is more likely a combination of diffusive and biochemical process, limited by both stomatal and non-stomatal factors (Nadal & Flexas, 2018). The recent work of Trueba et al. (2022) puts some light into this relationship by demonstrating that the ratio of stomatal number to mesophyll volume, rather than the stomata number alone, is positively correlated with g_s and negatively with WUE. Such result indicates that the combination of the whole three-dimensional leaf structure combined to stomatal density has a direct impact on leaf gas exchange and thus on physiological performance of the plant. Additionally, the mesophyll conductance (g_m) can also impose the same level of limitation to photosynthesis than stomata traits or biochemistry (Gago *et al.*, 2020). Indeed, the modification in leaf structure can influence

the gas- and liquid- phase conductance and thus the CO_2 diffusion efficiency for photosynthesis (Niinemets *et al.*, 2009; Gago *et al.*, 2020).

As a whole, leaves under amplified drought exhibited a lower leaf thickness (-7%) associated to higher SLA (+14%). The opposite response to increasing water stress has been however more documented (that is, SLA decrease is associated to higher leaf thickness), particularly in sclerophyllous species like *Q. coccifera* as a strategy to limit water transpiration and favor drought resistance (Peguero-Pina *et al.*, 2016b; Ormeño *et al.*, 2020a). *Q. pubescens* growth should have been halted in trees submitted to harsher drought conditions because there is always a negative relationship between growth and drought (Weber *et al.*, 2007; Vodnik *et al.*, 2019; Gea-Izquierdo *et al.*, 2021). Indeed, in our previous study, SLA was lower in summer leaves compared to spring leaves, but such decrease was less marked under amplified (Laoué *et al.*, 2023). This result indicates that trees growing under amplified drought – and related limited carbon uptake – will experience limited leaf growth compared to trees growing under natural drought conditions. When leaves possess higher SLA but also larger leaves, this is regarded as an acquisition resource-use strategy where light capture, photosynthesis and resource assimilation are maximized (Pérez-Ramos et al. 2013, Reich 2014). In our study, leaves under amplified drought conditions showed higher SLA (as also observed in *Q. pubescens* seedlings (Genard-Zielinski *et al.*, 2014)), but also a lower A_n and potentially smaller leaf surface. This result suggests a potential loss of competitive ability – due to prolonged water stress, negatively affecting CO_2 fixation and thus leaf growth – rather than an optimal adaptation strategy as already suggested for *Q. petraea* when submitted to water stress (Robakowski *et al.*, 2020). Despite *Q. pubescens* reduces both its capacity to fix CO_2 and potentially its leaf surface under amplified drought, this could be partially offset by enhancement in WUE - as evidenced through a negative correlation between leaf surface and WUE (also previously reported in Ackerly et al. 2001) - and could also be advantageous by reducing tissue construction costs. A reduction in leaf size has already been proposed as one of the key traits that allows different Mediterranean oaks to cope with drier conditions (Baldocchi & Xu, 2007; Peguero-Pina *et al.*, 2016b).

Despite the lower stomatal density under amplified drought, transpiration rate did not drop (as also reported in spring and autumn (Laoué *et al.*, 2023)), which could be an indicator of *Q. pubescens* capacity to acclimate to long-term water stress. This could be explained by both, partial stomatal closure to preserve hydraulic conductivity (Nardini & Pitt, 1999) but also by a higher non-glandular trichome density (+52%) which negatively correlated with transpiration in trees under amplified drought. These trichomes have indeed been suggested to limit transpiration by reducing the boundary layer conductance, thereby minimizing water loss (Buckley *et al.*, 2022). The higher density of non-glandular trichomes under amplified drought is consistent with several studies where water stress increased the density of leaf trichome to limit water loss eventually conferring drought resistance in *Quercus* species (Mediavilla *et al.*, 2019; Hernandez & Park, 2022) and other plant species (Gonzáles et al., 2008; Galdon-Armero et al., 2018; Chen et al., 2022).

Unlike unicellular non-glandular trichomes, multicellular glandular trichomes – identified in the abaxial leaf surface, as previously reported (Safou & Saint-Martin, 1989; Fortini *et al.*, 2009) – did not seem to provide any advantage against long-term amplified drought. The glandular trichome density was on average two-fold lower in trees under amplified drought compared to trees under natural drought and correlated negatively with the non-glandular trichome density, which indicates a trade-off between these two types of trichomes when trees are subjected to carbon-uptake-limiting conditions (as suggested by the drop in A_n). When water resources are limited during drought periods, the production of simple unicellular structures (i.e., non-glandular trichomes) may be prioritized over multicellular glandular trichomes, since the former is less costly (Hare *et al.*, 2003).

Another plausible explanation for the poorer density of glandular trichomes under amplified drought is the limited capacity of *Q. pubescens* to produce terpene-like defense compounds under pronounced water scarcity. Although further research is required to confirm this hypothesis, *Q. pubescens* leaves contain small amounts of monoterpene compounds (Santonja *et al.*, 2015) which are likely to be stored within glandular trichomes as in *Q. robur* leaves (Engel *et al.*, 1993). Furthermore, alike isoprene, whose synthesis was impacted since the third year of rain restriction in our field site (Saunier *et al.*, 2018), monoterpene synthesis and storage could also be reduced after 10 years of partial rain exclusion since isoprene and monoterpenes are produced from the same precursors, isopentenyl pyrophosphate (IPP) and dimethylallyl pyrophosphate (Zhao *et al.*, 2013). Producing a poor density of glandular trichomes under amplified drought would thus avoid an unnecessary extra-cost production for *Q. pubescens* when it grows under long-term amplified drought.

All these results suggest that the trade-off between both types of trichomes in favor of low-cost non-glandular trichomes confers a competitive advantage in terms of resistance to long-term drought (and more particularly, limiting leaf transpiration) despite the partial loss in the production of specialized defenses (isoprene, phenolic compounds) under amplified drought observed in previous studies (Saunier *et al.*, 2017b, 2022; Laoué *et al.*, 2023). Altogether, the decrease observed in all the different leaf traits analyzed express carbon limitation in trees under long-term amplified drought.

5. Conclusion

In conclusion, *Q. pubescens* functioning was clearly limited under long-term partial rain exclusion since net photosynthesis was two-fold lower (as a result of lower stomatal density and spongy thickness). Several leaf morphological and anatomical adjustments -

including a high non-glandular trichome density, a low stomatal density and a potential reduction in leaf surface - can contribute to maintain physiological functioning of *Q. pubescens* and confer protection under future drier Mediterranean climate. Another remarkable result was the trade-off between non-glandular and glandular trichomes reflecting an important adjustment where low-cost non-glandular trichomes are favored providing both, a more limited transpiration rate (also provided by partial stomatal closure) and lower production costs. Together with thinner and potentially smaller leaves, all these adjustments could contribute to minimize tissue construction cost and allow *Q. pubescens* to resist against more arid summer conditions expected in the future in the Mediterranean region.

6. Acknowledgements

This study was supported by the METAPHORES project funded by the 'Centre national de la recherche scientifique (CNRS)' (Grant agreement No. 250892; MITI and DGDS). We are grateful to CNRS-INEE, IMBE, ECCOREV and OSU Phyteas for managing O_3HP as well as AnaEE-France and AnaEE-ERIC networks (https://www.anaee-france.fr/service/experimentation-in-natura/ecosystemes-forestier/ecosystemes-forestiers-mediterraneens/o3hp) and specifically the PIA ("Plan d'Investissements d'Avenir") from ANR (ANR-11-INBS-0001 AnaEE France) for providing annual funding for the site functioning. We thank Ilja Reiter for providing climatic data and Jean-Philippe Orts for assistance during field work as well as Alain Tonetto, Sarah Boularand and Louis Godaert from PRATIM imaging platform at Aix-Marseille University for assistance and training using SEM.

CHAPTER VI: Impact of long-term amplified drought on central and specialized leaf metabolites over 2016-2022 period

A decade of rain exclusion in a Mediterranean forest reveals long-term memory and trade-offs of leaf chemical defenses

Justine Laoué[1*], Michel Havaux[2], Brigitte Ksas[2], Jean-Philippe Orts[1], Ilja M. Reiter[3], Catherine Fernandez[1], Elena Ormeno[1*]

[1]CNRS UMR 7263, Aix-Marseille University, Avignon University, IRD, IMBE, Marseille France

[2]Aix-Marseille Université, CEA, CNRS UMR7265, Institut de Bioscience et de Biotechnologie d'Aix-Marseille, CEA/Cadarache, Saint-Paul-lès-Durance, France

[3]CNRS FR30989, ECCOREV, Aix-en-Provence, France

Submitted in *Scientific reports.*

Abstract

Increasing aridity in the Mediterranean region will consist of longer and recurrent drought episodes, especially in summer. These changes will occur rapidly and could strongly modify plant defenses thus endangering tree protection and eventually survival. We investigate here the response of chemical defenses from central and specialized metabolism in *Quercus pubescens* Willd., one of the most widespread Mediterranean species, to future Mediterranean drought using a long-term drought experiment where trees have been submitted to amplified drought (~ -30% annual rain restriction) since April 2012 and compared to adjacent trees growing under natural drought conditions. We focused on leaf metabolites that provide photoprotection and protection against oxidative stress including chlorophylls and carotenoids (major groups of photosynthetic pigments from central metabolism) and flavonols (a major group of flavonoids issued from specialized metabolism). Measurements were performed in summer for seven years (2016 to 2022), that is from the 5th to the 11th year of rain restriction. Amplified drought led to higher concentrations of total photosynthetic pigments, especially chlorophylls, neoxanthin, β-carotene and lutein over the 2016-2022 period. However, it also led to significant concentration decreases of defenses conferring photoprotection and protection against oxidative stress (i.e. AZ/VAZ and flavonols, respectively). Additionally, chemical defenses of *Q. pubescens* exhibited a long-term memory to precipitation where low precipitation 1 year and/or 2 years preceding sampling were associated to low concentrations of VAZ, flavonol and high neoxanthin concentrations. Our study indicates that the pronounced decline of flavonol concentration under long-term drought is counterbalanced by a higher production of several central metabolites. This type of adjustment is the result of drought memory effects, highlighting the importance of performing long-term experimental studies *in natura* for assessing forest adaptation to climate change.

Keywords: adaptation, antioxidants, central and specialized metabolites, climate change, drought, flavonols, long-term stress, pigments, rainfall exclusion, trade-offs

1. Introduction

The Mediterranean region is a critical climate-change hotspot due to the expected rapid increase of temperatures and drought episodes (Lionello & Scarascia, 2018). In this region, climatic models forecast a decrease in annual precipitation of about 30%, longer summer periods and an increase in average surface temperatures up to 4–5°C by the end of the century, especially during the warm season where temperature could reach up to 7°C (Zittis *et al.*, 2019). Such increases in drought episodes will lead to tree mortality thereby threating forest ecosystems (Young *et al.*, 2017; Ogaya & Peñuelas, 2021). Although Mediterranean forests have demonstrated great resistance and resilience to water stress, expected rapid climate change could dramatically modify tree growth, survival and species distribution (Tague *et al.*, 2019).

One of the most important consequences of drought stress is a reduction in net photosynthesis through stomatal closure resulting in an excess of energy and a high accumulation of reactive oxygen species (ROS) eventually causing DNA damage and cell death (Cruz De Carvalho, 2008; Das & Roychoudhury, 2014). To limit photosynthetic damage and oxidative stress associated to water limitation and other abiotic constraints, plants have evolved diverse mechanisms including the production of a vast diversity of chemical defenses which are classified as central and specialized metabolites.

Plant central metabolites – also known as primary or universal metabolites – are essential for growth and development and for universal metabolic process such as photosynthesis whereas plant specialized metabolites (formerly named "secondary metabolites") are specifically involved in plant environmental interactions, stress responses and survival and account for supplementary plant defenses (Erb & Kliebenstein, 2020; Sytiuk *et al.*, 2023). Among central metabolites, chlorophylls are crucial pigments involved in photosynthesis which can be strongly affected by water deficit (Mohawesh, 2016; Noori *et al.*, 2018). In addition, carotenoid pigments such as β-carotene, lutein or those from the xanthophyll cycle (violaxanthin, zeaxanthin, antheraxanthin; hereafter referred to as VAZ) act as ROS scavengers (d'Alessandro & Havaux, 2019). Among carotenoids, the de-epoxidation of violaxanthin to antheraxanthin and zeaxanthin (denoted by increasing the ratio AZ/VAZ) is a major reaction indicator of the dissipation of excess energy in the antennae of the photosynthetic apparatus which plays a crucial role to cope with photo-oxidation in water-stressed photosynthetic tissues (Fernández-Marín *et al.*, 2020).

In addition to central antioxidant metabolites, specialized metabolites are widely spread in the plant kingdom where they play essential roles in plant defense. The major classes of plant specialized metabolites are terpenoids, phenolic compounds and alkaloids. Among phenolic compounds, flavonoids account for the most widespread group and include flavonols, well known for their role during drought stress, particularly as

antioxidants and UV-screening, thus conferring protection against oxidative stress and photoprotection (Pollastri & Tattini, 2011; Laoué *et al.*, 2022).

Foliage defenses deployed against short-term exposure to drought are well documented in various plant species both, in natural and controlled conditions (Spieß *et al.*, 2012; Genard-Zielinski *et al.*, 2014; Saunier *et al.*, 2018; Alam *et al.*, 2021) while long-term exposure, especially *in natura*, remains poorly explored (Rivas-Ubach *et al.*, 2014; Laoué *et al.*, 2023). Studies on *Quercus pubescens* Willd. – recognized for its resistance to relatively long drought periods (Nardini & Pitt, 1999; Genard-Zielinski *et al.*, 2018a; Saunier *et al.*, 2018) and highly spread in the northern Mediterranean basin (over 307,000 hectares in Southern France; IGN 2023) (Quézel & Médail, 2003) – reveal that amplified drought during the 1st (Genard-Zielinski et al., 2018), 3rd, 4th (Saunier et al., 2022, 2018, 2018) and 10th year (Laoué *et al.*, 2023) in the field clearly halts tree functioning through limited CO_2 fixation with moderate modifications of leaf metabolome and only clear drop in storage of some antioxidant metabolites (related to central and specialized metabolism). The common approach of all these studies is the comparison of tree response under natural and restricted precipitation during the current year, but neglect whether this response is influenced by precipitation from previous years (Forner *et al.*, 2018) or by precipitation during the growing season, which strongly influences plant growth (Zhang *et al.*, 2020; Wang *et al.*, 2022). Plant memory – described by Trewavas (2003) as "the ability to access past experience so that new responses incorporate relevant information from the past" – has been well related to plant growth (Julio Camarero *et al.*, 2018; Itter *et al.*, 2019; Peltier *et al.*, 2022; Marqués *et al.*, 2022) while few studies have tackled its influence on plant metabolome (Auler *et al.*, 2021; Kambona *et al.*, 2023; Kartashov *et al.*, 2023). Likewise, while monitoring of tree growth over years is a common approach to study tree growth pattern over climatic variability (King *et al.*, 2013; Etzold *et al.*, 2014; Joshi *et al.*, 2022), monitoring of central and specialized metabolism over several years has never been tested so far in forest ecosystems.

The present study aims to assess the response of central and specialized metabolites of *Q. pubescens* to long-term amplified drought expected in the Mediterranean area. For this purpose, we (i) compared *Q. pubescens* response growing under natural drought (ND) and amplified drought (AD) from the 5th to the 11th year of rain restriction, (ii) analyzed the precipitation memory effects in terms of leaf metabolic concentrations, and (iii) correlated central and specialized metabolites where a negative correlation would be indicator of a putative trade-off between central and specialized leaf defenses.

2. Materials and Methods

2.1. Study site, sampling design and campaigns

Q. pubescens was studied at the O_3HP (the Oak Observatory at the Observatoire de Haute-Provence), an *in natura* experimental site located in the French Mediterranean area (5°42′44″E, 43°55′54″N) which is part of the European research infrastructures AnaEE-France (Analysis and Experimentation on Ecosystems) and AnaEE-ERIC (European Research Infrastructure Consortium). The study site is located in a forest dominated by *Q. pubescens* and is characterized by a supra-Mediterranean sub-humid bioclimate with an average annual precipitation of 784 mm and annual mean temperature of 13.1 °C for the period 1993-2022. The O_3HP is equipped with dynamic rainfall exclusion system allowing to exclude annual precipitation by ~30% on a forest plot of 300 m^2 referred to as "amplified drought" (AD) (**Figure 35a,b**) and with a footbridge that provides access to the canopy (**Figure 35c**). Annual precipitation is partially excluded since April 2012 in the AD plot with a total exclusion of all rain events from the beginning of July to the end of September thus simulating a drier and longer summer season (Garnier *et al.*, 2021). Trees from this AD plot are compared to trees from an adjacent plot (300 m^2) which receives natural rainfall and is referred to as "natural drought" (ND) plot.

Metabolite and physiological traits were studied in summer within each drought condition (AD and ND). Central and specialized metabolites were characterized for seven years (2016 - 2022), 2016 and 2022 corresponding to tree response after 5 and 11 years of rain exclusion, respectively. The exact sampling dates were the following: July 26th 2016, August 2nd 2017, July 18th 2018, July 17th 2019, July 8th 2020, July 15th 2021 and July 21th 2022. Ombrothermic diagrams highlight drought intensity every year, monthly cumulative precipitation, and mean temperatures (**Figure S10**). A detailed description of climatic conditions over 2016-2022 is given in the results section. Physiological traits were studied during a more restricted period, from 2020-2022. The exact dates of physiological trait measurements were July 8th -9th 2020, July 12th -13th 2021 and July 18th -21st 2022.

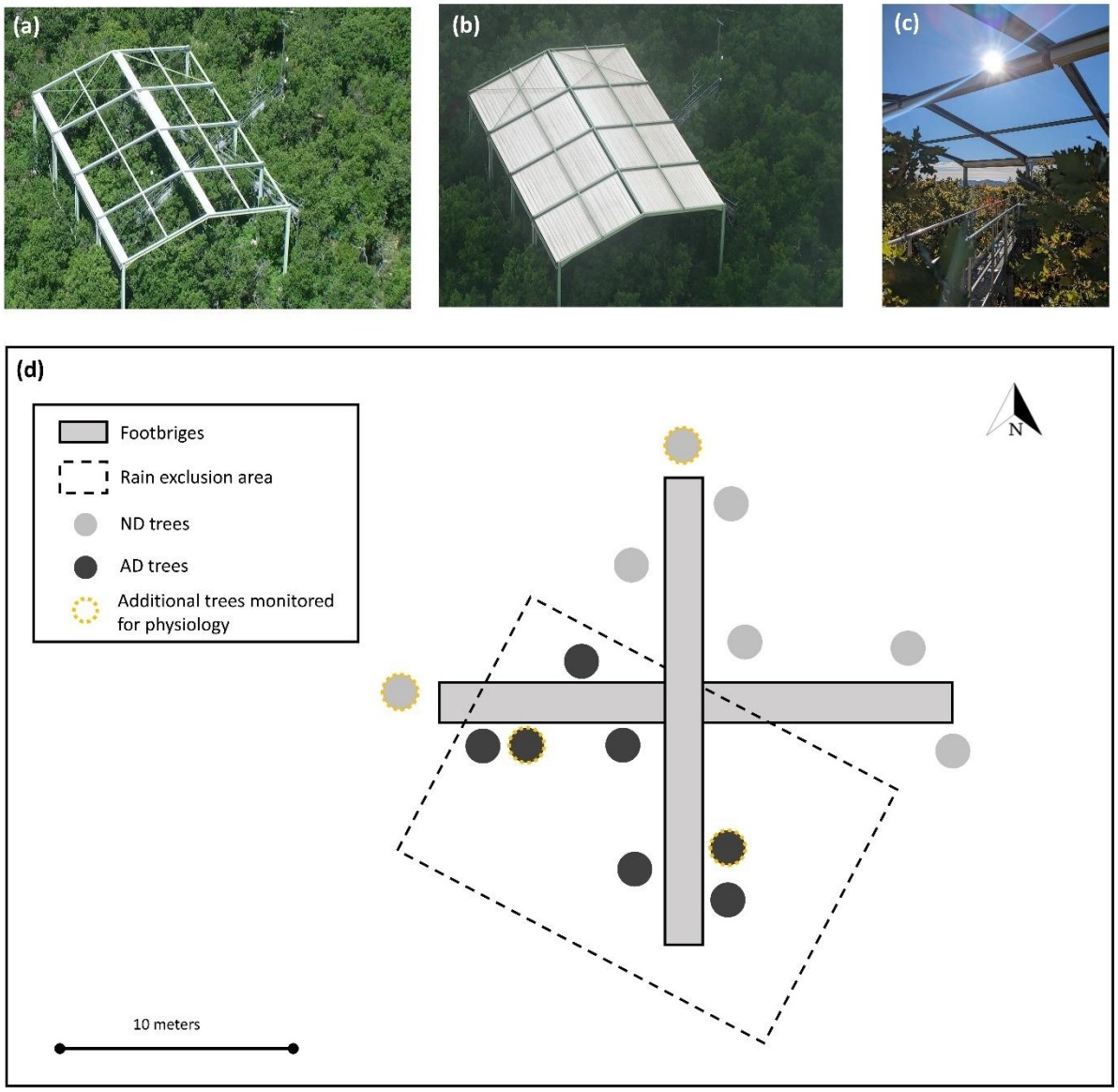

Figure 35: Experimental site at the Oak Observatory at the Observatoire de Haute Provence (O_3HP). Photo of the experimental site at the O_3HP with the exclusion device (a) opened and (b) closed. (c) Photo on the footbridge. (d) Scheme of the experimental site showing the distribution of the seven sampled trees. Trees under natural drought (ND) are shown in light grey and trees under amplified drought (AD) in dark grey. Trees circled in yellow are additional trees monitored for physiological measurements (seven trees by drought condition) and those not circled were used for metabolite analysis (five trees by drought condition).

2.2. Physiological traits

Water and CO_2 gas exchanges were measured on 7 trees per condition (**Figure 35d**) using sun-exposed leaves from the top canopy and 3 leaves by tree. Measurements were performed using an open-system gas analyzer (CIRAS-3, PP Systems, Amesbury, MA, USA) providing net CO_2 assimilation (A_n, µmol CO_2 m^{-2} s^{-1}) and stomatal conductance to water (g_s, mmol H_2O m^{-2} s^{-1}). The reference CO_2 concentration was maintained at 400 µmol mol^{-}

^{1}, the leaf chamber temperature was set to 27 °C, and the photosynthetically active radiation (PAR) was set to 1000 µmol m^{-2} s^{-1}.

Stem water potential was determined using stems containing 3 to 5 leaves on 4-7 trees per drought condition. Predawn water potential (Ψ_{pd}) was measured using a Scholander pressure chamber (PMS Instrument Co. USA; range 0–7 MPa) in the morning hours before sunrise.

2.3. Analysis of central (photosynthetic pigments) and specialized metabolites (flavonols)

Central and specialized metabolites were measured on 5 trees per condition. For each tree, 5-10 sun-exposed leaves were harvested from the top of each canopy during each sampling campaign. Leaves were immediately frozen in liquid nitrogen and stored at -80°C until analysis.

Regarding central metabolites, photosynthetic pigments of each tree were extracted using 20 to 50 mg (from 5-10 leaves previously ground using liquid nitrogen) and 2 ml of methanol. Leaf grinding was performed using liquid nitrogen and dry matter of each sample was measured after solvent volatilization and sample oven-drying in order to express results on a dry mass basis. Among photosynthetic pigments, we studied chlorophylls (chlorophyll *a* and *b*) and carotenoids from the xanthophyll cycle (VAZ: violaxanthin + antheraxanthin + zeaxanthin), as well as neoxanthin, lutein, and β-carotene. Quantification was performed by high-performance liquid chromatography (HPLC) as described in Havaux *et al.* (2007).

For specialized metabolites, flavonols were extracted for each tree using 10 mg dry matter (DM) (from 5 to 10 leaves previously ground using freeze-drying) and 1 mL of methanol containing 1% formic acid. The extract was processed using an Acquity UPLC-DAD-ESI-TQD system (Waters, USA). A C18 BEH column was used for separation, with an elution rate of 0.4 mL min^{-1} at a constant temperature of 30 °C. Flavonols were detected at 350 nm and verification of their identity or structure was accomplished using the triple quadrupole mass detector in negative ionization mode. The identity of flavonols was confirmed using external standards of monoglycosylated flavonols (quercetin and myricitrin) by triple quadrupole mass detector in negative ionization mode. More details are given in Laoué *et al.* (2023). Both, flavonols and photosynthetic pigments were finally quantified in µg g_{DM}^{-1}.

2.4. Statistical analysis

To explore metabolite and precipitation variability from 2016 to 2022 and between natural and amplified drought conditions (ND and AD) a principal component analysis (PCA) was carried out followed by a two-way PERMANOVA (with 9999 permutations). In order to assess relationship between metabolite concentrations and precipitation, Pearson's correlations were performed with drought conditions pooled together using the following precipitation: (i) total annual precipitation 1-year before sampling (from 1st January to 31st December), (ii) total annual precipitation 2-years before sampling (from 1st January to 31st December), (iii) precipitation during the growing season of the sampling year (from March 15th to leaf harvest date) and (iv) precipitation from 1st January to 15th March of the sampling year.

To highlight differences on photosynthetic pigments, flavonols and physiological traits (A_n, g_s, Ψ_{pd}) over years and drought conditions we performed a two-way ANOVA followed by post-hoc Tukey tests. Data were previously checked for normality and homoscedasticity and data were log-transformed if necessary.

The free software R v.4.0.3 (R Core Team, 2020) was employed using car, agricolae and multcomp packages for two-way ANOVA analysis. The PCA was performed using FactoMineR and factoextra packages (Husson *et al.*, 2010; Kassambara, 2020) for PCA and vegan package (Oksanen *et al.*, 2013) for the two-way PERMANOVA analyses. The correlation analyses were performed using "cor.test" function.

3. Results

3.1. Climatic conditions across years and drought conditions

The quantification of metabolites was performed in summer for seven years (from 2016 to 2022), that is from the 5th to the 11th year of rain restriction since precipitation restriction started in April 2012. Climatic data during 2014 and 2015 was considered in this study in order to determine whether precipitation during both, 1 and 2-years preceding the measurements could impact metabolite production. During the entire period of 9 years (2014-2022), ombrothermic diagrams revealed (i) six dry years (2015, 2016, 2017, 2020, 2021 and 2022) included the 2 driest years (2017 and 2020) with 3-5 dry months (**Figure 36a**, **Figure S10**) and (ii) three wet years (2014, 2018 and 2019) where total annual precipitation was well above 784 mm (**Figure 36a**). Between 2014

and 2022, from 13% to 48% of annual precipitation was excluded every year (**Figure 36a**).

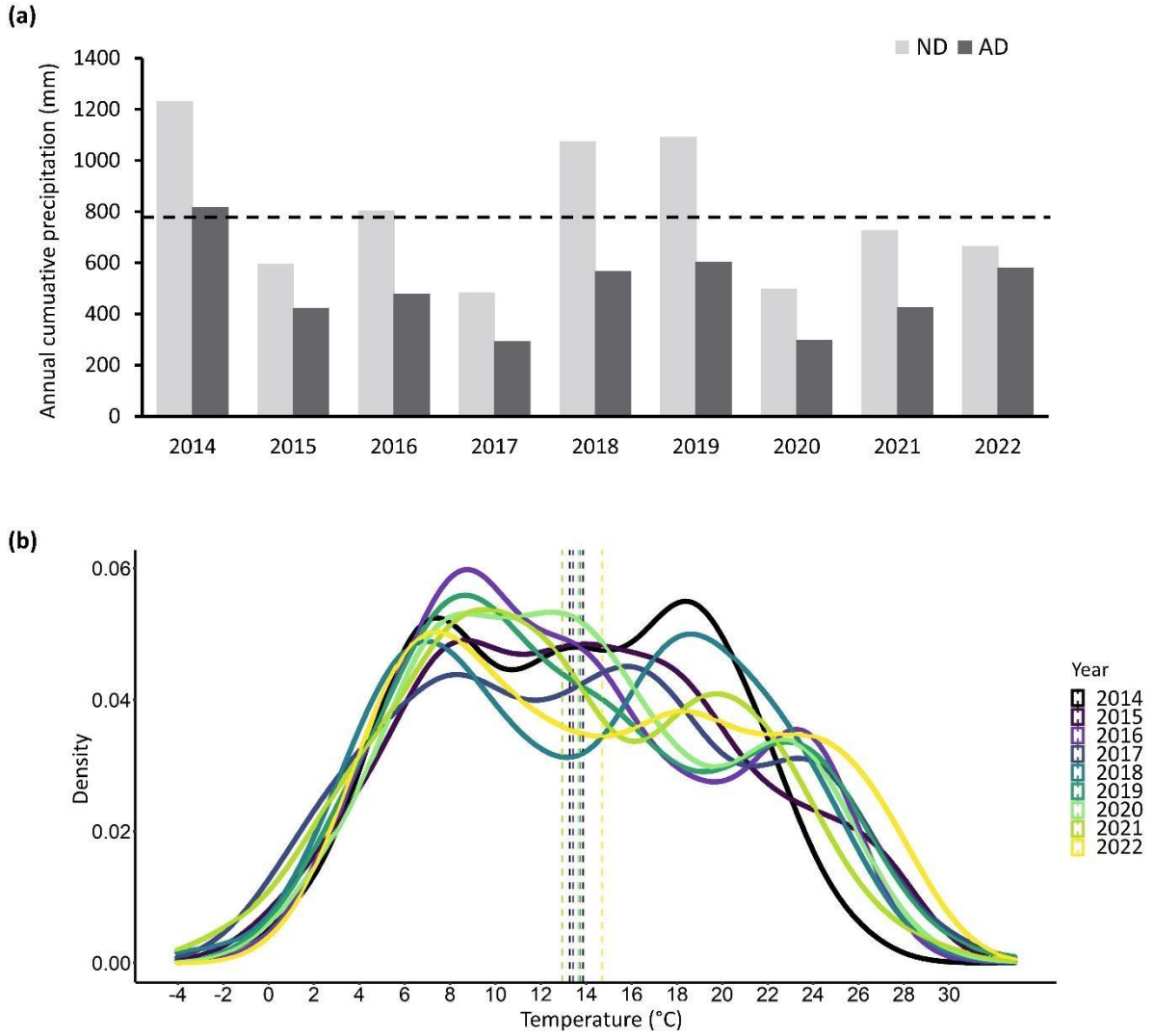

Figure 36: Climatic conditions on the experimental site from 2014 to 2022. (a) Annual cumulative precipitation for natural (ND, light gray) and amplified (AD, dark gray) drought plots for each year from 2014 to 2022. The dotted black line represents the annual mean precipitation calculated for the period 1993–2022 (784 mm). Under ND, when precipitation bars are below the 784 mm annual mean, the year is considered as "dry year" while when it is above the annual mean the year is considered as "wet year". (b) Density of temperature values for each year. The mean temperature for each year is represented by the dotted line and highlighted in the corresponding color.

Annual mean temperatures were quite similar between years excepting 2022 where it was 14.7 °C, that is, 1.6 °C above the annual mean temperature recorded in this site (i.e. 13.1 °C, over the 1993-2022 period) (**Figure 36b**). The monthly distribution of rainfall displayed different patterns according to the year (**Figure S10**). Both, 2017 and 2022 were naturally very dry displaying the highest number of dry months (up to 5 dry months under ND) and accordingly, trees under AD were also exposed to a high number

of dry months (5-7) while in 2018 trees were exposed to only two months of natural drought (**Figure S10**).

Regarding climatic conditions during the growing season (from March 15th to harvest date), precipitation was on average of 232 mm for the period 2014 to 2022. The rainiest growing season occurred in 2018 with 342 mm of precipitation while the driest growing season occurred in 2016 with only 146 mm (**Table 9**). Under AD, 43 % of precipitation was excluded during the growing season on average, while up to 72% precipitation was excluded in 2016 and no rain was excluded in 2022 since recorded temperatures were particularly high and precipitation was very low in spring 2022 (**Table 9**).

Table 9: Precipitation during both, the period from 1st January to 15th March and during the growing season (i.e. from 15th March to harvest date), and mean temperature during the growing season for 2014-2022 period.

Year	Precipitation from 1st January to 15th March (mm)		Growing season cumulative precipitation (mm)		Growing season mean temperature (°C)
	ND	AD	ND	AD	
2014	326	326	334	215	15.4
2015	144	144	160	92	16.8
2016	123	123	146	41	15.9
2017	82	43	218	84	17.7
2018	181	154	342	174	16.1
2019	62	44	213	144	15.7
2020	63	62	254	120	15.3
2021	115	107	243	158	14.4
2022	36	36	174	173	16.9

3.2. Physiological traits across years and drought conditions

Regarding physiological traits, only net CO_2 assimilation (A_n) tended to decrease by 50% under AD ($0.05 < P < 0.1$; **Figure 37a**) which represents a remarkable decline considering that A_n values under ND were rather low ranging from 3 to 11 (µmol CO_2 m^{-2}

s^{-1}) in 2020 to 2021. Tree physiology was especially slow-down in 2022 since net CO_2 assimilation was negative (**Figure 37a**) and stomatal conductance (g_s) (**Figure 37b**) and predawn water potential (Ψ_{pd}) reached the lowest values (**Figure 37c**), reflecting the extreme dry and warm conditions this year (**Table 9**).

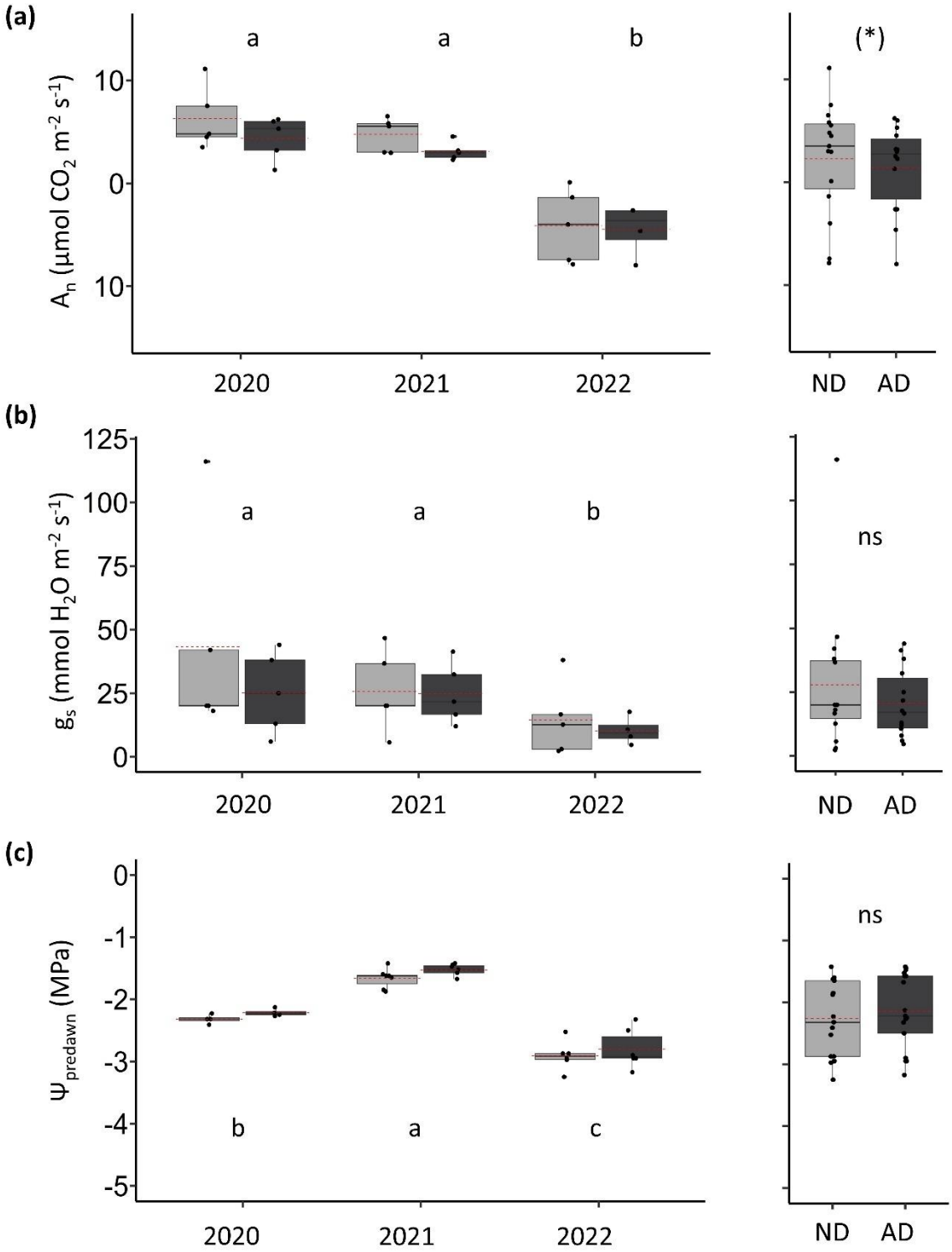

Figure 37: Physiological leaf traits. (a) Net CO_2 assimilation (A_n), (b) stomatal conductance to water (g_s) and predawn water potential ($\Psi_{predawn}$) through years (2020, 2021 and 2022) and drought conditions (natural drought (ND) in light gray and amplified drought (AD) in dark gray). Differences are tested with a two-way ANOVA. Since interaction between year and drought was not significant, significant differences across years and drought conditions are noted on separate graphs. Significant differences are denoted using letters (a > b > c) for the years and asterisks for the drought condition: (*): $0.05 < P < 0.1$. Ns is for not significant results. The horizontal black lines inside the boxes are the medians and the horizontal red dashed lines are the means (n = 4-7 trees).

3.3. Variation in photosynthetic pigments and flavonols across years and drought conditions

The PCA analysis followed by two-way PERMANOVA revealed two main principal components (PC) explaining 33% (PC1) and 15.2% (PC2) of the variance in metabolite concentrations and cumulated precipitations (**Figure 38**). This analysis highlighted a net effect of both, drought conditions and year ($P < 0.001$; **Figure 38a**). According to these axis, significant differences in metabolite concentrations were pointed out between trees growing under ND and AD where trees under AD featured higher concentration of photosynthetic pigments (lutein, neoxanthin and β-carotene and the total chlorophyll) which explained the positive part of PC1 and low concentrations of flavonols (quercetin derivatives) and AZ/VAZ represented in the negative part of PC1. Differences between drought conditions were also visible, to a lesser extent, across PC2, where trees under AD seemed to feature lower concentrations of kaempferol and myricetin derivatives.

The total annual precipitation 2 years preceding sampling was the most contributing variable to PC2 followed by the total annual precipitation 1-year preceding sampling (**Figure 38b**). Precipitation from January to March as well as during the growing season (from 15th March to harvest date) poorly contributed to the variation in the dataset (**Figure 38b**). The PCA also revealed a particular discrepancy between tree metabolite concentrations and precipitation in 2022, and the other years, where 2022 was a particularly dry and warm year and trees featured the lowest concentrations of both central and specialized metabolites.

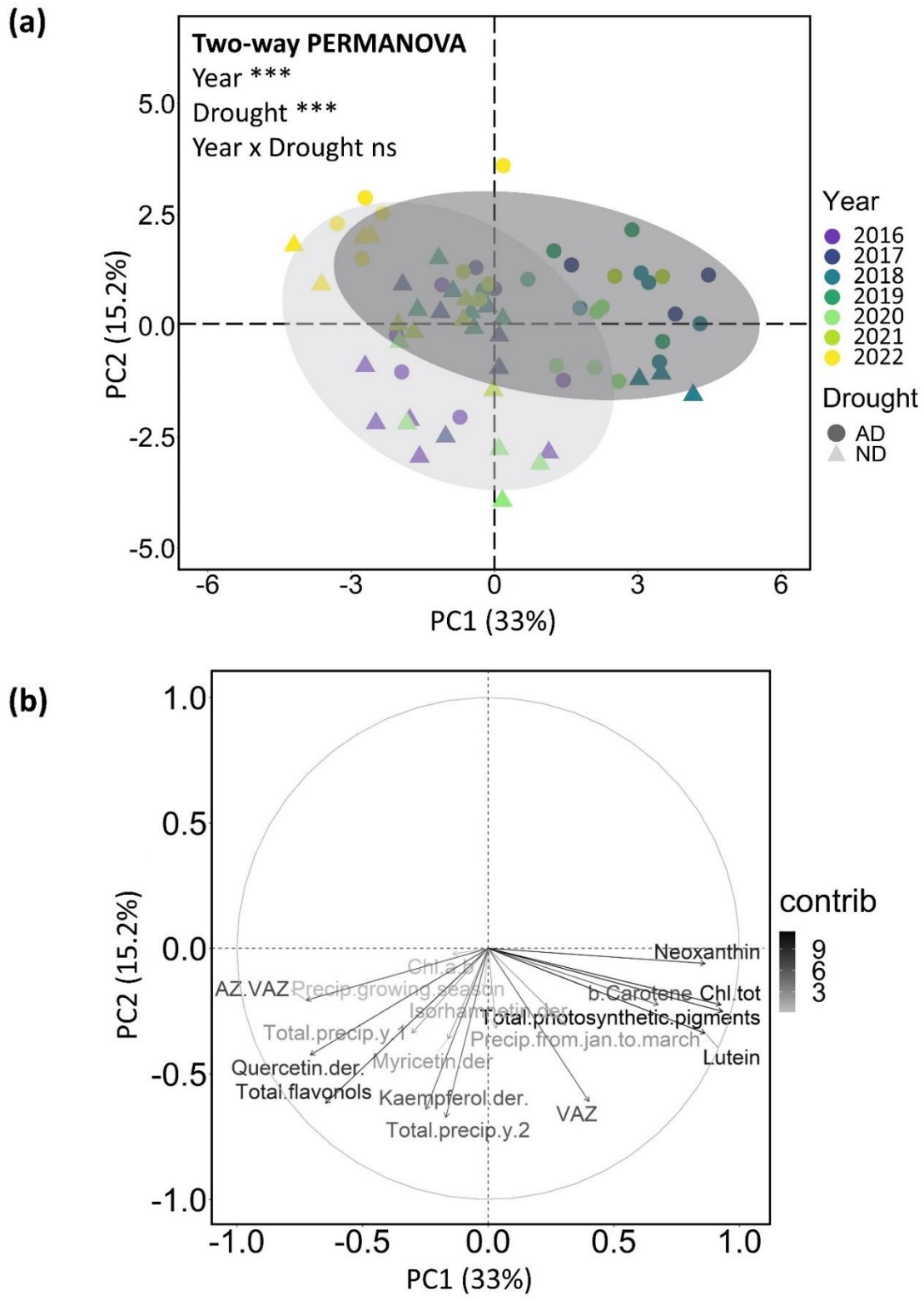

Figure 38: Principal component analysis (PCA) for the first two PCA axes of (a) individuals and (b) variables (metabolites and precipitation patterns), observed under natural drought (ND) and amplified drought (AD) from 2016 to 2022, with n = 5 for each condition. AZ / VAZ, de-epoxidation of violaxanthin to antheraxanthin and zeaxanthin; Chl. tot, total chlorophyll (chl. a + b); der., derivatives; Precip. growing season, precipitation during the growing season (from 15th March to harvest date); Precip jan. to march, precipitation from 1st January to 15th March of leaf harvest year; Total precip. y-1, Total annual precipitation 1-year before sampling; Total precip. y-2, Total annual precipitation 2-years before sampling.

Two-way ANOVA (**Figure 39, Figure 40**) also revealed significant differences in metabolite concentrations between drought conditions and across years and confirmed most differences described above. Trees under AD exhibited significantly higher concentrations in total photosynthetic pigments (**Figure 39a**) - including a 15% rise of total chlorophyll concentrations own to the increase in both chlorophyll *a* and *b* (**Figure S11**) although the ratio Chl a/b did not change (**Figure 39b, c**). In addition, the concentration of three carotenoids, namely neoxanthin, β-carotene and lutein, significantly raised under AD (up to 16% for neoxanthin) (**Figure 39d,e,f**). By contrast, the ratio AZ/VAZ significantly dropped by 23% under AD which was due to both, a clear drop of zeaxanthin concentration and a significant increase in violaxanthin under AD (**Figure S12**). The pool of metabolites from the xanthophyll cycle (VAZ) were not impacted by AD (**Figure 39g**).

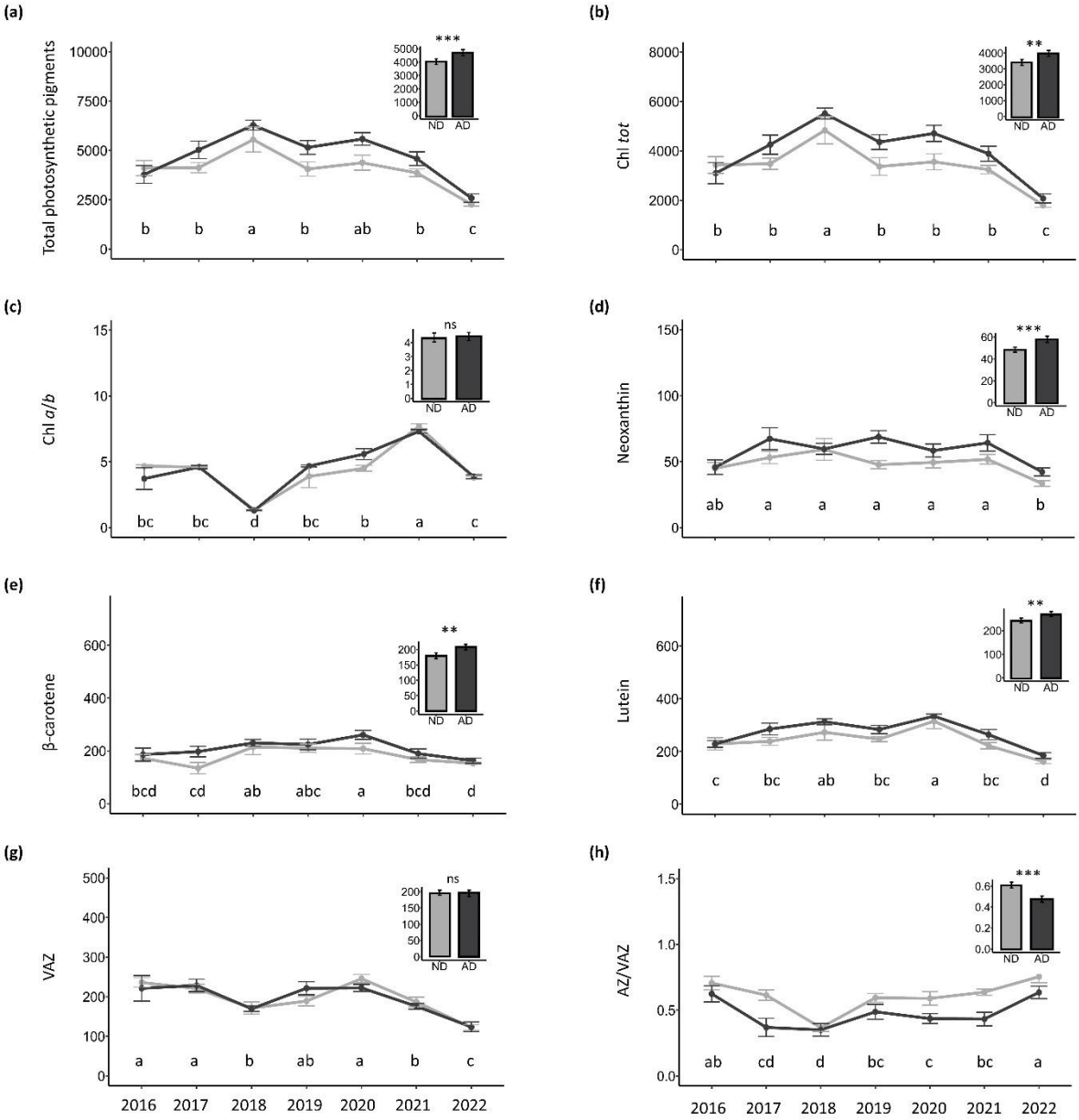

Figure 39: Leaf concentrations of photosynthetic pigments (µg g_{DM}^{-1}) according to years (from 2016 to 2022) and drought conditions. (a) Total photosynthetic pigments (carotenoids and chlorophyll). (b) Total chlorophyll (Chlorophyll *a* and *b*). (c) Ratio of chlorophyll *a* to *b* (Chl *a*/*b*). (d) Neoxanthin (carotenoid). (e) β-carotene (carotenoid). (f) Lutein (carotenoid). (g) Xanthophyll cycle (including three carotenoids: violaxanthin, antheraxanthin and zeaxanthin; VAZ). (h) De-epoxidation of violaxanthin to antheraxanthin and zeaxanthin (AZ/VAZ). Differences between years were tested with post hoc Tukey tests and are indicated with different letters (a > b > c > d). Differences between drought conditions were indicated by asterisks with **: 0.001 < *P* < 0.01 and ***: *P* < 0.001 and represented in a separate graph at the top right. Ns is for not significant results. Values are mean ± se (n =5 trees).

Regarding specialized metabolites, total flavonol concentrations significantly dropped under AD independently of the year (**Figure S13**), especially quercetin derivatives (quercetin galloyl glucose, quercetin-3-O-glucose and quercetin pentose; **Figure S14**) but

also isorhamnetin-3-glucuronique (**Figure S14**) and myricetin derivatives (myricitrin; **Figure S14**) (**Figure 40**).

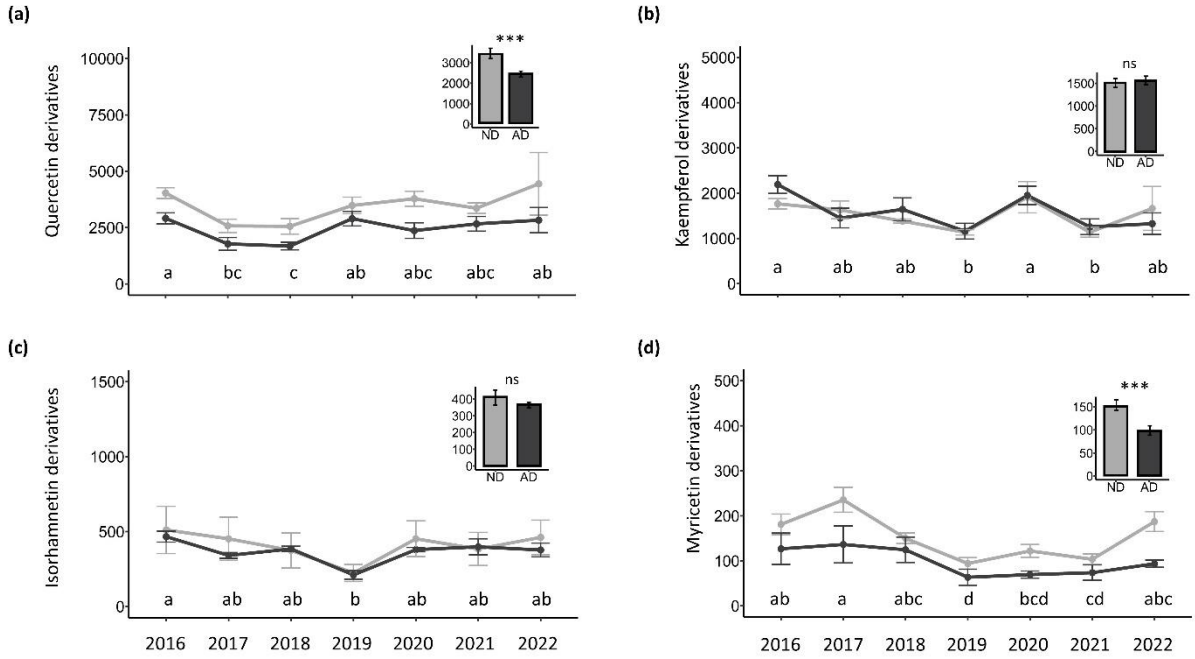

Figure 40: Leaf concentrations of flavonols (µg g_{DM}^{-1}) according to years (from 2016 to 2022) and drought conditions. (a) Quercetin derivatives. (b) Kaempferol derivatives. (c) Isorhamnetin derivatives. (d) Myricetin derivatives. Differences between years were tested with post hoc Tukey tests and are indicated with different letters (a > b > c > d). Differences between drought conditions were indicated by asterisks with ***: $P < 0.001$ and represented in a separate graph at the top right. Ns is for not significant results. Values are mean ± se (n =5 trees).

While total flavonol concentrations remained quite stable over years (**Figure S13**), the total photosynthetic pigment concentrations significantly dropped in 2022 due to the decrease in the total chlorophyll, lutein and VAZ concentrations (**Figure 39b,f,g**). Interestingly, the total photosynthetic pigments and flavonols were significantly and negatively correlated (r = -0.41, $P < 0.001$) likely indicating a trade-off between central and specialized metabolism (**Figure 41**).

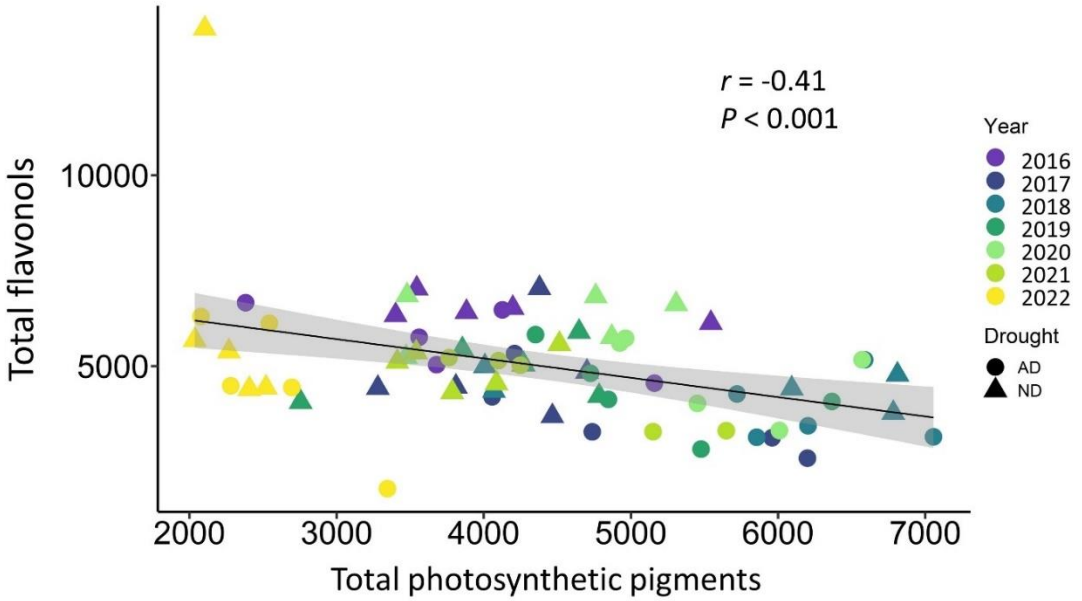

Figure 41: Linear Pearson correlation between total photosynthetic pigment and total flavonol concentrations (µg g_{DM}^{-1}). Solid line represents the regression line, both drought conditions pooled together with the shaded areas around the lines indicating the 95% of confidence interval. Circles represent trees under amplified drought (AD) and triangles represent trees under natural drought (ND). Pearson correlation coefficient (*r*) and *P*-values are indicated (n = 5 trees).

3.4. Correlations between metabolite concentration and precipitation

The PCA revealed that both, total photosynthetic pigments and flavonol concentrations were especially associated to the total annual precipitation 2-years before sampling and 1-year before sampling, rather than the precipitation during the growing season (**Figure 38**). For this reason, Pearson correlations were performed on these two cumulated precipitations. Low values of annual precipitation during the 2 years before sampling correlated to low concentrations of AZ/VAZ ($r = 0.27$, $P < 0.05$; **Figure 42a**), VAZ ($r = 0.34$, $P < 0.01$; **Figure 42b**) and total flavonols ($r = 0.41$, $P < 0.001$; **Figure 42c**). Furthermore, low annual precipitation 1-year before sampling was associated to high concentration in neoxanthin ($r = -0.24$, $P < 0.05$; **Figure 42d**) and low concentration in VAZ ($r = 0.23$, $P < 0.05$; **Figure 42e**) and total flavonol ($r = 0.31$, $P < 0.01$; **Figure 42f**).

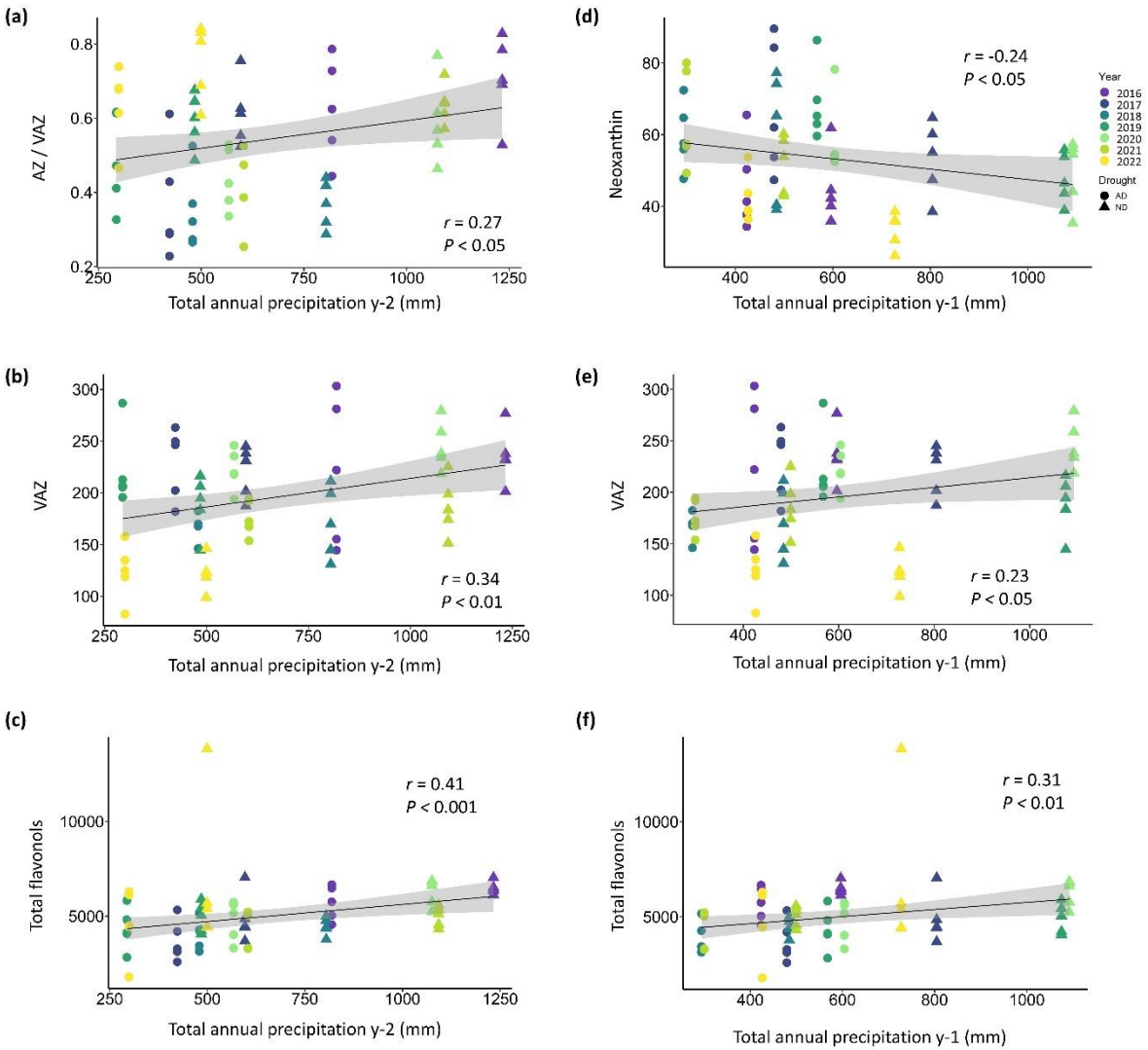

Figure 42: Linear Pearson correlations between the total annual precipitation 1 and 2-years before sampling and metabolite concentrations (µg g_{DM}^{-1}). Relationship between the total annual precipitation 2-years before sampling and (a) AZ / VAZ, (b) VAZ and (c) total flavonol concentrations, and between the total annual precipitation 1-year before sampling and (d) neoxanthin, (e) VAZ and (f) total flavonol concentrations. Solid line represents the regression line for both drought conditions pooled together with the shaded areas around the lines indicating the 95% of confidence intervals. Pearson correlation coefficient (*r*) and *P*-values are indicated.

4. Discussion

In the present study, we investigated the ability of *Q. pubescens* - a deciduous and largely distributed Mediterranean species characterized by its drought resistance - to cope with long-term precipitation restriction simulating future aridity conditions in the Mediterranean region. The original approach consisted of analyzing how both the central and specialized defenses of this species were modulated *in natura* through long-term amplified drought (AD) and the effects of cumulated precipitation across several years.

The rainfall exclusion in our field site (13 - 48% annual precipitation reduction since April 2012) implied a decline of net photosynthesis under AD from 2020 to 2022 which had already been shown during our previous studies on *Q. pubescens* in the same experimental site in 2014 and 2015 (Saunier *et al.,* 2018). Note that net photosynthesis was below zero in 2022 probably due to the very high temperatures recorded in July associated with water scarcity, pointing out the most severe climate stress on trees recorded so far for this experimental site (Genard-Zielinski *et al.*, 2018a; Saunier *et al.*, 2018; Laoué *et al.*, 2023). However, no difference occurred between both drought conditions regarding either trait, g_s and Ψ_{pd} (measured in July 2020, 2021 and 2022). Two strategies are argued to explain these results. First, *Q. pubescens* is described as an anisohydric species which only partially closes stomata during drought stress (Poyatos *et al.*, 2008), thus allowing to maintain some transpiration and photosynthesis rates even at very low leaf water potentials (Damesin & Rambal, 1995; Nardini & Pitt, 1999) such as those recorded in this study (up to -3.25 MPa). Second, *Q. pubescens* also possess a highly efficient hydraulic system as previously suggested by Nardini & Pitt (1999) allowing to maintain water content in leaves and impeding water potential drop. These two capabilities, namely partial stomatal closure and avoidance of the drop in water potential during drought stress, could explain that stomatal conductance and predawn water potential values remained stable between both drought conditions.

Regarding leaf metabolite concentrations, both 'drought conditions' and 'years' explained most of the variance (**Figure 38**). Importantly, among central metabolites, photosynthetic pigments were highly accumulated under AD. Some carotenoids, namely neoxanthin, β-carotene and lutein were triggered under AD during the 2016-2022 period, contrasting with Saunier *et al.* (2018) who observed a drop in neoxanthin and lutein concentrations during the 4th year of AD (in 2015). These metabolites play a crucial role against drought-related oxidative stress by acting as ROS scavengers (Havaux & Kloppstech, 2001; Rastogi *et al.*, 2014; Cazzaniga *et al.*, 2016). Additionally, the total chlorophyll concentration also increased under AD through the 2016-2022 period while the ratio of Chl a/b was similar between both drought conditions suggesting that the efficiency of photosynthetic process was not totally altered by AD despite the drop of net photosynthesis recorded herein and in previous studies (Saunier *et al.*, 2018; Laoué *et al.*, 2023). The accumulation of some carotenoids coupled with the increase in total chlorophyll concentration did not impede the photosynthesis decrease (- 50%) under AD over the 2020-2022 period. Since the drop of net CO_2 assimilation in summer was even stronger (- 60%) during the 4th year of rain restriction (Saunier *et al.* 2018) when such metabolic adjustments (accumulation of some carotenoids and chlorophylls) had not yet been observed, our results indicate upregulation of the synthesis of these central metabolites to cope with long-term water deficit. These observations are in line with Gallé *et al.*, (2007) who highlighted that *Q. pubescens* is able to preserve its photosynthetic apparatus during extreme drought through maintaining the concentration of the photosynthetic pigments (Chl *a* + *b* and associated carotenoids, e.g. β-carotene, lutein and

neoxanthin). Although these results give evidence of *Q. pubescens* acclimatation to harsher climatic conditions, it is worth noting that the ratio AZ/VAZ, which refers to the de-epoxidation state of the xanthophyll cycle, strongly dropped under AD in our study. Such decrease denotes a loss in dissipating excess energy required for protecting the photosynthetic apparatus (Peguero-Pina *et al.*, 2013). In addition, zeaxanthin concentrations also significantly dropped under AD. This carotenoid plays an important role as an antioxidant (Havaux *et al.*, 2005; Havaux & García-Plazaola, 2014) and its decrease could indicate the presence of oxidative stress under AD as suggested in Laoué et al. (2023) and endanger *Q. pubescens* functioning under very-long term precipitation decline.

Regarding specialized metabolites, the total flavonol concentration strongly dropped under AD over the 2016-2022 period according to results from previous years (2014 and 2015; Saunier *et al.*, 2022). Myricitrin derivatives displayed the highest decrease (-33%), followed by quercetin derivatives (-28%). Due to their chemical structure, quercetin and their derivatives possess the highest antioxidant activity compared to other flavonols (Laoué *et al.*, 2022). Although the glycosylated forms of these compounds possess a poorer antioxidant activity (Williamson *et al.*, 1999; Vogt & Jones, 2000), the drop of some flavonol derivatives under AD could reflect their antioxidant activity leading to their oxidation and thus in their consumption (Takahama, 2004; Hernandez *et al.*, 2006).

Our results indicate that *Q. pubescens* prioritizes the synthesis of central metabolites essential for photosynthesis (i.e. higher chlorophyll and carotenoid concentrations) rather than specialized defenses. This trade-off between specialized and central metabolites is also supported by the negative correlation between total flavonols and total photosynthetic pigments. Contrasting to our study, long-term amplified drought (more than 10 years) in a semi-arid Mediterranean site triggered foliar concentrations of flavonoids in the evergreen Mediterranean species (*Quercus ilex* L.),(Rivas-Ubach *et al.*, 2014). *Q. ilex* was however localized in a semi-arid Mediterranean site (average precipitation 610 mm) and submitted to a more drastic rain exclusion (compared to our study) leading to tree mortality after only 5 years of amplified drought. The effective role of flavonoids as antioxidants is currently intensively discussed and they have recently been described to act as a supplementary source of antioxidants when central antioxidants are unable to effectively neutralize ROS, especially in plants suffering from severe photooxidative stress (Agati *et al.*, 2020). This suggests that central antioxidant defenses of *Q. pubescens* may be sufficient to withstand long-term (10 years) amplified drought conditions present on our supra-Mediterranean study while harsher aridity conditions are required to upregulate specialized defenses as reported in *Q. ilex*.

The total annual precipitation 2-years before sampling contributed the most to metabolite concentration profile of the sampling year, followed by the total annual precipitation 1-year before sampling (**Figure 38**). Thus, poor precipitation cumulation was associated to poor concentrations of flavonols, VAZ and AZ/VAZ (**Figure 42**). This

result demonstrates that previous precipitation significantly drives the metabolic response of trees the current years and highlights the ability of *Q. pubescens* to memorize previous drought stress. Stress memory in plants refers to the plant ability to retain stress-related information allowing physiological and biochemical adjustments when confronted with the same stressor at a later time (Fleta-Soriano & Munné-Bosch, 2016; Crisp *et al.*, 2016). Plant memory has been well elucidated regarding forest tree growth (Julio Camarero et al., 2018; Itter et al., 2019; Peltier et al., 2022; Marqués et al., 2022) Concerning plant metabolism, many studies under greenhouse conditions have demonstrated drought-stress memory involving metabolic responses in several crop species such as coffee (Menezes-Silva *et al.*, 2017), rice (Auler *et al.*, 2021) and maize (Schulze *et al.*, 2021). However, there are few information regarding tree physiological and metabolite adjustments induced by recurrent drought over a long-term period (i.e. several years) (Tombesi *et al.*, 2018; Kartashov *et al.*, 2023). Recently, Kartashov *et al.* (2023) showed that even mild water deficits impact the expression of stress memory-related genes in naturally-grown coniferous tree species, Scots pine (*Pinus sylvestris* L.) and Norway spruce (*Picea abies* (L.) H. Karst), but the accumulation of stress-protective compounds was generally independent of stress memory effects in both species. In our study, low precipitation levels during both 1- and 2-years before sampling were strongly linked to low concentrations of VAZ and flavonols, in line with their drop when trees grow under amplified drought conditions. This result reinforces the idea that consecutive and long-term drought episodes strongly modulate plant chemical defenses (Peñuelas *et al.*, 2018) and can potentially impact tree growth as observed in Mediterranean holm oak forest (Barbeta *et al.*, 2013; Liu *et al.*, 2018; Ogaya & Peñuelas, 2021). However, it should be pointed out that severe drought conditions during the previous year also had a positive impact on some antioxidant defenses as shown by neoxanthin accumulation at low precipitation level suggesting that neoxanthin possess a remarkable antioxidant activity (Dall'Osto *et al.*, 2007; Giossi *et al.*, 2020).

5. Conclusion

In conclusion, our study provides valuable insights into how *Q. pubescens* will respond to future limited rain by analyzing the modulations in central (photosynthetic pigments) and specialized (flavonols) metabolites under intermediate to long-term scales (from the 5th to the 11th year of rain restriction). Despite a potential loss in photoprotection and antioxidant defenses due the respective decrease in AZ/VAZ and flavonol concentrations under amplified drought, the accumulation of other carotenoids (namely neoxanthin, β-carotene and lutein) and of chlorophylls, demonstrates a remarkable ability of *Q. pubescens* to adapt and maintain its photosynthetic efficiency and antioxidant defenses, potentially allowing the species to withstand long-term amplified drought. Nevertheless, further investigations should address whether this shift in defense metabolism

(upregulation of some central metabolites with a detrimental effect on flavonol concentration) could be dramatic for the species by favoring biotic stresses since these metabolites prevent invasion through plant signaling and act as a direct toxic substances against insects or pathogens (Ramaroson *et al.*, 2022). Another remarkable result of our study is that rainfall from the previous and two previous years were important drivers of metabolite concentrations, where previous dry years led to a decrease in VAZ and flavonol concentrations whereas precipitation of the previous year favored neoxanthin concentrations. As a whole, long-term (> 10 years) and very long-term (< 20 years) experiments in the field allow to assess memory precipitation effects on Mediterranean forest defenses.

6. Acknowledgements

This study was supported by the METAPHORES project funded by the 'Centre national de la recherche scientifique (CNRS)' (Grant agreement No. 250892; MITI and DGDS) and by the ECCOREV 2018 'Changements Métaboliques METAB80S' project. We are grateful to AnaEE-France and AnaEE-ERIC for the O_3HP facilities (https://www.anaee-france.fr/service/experimentation-in-natura/ecosystemes-forestier/ecosystemes-forestiers-mediterraneens/o3hp). We thank the P2M2 platform of the University of Rennes for the metabolic profiling of phenolic compounds. We thank Sylvie Dupouyet for the assistance in fieldwork. We are also grateful to the label "suivi à long-term du vivant" from INEE-CNRS. We acknowledge the use of the COOPERATE database (cooperate.obs-hp.fr/db/ and data by Meteo France for the stations St Michel-l'Observatoire and Dauphin.

CHAPTER VII: Discussion



Quercus pubescens Willd.

The general objective of this thesis was to study whether amplified and recurrent long-term drought (up to 10 years) under Mediterranean climate increased the physiological stress level of *Q. pubescens* at the leaf level and was associated to a modulation of leaf chemical and morpho-anatomical traits as means to trigger plant protection. **Chapter IV** (p. 85) focuses on the impact of amplified drought on central and specialized metabolism of *Q. pubescens* leaves over the course of a year (2021, that is, after 10 years of rain exclusion) and throughout the seasonal cycle (spring, summer and autumn). In view of the moderate changes shown in leaf metabolite production in Chapter IV, **Chapter V** (p. 108) explores the morpho-anatomical adjustments of *Q. pubescens* in response to amplified drought during the same year, with a focus on the summer season when drought is more pronounced. Finally, the goal of **Chapter VI** (p. 130), is to expand our understanding on the response of central and specialized metabolites over seven consecutive years of amplified drought (that is, after 5 to 11 years of rain exclusion) and how precipitation of current and previous years influenced metabolite concentration. In this discussion chapter, we synthesize and discuss the main physiological, chemical and physical responses found in an attempt to understand whether and how Downy oak will adapt to increasing limited precipitation in the Mediterranean area.

Over the last few decades, experimental drought on natural forests has enabled considerable progress in understanding the complex interactions between forests and changing climatic conditions (Jones *et al.*, 2022). Partial rain interception in the field for years is carried out in literature either through dynamic techniques - where a mobile roof is deployed part of the year (as in the present thesis) - or using static systems thereby simulating partial rain restriction all through the year (Limousin *et al.*, 2009; Moreno *et al.*, 2021b). For example, a study in a Mediterranean holm oak (*Q. ilex*) forest (Spain) subjected to 21 consecutive years of rain restriction (- 30% of annual rain exclusion) using a static system revealed that such reduction in precipitation had a significant negative impact on tree growth, mortality rate, and species composition (Ogaya & Peñuelas, 2021). Our research work was carried out on a *Q. pubescens* forest located at the O_3HP (Oak Observatory at Observatoire de Haute Provence), a forest non-exploited for the last 100 years where a dynamic rain exclusion system (roof) installed in April 2012 has enabled regular monitoring of forest functioning (leaf central and specialized metabolites, growth and physiology of Downy oak trees) upon partial rain withholding (i.e. amplified drought) from spring to fall resulting in roughly 30% less annual precipitation.

Past research conducted on this experimental site during the first 4 years of rain exclusion have demonstrated that such reduction in annual precipitation leads to a decrease in soil water availability at the study site, significantly increasing the **physiological leaf stress level** (Genard-Zielinski *et al.*, 2018a; Saunier *et al.*, 2018). As early as the third year of rain exclusion (in 2014), leaves exhibited a decline in net photosynthesis (A_n) and stomatal conductance (g_s) in trees subjected to amplified

drought, particularly in summer when water stress is more pronounced (Saunier *et al.*, 2018). Such physiological slowdown of trees under rain restriction was also of a higher magnitude during naturally dry years. For example, 2015 was a dry year since annual precipitation was only 598 mm while 2014 was a humid year with an annual precipitation of 1167 mm and, accordingly, trees displayed higher values of both, A_n and g_s, compared to 2015. This result underscores the importance of considering cumulative water restrictions within a given year as considered so far (Saunier *et al.*, 2017a, 2018) but also over several consecutive years.

In our study, conducted after 10 years of amplified drought (in 2021), the significant drop in stomatal conductance under amplified drought observed in 2015 did not occur. We argue that several parameters can explain this difference. First, precipitation in June was higher in 2015 compared to 2021, implying that rain exclusion in the amplified drought plot exacerbated the differences between both plots in 2015. Accordingly, there was a significantly lower predawn water potential (Ψ_{pd}) under amplified drought (-2.74 MPa) in 2015 compared to the natural drought plot (-2.41 MPa), resulting in greater stomatal closure (Saunier *et al.*, 2018). Second, in 2021, the maintenance of stomatal conductance under amplified drought is a typical response of anisohydric plants like *Q. pubescens*, which never completely close their stomata under moderate drought (Poyatos *et al.*, 2008), allowing them to maintain relatively high rates of carbon assimilation. In fact, in 2021, drought conditions were less severe on the site (Ψ_{pd} = -1.66 MPa) compared to 2015, leading to less pronounced stomatal closure (i.e. g_s = 19.1 mmol H_2O m^{-2} s^{-1} in 2021 compared to 3.8 mmol H_2O m^{-2} s^{-1} in 2015) and therefore higher net photosynthesis rate (A_n = 3.0 µmol CO_2 m^{-2} s^{-1} in 2021 compared to 1.3 µmol CO_2 m^{-2} s^{-1} in 2015). Nevertheless, despite the maintenance of stomatal conductance in 2021, carbon assimilation still strongly declined (-50% in summer) under amplified drought highlighting non-stomatal regulation of photosynthesis.

In summer 2015, two possible explanations were given to account for the decline in net photosynthesis. The first suggests that photosynthesis is mechanically inhibited (due to stomatal closure), and the second proposes a metabolic limitation own to a concentration decrease in the major photosynthetic pigments (including some carotenoids such as β-carotene, lutein, and neoxanthin) (Saunier *et al.*, 2018). In 2021, internal CO_2 concentrations (C_i) were higher under amplified drought, indicating that non-stomatal limitations of photosynthesis (e.g. metabolic impairment) were predominant when g_s was below a certain threshold value (here, < 22 mmol H_2O m^{-2} s^{-1}) (Flexas & Medrano, 2002; Medrano, 2002; Marino *et al.*, 2018).

Regarding changes in **central metabolites** in 2021, only concentrations of carotenoids from the xanthophyll cycle (i.e. violaxanthin, antheraxanthin, zeaxanthin; VAZ) significantly decreased under amplified drought (**Chapter IV**). Contrastingly, the photosynthetic system appeared maintained, notably through a significant increase in concentrations of chlorophylls *a* and *b*, as well as neoxanthin and lutein. Carotenoids

serve two primary functions in photosynthesis. They act both, as photoprotective agents preventing harmful photodynamic reactions, and as accessory pigments harvesting light, expanding the spectral range over which light drives photosynthesis (Cogdell & Gardiner, 1993). Xanthophyll cycle carotenoids (VAZ) are predominantly bound with chlorophyll molecules to proteins of integral membrane, forming light-harvesting complexes (Jansson, 1994) which play a crucial role in absorbing and transferring excitation energy to the photosynthetic reaction centers, facilitating electron transport. Additionally, to their role as light-harvesting pigments, xanthophylls are required for protecting the photosynthetic apparatus against high light (Niyogi *et al.*, 1997) through dissipation of the excess excitation energy in the antenna of photosystem II, which accumulates when stomatal closure limits photosynthesis (Demmig-Adams, 1990). Given these functions of carotenoids from the xanthophyll cycle, the observed decrease in their concentration after 10 years of amplified drought could indicate a loss of photoprotection rather than damage of the photosynthetic apparatus (since chlorophyll concentrations were maintained), reinforcing the idea that *Q. pubescens* is able to withstands extreme drought by preserving its photosynthetic apparatus through maintenance of photosynthetic pigments (in the present study: chlorophylls, β-carotene, lutein, and neoxanthin) (Gallé *et al.*, 2007).

Beyond chemical traits, changes in **leaf morphology and anatomy** can also strongly influence gas exchange since they permit plants to adjust their net CO_2 assimilation (A_n), stomatal conductance to water (g_s), transpiration (E) and water use efficiency (WUE) (Franks & Farquhar, 2007; Franks *et al.*, 2009). **Chapter V** focuses on the morpho-anatomical adjustments of leaves after 10 years of amplified drought and highlights that the reduction in both, spongy parenchyma thickness and stomatal density under amplified drought, could partly be involved in the limited photosynthesis rates based on the positive correlation between these traits. Indeed, spongy parenchyma and stomata constitute the physical basis for CO_2 conduction for photosynthesis by influencing the entry and diffusion of CO_2 to fixation sites (Flexas *et al.*, 2012; Borsuk *et al.*, 2022).

The reduction in spongy parenchyma under amplified drought, and more generally, the decrease in total leaf thickness – associated with a higher specific leaf area (SLA) – was interpreted in this study as a direct negative effect of drought on leaf growth rather than a shrinkage process observed upon leaf dehydration (Scoffoni *et al.*, 2014; Robakowski *et al.*, 2020). Indeed, together with lower photosynthesis levels and thinner/smaller leaves, it is likely that trees subjected to carbon limitation showed a limited carbon investment in plant growth. This result suggests that both, lower leaf area and leaf thickness, could be explained by the decline in cell expansion imposed by drought during leaf growth (Niinemets & Kull, 1998; Ogaya & Penuelas, 2006), since there is always a negative relationship between growth and drought (Weber *et al.*, 2007; Vodnik *et al.*, 2019; Gea-Izquierdo *et al.*, 2021). It is noteworthy that, unlike our study, a decrease in SLA (associated with greater leaf thickness) under water stress is well documented in sclerophyllous species such as *Q. coccifera*, as a mean to limit water transpiration and

promote drought resistance (Peguero-Pina *et al.*, 2016a; Ormeño *et al.*, 2020a). In other words, Downy oak did not harden its leaves under long-term amplified drought as expected in sclerophyllous species, at least, in the timescale (10 years) of our experimental rain exclusion.

It should be noted that when leaves possess a high SLA coupled with a large leaf size, this is regarded as an acquisition resource-use strategy where light capture, photosynthesis and resource assimilation are maximized (Pérez-Ramos *et al.*, 2013; Reich, 2014). Since in our study leaves under amplified drought increased their SLA, but also tended to exhibit a lower leaf surface and a drop in A_n, this result could likely indicate a negative physiological legacy in response to long-term water stress in terms of CO_2 fixation, rather than an optimal adaptation strategy, as observed in other broadleaf deciduous oak species like *Q. petraea* which reduced its leaf thickness under water stress (Robakowski *et al.*, 2020).

Although *Q. pubescens* reduced both its capacity to fix CO_2 and potentially its leaf area under long-term amplified drought, this could be partially offset by the improvement of water use efficiency (WUE) - as evidenced by the negative correlation between leaf area and WUE (Ackerly *et al.,* 2001). Reducing leaf size during drought stress confers the advantage of limiting tissue construction costs enabling Mediterranean oaks to cope with drier conditions (Baldocchi & Xu, 2007; Peguero-Pina *et al.*, 2016a).

As discussed above, as stomatal density decreased, net photosynthesis decreased in trees under amplified drought. However, no correlation was found between stomatal density and stomatal conductance or transpiration whereas several studies reported that the reduction in stomatal density is described as an advantageous strategy to limit both g_s and E (Liu *et al.*, 2015; Hughes *et al.*, 2017; Morales-Navarro *et al.*, 2018). The recent work of Trueba *et al.* (2022) provides an explanation to this lack of correlation since it demonstrates that the ratio between the number of stomata and the mesophyll volume (i.e. the three-dimensional structure of the leaves) rather than the number of stomata alone is a driver of g_s and WUE.

Despite the lower stomatal density under amplified drought, transpiration rate remained stable, which could be an indicator of *Q. pubescens* capacity to acclimate to long-term water stress. We hypothesize that these results are due to both, partial stomatal closure to preserve hydraulic conductivity (Nardini & Pitt, 1999; Poyatos *et al.*, 2008) and a higher non-glandular trichome density which negatively correlated with transpiration in trees under amplified drought. Non-glandular trichomes have indeed been suggested to limit transpiration by reducing the boundary layer conductance, thereby minimizing water loss (Buckley *et al.*, 2022). The higher density of non-glandular trichomes under amplified drought is consistent with several studies where water stress increased the density of leaf trichome to limit water loss eventually conferring drought resistance in

Quercus species (Mediavilla *et al.*, 2019; Hernandez & Park, 2022) and other plant species (Gonzáles et al., 2008; Galdon-Armero et al., 2018; Chen et al., 2022).

Another remarkable result of this work was the occurrence of a trade-off between glandular and non-glandular trichomes (**Chapter V**). Indeed, the density of glandular trichomes was, on average, two times lower in trees subjected to amplified drought than in trees under natural drought, and conversely, the density of non-glandular trichomes was two times higher. The negative correlation between these two types of trichomes indicates a trade-off favoring the production of simple unicellular structures (i.e. non-glandular trichomes), which are less costly, over multicellular glandular trichomes when water resources are limited, in line with the limitation of leaf growth to minimize tissue construction costs under amplified drought previously described.

The decrease in glandular trichome density under amplified drought might also express the decline in storage of monoterpene-like defenses, although further research is required to test this hypothesis. Our hypothesis relies on the fact that *Q. pubescens* leaves stores small amounts of monoterpenes (Santonja *et al.*, 2015) and this storage is likely to occur in the glandular trichomes, as observed in other deciduous oak species (*Q. robur*, Engel *et al.*, 1993). Moreover, considering that monoterpenes are synthesized from the same precursor than isoprene whose emissions were limited since the third year of rainfall restriction in Downy oak in the same study site (Saunier *et al.*, 2018), it is likely that the synthesis and storage of monoterpenes has also been reduced after 10 years of partial rain exclusion.

Glandular trichomes not only store and secrete terpenoids but also phenolic-like compounds such as phenolic acids in *Lamiaceae* species (Mahmoud *et al.*, 2021; Zhou *et al.*, 2021), or flavonoids in *Phillyrea latifolia* L. (Tattini *et al.*, 2000). Although the localization of phenolic compounds in the glandular trichomes of *Q. pubescens* could not be clarified during the exploratory tests of my PhD (cf. Raman imaging, p. 47) , we cannot exclude that there exists a relationship between the decrease in glandular trichome production and the decline in certain specialized metabolites, such as flavonols, under amplified drought. Further research is required to test this hypothesis using different imaging techniques.

Another major result of this thesis was the significant reduction in the concentration of total flavonols under amplified drought during the 2016-2022 period (**Chapter VI**), in agreement with our first hypothesis which puts forward a drop in the production of **specialized metabolite defenses** after ten years of amplified drought (as previously observed after 3-4 years of amplified drought). Our findings in Chapter VI contrast with the evolutionary concept proposed by Close & McArthur (2002), where an increase in the abundance of phenolic compounds is expected to occur as a mechanism to alleviate oxidative pressure through reactive oxygen species (ROS) quenching. As described in **Chapter III**, flavonols play major roles in plant protection under abiotic stresses (drought,

warming, UV radiation, and salinity) through their antioxidant properties, particularly due to their ROS-scavenging function attributed to the high reactivity of their hydroxyl substituents (Heim *et al.*, 2002). During drought stress, the restriction of CO_2 entrance upon stomatal closure leads to an imbalance in electron flow, then electron leakage and subsequent ROS generation which eventually triggers flavonol biosynthesis (Sierla *et al.*, 2016). This suggests that flavonols play a key role in plants inhabiting constraining environments such as the Mediterranean region (Di Ferdinando *et al.*, 2014). Consistently, an increase in flavonoid concentrations in response to drought has been reported in some Mediterranean species, including *Cistus clusii* (Hernández *et al.*, 2004), *Pinus pinaster* Ait. (de Miguel *et al.*, 2016) or *Q. ilex* (Rivas-Ubach *et al.*, 2014). In the later study (Rivas-Ubach *et al.* 2014), 10 years of partial rain exclusion in a natural *Q. ilex* forest resulted in higher leaf concentrations of flavonoids, while our results indicate that *Q. pubescens* prioritizes the synthesis of essential central metabolites for photosynthesis (i.e. higher concentrations of chlorophyll and carotenoids) over specialized defenses. The effective role of flavonoids as antioxidants is currently the subject of intense debate, and they have recently been described as an additional source of antioxidants when central antioxidants are unable to efficiently neutralize ROS, especially in plants experiencing severe photooxidative stress (Agati & Tattini, 2010). Our results suggest that the central antioxidant defenses of *Q. pubescens* (notably the increase in β-carotene, neoxanthin, and lutein during the period 2016-2022) may be sufficient to withstand the long-term amplified drought conditions (> 10 years) present at our study site. Furthermore, Rivas-Ubach *et al.* (2014) noted tree mortality after only 5 years of amplified drought in their experimental site with semi-arid Mediterranean climatic conditions, whereas there was no mortality in our site with less arid climatic conditions (i.e. sub-humid supra-Mediterranean), implying that *Q. ilex* was subjected to a more intense oxidative stress.

Previous studies carried out after 3-4 years of amplified drought at O_3HP showed that targeted (phenolic compounds) and untargeted metabolome of *Q. pubescens* leaves followed a strong seasonal pattern and remained relatively stable after 4 years of amplified and recurrent drought (Saunier *et al.*, 2018, 2022). Our study confirms a **strong impact of seasonality on Downy oak metabolome** (**Chapter IV**), consisting of a strong investment in (1) photosynthetic pigments in spring, (2) cuticular waxes in both summer and autumn, and (3) tocochromanols, plastoquinones, and flavanols in autumn.

The highest concentrations of **photosynthetic pigments** (chlorophylls and carotenoids) in spring correspond to favorable climatic conditions, with high soil water availability and optimal temperatures (12°C on average). During the growing season, plants invest heavily in photosynthetic processes to maximize their growth (Rivas-Ubach *et al.*, 2012; Rivas-Ubach *et al.*, 2014). In addition to photosynthetic pigments, certain specialized metabolites, such as phenolic acids and antioxidant flavonoids, also accumulated in spring. This observation supports the protective role of flavonoids and phenolic acids to cope with intense light irradiation at the start of the vegetative cycle and the associated oxidative stress (Ferreyra *et al.*, 2021; Roeber *et al.*, 2021).

Cuticular waxes, particularly triterpenoids (the major compounds within cuticular waxes in our study), showed the highest concentration in summer. In addition, other compound groups, such as fatty acid derivatives, tocopherols and alkanes, showed the highest concentrations in both summer and autumn. Cuticular triterpenoids do not act as a direct barrier against cuticular transpiration, but rather prevent thermal damage by stabilizing the cuticular structure as recently reviewed (Jetter & Riederer, 2016; Schuster *et al.*, 2016). They can account for up to 60% of total cuticular wax concentrations in some oak species (Bueno *et al.*, 2020) and represent 37% of the cuticular fraction of *Q. pubescens* leaves. Our study highlighted the importance of these specialized metabolites in *Q. pubescens* resistance to summer drought since they could confer protection against heat stress during warm periods, contributing to leaf protection during simultaneous periods of drought and heat stress. Seasonal variation in cuticular waxes has also been observed in other deciduous trees such as *Fagus sylvatica* L. (Prasad & Giilz, 1990) and *Quercus robur* (Gülz & Müller, 1992), the latter displaying also higher cuticular wax accumulation in summer and autumn as reported in our study. Despite the importance of cuticular waxes to cope with drier and warmer climatic conditions in summer, there was no clear impact of long-term drought on cuticular wax concentrations. This results contrasts with our hypothesis (we expected leaf enrichment in cuticular waxes under amplified drought), based on studies showing that increasing cuticular wax concentrations is associated with water shortage and enhancement of drought tolerance in *Arabidopsis thaliana* (Aharoni *et al.*, 2004; Kosma *et al.*, 2009; Yang *et al.*, 2011) and in various crop species (Xue *et al.*, 2017). *Q. pubescens* did not exhibit the strategy of increasing cuticular wax concentrations under rain exclusion, at least after 10 years of amplified drought.

Seasonal metabolic profile changes can also denote tree physiological functioning. For example, the recovery of photosynthetic activity in autumn, despite the decline in photosynthetic pigment concentrations, can be explained by the accumulation of plastoquinones and three other antioxidants (PC-8, α-tocopherol, and the flavanol catechin) which confer a strong protection of the photosynthetic apparatus against oxidative stress still present in autumn (Bernatoniene & Kopustinskiene, 2018; Muñoz & Munné-Bosch, 2019; Kumar *et al.*, 2020a).

All the studies mentioned above, as well as a major part of this thesis (**Chapters IV, V**), compare the response of trees growing under different water stress conditions within the current year and reveal that prolonged drought, from 3 to 10 years, clearly hampers the physiological functioning of trees by limiting CO_2 fixation, accompanied by moderate increases or decreases in leaf metabolome. The novelty of **Chapter VI** is to address whether central and specialized metabolites of *Q. pubescens* are influenced by precipitation from past years (implying a precipitation memory effect) or by precipitation during the growing season (Zhang *et al.*, 2020; Wang *et al.*, 2022). Plant memory – described by Trewavas (2003) as "the ability to access past experience so that new

responses incorporate relevant information from the past" – has been well related to tree growth (Julio Camarero *et al.*, 2018; Itter *et al.*, 2019; Peltier *et al.*, 2022; Marqués *et al.*, 2022) while few studies have tackled its influence on plant metabolome (Auler *et al.*, 2021; Kambona *et al.*, 2023; Kartashov *et al.*, 2023), especially regarding tree metabolome under recurrent drought over several years (Tombesi *et al.*, 2018; Kartashov *et al.*, 2023). In our study, low precipitation levels during both 1- and 2-years before leaf sampling were strongly linked to low concentrations of VAZ and flavonols, in line with their concentration decline in trees growing under amplified drought conditions. This result reinforces the idea that consecutive years of limited precipitation strongly slow-down the production of some chemical defenses in the long-term (Peñuelas *et al.*, 2018) and can potentially limit tree growth as observed in the Mediterranean holm oak forest (Barbeta *et al.*, 2013; Liu *et al.*, 2018; Ogaya & Peñuelas, 2021). In addition, such impact of previous precipitation can also have a positive effect on some plant chemical defenses as shown by neoxanthin accumulation under the lowest precipitation levels suggesting an important function of this central metabolite to cope with oxidative stress under long-term drought and avoid strong damage to the photosynthetic apparatus (Gallé *et al.*, 2007; Dall'Osto *et al.*, 2007; Giossi *et al.*, 2020).

CHAPTER VIII: Conclusion and perspectives



Sunset at Saint-Michel- l'Observatoire, Alpes-de-Haute-Provence, France

This thesis highlights that *Q. pubescens* exhibits a slow-down of leaf physiological functioning under long-term rain restriction and responds to this stress by modulating central and specialized metabolism as well as morpho-anatomical traits. Such modulations may represent chemical and physical defenses respectively but are also indicative of leaf growth (e.g. leaf thickness, leaf surface). The take-home message of this thesis is that the reported physico-chemical changes of Downy oak enable this species to (1) avoid excessive damage to the photosynthetic apparatus, mainly through an increase in central metabolite concentrations (chlorophylls, lutein, β-carotene, and neoxanthin), (2) limit water loss (through higher non-glandular trichome density) and (3) reduce production-cost (low glandular trichome density and reduced leaf thickness and size).

Unpublished data on *Q. pubescens* growth in our experimental site shows a negative impact of amplified drought on leaf biomass production from the 5th year (2016) of rain exclusion (Priscille Wenger; Master thesis 2022) and the present thesis highlights a trade-off in the chemical defense strategy occurring as early as the 5th year of amplified drought. However, no mortality has been observed unlike for other Mediterranean species is Southern latitudes, suggesting that *Q. pubescens* can withstand 10 years of amplified drought while maintaining vital functions.

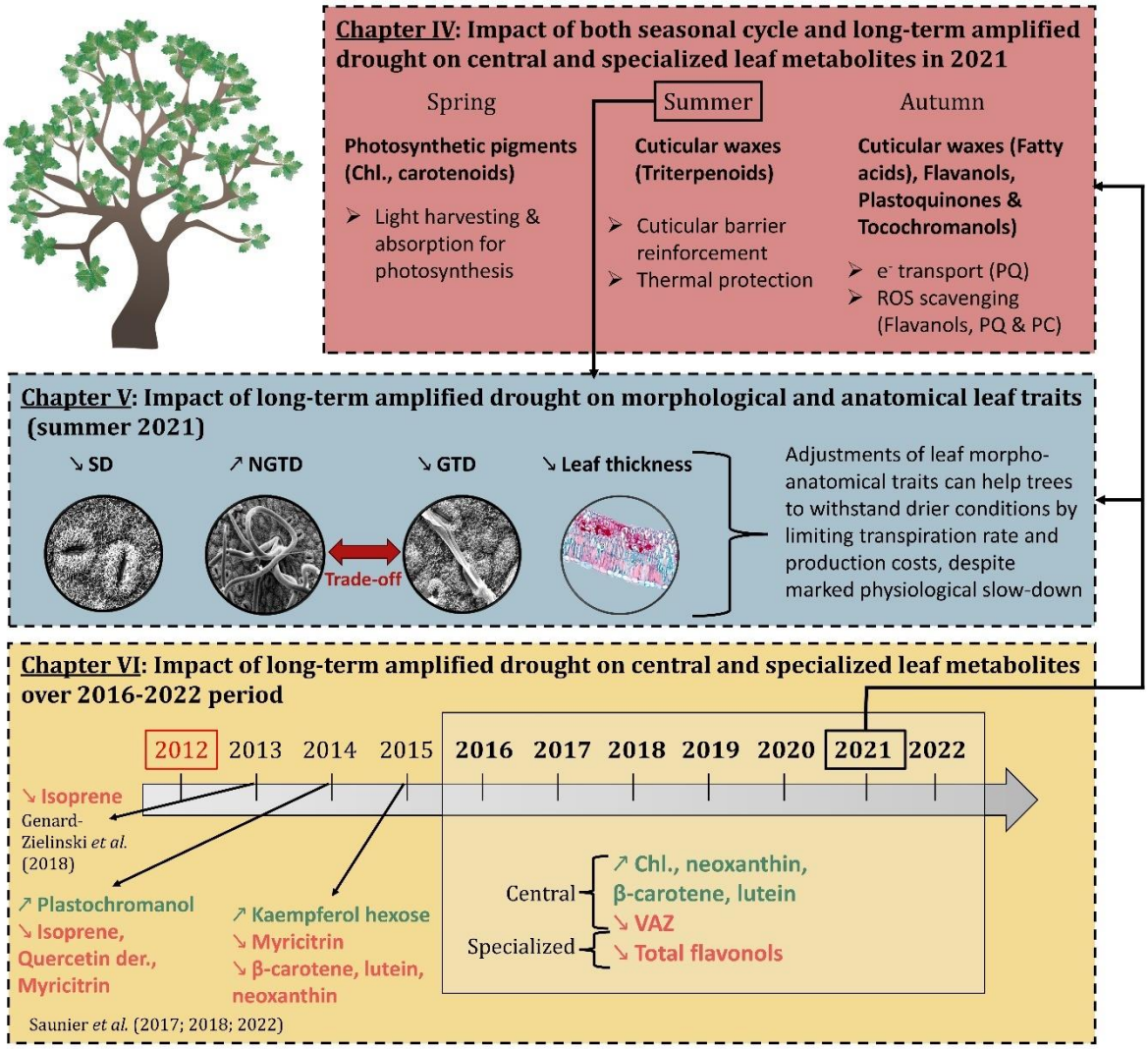

Figure 43: concluding schema of the main results obtained in this thesis. Abbreviations are as follows: e-, electron; Chl, chlorophylls (*a* and *b*); GTD, glandular trichome density; NGTD, non-glandular trichome density; PC, plastochromanol; PQ, plastoquinones; ROS, reactive oxygen species; SD, stomatal density; VAZ, xanthophyll cycle (violaxanthin, antheraxanthin, zeaxanthin).

Some morpho-anatomical adjustments of leaves, notably a high density of non-glandular trichomes, low stomatal density, and a potential reduction in leaf surface, could contribute to maintain the physiological functioning of *Q. pubescens* and provide protection under future drier Mediterranean climate. Moreover, some trade-offs, such as favoring the production of non-glandular trichomes over glandular trichomes, may reflect a significant shift where low-cost structures (non-glandular trichomes) are favored, permitting limited transpiration rates and lower production costs. The low leaf construction cost and the fast recovery of the photosynthetic activity in autumn (probably related to metabolome adjustments) could permit the success of these species to withstand increasing prolonged and severe drought expected in the future. These results confirm that, among European oak species (e.g. *Q. petraea* and *Q. robur*), *Q. pubescens* is more tolerant to drought stress (Cochard *et al.*, 1992; Früchtenicht *et al.*, 2018). *Q.*

pubescens could be a species of choice for foresters in the context of assisted migration, for example in northern France, gradually replacing *Q. petraea* or *Q. robur* which is becoming increasingly vulnerable to climate change (Sardin *et al.*, 2022).

It is worth noting that, as already shown after 3-4 years of amplified drought (Saunier *et al.*, 2022), specialized metabolism (phenolic compounds) of *Q. pubescens* did not respond to 10 years of rain exclusion as expected by the GDBH (growth-differentiation balance hypothesis). Indeed, if we consider that water resources were moderately available under amplified drought in this sub-humid site, the GDBH expects that under such conditions growth is limited while carbon assimilation is maintained, resulting in an increase in carbon allocation for the synthesis of defense specialized metabolites. Instead, our study showed that photosynthesis, some indicators of leaf growth (e.g. leaf thickness and surface area) and, to some extent, flavonol concentration (**Chapters V, VI**) were reduced in trees subjected to amplified drought and that, as previously highlighted, the synthesis of central antioxidant defenses (β-carotene, neoxanthin, and lutein during the period 2016-2022) are prioritized as they appear to be sufficient to withstand such long-term amplified drought conditions/moderate water scarcity. These results thus confirm the limited utility of the GDBH to predict forest functioning according to water availability.

In **perspectives**, future studies should continue to address the memory precipitation effects on forest functioning using long-time data series. Importantly, more in-depth analyses on forest growth should be carried out by considering measurements of both, primary growth (length of new shoots) and secondary growth (diameter at breast height; DBH), as well as the leaf productivity of *Q. pubescens.* The use of LiDAR (Light Detection and Ranging) technology could also be relevant to capture detailed information about changes in canopy structure (canopy cover, leaf area) in response to amplified drought (Smith *et al.*, 2019; Tang *et al.*, 2019).

Further studies imaging techniques could also provide valuable information on localization of specialized metabolites within leaf structures. Indeed, the functions played by metabolites within plants are related to both, their concentration and localization within the plant organ. Specifically, future studies are required to confirm the presence of monoterpenoids within glandular trichomes of Downy oak leaves and precise the localization of flavonoids within leaf tissues.

From an experimental point of view, it is also necessary to tackle the response of Mediterranean forest to both, warming and limited rain since both climate constraints will become more exacerbated in the Mediterranean area in the future. At O_3HP, but also at the *Q. ilex* forest in Puéchabon, this will be possible in the close future, by deploying long-term experimental systems *in natura* which are under development. Moreover, in view of the frequency of dry years in the Mediterranean area, it would be necessary to implement *in natura* sites with an irrigation plot allowing to simulate an "optimal precipitation condition" thus overcoming the impact of particularly hot and dry years,

such as 2022, where differences in the physiological functioning of trees were masked because trees under natural conditions also underwent a high water stress level.

To conclude, although *Q. pubescens* has readjusted part of its physical and chemical traits to maintain its physiological functions and protect its photosynthetic apparatus (due to an increase in carotenoids and chlorophyll), it does so at the expense of flavonol production. However, it is not yet known how the reduction in flavonols and the increase in carotenoids influence attacks by pathogens and herbivores, and/or how potential nutritional benefits for herbivores modify their abundance. Flavonol concentration decreases could potentially weaken the ability of Downy oak to defend against biotic stresses since they act as a chemical barrier to prevent invasion, or as a direct toxic against insects or pathogens (Ramaroson *et al.*, 2022). From an ecological perspective this shift in defense metabolism may be quite dramatic, even if such aspect should also be tackled in future studies.

References

A. Lal M. **2018**. Photosynthesis. In: Bhatla SC, A. Lal M, eds. Plant Physiology, Development and Metabolism. Singapore: Springer, 159–226.

Abrahams S, Tanner GJ, Larkin PJ, Ashton AR. **2002**. Identification and Biochemical Characterization of Mutants in the Proanthocyanidin Pathway in *Arabidopsis*. *Plant Physiology* **130**: 561–576.

Ackerly D, Knight C, Weiss S, Barton K, Starmer KP. **2001**. Leaf size, specific leaf area and microhabitat distribution of chaparral woody plants: Contrasting patterns in species level and community level analyses. *Oecologia* **130**: 449–457.

Afzal A, Duiker SW, Watson JE. **2017**. Leaf thickness to predict plant water status. *Biosystems Engineering* **156**: 148–156.

Agati G, Azzarello E, Pollastri S, Tattini M. **2012**. Flavonoids as antioxidants in plants: Location and functional significance. *Plant Science* **196**: 67–76.

Agati G, Biricolti S, Guidi L, Ferrini F, Fini A, Tattini M. **2011**. The biosynthesis of flavonoids is enhanced similarly by UV radiation and root zone salinity in L. *vulgare* leaves. *Journal of Plant Physiology* **168**: 204–212.

Agati G, Brunetti C, Di Ferdinando M, Ferrini F, Pollastri S, Tattini M. **2013**. Functional roles of flavonoids in photoprotection: New evidence, lessons from the past. *Plant Physiology and Biochemistry* **72**: 35–45.

Agati G, Brunetti C, Fini A, Gori A, Guidi L, Landi M, Sebastiani F, Tattini M. **2020**. Are Flavonoids Effective Antioxidants in Plants? Twenty Years of Our Investigation. *Antioxidants* **9**: 1098.

Agati G, Tattini M. **2010**. Multiple functional roles of flavonoids in photoprotection. *New Phytologist* **186**: 786–793.

Agrawal AD. **2011**. Pharmacological Activities of Flavonoids: A Review. *International Journal of Pharmaceutical Sciences and Nanotechnology* **4**: 1394–1398.

Aharoni A, Dixit S, Jetter R, Thoenes E, van Arkel G, Pereira A. **2004**. The SHINE Clade of AP2 Domain Transcription Factors Activates Wax Biosynthesis, Alters Cuticle Properties, and Confers Drought Tolerance when Overexpressed in *Arabidopsis*. *The Plant Cell* **16**: 2463–2480.

Aherne SA, O'Brien NM. **2002**. Dietary flavonols: chemistry, food content, and metabolism. *Nutrition* **18**: 75–81.

Ahuja I, de Vos RCH, Bones AM, Hall RD. **2010**. Plant molecular stress responses face climate change. *Trends in Plant Science* **15**: 664–674.

Alam H, Khattak JZ, Ksiksi TS, Saleem MH, Fahad S, Sohail H, Ali Q, Zamin M, El-Esawi MA, Saud S. **2021**. Negative impact of long-term exposure of salinity and drought stress on native *Tetraena mandavillei* L. *Physiologia Plantarum* **172**: 1336–1351.

d'Alessandro S, Havaux M. **2019**. Sensing β-carotene oxidation in photosystem II to master plant stress tolerance. *New Phytologist* **223**: 1776–1783.

Altangerel N, Ariunbold GO, Gorman C, Alkahtani MH, Borrego EJ, Bohlmeyer D, Hemmer P, Kolomiets MV, Yuan JS, Scully MO. **2017**. In vivo diagnostics of early abiotic plant stress response via Raman spectroscopy. *Proceedings of the National Academy of Sciences* **114**: 3393–3396.

Anderegg WRL, Schwalm C, Biondi F, Camarero JJ, Koch G, Litvak M, Ogle K, Shaw JD, Shevliakova E, Williams AP, *et al.* 2015. Pervasive drought legacies in forest ecosystems and their implications for carbon cycle models. *Science* **349**: 528–532.

Anjum SA, Xie X, Wang L, Saleem MF, Man C, Lei W. **2011**. Morphological, physiological and biochemical responses of plants to drought stress. *African Journal of Agricultural Research* **6**: 2026–2032.

Auler PA, Souza GM, da Silva Engela MRG, do Amaral MN, Rossatto T, da Silva MGZ, Furlan CM, Maserti B, Braga EJB. **2021**. Stress memory of physiological, biochemical and metabolomic responses in two different rice genotypes under drought stress: The scale matters. *Plant Science* **311**: 110994.

Bahamonde HA, Gil L, Fernández V. **2018**. Surface Properties and Permeability to Calcium Chloride of Fagus sylvatica and *Quercus petraea* Leaves of Different Canopy Heights. *Frontiers in Plant Science* **9**: 494.

Baldocchi DD, Xu L. **2007**. What limits evaporation from Mediterranean oak woodlands – The supply of moisture in the soil, physiological control by plants or the demand by the atmosphere? *Advances in Water Resources* **30**: 2113–2122.

Baldoni E, Genga A, Cominelli E. **2015**. Plant MYB Transcription Factors: Their Role in Drought Response Mechanisms. *International Journal of Molecular Sciences* **16**: 15811–15851.

Barbeta A, Ogaya R, Peñuelas J. **2013**. Dampening effects of long-term experimental drought on growth and mortality rates of a Holm oak forest. *Global Change Biology* **19**: 3133–3144.

Barnes PW, Tobler MA, Keefover-Ring K, Flint SD, Barkley AE, Ryel RJ, Lindroth RL. **2016**. Rapid modulation of ultraviolet shielding in plants is influenced by solar ultraviolet radiation and linked to alterations in flavonoids. *Plant, Cell & Environment* **39**: 222–230.

Basu S, Ramegowda V, Kumar A, Pereira A. **2016**. Plant adaptation to drought stress. *F1000Research* **5**: F1000 Faculty Rev-1554.

Bazzaz FA, Chiariello NR, Coley PD, Pitelka LF. **1987**. Allocating Resources to Reproduction and Defense. *BioScience* **37**: 58–67.

Behr M, Neutelings G, El Jaziri M, Baucher M. **2020**. You Want it Sweeter: How Glycosylation Affects Plant Response to Oxidative Stress. *Frontiers in Plant Science* **11**: 1443.

Ben Abdallah S, Aung B, Amyot L, Lalin I, Lachâal M, Karray-Bouraoui N, Hannoufa A. **2016**. Salt stress (NaCl) affects plant growth and branch pathways of carotenoid and flavonoid biosyntheses in Solanum nigrum. *Acta Physiologiae Plantarum* **38**: 72.

Bennett RN, Wallsgrove RM. **1994**. Secondary metabolites in plant defence mechanisms. *New Phytologist* **127**: 617–633.

Bernatoniene J, Kopustinskiene DM. **2018**. The Role of Catechins in Cellular Responses to Oxidative Stress. *Molecules* **23**: 965.

Bertolino LT, Caine RS, Gray JE. **2019**. Impact of Stomatal Density and Morphology on Water-Use Efficiency in a Changing World. *Frontiers in Plant Science* **10**: 225.

Bickford CP. **2016**. Ecophysiology of leaf trichomes. *Functional Plant Biology* **43**: 807.

Blanco-Sánchez M, Ramos-Muñoz M, Pías B, Ramírez-Valiente JA, Díaz-Guerra L, Escudero A, Matesanz S. **2022**. Natural selection favours drought escape and an acquisitive resource-use strategy in semi-arid Mediterranean shrubs. *Functional Ecology* **36**: 2289–2302.

Bornman JF, Barnes PW, Robson TM, Robinson SA, Jansen MAK, Ballaré CL, Flint SD. **2019**. Linkages between stratospheric ozone, UV radiation and climate change and their implications for terrestrial ecosystems. *Photochemical & Photobiological Sciences* **18**: 681–716.

Borsuk AM, Roddy AB, Théroux-Rancourt G, Brodersen CR. **2022**. Structural organization of the spongy mesophyll. *New Phytologist* **234**: 946–960.

Bourgaud F, Gravot A, Milesi S, Gontier E. **2001**. Production of plant secondary metabolites: a historical perspective. *Plant Science* **161**: 839–851.

Brewer CA, Smith WK, Vogelmann TC. **1991**. Functional interaction between leaf trichomes, leaf wettability and the optical properties of water droplets. *Plant, Cell & Environment* **14**: 955–962.

Brossa R, Casals I, Pintó-Marijuan M, Fleck I. **2009**. Leaf flavonoid content in *Quercus ilex* L. resprouts and its seasonal variation. *Trees* **23**: 401–408.

Brown EJ, Khodr H, Hider CR, Rice-Evans CA. **1998**. Structural dependence of flavonoid interactions with Cu^{2+} ions: implications for their antioxidant properties. *Biochemical Journal* **330**: 1173–1178.

Brown DE, Rashotte AM, Murphy AS, Normanly J, Tague BW, Peer WA, Taiz L, Muday GK. **2001**. Flavonoids Act as Negative Regulators of Auxin Transport *in Vivo* in *Arabidopsis*. *Plant Physiology* **126**: 524–535.

Brunetti C, Di Ferdinando M, Fini A, Pollastri S, Tattini M. **2013**. Flavonoids as Antioxidants and Developmental Regulators: Relative Significance in Plants and Humans. *International Journal of Molecular Sciences* **14**: 3540–3555.

Brunetti C, Fini A, Sebastiani F, Gori A, Tattini M. **2018**. Modulation of Phytohormone Signaling: A Primary Function of Flavonoids in Plant–Environment Interactions. *Frontiers in Plant Science* **9**: 1042.

Brunetti C, Sebastiani F, Tattini M. **2019a**. Review: ABA, flavonols, and the evolvability of land plants. *Plant Science* **280**: 448–454.

Brunetti C, Tattini M, Guidi L, Velikova V, Ferrini F, Fini A. **2019b**. An integrated overview of physiological and biochemical responses of *Celtis australis* to drought stress. *Urban Forestry & Urban Greening* **46**: 126480.

Buckley T, Pierce MA, Sack L. **2022**. *Leaf trichomes reduce boundary layer conductance*. Preprints.

Bueno A, Sancho-Knapik D, Gil-Pelegrín E, Leide J, Peguero-Pina JJ, Burghardt M, Riederer M. **2020**. Cuticular wax coverage and its transpiration barrier properties in *Quercus coccifera* L. leaves: does the environment matter? *Tree Physiology* **40**: 827–840.

Buer CS, Muday GK. **2004**. The transparent testa4 mutation prevents flavonoid synthesis and alters auxin transport and the response of *Arabidopsis* roots to gravity and light. *The Plant Cell* **16**: 1191–1205.

Buer CS, Muday GK, Djordjevic MA. **2007**. Flavonoids Are Differentially Taken Up and Transported Long Distances in *Arabidopsis*. *Plant Physiology* **145**: 478–490.

Cailleret M, Nourtier M, Amm A, Durand-Gillmann M, Davi H. **2014**. Drought-induced decline and mortality of silver fir differ among three sites in Southern France. *Annals of Forest Science* **71**: 643–657.

Caldwell MM, Flint SD. **1994**. Stratospheric ozone reduction, solar UV-B radiation and terrestrial ecosystems. *Climatic Change* **28**: 375–394.

Caldwell MM, Robberecht R, Flint SD. **1983**. Internal filters: prospects for UV-acclimation in higher plants. *Physiologia plantarum* **58**: 445–450.

Catoni C, Peters A, Martin Schaefer H. **2008**. Life history trade-offs are influenced by the diversity, availability and interactions of dietary antioxidants. *Animal Behaviour* **76**: 1107–1119.

Cazzaniga S, Bressan M, Carbonera D, Agostini A, Dall'Osto L. **2016**. Differential Roles of Carotenes and Xanthophylls in Photosystem I Photoprotection. *Biochemistry* **55**: 3636–3649.

Chaves MM. **2002**. How Plants Cope with Water Stress in the Field? Photosynthesis and Growth. *Annals of Botany* **89**: 907–916.

Chaves N, Escudero JC, Gutierrez-Merino C. **1993**. Seasonal variation of exudate of *Cistus ladanifer*. *Journal of Chemical Ecology* **19**: 2577–2591.

Chaves N, Escudero JC, Gutierrez-Merino C. **1997**. Role of Ecological Variables in the Seasonal Variation of Flavonoid Content of *Cistus ladanifer* Exudate. *Journal of Chemical Ecology* **23**: 579–603.

Chen Z, Li S, Wan X, Liu S. **2022a**. Strategies of tree species to adapt to drought from leaf stomatal regulation and stem embolism resistance to root properties. *Frontiers in Plant Science* **13**: 926535.

Chen J-J, Sun Y, Kopp K, Oki L, Jones SB, Hipps L. **2022b**. Effects of Water Availability on Leaf Trichome Density and Plant Growth and Development of *Shepherdia ×utahensis*. *Frontiers in Plant Science* **13**: 855858.

Close DC, McArthur C. **2002**. Rethinking the Role of Many Plant Phenolics: Protection from Photodamage Not Herbivores? *Oikos* **99**: 166–172.

Cochard HH, Bréda N, Granier AA, Aussenac G. **1992**. Vulnerability to air embolism of three European oak species (*Quercus petraea* (Matt) Liebl, *Q pubescens* Willd, *Q robur* L). *Annales des sciences forestières* **49**: 225–233.

Cogdell RJ, Gardiner AT. **1993**. Functions of carotenoids in photosynthesis. In: Carotenoids Part B: Metabolism, Genetics, and Biosynthesis. Methods in Enzymology. Academic Press, 185–193.

Cook NC, Samman S. **1996**. Flavonoids—Chemistry, metabolism, cardioprotective effects, and dietary sources. *The Journal of Nutritional Biochemistry* **7**: 66–76.

Corwin DL. **2021**. Climate change impacts on soil salinity in agricultural areas. *European Journal of Soil Science* **72**: 842–862.

Cos J, Doblas-Reyes F, Jury M, Marcos R, Bretonnière P-A, Samsó M. **2022**. The Mediterranean climate change hotspot in the CMIP5 and CMIP6 projections. *Earth System Dynamics* **13**: 321–340.

Cramer W, Guiot J, Fader M, Garrabou J, Gattuso J-P, Iglesias A, Lange MA, Lionello P, Llasat MC, Paz S, *et al.* 2018. Climate change and interconnected risks to sustainable development in the Mediterranean. *Nature Climate Change* **8**: 972–980.

Crisp PA, Ganguly D, Eichten SR, Borevitz JO, Pogson BJ. **2016**. Reconsidering plant memory: Intersections between stress recovery, RNA turnover, and epigenetics. *Science Advances* **2**: e1501340.

Crozier A, Jaganath IB, Clifford MN. **2006**. Phenols, polyphenols and tannins: an overview. *Plant secondary metabolites: Occurrence, structure and role in the human diet* **1**: 1–25.

Crupi P, Faienza MF, Naeem MY, Corbo F, Clodoveo ML, Muraglia M. **2023**. Overview of the Potential Beneficial Effects of Carotenoids on Consumer Health and Well-Being. *Antioxidants* **12**: 1069.

Cruz De Carvalho MH. **2008**. Drought stress and reactive oxygen species: production, scavenging and signaling. *Plant Signaling & Behavior* **3**: 156–165.

Csepregi K, Coffey A, Cunningham N, Prinsen E, Hideg É, Jansen MAK. **2017**. Developmental age and UV-B exposure co-determine antioxidant capacity and flavonol accumulation in *Arabidopsis* leaves. *Environmental and Experimental Botany* **140**: 19–25.

Czemmel S, Stracke R, Weisshaar B, Cordon N, Harris NN, Walker AR, Robinson SP, Bogs J. **2009**. The Grapevine R2R3-MYB Transcription Factor VvMYBF1 Regulates Flavonol Synthesis in Developing Grape Berries. *Plant Physiology* **151**: 1513–1530.

Daliakopoulos IN, Tsanis IK, Koutroulis A, Kourgialas NN, Varouchakis AE, Karatzas GP, Ritsema CJ. **2016**. The threat of soil salinity: A European scale review. *Science of The Total Environment* **573**: 727–739.

Dall'Osto L, Cazzaniga S, North H, Marion-Poll A, Bassi R. **2007**. The *Arabidopsis aba4-1* Mutant Reveals a Specific Function for Neoxanthin in Protection against Photooxidative Stress. *The Plant Cell* **19**: 1048–1064.

Damesin C, Rambal S. **1995**. Field study of leaf photosynthetic performance by a Mediterranean deciduous oak tree (*Quercus pubescens*) during a severe summer drought. *New Phytologist* **131**: 159–167.

Das K, Roychoudhury A. **2014**. Reactive oxygen species (ROS) and response of antioxidants as ROS-scavengers during environmental stress in plants. *Frontiers in Environmental Science* **2**: 53.

Davies KM, Albert NW, Zhou Y, Schwinn KE. **2018**. Functions of Flavonoid and Betalain Pigments in Abiotic Stress Tolerance in Plants. In: Annual Plant Reviews online. John Wiley & Sons, Ltd, 21–62.

Davies KM, Schwinn KE, Deroles SC, Manson DG, Lewis DH, Bloor SJ, Bradley JM. **2003**. Enhancing anthocyanin production by altering competition for substrate between flavonol synthase and dihydroflavonol 4-reductase. *Euphytica* **131**: 259–268.

Davis MB. **2001**. Range Shifts and Adaptive Responses to Quaternary Climate Change. *Science* **292**: 673–679.

De Micco V, Aronne G. **2012**. Morpho-Anatomical Traits for Plant Adaptation to Drought. In: Aroca R, ed. Plant Responses to Drought Stress: From Morphological to Molecular Features. Berlin, Heidelberg: Springer, 37–61.

Debeaujon I, Peeters AJM, Léon-Kloosterziel KM, Koornneef M. **2001**. The TRANSPARENT TESTA12 Gene of *Arabidopsis* Encodes a Multidrug Secondary Transporter-like Protein Required for Flavonoid Sequestration in Vacuoles of the Seed Coat Endothelium. *The Plant Cell* **13**: 853–871.

Della Torre F, Ferreira BG, Lima JE, Lemos-Filho JP, Rossiello ROP, França MGC. **2021**. Leaf morphophysiological changes induced by long-term drought in *Jatropha* curcas plants explain the resilience to extreme drought. *Journal of Arid Environments* **185**: 104381.

DellaPenna D, Last RL. **2006**. Progress in the dissection and manipulation of plant vitamin E biosynthesis. *Physiologia Plantarum* **126**: 356–368.

Demmig-Adams B. **1990**. Carotenoids and photoprotection in plants: A role for the xanthophyll zeaxanthin. *Biochimica et Biophysica Acta (BBA) - Bioenergetics* **1020**: 1–24.

Demmig-Adams B, Stewart JJ, López-Pozo M, Polutchko SK, Adams WW. **2020**. Zeaxanthin, a Molecule for Photoprotection in Many Different Environments. *Molecules* **25**: 5825.

Di Ferdinando M, Brunetti C, Agati G, Tattini M. **2014**. Multiple functions of polyphenols in plants inhabiting unfavorable Mediterranean areas. *Environmental and Experimental Botany* **103**: 107–116.

Dias MC, Pinto DCGA, Silva AMS. **2021**. Plant Flavonoids: Chemical Characteristics and Biological Activity. *Molecules* **26**: 5377.

Drake PL, Froend RH, Franks PJ. **2013**. Smaller, faster stomata: scaling of stomatal size, rate of response, and stomatal conductance. *Journal of Experimental Botany* **64**: 495–505.

Dyal SC. **1936**. A Key to the Species of Oaks of Eastern North America Based on Foliage and Twig Characters. *Rhodora* **38**: 53–63.

Edwards D. **1996**. Cuticles of early land plants: a palaeoecophysiological evaluation. *Plant Cuticles an Integrated Functional Approach*: 1–31.

Engel R, Gülz P-G, Herrmann T, Nahrstedt A. **1993**. Glandular Trichomes and the Yolatiles Obtained by Steam Distillation of *Quercus robur* Leaves. *Zeitschrift für Naturforschung C* **48**: 736–744.

Epron D, Dreyer E. **1993**. Long-term effects of drought on photosynthesis of adult oak trees [*Quercus petraea* (Matt.) Liebl. and *Quercus robur* L.] in a natural stand. *New Phytologist* **125**: 381–389.

Erb M, Kliebenstein DJ. **2020**. Plant secondary metabolites as defenses, regulators, and primary metabolites: the blurred functional trichotomy. *Plant physiology* **184**: 39–52.

Esteban R, Moran JF, Becerril JM, García-Plazaola JI. **2015**. Versatility of carotenoids: An integrated view on diversity, evolution, functional roles and environmental interactions. *Environmental and Experimental Botany* **119**: 63–75.

Etzold S, Waldner P, Thimonier A, Schmitt M, Dobbertin M. **2014**. Tree growth in Swiss forests between 1995 and 2010 in relation to climate and stand conditions: Recent disturbances matter. *Forest Ecology and Management* **311**: 41–55.

Fageria NK, Gheyi HR, Moreira A. **2011**. Nutrient Bioavailability in Salt Affected Soils. *Journal of Plant Nutrition* **34**: 945–962.

Falk J, Munné-Bosch S. **2010**. Tocochromanol functions in plants: antioxidation and beyond. *Journal of Experimental Botany* **61**: 1549–1566.

Fang C, Fernie AR, Luo J. **2019**. Exploring the Diversity of Plant Metabolism. *Trends in Plant Science* **24**: 83–98.

Farquhar GD, Sharkey TD. **1982**. Stomatal Conductance and Photosynthesis. *Annual Review of Plant Physiology* **33**: 317–345.

Fernández V, Sancho-Knapik D, Guzmán P, Peguero-Pina JJ, Gil L, Karabourniotis G, Khayet M, Fasseas C, Heredia-Guerrero JA, Heredia A, *et al.* 2014. Wettability, Polarity, and Water Absorption of Holm Oak Leaves: Effect of Leaf Side and Age. *Plant Physiology* **166**: 168–180.

Fernández-Marcos M, Sanz L, Lewis DR, Muday GK, Lorenzo O. **2013**. Control of Auxin Transport by Reactive Oxygen and Nitrogen Species. In: Chen R, Baluška F, eds. Signaling and Communication in Plants. Polar Auxin Transport. Berlin, Heidelberg: Springer, 103–117.

Fernández-Marín B, Nadal M, Gago J, Fernie AR, López-Pozo M, Artetxe U, García-Plazaola JI, Verhoeven A. **2020**. Born to revive: molecular and physiological mechanisms of double tolerance in a paleotropical and resurrection plant. *New Phytologist* **226**: 741–759.

Ferrer J-L, Austin MB, Stewart C, Noel JP. **2008**. Structure and function of enzymes involved in the biosynthesis of phenylpropanoids. *Plant Physiology and Biochemistry* **46**: 356–370.

Ferreyra MLF, Serra P, Casati P. **2021**. Recent advances on the roles of flavonoids as plant protective molecules after UV and high light exposure. *Physiologia Plantarum* **173**: 736–749.

Férriz M, Martin-Benito D, Fernández-de-Simón MB, Conde M, García-Cervigón AI, Aranda I, Gea-Izquierdo G. **2023**. Functional phenotypic plasticity mediated by water stress and [CO_2] explains differences in drought tolerance of two phylogenetically close conifers (R Tognetti, Ed.). *Tree Physiology* **43**: 909–924.

Fini A, Guidi L, Ferrini F, Brunetti C, Di Ferdinando M, Biricolti S, Pollastri S, Calamai L, Tattini M. **2012**. Drought stress has contrasting effects on antioxidant enzymes activity and phenylpropanoid biosynthesis in *Fraxinus ornus* leaves: An excess light stress affair? *Journal of Plant Physiology* **169**: 929–939.

Fischbach RJ, Kossmann B, Panten H, Steinbrecher R, Heller W, Seidlitz HK, Sandermann H, Hertkorn N, Schnitzler J-P. **1999**. Seasonal accumulation of ultraviolet-B screening pigments in needles of Norway spruce (*Picea abies* (L.) Karst.). *Plant, Cell & Environment* **22**: 27–37.

Fleta-Soriano E, Munné-Bosch S. **2016**. Stress Memory and the Inevitable Effects of Drought: A Physiological Perspective. *Frontiers in Plant Science* **7**: 143.

Flexas J, Barbour MM, Brendel O, Cabrera HM, Carriquí M, Díaz-Espejo A, Douthe C, Dreyer E, Ferrio JP, Gago J, *et al.* 2012. Mesophyll diffusion conductance to CO_2: An unappreciated central player in photosynthesis. *Plant Science* **193–194**: 70–84.

Flexas J, Diaz-Espejo A, Gago J, Gallé A, Galmés J, Gulías J, Medrano H. **2014**. Photosynthetic limitations in Mediterranean plants: A review. *Environmental and Experimental Botany* **103**: 12–23.

Flexas J, Gulías J, Jonasson S, Medrano H, Mus M. **2001**. Seasonal patterns and control of gas exchange in local populations of the Mediterranean evergreen shrub *Pistacia lentiscus* L. *Acta Oecologica* **22**: 33–43.

Flexas J, Medrano H. **2002**. Drought-inhibition of Photosynthesis in C3 Plants: Stomatal and Non-stomatal Limitations Revisited. *Annals of Botany* **89**: 183–189.

Forner A, Valladares F, Bonal D, Granier A, Grossiord C, Aranda I. **2018**. Extreme droughts affecting Mediterranean tree species' growth and water-use efficiency: the importance of timing. *Tree Physiology* **38**: 1127–1137.

Fortini P, Antonecchia G, Di Marzio P, Maiuro L, Viscosi V. **2013**. Role of micromorphological leaf traits and molecular data in taxonomy of three sympatric white oak species and their hybrids (*Quercus* L.). *Plant Biosystems - An International Journal Dealing with all Aspects of Plant Biology* **149**: 546–558.

Fortini P, Viscosi V, Maiuro L, Fineschi S, Vendramin GG. **2009**. Comparative leaf surface morphology and molecular data of five oaks of the subgenus *Quercus* Oerst (Fagaceae). *Plant Biosystems - An International Journal Dealing with all Aspects of Plant Biology* **143**: 543–554.

Fotelli MN, Radoglou KM, Constantinidou H-IA. **2000**. Water stress responses of seedlings of four Mediterranean oak species. *Tree Physiology* **20**: 1065–1075.

Franks PJ, Drake PL, Beerling DJ. **2009**. Plasticity in maximum stomatal conductance constrained by negative correlation between stomatal size and density: an analysis using *Eucalyptus globulus*. *Plant, Cell & Environment* **32**: 1737–1748.

Franks PJ, Farquhar GD. **2007**. The Mechanical Diversity of Stomata and Its Significance in Gas-Exchange Control. *Plant Physiology* **143**: 78–87.

Früchtenicht E, Neumann L, Klein N, Bonal D, Brüggemann W. **2018**. Response of *Quercus robur* and two potential climate change winners—*Quercus pubescens* and *Quercus ilex*—To two years summer drought in a semi-controlled competition study: I—Tree water status. *Environmental and Experimental Botany* **152**: 107–117.

Gachon CMM, Langlois-Meurinne M, Saindrenan P. **2005**. Plant secondary metabolism glycosyltransferases: the emerging functional analysis. *Trends in Plant Science* **10**: 542–549.

Gago J, Daloso DM, Carriquí M, Nadal M, Morales M, Araújo WL, Nunes-Nesi A, Flexas J. **2020**. Mesophyll conductance: the leaf corridors for photosynthesis. *Biochemical Society Transactions* **48**: 429–439.

Galdon-Armero J, Fullana-Pericas M, Mulet PA, Conesa MA, Martin C, Galmes J. **2018**. The ratio of trichomes to stomata is associated with water use efficiency in *Solanum lycopersicum* (tomato). *The Plant Journal* **96**: 607–619.

Gallé A, Haldimann P, Feller U. **2007**. Photosynthetic performance and water relations in young pubescent oak (*Quercus pubescens*) trees during drought stress and recovery. *New Phytologist* **174**: 799–810.

Galmés J, Ochogavía JM, Gago J, Roldán EJ, Cifre J, Conesa MÀ. **2013**. Leaf responses to drought stress in Mediterranean accessions of *Solanum lycopersicum*: anatomical adaptations in relation to gas exchange parameters. *Plant, Cell & Environment* **36**: 920–935.

García-Plazaola JI, Becerril JM. **2000**. Effects of drought on photoprotective mechanisms in European beech (*Fagus sylvatica* L.) seedlings from different provenances. *Trees* **14**: 485–490.

García-Plazaola JI, Esteban R, Hormaetxe K, Fernández-Marín B, Becerril JM. **2008**. Photoprotective responses of Mediterranean and Atlantic trees to the extreme heat-wave of summer 2003 in Southwestern Europe. *Trees* **22**: 385–392.

Garnier S, Giordanengo E, Saatkamp A, Santonja M, Reiter IM, Orts J-P, Gauquelin T, Meineri E. **2021**. Amplified drought induced by climate change reduces seedling emergence and increases seedling mortality for two Mediterranean perennial herbs. *Ecology and Evolution* **11**: 16143–16152.

Gayomba SR, Watkins JM, Muday GK. **2016**. Flavonols regulate plant growth and development through regulation of auxin transport and cellular redox status. *Recent advances in polyphenol research* **5**: 143–170.

Gea-Izquierdo G, Aranda I, Cañellas I, Dorado-Liñán I, Olano JM, Martin-Benito D. **2021**. Contrasting species decline but high sensitivity to increasing water stress on a mixed pine–oak ecotone. *Journal of Ecology* **109**: 109–124.

Genard-Zielinski A-C, Boissard C, Fernandez C, Kalogridis C, Lathière J, Gros V, Bonnaire N, Ormeño E. **2015**. Variability of BVOC emissions from a Mediterranean mixed forest in southern France with a focus on *Quercus pubescens*. *Atmospheric Chemistry and Physics* **15**: 431–446.

Genard-Zielinski A-C, Boissard C, Ormeño E, Lathière J, Reiter IM, Wortham H, Orts J-P, Temime-Roussel B, Guenet B, Bartsch S. **2018a**. Seasonal variations of *Quercus pubescens* isoprene emissions from an in natura forest under drought stress and sensitivity to future climate change in the Mediterranean area. *Biogeosciences* **15**: 4711–4730.

Genard-Zielinski A-C, Boissard C, Ormeño E, Lathière J, Reiter IM, Wortham H, Orts J-P, Temime-Roussel B, Guenet B, Bartsch S. **2018b**. Seasonal variations of Quercus pubescens isoprene emissions from an in natura forest under drought stress and sensitivity to future climate change in the Mediterranean area. *Biogeosciences* **15**: 4711–4730.

Genard-Zielinski A-C, Ormeño E, Boissard C, Fernandez C. **2014**. Isoprene Emissions from Downy Oak under Water Limitation during an Entire Growing Season: What Cost for Growth? *PLOS ONE* **9**: e112418.

Gerhardt KE, Lampi MA, Greenberg BM. **2008**. The effects of far-red light on plant growth and flavonoid accumulation in *Brassica napus* in the presence of ultraviolet B radiation. *Photochemistry and Photobiology* **84**: 1445–1454.

Gharibi S, Sayed Tabatabaei BE, Saeidi G, Talebi M, Matkowski A. **2019**. The effect of drought stress on polyphenolic compounds and expression of flavonoid biosynthesis related genes in *Achillea pachycephala* Rech.f. *Phytochemistry* **162**: 90–98.

Giorgi F, Lionello P. **2008**. Climate change projections for the Mediterranean region. *Global and Planetary Change* **63**: 90–104.

Giossi C, Cartaxana P, Cruz S. **2020**. Photoprotective Role of Neoxanthin in Plants and Algae. *Molecules* **25**: 4617.

Girard F, Vennetier M, Guibal F, Corona C, Ouarmim S, Herrero A. **2012**. *Pinus halepensis* Mill. crown development and fruiting declined with repeated drought in Mediterranean France. *European Journal of Forest Research* **131**: 919–931.

Gonzáles WL, Negritto MA, Suárez LH, Gianoli E. **2008**. Induction of glandular and non-glandular trichomes by damage in leaves of Madia sativa under contrasting water regimes. *Acta Oecologica* **33**: 128–132.

Gori A, Nascimento LB, Ferrini F, Centritto M, Brunetti C. **2020**. Seasonal and Diurnal Variation in Leaf Phenolics of Three Medicinal Mediterranean Wild Species: What Is the Best Harvesting Moment to Obtain the Richest and the Most Antioxidant Extracts? *Molecules* **25**: 956.

Gori A, Tattini M, Centritto M, Ferrini F, Marino G, Mori J, Guidi L, Brunetti C. **2019**. Seasonal and daily variations in primary and secondary metabolism of three maquis shrubs unveil different adaptive responses to Mediterranean climate. *Conservation Physiology* **7**: coz070.

Gouveia AC, Freitas H. **2009**. Modulation of leaf attributes and water use efficiency in *Quercus suber* along a rainfall gradient. *Trees* **23**: 267–275.

Gratani L, Pesoli P, Crescente MF, Aichner K, Larcher W. **2000**. Photosynthesis as a temperature indicator in *Quercus ilex* L. *Global and Planetary Change* **24**: 153–163.

Grattan SR, Grieve CM. **1999**. Mineral nutrient acquisition and response by plants grown in saline environments. *Handbook of plant and crop stress* **2**: 203–229.

Griesser M, Weingart G, Schoedl-Hummel K, Neumann N, Becker M, Varmuza K, Liebner F, Schuhmacher R, Forneck A. **2015**. Severe drought stress is affecting selected primary metabolites, polyphenols, and volatile metabolites in grapevine leaves (*Vitis vinifera* cv. Pinot noir). *Plant Physiology and Biochemistry* **88**: 17–26.

Griffin-Nolan RJ, Blumenthal DM, Collins SL, Farkas TE, Hoffman AM, Mueller KE, Ocheltree TW, Smith MD, Whitney KD, Knapp AK. **2019**. Shifts in plant functional composition following long-term drought in grasslands. *Journal of Ecology* **107**: 2133–2148.

Grunewald W, Smet ID, Lewis DR, Löfke C, Jansen L, Goeminne G, Bossche RV, Karimi M, Rybel BD, Vanholme B, *et al.* 2012. Transcription factor WRKY23 assists auxin distribution patterns during *Arabidopsis* root development through local control on flavonol biosynthesis. *Proceedings of the National Academy of Sciences* **109**: 1554–1559.

Gruszka J, Pawlak A, Kruk J. 2008. Tocochromanols, plastoquinol, and other biological prenyllipids as singlet oxygen quenchers—determination of singlet oxygen quenching rate constants and oxidation products. *Free Radical Biology and Medicine* **45**: 920–928.

Guerfel M, Baccouri O, Boujnah D, Chaïbi W, Zarrouk M. 2009. Impacts of water stress on gas exchange, water relations, chlorophyll content and leaf structure in the two main Tunisian olive (*Olea europaea* L.) cultivars. *Scientia Horticulturae* **119**: 257–263.

Guiot J, Cramer W. 2016. Climate change: The 2015 Paris Agreement thresholds and Mediterranean basin ecosystems. *Science* **354**: 465–468.

Gülz P-G, Müller E. 1992. Seasonal Variation In The Composition Of Epicuticular Waxes Of *Quercus Robur* Leaves. *Zeitschrift für Naturforschung C* **47**: 800–806.

Haas K, Bauer M, Wollenweber E. 2003. Cuticular Waxes and Flavonol Aglycones of Mistletoes. *Zeitschrift für Naturforschung C* **58**: 464–470.

Haberstroh S, Kreuzwieser J, Lobo-do-Vale R, Caldeira MC, Dubbert M, Werner C. 2018. Terpenoid Emissions of Two Mediterranean Woody Species in Response to Drought Stress. *Frontiers in Plant Science* **9**: 1071.

Haldimann P, Galle A, Feller U. 2008. Impact of an exceptionally hot dry summer on photosynthetic traits in oak (*Quercus pubescens*) leaves. *Tree physiology* **28**: 785–95.

Hardin JW. 1975. Hybridization and Introgression in *Quercus Alba*. *Journal of the Arnold Arboretum* **56**: 336–363.

Hardin JW. 1976. Terminology and Classification of *Quercus* Trichomes. *Journal of the Elisha Mitchell Scientific Society* **92**: 151–161.

Hardin JW. 1979. Patterns of Variation in Foliar Trichomes of Eastern North American *Quercus*. **66**: 576–585.

Hare JD, Elle E, van Dam NM. 2003. Costs of Glandular Trichomes in Datura Wrightii: A Three-Year Study. *Evolution* **57**: 793–805.

Harrell Jr FE. 2014. Hmisc: Harrell Miscellaneous (Version 3.14–4)[Computer program, R package]. *Nashville, TN: Author Retrieved from CRAN R-project org/package= Hmisc*.

Hartmann H, Bastos A, Das AJ, Esquivel-Muelbert A, Hammond WM, Martínez-Vilalta J, McDowell NG, Powers JS, Pugh TAM, Ruthrof KX, *et al.* 2022. Climate Change Risks to Global Forest Health: Emergence of Unexpected Events of Elevated Tree Mortality Worldwide. *Annual Review of Plant Biology* **73**: 673–702.

Hasanuzzaman M, Nahar K, Alam MM, Roychowdhury R, Fujita M. **2013**. Physiological, Biochemical, and Molecular Mechanisms of Heat Stress Tolerance in Plants. *International Journal of Molecular Sciences* **14**: 9643–9684.

Havaux M. **2020**. Plastoquinone In and Beyond Photosynthesis. *Trends in Plant Science* **25**: 1252–1265.

Havaux M, Dall'Osto L, Bassi R. **2007**. Zeaxanthin Has Enhanced Antioxidant Capacity with Respect to All Other Xanthophylls in *Arabidopsis* Leaves and Functions Independent of Binding to PSII Antennae. *Plant Physiology* **145**: 1506–1520.

Havaux M, Eymery F, Porfirova S, Rey P, Dörmann P. **2005**. Vitamin E Protects against Photoinhibition and Photooxidative Stress in *Arabidopsis thaliana*. *The Plant Cell* **17**: 3451–3469.

Havaux M, García-Plazaola JI. **2014**. Beyond Non-Photochemical Fluorescence Quenching: The Overlapping Antioxidant Functions of Zeaxanthin and Tocopherols. In: Demmig-Adams B, Garab G, Adams III W, Govindjee, eds. Advances in Photosynthesis and Respiration. Non-Photochemical Quenching and Energy Dissipation in Plants, Algae and Cyanobacteria. Dordrecht: Springer Netherlands, 583–603.

Havaux M, Kloppstech K. **2001**. The protective functions of carotenoid and flavonoid pigments against excess visible radiation at chilling temperature investigated in *Arabidopsis* npq and tt mutants. *Planta* **213**: 953–966.

Hectors K, van Oevelen S, Guisez Y, Prinsen E, Jansen MA. **2012**. The phytohormone auxin is a component of the regulatory system that controls UV-mediated accumulation of flavonoids and UV-induced morphogenesis. *Physiologia plantarum* **145**: 594–603.

Hectors K, Van Oevelen S, Geuns J, Guisez Y, Jansen MAK, Prinsen E. **2014**. Dynamic changes in plant secondary metabolites during UV acclimation in *Arabidopsis thaliana*. *Physiologia Plantarum* **152**: 219–230.

Heim KE, Tagliaferro AR, Bobilya DJ. **2002**. Flavonoid antioxidants: chemistry, metabolism and structure-activity relationships. *The Journal of Nutritional Biochemistry* **13**: 572–584.

Heine GF, Hernandez JM, Grotewold E. **2004**. Two Cysteines in Plant R2R3 MYB Domains Participate in REDOX-dependent DNA Binding*. *Journal of Biological Chemistry* **279**: 37878–37885.

Henry C, John GP, Pan R, Bartlett MK, Fletcher LR, Scoffoni C, Sack L. **2019**. A stomatal safety-efficiency trade-off constrains responses to leaf dehydration. *Nature Communications* **10**: 3398.

Henry LK, Thomas ST, Widhalm JR, Lynch JH, Davis TC, Kessler SA, Bohlmann J, Noel JP, Dudareva N. **2018**. Contribution of isopentenyl phosphate to plant terpenoid metabolism. *Nature Plants* **4**: 721–729.

Heredia-Guerrero JA, Benítez JJ, Domínguez E, Bayer IS, Cingolani R, Athanassiou A, Heredia A. **2016**. Infrared spectroscopy as a tool to study plant cuticles. **28**: 4.

Herms DA, Mattson WJ. **1992**. The dilemma of plants: to grow or defend. *The quarterly review of biology* **67**: 283–335.

Hernández I, Alegre L, Munné-Bosch S. **2004**. Drought-induced changes in flavonoids and other low molecular weight antioxidants in *Cistus clusii* grown under Mediterranean field conditions. *Tree Physiology* **24**: 1303–1311.

Hernandez I, Alegre L, Munnebosch S. **2006**. Enhanced oxidation of flavan-3-ols and proanthocyanidin accumulation in water-stressed tea plants. *Phytochemistry* **67**: 1120–1126.

Hernández I, Alegre L, Van Breusegem F, Munné-Bosch S. **2009**. How relevant are flavonoids as antioxidants in plants? *Trends in Plant Science* **14**: 125–132.

Hernández I, Cela J, Alegre L, Munné-Bosch S. **2012**. Antioxidant defenses against drought stress. In: Plant responses to drought stress. Springer, 231–258.

Hernandez JO, Park BB. **2022**. The Leaf Trichome, Venation, and Mesophyll Structural Traits Play Important Roles in the Physiological Responses of Oak Seedlings to Water-Deficit Stress. *International Journal of Molecular Sciences* **23**: 8640.

Herrmann K. **1988**. On the occurrence of flavonol and flavone glycosides in vegetables. *Zeitschrift für Lebensmittel-Untersuchung und Forschung* **186**: 1–5.

Hichri I, Barrieu F, Bogs J, Kappel C, Delrot S, Lauvergeat V. **2011**. Recent advances in the transcriptional regulation of the flavonoid biosynthetic pathway. *Journal of Experimental Botany* **62**: 2465–2483.

Hodaei M, Rahimmalek M, Arzani A, Talebi M. **2018**. The effect of water stress on phytochemical accumulation, bioactive compounds and expression of key genes involved in flavonoid biosynthesis in Chrysanthemum morifolium L. *Industrial Crops and Products* **120**: 295–304.

Holloway PJ. **1994**. Plant Cuticles: Physicochemical Characteristics and Biosynthesis. In: Percy KE, Cape JN, Jagels R, Simpson CJ, eds. Air Pollutants and the Leaf Cuticle. Berlin, Heidelberg: Springer Berlin Heidelberg, 1–13.

Hughes J, Hepworth C, Dutton C, Dunn JA, Hunt L, Stephens J, Waugh R, Cameron DD, Gray JE. **2017**. Reducing Stomatal Density in Barley Improves Drought Tolerance without Impacting on Yield. *Plant Physiology* **174**: 776–787.

Hundal T, Forsmark-Andrée P, Ernster L, Andersson B. **1995**. Antioxidant Activity of Reduced Plastoquinone in Chloroplast Thylakoid Membranes. *Archives of Biochemistry and Biophysics* **324**: 117–122.

Hussain S, Junaid Rao M, Anjum MA, Ejaz S, Zakir I, Ali MA, Ahmad N, Ahmad S. **2019**. Oxidative Stress and Antioxidant Defense in Plants Under Drought Conditions. In: 207–219.

Husson F, Josse J, Pages J. **2010**. Principal component methods-hierarchical clustering-partitional clustering: why would we need to choose for visualizing data. *Applied Mathematics Department* **17**.

Hutzler P, Fischbach R, Heller W, Jungblut TP, Reuber S, Schmitz R, Veit M, Weissenböck G, Schnitzler J-P. **1998**. Tissue localization of phenolic compounds in plants by confocal laser scanning microscopy. *Journal of Experimental Botany* **49**: 953–965.

Ibrahim RK, De Luca V, Khouri H, Latchinian L, Brisson L, Charest PM. **1987**. Enzymology and compartmentation of polymethylated flavonol glucosides in *chrysosplenium americanum*. *Phytochemistry* **26**: 1237–1245.

Imlay JA, Chin SM, Linn S. **1988**. Toxic DNA Damage by Hydrogen Peroxide Through the Fenton Reaction in Vivo and in Vitro. *Science* **240**: 640–642.

Itter MS, D'Orangeville L, Dawson A, Kneeshaw D, Duchesne L, Finley AO. **2019**. Boreal tree growth exhibits decadal-scale ecological memory to drought and insect defoliation, but no negative response to their interaction. *Journal of Ecology* **107**: 1288–1301.

Iwashina T. **2000**. The structure and distribution of the flavonoids in plants. *Journal of Plant Research* **113**: 287.

Jacobs M, Rubery PH. **1988**. Naturally Occurring Auxin Transport Regulators. *Science* **241**: 346–349.

Jansen MA. **2002**. Ultraviolet-B radiation effects on plants: induction of morphogenic responses. *Physiologia Plantarum* **116**: 423–429.

Jansson S. **1994**. The light-harvesting chlorophyll ab-binding proteins. *Biochimica et Biophysica Acta (BBA) - Bioenergetics* **1184**: 1–19.

Javelle M, Vernoud V, Rogowsky PM, Ingram GC. **2011**. Epidermis: the formation and functions of a fundamental plant tissue. *New Phytologist* **189**: 17–39.

Jenks MA, Hasegawa PM, Jain SM (Eds.). **2007**. *Advances in Molecular Breeding Toward Drought and Salt Tolerant Crops*. Dordrecht: Springer Netherlands.

Jetter R, Riederer M. **2016**. Localization of the Transpiration Barrier in the Epi- and Intracuticular Waxes of Eight Plant Species: Water Transport Resistances Are Associated with Fatty Acyl Rather Than Alicyclic Components. *Plant Physiology* **170**: 921–934.

Jogawat A, Yadav B, Chhaya, Lakra N, Singh AK, Narayan OP. **2021**. Crosstalk between phytohormones and secondary metabolites in the drought stress tolerance of crop plants: A review. *Physiologia Plantarum* **172**: 1106–1132.

Jones AG, Clymans W, Palmer DJ, Crockatt ME. **2022**. Revaluating forest drought experiments according to future precipitation patterns, ecosystem carbon and decomposition rate responses: A meta-analysis. *Ambio* **51**: 1227–1238.

Jorge TF, Tohge T, Wendenburg R, Ramalho JC, Lidon FC, Ribeiro-Barros AI, Fernie AR, António C. 2019. Salt-stress secondary metabolite signatures involved in the ability of Casuarina glauca to mitigate oxidative stress. *Environmental and Experimental Botany* **166**: 103808.

Joshi RC, Sheridan GJ, Ryu D, Lane PNJ. 2022. How long is the memory of forest growth to rainfall in asynchronous climates? *Ecological Indicators* **140**: 109057.

Julio Camarero J, Gazol A, Sangüesa-Barreda G, Cantero A, Sánchez-Salguero R, Sánchez-Miranda A, Granda E, Serra-Maluquer X, Ibáñez R. 2018. Forest Growth Responses to Drought at Short- and Long-Term Scales in Spain: Squeezing the Stress Memory from Tree Rings. *Frontiers in Ecology and Evolution* **6**: 9.

Kamal-Eldin A, Appelqvist L-Å. 1996. The chemistry and antioxidant properties of tocopherols and tocotrienols. *Lipids* **31**: 671–701.

Kambona CM, Koua PA, Léon J, Ballvora A. 2023. Stress memory and its regulation in plants experiencing recurrent drought conditions. *Theoretical and Applied Genetics* **136**: 26.

Kapoor D, Bhardwaj S, Landi M, Sharma A, Ramakrishnan M, Sharma A. 2020. The Impact of Drought in Plant Metabolism: How to Exploit Tolerance Mechanisms to Increase Crop Production. *Applied Sciences* **10**: 5692.

Karabourniotis G, Liakopoulos G, Nikolopoulos D, Bresta P. 2020. Protective and defensive roles of non-glandular trichomes against multiple stresses: structure–function coordination. *Journal of Forestry Research* **31**: 1–12.

Kartashov AV, Zlobin IE, Pashkovskiy PP, Pojidaeva ES, Ivanov YV, Ivanova AI, Ivanov VP, Marchenko SI, Nartov DI, Kuznetsov VV. 2023. Effects of drought stress memory on the accumulation of stress-protective compounds in naturally grown pine and spruce. *Plant Physiology and Biochemistry* **200**: 107761.

Kassambara A. 2020. Mundt. F.(2020). Factoextra: Extract and visualize the results of multivariate data analyses. *R package version* **1**.

Kellomäki S, Wang K-Y. 2001. Growth and Resource Use of Birch Seedlings Under Elevated Carbon Dioxide and Temperature. *Annals of Botany* **87**: 669–682.

Khorobrykh S, Tyystjärvi E. 2018. Plastoquinol generates and scavenges reactive oxygen species in organic solvent: Potential relevance for thylakoids. *Biochimica et Biophysica Acta (BBA) - Bioenergetics* **1859**: 1119–1131.

Kim S, Schlicke H, Ree K, Karvonen K, Subramaniam A, Richter A, Grimm B, Braam J. 2013. *Arabidopsis* Chlorophyll Biosynthesis: An Essential Balance between the Methylerythritol Phosphate and Tetrapyrrole Pathways. *The Plant cell* **25**.

King G, Fonti P, Nievergelt D, Büntgen U, Frank D. 2013. Climatic drivers of hourly to yearly tree radius variations along a 6°C natural warming gradient. *Agricultural and Forest Meteorology* **168**: 36–46.

Kissling P. **1977**. Les poils de quatre espèces de chênes du Jura (*Quercus pubescens*, *Q. petraea*, *Q. robur* et *Q. cerris*). **87**: 1–18.

Klein T. **2015**. Drought-induced tree mortality: from discrete observations to comprehensive research. *Tree Physiology* **35**: 225–228.

Konrad W, Burkhardt J, Ebner M, Roth-Nebelsick A. **2015**. Leaf pubescence as a possibility to increase water use efficiency by promoting condensation. *Ecohydrology* **8**: 480–492.

Kosma DK, Bourdenx B, Bernard A, Parsons EP, Lü S, Joubès J, Jenks MA. **2009**. The Impact of Water Deficiency on Leaf Cuticle Lipids of *Arabidopsis*. *Plant Physiology* **151**: 1918–1929.

Kotilainen T, Tegelberg R, Julkunen-Tiitto R, Lindfors A, Aphalo PJ. **2008**. Metabolite specific effects of solar UV-A and UV-B on alder and birch leaf phenolics. *Global Change Biology* **14**: 1294–1304.

Krieger-Liszkay A, Fufezan C, Trebst A. **2008**. Singlet oxygen production in photosystem II and related protection mechanism. *Photosynthesis Research* **98**: 551–564.

Krinsky NI. **1989**. Antioxidant functions of carotenoids. *Free Radical Biology and Medicine* **7**: 617–635.

Król A, Amarowicz R, Weidner S. **2014**. Changes in the composition of phenolic compounds and antioxidant properties of grapevine roots and leaves (*Vitis vinifera* L.) under continuous of long-term drought stress. *Acta Physiologiae Plantarum* **36**: 1491–1499.

Kruk J, Szymańska R, Cela J, Munne-Bosch S. **2014**. Plastochromanol-8: Fifty years of research. *Phytochemistry* **108**: 9–16.

Ksas B, Becuwe N, Chevalier A, Havaux M. **2015**. Plant tolerance to excess light energy and photooxidative damage relies on plastoquinone biosynthesis. *Scientific Reports* **5**: 10919.

Ksas B, Légeret B, Ferretti U, Chevalier A, Pospíšil P, Alric J, Havaux M. **2018**. The plastoquinone pool outside the thylakoid membrane serves in plant photoprotection as a reservoir of singlet oxygen scavengers. *Plant, Cell & Environment* **41**: 2277–2287.

Kuhn BM, Geisler M, Bigler L, Ringli C. **2011**. Flavonols Accumulate Asymmetrically and Affect Auxin Transport in *Arabidopsis*. *Plant Physiology* **156**: 585–595.

Kumar S, Abedin MM, Singh A, Das S. **2020a**. Role of Phenolic Compounds in Plant-Defensive Mechanisms. In: Plant Phenolics in Sustainable Agriculture. 517–532.

Kumar K, Debnath P, Singh S, Kumar N. **2023**. An Overview of Plant Phenolics and Their Involvement in Abiotic Stress Tolerance. *Stresses* **3**: 570–585.

Kumar V, Kodandaramaiah J, Rajan M. **2012**. Leaf and anatomical traits in relation to physiological characteristics in mulberry (Morus sp.) cultivars. *Turkish Journal of Botany* **36**: 683–689.

Kumar S, Pandey AK. **2013**. Chemistry and Biological Activities of Flavonoids: An Overview (KP Lu and J Sastre, Eds.). *The Scientific World Journal* **2013**: 162750.

Kumar A, Prasad A, Sedlářová M, Ksas B, Havaux M, Pospíšil P. **2020b**. Interplay between antioxidants in response to photooxidative stress in *Arabidopsis*. *Free Radical Biology and Medicine* **160**: 894–907.

Laoué J, Fernandez C, Ormeño E. **2022**. Plant Flavonoids in Mediterranean Species: A Focus on Flavonols as Protective Metabolites under Climate Stress. *Plants* **11**: 172.

Laoué J, Havaux M, Ksas B, Tuccio B, Lecareux C, Fernandez C, Ormeño E. **2023**. Long-term rain exclusion in a Mediterranean forest: response of physiological and physico-chemical traits of *Quercus pubescens* across seasons. *The Plant Journal* **116**: 1293–1308.

Lattanzio V, Lattanzino VMT, Cardinali A. **2006**. Role of phenolics in the resistance mechanisms of plants against fungal pathogens and insects. **661**: 23–67.

Lawlor. **1995**. The effects of water deficit on photosynthesis. *Environment and Plant Metabolism.*: 129–160.

Le Provost G, Domergue F, Lalanne C, Ramos Campos P, Grosbois A, Bert D, Meredieu C, Danjon F, Plomion C, Gion J-M. **2013**. Soil water stress affects both cuticular wax content and cuticle-related gene expression in young saplings of maritime pine (*Pinus pinaster* Ait). *BMC Plant Biology* **13**: 95.

Le Roy J, Huss B, Creach A, Hawkins S, Neutelings G. **2016**. Glycosylation Is a Major Regulator of Phenylpropanoid Availability and Biological Activity in Plants. *Frontiers in Plant Science* **7**: 735.

Leopoldini M, Russo N, Chiodo S, Toscano M. **2006**. Iron Chelation by the Powerful Antioxidant Flavonoid Quercetin. *Journal of Agricultural and Food Chemistry* **54**: 6343–6351.

Lepiniec L, Debeaujon I, Routaboul J-M, Baudry A, Pourcel L, Nesi N, Caboche M. **2006**. Genetics and Biochemistry of Seed Flavonoids. *Annual Review of Plant Biology* **57**: 405–430.

Levitt J. **1980**. *Responses of plants to environmental stresses / J. Levitt*. New York: Academic Press.

Lewis DR, Ramirez MV, Miller ND, Vallabhaneni P, Ray WK, Helm RF, Winkel BSJ, Muday GK. **2011**. Auxin and Ethylene Induce Flavonol Accumulation through Distinct Transcriptional Networks. *Plant Physiology* **156**: 144–164.

Li X, Kim YB, Kim Y, Zhao S, Kim HH, Chung E, Lee J-H, Park SU. **2013**. Differential stress-response expression of two flavonol synthase genes and accumulation of flavonols in tartary buckwheat. *Journal of Plant Physiology* **170**: 1630–1636.

Li S, Lu S, Wang J, Chen Z, Zhang Y, Duan J, Liu P, Wang X, Guo J. **2023a**. Responses of Physiological, Morphological and Anatomical Traits to Abiotic Stress in Woody Plants. *Forests* **14**: 1784.

Li C, Mo Y, Wang N, Xing L, Qu Y, Chen Y, Yuan Z, Ali A, Qi J, Fernández V, *et al.* 2023b. The overlooked functions of trichomes: Water absorption and metal detoxication. *Plant, Cell & Environment* **46**: 669–687.

Libutti A, Cammerino ARB, Monteleone M. **2018**. Risk Assessment of Soil Salinization Due to Tomato Cultivation in Mediterranean Climate Conditions. *Water* **10**: 1503.

Liebelt DJ, Jordan JT, Doherty CJ. **2019**. Only a matter of time: the impact of daily and seasonal rhythms on phytochemicals. *Phytochemistry Reviews* **18**: 1409–1433.

Limousin JM, Rambal S, Ourcival JM, Rocheteau A, Joffre R, Rodriguez-Cortina R. **2009**. Long-term transpiration change with rainfall decline in a Mediterranean *Quercus ilex* forest. *Global Change Biology* **15**: 2163–2175.

Limousin J-M, Roussel A, Rodríguez-Calcerrada J, Torres-Ruiz JM, Moreno M, Garcia de Jalon L, Ourcival J-M, Simioni G, Cochard H, Martin-StPaul N. **2022**. Drought acclimation of *Quercus ilex* leaves improves tolerance to moderate drought but not resistance to severe water stress. *Plant, Cell & Environment* **45**: 1967–1984.

Lin-Wang K, Micheletti D, Palmer J, Volz R, Lozano L, Espley R, Hellens RP, Chagnè D, Rowan DD, Troggio M, *et al.* 2011. High temperature reduces apple fruit colour via modulation of the anthocyanin regulatory complex. *Plant, Cell & Environment* **34**: 1176–1190.

Lionello P, Abrantes F, Gacic M, Planton S, Trigo R, Ulbrich U. **2014**. The climate of the Mediterranean region: research progress and climate change impacts. *Regional Environmental Change* **14**: 1679–1684.

Lionello P, Scarascia L. **2018**. The relation between climate change in the Mediterranean region and global warming. *Regional Environmental Change* **18**: 1481–1493.

Liu M, Li X, Liu Y, Cao B. **2013**. Regulation of flavanone 3-hydroxylase gene involved in the flavonoid biosynthesis pathway in response to UV-B radiation and drought stress in the desert plant, *Reaumuria soongorica*. *Plant Physiology and Biochemistry* **73**: 161–167.

Liu D, Ogaya R, Barbeta A, Yang X, Peñuelas J. **2018**. Long-term experimental drought combined with natural extremes accelerate vegetation shift in a Mediterranean holm oak forest. *Environmental and Experimental Botany* **151**: 1–11.

Liu Y, Qin L, Han L, Xiang Y, Zhao D. **2015**. Overexpression of maize SDD1 (ZmSDD1) improves drought resistance in *Zea mays* L. by reducing stomatal density. *Plant Cell, Tissue and Organ Culture (PCTOC)* **122**: 147–159.

Lo Gullo MA, Salleo S. **1988**. Different strategies of drought resistance in three Mediterranean sclerophyllous trees growing in the same environmental conditions. *New Phytologist* **108**: 267–276.

Mahmoud SS, Maddock S, Adal AM. **2021**. Isoprenoid Metabolism and Engineering in Glandular Trichomes of *Lamiaceae*. *Frontiers in Plant Science* **12**.

Mamari HHA. **2021**. Phenolic Compounds: Classification, Chemistry, and Updated Techniques of Analysis and Synthesis. In: Phenolic Compounds - Chemistry, Synthesis, Diversity, Non-Conventional Industrial, Pharmaceutical and Therapeutic Applications. IntechOpen, 73–94.

Mandal R, Dutta G. **2020**. From photosynthesis to biosensing: Chlorophyll proves to be a versatile molecule. *Sensors International* **1**: 100058.

Maoka T. **2020**. Carotenoids as natural functional pigments. *Journal of Natural Medicines* **74**: 1–16.

Marchi S, Tognetti R, Minnocci A, Borghi M, Sebastiani L, Biolabs Á, Superiore S, Anna S. **2008**. Variation in mesophyll anatomy and photosynthetic capacity during leaf development in a deciduous mesophyte fruit tree(Prunus persica) and an evergreen sclerophyllous Mediterranean shrub (Olea europaea). *Trees* **22**: 559–571.

Marchin RM, Medlyn BE, Tjoelker MG, Ellsworth DS. **2023**. Decoupling between stomatal conductance and photosynthesis occurs under extreme heat in broadleaf tree species regardless of water access. *Global Change Biology* **29**: 6319–6335.

Marenco RA, Antezana-Vera SA, Nascimento HCS. **2009**. Relationship between specific leaf area, leaf thickness, leaf water content and SPAD-502 readings in six Amazonian tree species. *Photosynthetica* **47**: 184–190.

Marino G, Caruso T, Ferguson L, Marra F. **2018**. Gas Exchanges and Stem Water Potential Define Stress Thresholds for Efficient Irrigation Management in Olive (*Olea europea* L.). *Water* **10**: 342.

Marinova K, Pourcel L, Weder B, Schwarz M, Barron D, Routaboul J-M, Debeaujon I, Klein M. **2007**. The *Arabidopsis* MATE transporter TT12 acts as a vacuolar flavonoid/H+-antiporter active in proanthocyanidin-accumulating cells of the seed coat. *The Plant Cell* **19**: 2023–2038.

Markham KR, Porter LJ. **1979**. Flavonoids of the primitive liverwort Takakia and their taxonomic and phylogenetic significance. *Phytochemistry* **18**: 611–615.

Marqués L, Ogle K, Peltier DMP, Camarero JJ. **2022**. Altered climate memory characterizes tree growth during forest dieback. *Agricultural and Forest Meteorology* **314**: 108787.

Martinez V, Mestre TC, Rubio F, Girones-Vilaplana A, Moreno DA, Mittler R, Rivero RM. **2016**. Accumulation of Flavonols over Hydroxycinnamic Acids Favors Oxidative Damage Protection under Abiotic Stress. *Frontiers in Plant Science* **7**: 838.

Martins CMC, Mesquita SMM, Vaz WLC. **1999**. Cuticular waxes of the holm (*Quercus ilex* l. subsp. *ballota* (desf.) samp.) and cork (*Q. suber* l.) oaks. *Phytochemical Analysis* **10**: 1–5.

Matesanz S, Valladares F. **2014**. Ecological and evolutionary responses of Mediterranean plants to global change. *Environmental and Experimental Botany* **103**: 53–67.

McDowell NG. **2011**. Mechanisms Linking Drought, Hydraulics, Carbon Metabolism, and Vegetation Mortality. *Plant Physiology* **155**: 1051–1059.

McDowell N, Pockman WT, Allen CD, Breshears DD, Cobb N, Kolb T, Plaut J, Sperry J, West A, Williams DG, *et al.* 2008. Mechanisms of plant survival and mortality during drought: why do some plants survive while others succumb to drought? *New Phytologist* **178**: 719–739.

Mediavilla S, Escudero A. **2003**. Stomatal responses to drought at a Mediterranean site: a comparative study of co-occurring woody species differing in leaf longevity. *Tree Physiology* **23**: 987–996.

Mediavilla S, Martín I, Babiano J, Escudero A. **2019**. Foliar plasticity related to gradients of heat and drought stress across crown orientations in three Mediterranean *Quercus* species. *PLOS ONE* **14**: e0224462.

Medrano H. **2002**. Regulation of Photosynthesis of C3 Plants in Response to Progressive Drought: Stomatal Conductance as a Reference Parameter. *Annals of Botany* **89**: 895–905.

Melidou M, Riganakos K, Galaris D. **2005**. Protection against nuclear DNA damage offered by flavonoids in cells exposed to hydrogen peroxide: The role of iron chelation. *Free Radical Biology and Medicine* **39**: 1591–1600.

Menezes-Silva PE, Sanglard LMVP, Ávila RT, Morais LE, Martins SCV, Nobres P, Patreze CM, Ferreira MA, Araújo WL, Fernie AR, *et al.* 2017. Photosynthetic and metabolic acclimation to repeated drought events play key roles in drought tolerance in coffee. *Journal of Experimental Botany* **68**: 4309–4322.

de Miguel M, Guevara MÁ, Sánchez-Gómez D, de María N, Díaz LM, Mancha JA, Fernández de Simón B, Cadahía E, Desai N, Aranda I, *et al.* 2016. Organ-specific metabolic responses to drought in *Pinus pinaster* Ait. *Plant Physiology and Biochemistry* **102**: 17–26.

Miller G, Suzuki N, Ciftci-Yilmaz S, Mittler R. **2010**. Reactive oxygen species homeostasis and signalling during drought and salinity stresses. *Plant, Cell & Environment* **33**: 453–467.

Mittler R. **2006**. Abiotic stress, the field environment and stress combination. *Trends in Plant Science* **11**: 15–19.

Mittler R, Blumwald E. **2015**. The Roles of ROS and ABA in Systemic Acquired Acclimation. *The Plant Cell* **27**: 64–70.

Moghe GD, Kruse LH. **2018**. The study of plant specialized metabolism: Challenges and prospects in the genomics era. *American Journal of Botany* **105**: 959–962.

Moghe GD, Leong BJ, Hurney SM, Daniel Jones A, Last RL. **2017**. Evolutionary routes to biochemical innovation revealed by integrative analysis of a plant-defense related specialized metabolic pathway. *eLife* **6**: e28468.

Mohawesh O. **2016**. Utilizing deficit irrigation to enhance growth performance and water-use efficiency of eggplant in arid environments. *Journal of Agricultural Science and Technology* **18**: 265–276.

Morales-Navarro S, Pérez-Díaz R, Ortega A, de Marcos A, Mena M, Fenoll C, González-Villanueva E, Ruiz-Lara S. **2018**. Overexpression of a *SDD1-Like* Gene From Wild Tomato Decreases Stomatal Density and Enhances Dehydration Avoidance in *Arabidopsis* and Cultivated Tomato. *Frontiers in plant science* **9**: 940.

Moran JoseF, Becana M, Iturbe-Ormaetxe I, Frechilla S, Klucas RobertV, Aparicio-Tejo P. **1994**. Drought induces oxidative stress in pea plants. *Planta* **194**: 346–352.

Moreira X, Abdala-Roberts L, Hidalgo-Galvez MD, Vázquez-González C, Pérez-Ramos IM. **2020**. Micro-climatic effects on plant phenolics at the community level in a Mediterranean savanna. *Scientific Reports* **10**: 14757.

Moreira X, Castagneyrol B, Abdala-Roberts L, Berny-Mier y Teran JC, Timmermans BGH, Bruun HH, Covelo F, Glauser G, Rasmann S, Tack AJM. **2018**. Latitudinal variation in plant chemical defences drives latitudinal patterns of leaf herbivory. *Ecography* **41**: 1124–1134.

Moreira X, Mooney KA, Rasmann S, Petry WK, Carrillo-Gavilán A, Zas R, Sampedro L. **2014**. Trade-offs between constitutive and induced defences drive geographical and climatic clines in pine chemical defences. *Ecology Letters* **17**: 537–546.

Moreno JC, Mi J, Alagoz Y, Al-Babili S. **2021a**. Plant apocarotenoids: from retrograde signaling to interspecific communication. *The Plant Journal* **105**: 351–375.

Moreno M, Simioni G, Cailleret M, Ruffault J, Badel E, Carrière S, Davi H, Gavinet J, Huc R, Limousin J-M, *et al.* 2021b. Consistently lower sap velocity and growth over nine years of rainfall exclusion in a Mediterranean mixed pine-oak forest. *Agricultural and Forest Meteorology* **308–309**: 108472.

Morita Y, Takagi K, Fukuchi-Mizutani M, Ishiguro K, Tanaka Y, Nitasaka E, Nakayama M, Saito N, Kagami T, Hoshino A. **2014**. A chalcone isomerase-like protein enhances flavonoid production and flower pigmentation. *The Plant Journal* **78**: 294–304.

Movahed N, Pastore C, Cellini A, Allegro G, Valentini G, Zenoni S, Cavallini E, D'Incà E, Tornielli GB, Filippetti I. **2016**. The grapevine VviPrx31 peroxidase as a candidate gene involved in anthocyanin degradation in ripening berries under high temperature. *Journal of Plant Research* **129**: 513–526.

Mrázová A, Belay SA, Eliášová A, Perez-Delgado C, Kaducová M, Betti M, Vega JM, Paľove-Balang P. **2017**. Expression, activity of phenylalanine-ammonia-lyase and accumulation of phenolic compounds in Lotus japonicus under salt stress. *Biologia* **72**: 36–42.

Munné-Bosch S. **2005**. The role of -tocopherol in plant stress tolerance. *Journal of Plant Physiology* **162**: 743–748.

Munné-Bosch S, Alegre L. **2001**. Subcellular Compartmentation of the Diterpene Carnosic Acid and Its Derivatives in the Leaves of Rosemary. *Plant Physiology* **125**: 1094–1102.

Munné-Bosch S, Alegre L. **2002**. The Function of Tocopherols and Tocotrienols in Plants. *Critical Reviews in Plant Sciences* **21**: 31–57.

Munné-Bosch S, Schwarz K, Alegre L. **1999**. Enhanced Formation of α-Tocopherol and Highly Oxidized Abietane Diterpenes in Water-Stressed Rosemary Plants. *Plant Physiology* **121**: 1047–1052.

Muñoz P, Munné-Bosch S. **2019**. Vitamin E in Plants: Biosynthesis, Transport, and Function. *Trends in Plant Science* **24**: 1040–1051.

Nadal M, Flexas J. **2018**. Mesophyll Conductance to CO_2 Diffusion: Effects of Drought and Opportunities for Improvement. In: García Tejero IF, Durán Zuazo VH, eds. Water Scarcity and Sustainable Agriculture in Semiarid Environment. Academic Press, 403–438.

Naikoo MI, Dar MI, Raghib F, Jaleel H, Ahmad B, Raina A, Khan FA, Naushin F. **2019**. Role and regulation of plants phenolics in abiotic stress tolerance: an overview. In: Plant signaling molecules. Elsevier, 157–168.

Nakabayashi R, Mori T, Saito K. **2014a**. Alternation of flavonoid accumulation under drought stress in *Arabidopsis thaliana*. *Plant Signaling & Behavior* **9**: e29518.

Nakabayashi R, Yonekura-Sakakibara K, Urano K, Suzuki M, Yamada Y, Nishizawa T, Matsuda F, Kojima M, Sakakibara H, Shinozaki K, *et al.* 2014b. Enhancement of oxidative and drought tolerance in *Arabidopsis* by overaccumulation of antioxidant flavonoids. *The Plant Journal* **77**: 367–379.

Narayana KR, Reddy MS, Chaluvadi MR, Krishna DR. **2001**. Bioflavonoids classification, pharmacological, biochemical effects and therapeutic potential. *Indian Journal of Pharmacology* **33**: 2–16.

Nardini A, Pitt F. **1999**. Drought resistance of *Quercus pubescens* as a function of root hydraulic conductance, xylem embolism and hydraulic architecture. *The New Phytologist* **143**: 485–493.

Ni X, Sun L, Cai Q, Ma S, Feng Y, Sun Y, An L, Ji C. **2022**. Variation and determinants of leaf anatomical traits from boreal to tropical forests in eastern China. *Ecological Indicators* **140**: 108992.

Nichols SN, Hofmann RW, Williams WM. **2015**. Physiological drought resistance and accumulation of leaf phenolics in white clover interspecific hybrids. *Environmental and Experimental Botany* **119**: 40–47.

Niinemets Ü. **2015**. Is there a species spectrum within the world-wide leaf economics spectrum? Major variations in leaf functional traits in the Mediterranean sclerophyll *Quercus ilex*. *New Phytologist* **205**: 79–96.

Niinemets U, Kull O. **1998**. Stoichiometry of foliar carbon constituents varies along light gradients in temperate woody canopies: implications for foliage morphological plasticity. *Tree Physiology* **18**: 467–479.

Niinemets Ü, Wright IJ, Evans JR. **2009**. Leaf mesophyll diffusion conductance in 35 Australian sclerophylls covering a broad range of foliage structural and physiological variation. *Journal of Experimental Botany* **60**: 2433–2449.

Nissinen K, Nybakken L, Virjamo V, Julkunen-Tiitto R. **2016**. Slow-growing Salix repens (*Salicaceae*) benefits from changing climate. *Environmental and Experimental Botany* **128**: 59–68.

Nissinen K, Virjamo V, Randriamanana T, Sobuj N, Sivadasan U, Mehtätalo L, Beuker E, Julkunen-Tiitto R, Nybakken L. **2017**. Responses of growth and leaf phenolics in European aspen (*Populus tremula*) to climate change during juvenile phase change. *Canadian Journal of Forest Research* **47**: 1350–1363.

Niyogi KK, Björkman O, Grossman AR. **1997**. The roles of specific xanthophylls in photoprotection. *Proceedings of the National Academy of Sciences* **94**: 14162–14167.

Noori M, Azar AM, Saidi M, Panahandeh J, Haghi DZ. **2018**. Evaluation of water deficiency impacts on antioxidant enzymes activity and lipid peroxidation in some tomato (*Solanum lycopersicum* L.) lines. *Indian Journal of Agricultural Research* **52**: 228–235.

Ogaya R, Penuelas J. **2006**. Contrasting foliar responses to drought in *Quercus ilex* and *Phillyrea latifolia*. *Biologia plantarum* **50**: 373–382.

Ogaya R, Peñuelas J. **2021**. Climate Change Effects in a Mediterranean Forest Following 21 Consecutive Years of Experimental Drought. *Forests* **12**: 306.

Oksanen J, Blanchet FG, Kindt R, Legendre P, Minchin PR, O'hara RB, Simpson GL, Solymos P, Stevens MHH, Wagner H. **2013**. Package 'vegan'. *Community ecology package, version* **2**: 1–295.

Ormeño E, Ruffault J, Gutigny C, Madrigal J, Guijarro M, Hernando C, Ballini C. **2020a**. Increasing cuticular wax concentrations in a drier climate promote litter flammability. *Forest Ecology and Management* **473**: 118242.

Ormeño E, Viros J, Mévy J-P, Tonetto A, Saunier A, Bousquet-Mélou A, Fernandez C. **2020b**. Exogenous Isoprene Confers Physiological Benefits in a Negligible Isoprene Emitter (*Acer monspessulanum* L.) under Water Deficit. *Plants* **9**: 159.

Osmond CB, Foyer CH, Bock G, Grace SC, Logan BA. **2000**. Energy dissipation and radical scavenging by the plant phenylpropanoid pathway. *Philosophical Transactions of the Royal Society of London. Series B: Biological Sciences* **355**: 1499–1510.

Owens DK, Alerding AB, Crosby KC, Bandara AB, Westwood JH, Winkel BSJ. **2008**. Functional Analysis of a Predicted Flavonol Synthase Gene Family in Arabidopsis. *Plant Physiology* **147**: 1046–1061.

Panche AN, Diwan AD, Chandra SR. **2016**. Flavonoids: an overview. *Journal of Nutritional Science* **5**: e47.

Pandey KB, Rizvi SI. **2009**. Plant Polyphenols as Dietary Antioxidants in Human Health and Disease. *Oxidative Medicine and Cellular Longevity* **2**: 270–278.

Pang Y, Wenger JP, Saathoff K, Peel GJ, Wen J, Huhman D, Allen SN, Tang Y, Cheng X, Tadege M, *et al.* 2009. A WD40 Repeat Protein from *Medicago truncatula* Is Necessary for Tissue-Specific Anthocyanin and Proanthocyanidin Biosynthesis But Not for Trichome Development. *Plant Physiology* **151**: 1114–1129.

Parihar P, Singh S, Singh R, Singh VP, Prasad SM. **2015**. Effect of salinity stress on plants and its tolerance strategies: a review. *Environmental Science and Pollution Research* **22**: 4056–4075.

Park M, Somborn A, Schlehuber D, Keuter V, Deerberg G. **2023**. Raman spectroscopy in crop quality assessment: focusing on sensing secondary metabolites: a review. *Horticulture Research* **10**: uhad074.

Pasta S, de Rigo D, Caudullo G. **2016**. *Quercus pubescens* in Europe: distribution, habitat, usage and threats. *European Atlas of forest tree species*: 156–157.

Pastore C, Dal Santo S, Zenoni S, Movahed N, Allegro G, Valentini G, Filippetti I, Tornielli GB. **2017**. Whole Plant Temperature Manipulation Affects Flavonoid Metabolism and the Transcriptome of Grapevine Berries. *Frontiers in Plant Science* **8**: 929.

Paula S, Pausas JG. **2006**. Leaf traits and resprouting ability in the Mediterranean basin. *Functional Ecology* **20**: 941–947.

Paul-Victor C, Züst T, Rees M, Kliebenstein DJ, Turnbull LA. **2010**. A new method for measuring relative growth rate can uncover the costs of defensive compounds in Arabidopsis thaliana. *New Phytologist* **187**: 1102–1111.

Peer WA, Murphy AS. **2006**. Flavonoids as Signal Molecules: Targets of Flavonoid Action. In: Grotewold E, ed. The Science of Flavonoids. New York, NY: Springer, 239–268.

Peer WA, Murphy AS. **2007**. Flavonoids and auxin transport: modulators or regulators? *Trends in Plant Science* **12**: 556–563.

Peguero-Pina JJ, Gil-Pelegrín E, Morales F. **2013**. Three pools of zeaxanthin in *Quercus coccifera* leaves during light transitions with different roles in rapidly reversible photoprotective energy dissipation and photoprotection. *Journal of Experimental Botany* **64**: 1649–1661.

Peguero-Pina JJ, Sisó S, Fernández-Marín B, Flexas J, Galmés J, García-Plazaola JI, Niinemets Ü, Sancho-Knapik D, Gil-Pelegrín E. **2016a**. Leaf functional plasticity

decreases the water consumption without further consequences for carbon uptake in *Quercus coccifera* L. under Mediterranean conditions. *Tree Physiology* **36**: 356–367.

Peguero-Pina JJ, Sisó S, Sancho-Knapik D, Díaz-Espejo A, Flexas J, Galmés J, Gil-Pelegrín E. 2016b. Leaf morphological and physiological adaptations of a deciduous oak (*Quercus faginea* Lam.) to the Mediterranean climate: a comparison with a closely related temperate species (*Quercus robur* L.). *Tree Physiology* **36**: 287–299.

Peiffer M, Tooker JF, Luthe DS, Felton GW. 2009. Plants on early alert: glandular trichomes as sensors for insect herbivores. *New Phytologist* **184**: 644–656.

Peltier DMP, Anderegg WRL, Guo JS, Ogle K. 2022. Contemporary tree growth shows altered climate memory. *Ecology Letters* **25**: 2663–2674.

Peñuelas J, Sardans J, Filella I, Estiarte M, Llusià J, Ogaya R, Carnicer J, Bartrons M, Rivas-Ubach A, Grau O, *et al.* 2018. Assessment of the impacts of climate change on Mediterranean terrestrial ecosystems based on data from field experiments and long-term monitored field gradients in Catalonia. *Environmental and Experimental Botany* **152**: 49–59.

Pérez-Ramos IM, Volaire F, Fattet M, Blanchard A, Roumet C. 2013. Tradeoffs between functional strategies for resource-use and drought-survival in Mediterranean rangeland species. *Environmental and Experimental Botany* **87**: 126–136.

Petrussa E, Braidot E, Zancani M, Peresson C, Bertolini A, Patui S, Vianello A. 2013. Plant Flavonoids—Biosynthesis, Transport and Involvement in Stress Responses. *International Journal of Molecular Sciences* **14**: 14950–14973.

Pirasteh-Anosheh H, Saed-Moucheshi A, Pakniyat H, Pessarakli M. 2016. Stomatal responses to drought stress. In: Ahmad P, ed. Water Stress and Crop Plants. Chichester, UK: John Wiley & Sons, Ltd, 24–40.

Pollastri S, Tattini M. 2011. Flavonols: old compounds for old roles. *Annals of Botany* **108**: 1225–1233.

Polyakov NE, Focsan AL, Gao Y, Kispert LD. 2023. The Endless World of Carotenoids—Structural, Chemical and Biological Aspects of Some Rare Carotenoids. *International Journal of Molecular Sciences* **24**: 9885.

Ponton S, Dupouey J-L, Bréda N. 2002. Comparison of water-use efficiency of seedlings from two sympatric oak species: genotype × environment interactions. *Tree Physiology* **22**: 413–422.

Poorter H, Niinemets Ü, Poorter L, Wright IJ, Villar R. 2009. Causes and consequences of variation in leaf mass per area (LMA): a meta-analysis. *New Phytologist* **182**: 565–588.

Popović BM, Štajner D, Ždero-Pavlović R, Tumbas-Šaponjac V, Čanadanović-Brunet J, Orlović S. 2016. Water stress induces changes in polyphenol profile and antioxidant capacity in poplar plants (*Populus* spp.). *Plant Physiology and Biochemistry* **105**: 242–250.

Poyatos R, Llorens P, Piñol J, Rubio C. 2008. Response of Scots pine (*Pinus sylvestris* L.) and pubescent oak (*Quercus pubescens* Willd.) to soil and atmospheric water deficits under Mediterranean mountain climate. *Annals of Forest Science* **65**: 306–306.

Prasad RBN, Giilz P-G. 1990. Developmental and Seasonal Variations in the Epicuticular Waxes of Beech Leaves (*Fagus sylvatica* L.). *Zeitschrift für Naturforschung C* **45**: 805–812.

Prasad RBN, Gülz P-G. 1990. Surface Structure and Chemical Composition of Leaf Waxes from *Quercus robur* L., *Acer pseudoplatanus* L. and *JugIans regia* L. *Zeitschrift für Naturforschung C* **45**: 813–817.

Qian Y, Lynch JH, Guo L, Rhodes D, Morgan JA, Dudareva N. 2019. Completion of the cytosolic post-chorismate phenylalanine biosynthetic pathway in plants. *Nature Communications* **10**: 15.

Quattrocchio F, Baudry A, Lepiniec L, Grotewold E. 2006. The Regulation of Flavonoid Biosynthesis. In: Grotewold E, ed. The Science of Flavonoids. New York, NY: Springer, 97–122.

Quézel P, Médail F. 2003. *Ecologie et biogéographie des forêts du bassin méditérranéen*. Paris: Elsevier.

Rahimi Y, Taleei A, Ranjbar M. 2018. Long-term water deficit modulates antioxidant capacity of peppermint (*Mentha piperita* L.). *Scientia Horticulturae* **237**: 36–43.

Ramaroson M-L, Koutouan C, Helesbeux J-J, Le Clerc V, Hamama L, Geoffriau E, Briard M. 2022. Role of Phenylpropanoids and Flavonoids in Plant Resistance to Pests and Diseases. *Molecules* **27**: 8371.

Ramírez-Valiente JA, Center A, Sparks JP, Sparks KL, Etterson JR, Longwell T, Pilz G, Cavender-Bares J. 2017. Population-Level Differentiation in Growth Rates and Leaf Traits in Seedlings of the Neotropical Live Oak *Quercus* oleoides Grown under Natural and Manipulated Precipitation Regimes. *Frontiers in Plant Science* **8**: 585.

Ramírez-Valiente JA, López R, Hipp AL, Aranda I. 2020. Correlated evolution of morphology, gas exchange, growth rates and hydraulics as a response to precipitation and temperature regimes in oaks (*Quercus*). *New Phytologist* **227**: 794–809.

Rastogi A, Yadav DK, Szymańska R, Kruk J, Sedlářová M, Pospíšil P. 2014. Singlet oxygen scavenging activity of tocopherol and plastochromanol in *Arabidopsis thaliana*: relevance to photooxidative stress. *Plant, Cell & Environment* **37**: 392–401.

Ravaglia D, Espley RV, Henry-Kirk RA, Andreotti C, Ziosi V, Hellens RP, Costa G, Allan AC. 2013. Transcriptional regulation of flavonoid biosynthesis in nectarine (*Prunus persica*) by a set of R2R3 MYB transcription factors. *BMC Plant Biology* **13**: 68.

Rea PA. 2007. Plant ATP-Binding Cassette Transporters. *Annual Review of Plant Biology* **58**: 347–375.

Read J, Sanson GD. 2003. Characterizing sclerophylly: the mechanical properties of a diverse range of leaf types. *New Phytologist* **160**: 81–99.

Reddy AR, Chaitanya KV, Vivekanandan M. **2004**. Drought-induced responses of photosynthesis and antioxidant metabolism in higher plants. *Journal of plant physiology* **161**: 1189–1202.

Reich PB. **2014**. The world-wide 'fast–slow' plant economics spectrum: a traits manifesto. *Journal of Ecology* **102**: 275–301.

Riahi K, Rao S, Krey V, Cho C, Chirkov V, Fischer G, Kindermann G, Nakicenovic N, Rafaj P. **2011**. RCP 8.5—A scenario of comparatively high greenhouse gas emissions. *Climatic Change* **109**: 33.

Rice-evans CA, Miller NJ, Bolwell PG, Bramley PM, Pridham JB. **1995**. The Relative Antioxidant Activities of Plant-Derived Polyphenolic Flavonoids. *Free Radical Research* **22**: 375–383.

Rice-Evans CA, Miller NJ, Paganga G. **1996**. Structure-antioxidant activity relationships of flavonoids and phenolic acids. *Free Radical Biology and Medicine* **20**: 933–956.

Rice-Evans C, Miller N, Paganga G. **1997**. Antioxidant properties of phenolic compounds. *Trends in Plant Science* **2**: 152–159.

Riederer M, Schneider G. **1990**. The effect of the environment on the permeability and composition of *Citrus* leaf cuticles. *Planta* **180**: 154–165.

Riederer M, Schreiber L. **1995**. Waxes—the transport barriers of plant cuticles. In: Hamilton R, ed. Waxes : chemistry, molecular biology and functions. Dundee: The Oily Press: Oily Press, 131–156.

Rivas-Ubach A, Gargallo-Garriga A, Sardans J, Oravec M, Mateu-Castell L, Pérez-Trujillo M, Parella T, Ogaya R, Urban O, Peñuelas J. **2014**. Drought enhances folivory by shifting foliar metabolomes in *Quercus ilex* trees. *New Phytologist* **202**: 874–885.

Rivas-Ubach A, Sardans J, Pérez-Trujillo M, Estiarte M, Peñuelas J. **2012**. Strong relationship between elemental stoichiometry and metabolome in plants. *Proceedings of the National Academy of Sciences* **109**: 4181–4186.

Robakowski P, Wyka TP, Kowalkowski W, Barzdajn W, Pers-Kamczyc E, Jankowski A, Politycka B. **2020**. Practical Implications of Different Phenotypic and Molecular Responses of Evergreen Conifer and Broadleaf Deciduous Forest Tree Species to Regulated Water Deficit in a Container Nursery. *Forests* **11**: 1011.

Roca M, Pérez-Gálvez A. **2021**. Metabolomics of Chlorophylls and Carotenoids: Analytical Methods and Metabolome-Based Studies. *Antioxidants* **10**: 1622.

Roeber VM, Bajaj I, Rohde M, Schmülling T, Cortleven A. **2021**. Light acts as a stressor and influences abiotic and biotic stress responses in plants. *Plant, Cell & Environment* **44**: 645–664.

Romero-Aranda R, Soria T, Cuartero J. **2001**. Tomato plant-water uptake and plant-water relationships under saline growth conditions. *Plant Science* **160**: 265–272.

Ruiz-Sola MÁ, Rodríguez-Concepción M. **2012**. Carotenoid Biosynthesis in *Arabidopsis*: A Colorful Pathway. *The Arabidopsis Book / American Society of Plant Biologists* **10**: e0158.

Ryan KG, Markham KR, Bloor SJ, Bradley JM, Mitchell KA, Jordan BR. **1998**. UVB Radiation Induced Increase in Quercetin: Kaempferol Ratio in Wild-Type and Transgenic Lines of Petunia. *Photochemistry and Photobiology* **68**: 323–330.

Ryan KG, Swinny EE, Markham KR, Winefield C. **2002**. Flavonoid gene expression and UV photoprotection in transgenic and mutant *Petunia* leaves. *Phytochemistry* **59**: 23–32.

Safou O, Saint-Martin M. **1989**. Le trichome foliaire de quelques *Quercus* périméditerranéens. *Bulletin de la Société Botanique de France. Lettres Botaniques* **136**: 291–304.

Sah SK, Reddy KR, Li J. **2016**. Abscisic Acid and Abiotic Stress Tolerance in Crop Plants. *Frontiers in Plant Science* **7**: 571.

Sairam RK, Tyagi A. **2004**. Physiology and molecular biology of salinity stress tolerance in plants. *Current Science* **86**: 407–421.

Saltveit ME. **2010**. Synthesis and metabolism of phenolic compounds. *Fruit and vegetable phytochemicals: chemistry, nutritional value and stability. Wiley-Blackwell, Ames*: 89–100.

Šamec D, Karalija E, Šola I, Vujčić Bok V, Salopek-Sondi B. **2021**. The Role of Polyphenols in Abiotic Stress Response: The Influence of Molecular Structure. *Plants* **10**: 118.

Sánchez-Rodríguez E, Moreno DA, Ferreres F, Rubio-Wilhelmi M del M, Ruiz JM. **2011**. Differential responses of five cherry tomato varieties to water stress: Changes on phenolic metabolites and related enzymes. *Phytochemistry* **72**: 723–729.

Santonja M, Fernandez C, Gauquelin T, Baldy V. **2015**. Climate change effects on litter decomposition: intensive drought leads to a strong decrease of litter mixture interactions. *Plant and Soil* **393**: 69–82.

Santos EL, Maia B, Ferriani AP, Teixeira SD. **2017**. *Flavonoids: Classification, biosynthesis and chemical ecology*. InTech.

Santos Tozin LR dos, de Melo Silva SC, Rodrigues TM. **2016**. Non-glandular trichomes in *Lamiaceae* and *Verbenaceae* species: morphological and histochemical features indicate more than physical protection. *New Zealand Journal of Botany* **54**: 446–457.

Santos-Sánchez NF, Salas-Coronado R, Hernández-Carlos B, Villanueva-Cañongo C. **2019**. *Shikimic Acid Pathway in Biosynthesis of Phenolic Compounds*. London, UK: IntechOpen.

Sardans J, Peñuelas J. **2013**. Plant-soil interactions in Mediterranean forest and shrublands: impacts of climatic change. *Plant and Soil* **365**: 1–33.

Sardans J, Peñuelas J, Rivas-Ubach A. **2011**. Ecological metabolomics: overview of current developments and future challenges. *Chemoecology* **21**: 191–225.

Sardin T, Micheneau C, Nicolas L, Claude S, François D. **2022**. Chêne sessile et chêne pédonculé face au changement climatique : quels choix sylvicoles ? *Rendez-vous Techniques de l'ONF*: 18–25.

Saslowsky DE, Warek U, Winkel BSJ. **2005**. Nuclear Localization of Flavonoid Enzymes in *Arabidopsis**. *Journal of Biological Chemistry* **280**: 23735–23740.

Saunier A, Greff S, Blande JD, Lecareux C, Baldy V, Fernandez C, Ormeño E. **2022**. Amplified Drought and Seasonal Cycle Modulate *Quercus pubescens* Leaf Metabolome. *Metabolites* **12**: 307.

Saunier A, Ormeño E, Boissard C, Wortham H, Temime-Roussel B, Lecareux C, Armengaud A, Fernandez C. **2017a**. Effect of mid-term drought on *Quercus pubescens* BVOCs' emission seasonality and their dependency on light and/or temperature. *Atmospheric Chemistry and Physics* **17**: 7555–7566.

Saunier A, Ormeño E, Havaux M, Wortham H, Ksas B, Temime-Roussel B, Blande JD, Lecareux C, Mévy J-P, Bousquet-Mélou A. **2018**. Resistance of native oak to recurrent drought conditions simulating predicted climatic changes in the Mediterranean region. *Plant, cell & environment* **41**: 2299–2312.

Saunier A, Ormeño E, Piga D, Armengaud A, Boissard C, Lathière J, Szopa S, Genard-Zielinski A-C, Fernandez C. **2020**. Isoprene contribution to ozone production under climate change conditions in the French Mediterranean area. *Regional Environmental Change* **20**: 111.

Saunier A, Ormeño E, Wortham H, Temime-Roussel B, Lecareux C, Boissard C, Fernandez C. **2017b**. Chronic drought decreases anabolic and catabolic BVOC emissions of *Quercus pubescens* in a Mediterranean forest. *Frontiers in plant science* **8**: 71.

Schulze WX, Altenbuchinger M, He M, Kränzlein M, Zörb C. **2021**. Proteome profiling of repeated drought stress reveals genotype-specific responses and memory effects in maize. *Plant Physiology and Biochemistry* **159**: 67–79.

Schuster A-C, Burghardt M, Alfarhan A, Bueno A, Hedrich R, Leide J, Thomas J, Riederer M. **2016**. Effectiveness of cuticular transpiration barriers in a desert plant at controlling water loss at high temperatures. *AoB PLANTS* **8**: plw027.

Scoffoni C, Vuong C, Diep S, Cochard H, Sack L. **2014**. Leaf Shrinkage with Dehydration: Coordination with Hydraulic Vulnerability and Drought Tolerance. *Plant Physiology* **164**: 1772–1788.

Sebastiani F, Torre S, Gori A, Brunetti C, Centritto M, Ferrini F, Tattini M. **2019**. Dissecting Adaptation Mechanisms to Contrasting Solar Irradiance in the Mediterranean Shrub *Cistus incanus*. *International Journal of Molecular Sciences* **20**: 3599.

Serra S. **2015**. Recent Advances in the Synthesis of Carotenoid-Derived Flavours and Fragrances. *Molecules* **20**: 12817–12840.

Seufert P, Staiger S, Arand K, Bueno A, Burghardt M, Riederer M. **2022**. Building a Barrier: The Influence of Different Wax Fractions on the Water Transpiration Barrier of Leaf Cuticles. *Frontiers in Plant Science* **12**: 766602.

Shah A, Smith DL. **2020**. Flavonoids in Agriculture: Chemistry and Roles in, Biotic and Abiotic Stress Responses, and Microbial Associations. *Agronomy* **10**: 1209.

Shahzad M, Khan Z, Nazeer W, Arshad SF, Ahmad F. **2021**. Effect of Drought on Trichome Density and Length in Cotton (*Gossypium Hirsutum*). *Journal of Bioresource Management* **8**: 154–167.

Sharma A, Shahzad B, Rehman A, Bhardwaj R, Landi M, Zheng B. **2019**. Response of Phenylpropanoid Pathway and the Role of Polyphenols in Plants under Abiotic Stress. *Molecules* **24**: 2452.

Shepherd T, Wynne Griffiths D. **2006**. The effects of stress on plant cuticular waxes. *New Phytologist* **171**: 469–499.

Shi H, Chen L, Ye T, Liu X, Ding K, Chan Z. **2014**. Modulation of auxin content in *Arabidopsis* confers improved drought stress resistance. *Plant Physiology and Biochemistry* **82**: 209–217.

Shibuya T, Itagaki K, Ueyama S, Hirai N, Endo R. **2016**. Atmospheric Humidity Influences Oviposition Rate of *Tetranychus urticae* (Acari: Tetranychidae) Through Morphological Responses of Host *Cucumis sativus* Leaves. *Journal of Economic Entomology* **109**: 255–258.

Shipley B, Vile D, Garnier E, Wright IJ, Poorter H. **2005**. Functional linkages between leaf traits and net photosynthetic rate: reconciling empirical and mechanistic models. *Functional Ecology* **19**: 602–615.

Shukla PR, Skea J, Calvo Buendia E, Masson-Delmotte V, Pörtner HO, Roberts DC, Zhai P, Slade R, Connors S, Van Diemen R. **2019**. IPCC, 2019: Climate Change and Land: an IPCC special report on climate change, desertification, land degradation, sustainable land management, food security, and greenhouse gas fluxes in terrestrial ecosystems.

Sierla M, Waszczak C, Vahisalu T, Kangasjärvi J. **2016**. Reactive Oxygen Species in the Regulation of Stomatal Movements. *Plant Physiology* **171**: 1569–1580.

Simões R, Miranda I, Pereira H. **2022**. Effect of Seasonal Variation on Leaf Cuticular Waxes' Composition in the Mediterranean Cork Oak (*Quercus suber* L.). *Forests* **13**: 1236.

Simões R, Rodrigues A, Ferreira-Dias S, Miranda I, Pereira H. **2020**. Chemical Composition of Cuticular Waxes and Pigments and Morphology of Leaves of *Quercus suber* Trees of Different Provenance. *Plants* **9**: 1165.

de Simón BF, Sanz M, Cervera MT, Pinto E, Aranda I, Cadahía E. **2017**. Leaf metabolic response to water deficit in Pinus pinaster Ait. relies upon ontogeny and genotype. *Environmental and Experimental Botany* **140**: 41–55.

Smith GJ, Markham KR. **1998**. Tautomerism of flavonol glucosides: relevance to plant UV protection and flower colour. *Journal of Photochemistry and Photobiology A: Chemistry* **118**: 99–105.

Smith MN, Stark SC, Taylor TC, Ferreira ML, de Oliveira E, Restrepo-Coupe N, Chen S, Woodcock T, dos Santos DB, Alves LF, *et al.* 2019. Seasonal and drought-related changes in leaf area profiles depend on height and light environment in an Amazon forest. *New Phytologist* **222**: 1284–1297.

Somavilla NS, Kolb RM, Rossatto DR. **2014**. Leaf anatomical traits corroborate the leaf economic spectrum: a case study with deciduous forest tree species. *Brazilian Journal of Botany* **37**: 69–82.

Sosa T, Alías JC, Escudero JC, Chaves N. **2005**. Interpopulational variation in the flavonoid composition of *Cistus ladanifer* L. exudate. *Biochemical Systematics and Ecology* **33**: 353–364.

Soufi O, Romero C, Louaileche H. **2014**. Ortho-diphenol profile and antioxidant activity of Algerian black olive cultivars: Effect of dry salting process. *Food Chemistry* **157**: 504–510.

Spieß N, Oufir M, Matušíková I, Stierschneider M, Kopecky D, Homolka A, Burg K, Fluch S, Hausman J-F, Wilhelm E. **2012**. Ecophysiological and transcriptomic responses of oak (*Quercus robur*) to long-term drought exposure and rewatering. *Environmental and Experimental Botany* **77**: 117–126.

Stapleton A. **1992**. Ultraviolet Radiation and Plants: Burning Questions. *The Plant Cell* **4**: 1353–1358.

Stirbet A, Lazár D, Guo Y, Govindjee G. **2020**. Photosynthesis: basics, history and modelling. *Annals of Botany* **126**: 511–537.

Stracke R, Ishihara H, Huep G, Barsch A, Mehrtens F, Niehaus K, Weisshaar B. **2007**. Differential regulation of closely related R2R3-MYB transcription factors controls flavonol accumulation in different parts of the *Arabidopsis thaliana* seedling. *The Plant Journal* **50**: 660–677.

Struve DK, Ferrini F, Fini A, Pennati L. **2009**. Relative Growth and Water Use of Seedlings from Three Italian *Quercus* Species. *Arboriculture & Urban Forestry* **35**: 113–121.

Sun P, Schuurink RC, Caissard J-C, Hugueney P, Baudino S. **2016**. My Way: Noncanonical Biosynthesis Pathways for Plant Volatiles. *Trends in Plant Science* **21**: 884–894.

Swain T, Williams CA. **1970**. The role of phenylalanine in flavonoid biosynthesis. *Phytochemistry* **9**: 2115–2122.

Symonowicz M, Kolanek M. **2012**. Flavonoids and their properties to form chelate complexes.

Sytiuk A, Hamard S, Céréghino R, Dorrepaal E, Geissel H, Küttim M, Lamentowicz M, Tuittila ES, Jassey VEJ. **2023**. Linkages between *Sphagnum* metabolites and peatland CO_2 uptake are sensitive to seasonality in warming trends. *New Phytologist* **237**: 1164–1178.

Szewczyk K, Chojnacka A, Górnicka M. **2021**. Tocopherols and Tocotrienols—Bioactive Dietary Compounds; What Is Certain, What Is Doubt? *International Journal of Molecular Sciences* **22**: 6222.

Szőllősi E, Oláh V, Kanalas P, Kis J, Fenyvesi A, Mészáros I. **2010**. Seasonal variation of leaf ecophysiological traits within the canopy of *Quercus petraea* (Matt.) Liebl. trees. *Acta Biologica Hungarica* **61**: 172–188.

Szymańska R, Nowicka B, Kruk J. **2014**. Hydroxy-plastochromanol and plastoquinone-C as singlet oxygen products during photo-oxidative stress in *Arabidopsis*. *Plant, Cell & Environment* **37**: 1464–1473.

Tague CL, Moritz M, Hanan E. **2019**. The changing water cycle: The eco-hydrologic impacts of forest density reduction in Mediterranean (seasonally dry) regions. *Wiley Interdisciplinary Reviews: Water* **6**: e1350.

Takahama U. **2004**. Oxidation of vacuolar and apoplastic phenolic substrates by peroxidase: Physiological significance of the oxidation reactions. *Phytochemistry Reviews* **3**: 207–219.

Tanaka Y, Sugano SS, Shimada T, Hara-Nishimura I. **2013**. Enhancement of leaf photosynthetic capacity through increased stomatal density in *Arabidopsis*. *New Phytologist* **198**: 757–764.

Tang H, Armston J, Hancock S, Marselis S, Goetz S, Dubayah R. **2019**. Characterizing global forest canopy cover distribution using spaceborne lidar. *Remote Sensing of Environment* **231**: 111262.

Tardieu F, Simonneau T. **1998**. Variability among species of stomatal control under fluctuating soil water status and evaporative demand: modelling isohydric and anisohydric behaviours. *Journal of Experimental Botany* **49**: 419–432.

Tattini M, Galardi C, Pinelli P, Massai R, Remorini D, Agati G. **2004**. Differential accumulation of flavonoids and hydroxycinnamates in leaves of *Ligustrum vulgare* under excess light and drought stress. *New Phytologist* **163**: 547–561.

Tattini M, Gravano E, Pinelli P, Mulinacci N, Romani A. **2000**. Flavonoids accumulate in leaves and glandular trichomes of *Phillyrea latifolia* exposed to excess solar radiation. *The New Phytologist* **148**: 69–77.

Tattini M, Matteini P, Saracini E, Traversi ML, Giordano C, Agati G. **2007**. Morphology and Biochemistry of Non-Glandular Trichomes in *Cistus salvifolius* L. Leaves Growing in Extreme Habitats of the Mediterranean Basin. *Plant Biology* **9**: 411–419.

Tattini M, Remorini D, Pinelli P, Agati G, Saracini E, Traversi ML, Massai R. **2006**. Morpho-anatomical, physiological and biochemical adjustments in response to root zone

salinity stress and high solar radiation in two Mediterranean evergreen shrubs, *Myrtus communis* and *Pistacia lentiscus*. *New Phytologist* **170**: 779–794.

Tattini M, Traversi ML, Castelli S, Biricolti S, Guidi L, Massai R, Tattini M, Traversi ML, Castelli S, Biricolti S, *et al.* 2009. Contrasting response mechanisms to root-zone salinity in three co-occurring Mediterranean woody evergreens: a physiological and biochemical study. *Functional Plant Biology* **36**: 551–563.

Taylor LP, Grotewold E. 2005. Flavonoids as developmental regulators. *Current Opinion in Plant Biology* **8**: 317–323.

Teale WD, Pasternak T, Dal Bosco C, Dovzhenko A, Kratzat K, Bildl W, Schwörer M, Falk T, Ruperti B, V Schaefer J. 2021. Flavonol-mediated stabilization of PIN efflux complexes regulates polar auxin transport. *The EMBO Journal* **40**: e104416.

Team RC. 2020. R Core Team R: a language and environment for statistical computing. *Foundation for Statistical Computing*.

Terashima I, Hanba YT, Tholen D, Niinemets Ü. 2011. Leaf Functional Anatomy in Relation to Photosynthesis. *Plant Physiology* **155**: 108–116.

Thomas FM, Gausling T. 2000. Morphological and physiological responses of oak seedlings (*Quercus petraea* and *Q. robur*) to moderate drought. *Annals of Forest Science* **57**: 325–333.

Thompson JD. 2020. *Plant Evolution in the Mediterranean: Insights for Conservation*. Oxford University Press.

Thomson PM, Mohlenbrock RH. 1979. Foliar Trichomes of *Quercus Subgenus Quercus* in the Eastern United States. *Journal of the Arnold Arboretum* **60**: 350–366.

Tirumalai V, Swetha C, Nair A, Pandit A, Shivaprasad PV. 2019. miR828 and miR858 regulate VvMYB114 to promote anthocyanin and flavonol accumulation in grapes. *Journal of Experimental Botany* **70**: 4775–4792.

Tixier A, Guzmán-Delgado P, Sperling O, Amico Roxas A, Laca E, Zwieniecki MA. 2020. Comparison of phenological traits, growth patterns, and seasonal dynamics of non-structural carbohydrate in Mediterranean tree crop species. *Scientific Reports* **10**: 347.

Tognetti R, Cherubini P, Marchi S, Raschi A. 2007. Leaf traits and tree rings suggest different water-use and carbon assimilation strategies by two co-occurring *Quercus* species in a Mediterranean mixed-forest stand in Tuscany, Italy. *Tree Physiology* **27**: 1741–1751.

Tognetti R, Longobucco A, Miglietta F, Raschi A. 1998a. Transpiration and stomatal behaviour of *Quercus ilex* plants during the summer in a Mediterranean carbon dioxide spring. *Plant, Cell & Environment* **21**: 613–622.

Tognetti R, Longobucco A, Raschi A. 1998b. Vulnerability of xylem to embolism in relation to plant hydraulic resistance in *Quercus pubescens* and *Quercus ilex* co-occurring in a Mediterranean coppice stand in central Italy. *New Phytologist* **139**: 437–447.

Tombesi S, Frioni T, Poni S, Palliotti A. **2018**. Effect of water stress "memory" on plant behavior during subsequent drought stress. *Environmental and Experimental Botany* **150**: 106–114.

Treutter D. **2006**. Significance of flavonoids in plant resistance: a review. *Environmental Chemistry Letters* **4**: 147.

Trewavas A. **2003**. Aspects of Plant Intelligence. *Annals of Botany* **92**: 1–20.

Trueba S, Théroux-Rancourt G, Earles JM, Buckley TN, Love D, Johnson DM, Brodersen C. **2022**. The three-dimensional construction of leaves is coordinated with water use efficiency in conifers. *New Phytologist* **233**: 851–861.

Tschan GF, Denk T. **2012**. Trichome types, foliar indumentum and epicuticular wax in the Mediterranean gall oaks, *Quercus* subsection *Galliferae* (Fagaceae): implications for taxonomy, ecology and evolution: Trichome types in gall oaks. *Botanical Journal of the Linnean Society* **169**: 611–644.

Tsubaki S, Sugimura K, Teramoto Y, Yonemori K, Azuma J. **2013**. Cuticular Membrane of *Fuyu* Persimmon Fruit Is Strengthened by Triterpenoid Nano-Fillers. *PLOS ONE* **8**: e75275.

Tuteja N. **2007**. Abscisic Acid and Abiotic Stress Signaling. *Plant Signaling & Behavior* **2**: 135–138.

Ullah A, Manghwar H, Shaban M, Khan AH, Akbar A, Ali U, Ali E, Fahad S. **2018**. Phytohormones enhanced drought tolerance in plants: a coping strategy. *Environmental Science and Pollution Research* **25**: 33103–33118.

Vaz M, Pereira JS, Gazarini LC, David TS, David JS, Rodrigues A, Maroco J, Chaves MM. **2010**. Drought-induced photosynthetic inhibition and autumn recovery in two Mediterranean oak species (*Quercus ilex* and *Quercus suber*). *Tree Physiology* **30**: 946–956.

Velikova V, Várkonyi Z, Szabó M, Maslenkova L, Nogues I, Kovács L, Peeva V, Busheva M, Garab G, Sharkey TD, *et al.* 2011. Increased Thermostability of Thylakoid Membranes in Isoprene-Emitting Leaves Probed with Three Biophysical Techniques. *Plant Physiology* **157**: 905–916.

Vickers CE, Gershenzon J, Lerdau MT, Loreto F. **2009**. A unified mechanism of action for volatile isoprenoids in plant abiotic stress. *Nature Chemical Biology* **5**: 283–291.

Vile D, Garnier É, Shipley B, Laurent G, Navas M-L, Roumet C, Lavorel S, Díaz S, Hodgson JG, Lloret F, *et al.* 2005. Specific Leaf Area and Dry Matter Content Estimate Thickness in Laminar Leaves. *Annals of Botany* **96**: 1129–1136.

Vodnik D, Gričar J, Lavrič M, Ferlan M, Hafner P, Eler K. **2019**. Anatomical and physiological adjustments of pubescent oak (*Quercus pubescens* Willd.) from two adjacent sub-Mediterranean ecosites. *Environmental and Experimental Botany* **165**: 208–218.

Vogt T, Jones P. **2000**. Glycosyltransferases in plant natural product synthesis: characterization of a supergene family. *Trends in Plant Science* **5**: 380–386.

Vogt T, Proksch P, Gülz P-G. **1987**. Epicuticular Flavonoid Aglycones in the Genus *Cistus*, *Cistaceae*. *Journal of Plant Physiology* **131**: 25–36.

Vranová E, Coman Schmid D, Gruissem W. **2013**. Network Analysis of the MVA and MEP Pathways for Isoprenoid Synthesis. *Annual review of plant biology* **64**.

Vuillemin J. **1982**. Ecophysiologie comparée du développement initial de *Quercus pubescens* Willd. et de *Quercus ilex* L. I. Développement des semis in situ. *Ecologia Mediterranea* **8**: 139–146.

Wagner GJ, Hrazdina G. **1984**. Endoplasmic reticulum as a site of phenylpropanoid and flavonoid metabolism in *Hippeastrum*. *Plant physiology* **74**: 901–906.

Wang S, Alseekh S, Fernie AR, Luo J. **2019**. The Structure and Function of Major Plant Metabolite Modifications. *Molecular Plant* **12**: 899–919.

Wang T, Li Q, Bi K. **2018a**. Bioactive flavonoids in medicinal plants: Structure, activity and biological fate. *Asian Journal of Pharmaceutical Sciences* **13**: 12–23.

Wang X, Shen C, Meng P, Tan G, Lv L. **2021**. Analysis and review of trichomes in plants. *BMC Plant Biology* **21**: 70.

Wang P, Song C-P. **2008**. Guard-cell signalling for hydrogen peroxide and abscisic acid. *New Phytologist* **178**: 703–718.

Wang X, Wang R, Gao J. **2022**. Precipitation and soil nutrients determine the spatial variability of grassland productivity at large scales in China. *Frontiers in Plant Science* **13**: 996313.

Wang X, Wang W, Huang J, Peng S, Xiong D. **2018b**. Diffusional conductance to CO_2 is the key limitation to photosynthesis in salt-stressed leaves of rice (*Oryza sativa*). *Physiologia Plantarum* **163**: 45–58.

Wang F, Zhu H, Chen D, Li Z, Peng R, Yao Q. **2016**. A grape bHLH transcription factor gene, VvbHLH1, increases the accumulation of flavonoids and enhances salt and drought tolerance in transgenic *Arabidopsis thaliana*. *Plant Cell, Tissue and Organ Culture (PCTOC)* **125**: 387–398.

Watkins JM, Chapman JM, Muday GK. **2017**. Abscisic Acid-Induced Reactive Oxygen Species Are Modulated by Flavonols to Control Stomata Aperture. *Plant Physiology* **175**: 1807–1825.

Weber P, Bugmann H, Rigling A. **2007**. Radial growth responses to drought of *Pinus sylvestris* and *Quercus pubescens* in an inner-Alpine dry valley. *Journal of Vegetation Science* **18**: 777–792.

Wellstein C, Poschlod P, Gohlke A, Chelli S, Campetella G, Rosbakh S, Canullo R, Kreyling J, Jentsch A, Beierkuhnlein C. **2017**. Effects of extreme drought on specific leaf area of grassland species: A meta-analysis of experimental studies in temperate and sub-Mediterranean systems. *Global Change Biology* **23**: 2473–2481.

Widhalm JR, Gutensohn M, Yoo H, Adebesin F, Qian Y, Guo L, Jaini R, Lynch JH, McCoy RM, Shreve JT, *et al.* 2015. Identification of a plastidial phenylalanine exporter that influences flux distribution through the phenylalanine biosynthetic network. *Nature Communications* **6**: 8142.

Williamson G, Plumb GW, Garcia-Conesa MT. **1999**. Glycosylation, Esterification, and Polymerization of Flavonoids and Hydroxycinnamates: Effects on Antioxidant Properties. In: Gross GG, Hemingway RW, Yoshida T, Branham SJ, eds. Basic Life Sciences. Plant Polyphenols 2: Chemistry, Biology, Pharmacology, Ecology. Boston, MA: Springer US, 483–494.

Wilson PJ, Thompson K, Hodgson JG. **1999**. Specific leaf area and leaf dry matter content as alternative predictors of plant strategies. *New Phytologist* **143**: 155–162.

Winkel BSJ. **2004**. Metabolic Channeling in Plants. *Annual Review of Plant Biology* **55**: 85–107.

Winkel-Shirley B. **1999**. Evidence for enzyme complexes in the phenylpropanoid and flavonoid pathways. *Physiologia Plantarum* **107**: 142–149.

Wright IJ, Reich PB, Westoby M, Ackerly DD, Baruch Z, Bongers F, Cavender-Bares J, Chapin T, Cornelissen JHC, Diemer M, *et al.* 2004. The worldwide leaf economics spectrum. *Nature* **428**: 821–827.

Xiao K, Mao X, Lin Y. **2016**. Trichome, a Functional Diversity Phenotype in Plant. *Molecular Biology* **s1**.

Xu W, Dubos C, Lepiniec L. **2015**. Transcriptional control of flavonoid biosynthesis by MYB–bHLH–WDR complexes. *Trends in Plant Science* **20**: 176–185.

Xu C, He CG, Wang YJ, Bi YF, Jiang H. **2020a**. Effect of drought and heat stresses on photosynthesis, pigments, and xanthophyll cycle in alfalfa (*Medicago sativa* L.). *Photosynthetica* **58**: 1226–1236.

Xu W, Jia L, Shi W, Liang J, Zhou F, Li Q, Zhang J. **2013**. Abscisic acid accumulation modulates auxin transport in the root tip to enhance proton secretion for maintaining root growth under moderate water stress. *New Phytologist* **197**: 139–150.

Xu Z, Zhou G. **2008**. Responses of leaf stomatal density to water status and its relationship with photosynthesis in a grass. *Journal of Experimental Botany* **59**: 3317–3325.

Xu Z, Zhou J, Ren T, Du H, Liu H, Li Y, Zhang C. **2020b**. Salt stress decreases seedling growth and development but increases quercetin and kaempferol content in *Apocynum venetum*. *Plant Biology* **22**: 813–821.

Xue D, Zhang X, Lu X, Chen G, Chen Z-H. **2017**. Molecular and Evolutionary Mechanisms of Cuticular Wax for Plant Drought Tolerance. *Frontiers in Plant Science* **8**: 621.

Yadav B, Jogawat A, Rahman M, Narayan O. **2021**. Secondary metabolites in the drought stress tolerance of crop plants: A review. *Gene Reports* **23**: 101040.

Yamasaki H, Sakihama Y, Ikehara N. **1997**. Flavonoid-Peroxidase Reaction as a Detoxification Mechanism of Plant Cells against H_2O_2. *Plant Physiology* **115**: 1405–1412.

Yang J, Ordiz MI, Jaworski JG, Beachy RN. **2011**. Induced accumulation of cuticular waxes enhances drought tolerance in *Arabidopsis* by changes in development of stomata. *Plant Physiology and Biochemistry* **49**: 1448–1455.

Yang L, Wen K-S, Ruan X, Zhao Y-X, Wei F, Wang Q. **2018**. Response of Plant Secondary Metabolites to Environmental Factors. *Molecules* **23**: 762.

Yeats TH, Rose JKC. **2013**. The Formation and Function of Plant Cuticles. *Plant Physiology* **163**: 5–20.

Yin R, Han K, Heller W, Albert A, Dobrev PI, Zažímalová E, Schäffner AR. **2014**. Kaempferol 3-O-rhamnoside-7-O-rhamnoside is an endogenous flavonol inhibitor of polar auxin transport in *Arabidopsis* shoots. *New Phytologist* **201**: 466–475.

Young DJ, Stevens JT, Earles JM, Moore J, Ellis A, Jirka AL, Latimer AM. **2017**. Long-term climate and competition explain forest mortality patterns under extreme drought. *Ecology letters* **20**: 78–86.

Zandalinas SI, Sales C, Beltrán J, Gómez-Cadenas A, Arbona V. **2017**. Activation of Secondary Metabolism in Citrus Plants Is Associated to Sensitivity to Combined Drought and High Temperatures. *Frontiers in Plant Science* **7**: 1954.

Zaprometov MN, Nikolaeva TN. **2003**. Chloroplasts Isolated from Kidney Bean Leaves Are Capable of Phenolic Compound Biosynthesis. *Russian Journal of Plant Physiology* **50**: 623–626.

Zhang S-B, Sun M, Cao K-F, Hu H, Zhang J-L. **2014**. Leaf Photosynthetic Rate of Tropical Ferns Is Evolutionarily Linked to Water Transport Capacity (C Ng, Ed.). *PLoS ONE* **9**: e84682.

Zhang Y, Virjamo V, Du W, Yin Y, Nissinen K, Nybakken L, Guo H, Julkunen-Tiitto R. **2018**. Effects of soil pyrene contamination on growth and phenolics in Norway spruce (*Picea abies*) are modified by elevated temperature and CO_2. *Environmental Science and Pollution Research* **25**: 12788–12799.

Zhang J, Zuo X, Zhao X, Ma J, Medina-Roldán E. **2020**. Effects of rainfall manipulation and nitrogen addition on plant biomass allocation in a semiarid sandy grassland. *Scientific Reports* **10**: 9026.

Zhao Y. **2010**. Auxin Biosynthesis and Its Role in Plant Development. *Annual Review of Plant Biology* **61**: 49–64.

Zhao J. **2015**. Flavonoid transport mechanisms: how to go, and with whom. *Trends in Plant Science* **20**: 576–585.

Zhao L, Chang W, Xiao Y, Liu H, Liu P. **2013**. Methylerythritol Phosphate Pathway of Isoprenoid Biosynthesis. *Annual review of biochemistry* **82**: 497–530.

Zhao J, Dixon RA. **2010**. The 'ins' and 'outs' of flavonoid transport. *Trends in Plant Science* **15**: 72–80.

Zhao W, Sun Y, Kjelgren R, Liu X. **2015**. Response of stomatal density and bound gas exchange in leaves of maize to soil water deficit. *Acta Physiologiae Plantarum* **37**: 1704.

Zhou P, Yin M, Dai S, Bao K, Song C, Liu C, Wu Q. **2021**. Multi-omics analysis of the bioactive constituents biosynthesis of glandular trichome in *Perilla frutescens*. *BMC Plant Biology* **21**: 277.

Zittis G, Bruggeman A, Lelieveld J. **2021**. Revisiting future extreme precipitation trends in the Mediterranean. *Weather and Climate Extremes* **34**: 100380.

Zittis G, Hadjinicolaou P, Klangidou M, Proestos Y, Lelieveld J. **2019**. A multi-model, multi-scenario, and multi-domain analysis of regional climate projections for the Mediterranean. *Regional Environmental Change* **19**: 2621–2635.

Zweifel R, Zimmermann L, Zeugin F, Newbery DM. **2006**. Intra-annual radial growth and water relations of trees: implications towards a growth mechanism. *Journal of Experimental Botany* **57**: 1445–1459.

List of figures

Figure 1: Historic warming of the atmosphere globally and in the Mediterranean Basin. Annual mean air temperature anomalies are shown with respect to the period 1880–1899, with the Mediterranean Basin (blue) and the globe (green) presented with (light curves) and without (dark curves) smoothing (Cramer *et al.*, 2018). 18

Figure 2: Projected changes of (a) mean annual temperature and (b) mean annual precipitation for the end (END 2081-2100) of the 21st century with respect to the reference period (CTL 1986–2005), for two Representative Concentration Pathways (RCP4.5: top row and RCP8.5: bottom row) in the Mediterranean region. Modified from Zittis *et al.* (2019). 19

Figure 3: Examples of morphology of different trichome types found in different plant species (Li *et al.*, 2023b). 23

Figure 4: Different types of glandular and non-glandular trichomes found in *Quercus* species (Hardin, 1976). 24

Figure 5: Leaf anatomical traits of *Q. pubescens* leaf. Leaf cross-sections were stained with safranin (lignified tissues) and astra blue (non-lignified tissues). Ab. Ep., abaxial epidermis; Ad Ep., adaxial epidermis; LT, leaf thickness; and VBD, midrib vascular bundle diameter. 26

Figure 6: Simplified schema of the response of plants to drought stress and the mechanisms (ROS scavenger, UV screener, energy dissipation) whereby plant defenses reduce cell oxidation. 28

Figure 7: Simplified biosynthetic pathways of metabolites targeted in this study. Compounds forming cuticular waxes are indicated with a star although they are not exclusive to waxes. Abbreviations are as follows: 3-DHS, 3-dehydroshikimate; 5 IPP, 5 Isopentenyl diphosphate; CoA, coenzyme A; DMAPP, dimethylallyl-diphosphate; DXP, 1-deoxy-D-xylulose-5-phosphate; FAD, fatty acids and derivatives; FPP, farnesyl pyrophosphate; GGPP, geranylgeranyl pyrophosphate; GPP, Geranyl pyrophosphate; HGA, homogentisic acid or homogentisate (phenolic acid); HPP, hydroxyphenylpyruvate; IPP, isopentenyl diphosphate; MEP, 2-C-methyl-D-Erythritol-4-phosphate; MPBQ, methylphytylbenzoquinol; MVA, (R)-mevalonate; Phytyl-PP, phytyl-diphosphate; MSBQ, methyl-solanesyl-enzoquinone; SDP, solanesyl diphosphate; VLCFA, Very Long Chain Fatty Acid. Modified from Laoué *et al.* (2023). 30

Figure 8: Photosynthetic pigments found in plants. (a) Structure of chlorophyll *a* and *b*. (b) Biosynthesis of carotenoids from lycopene as well as interconversions of zeaxanthin, antheraxanthin and violaxanthin in the xanthophyl cycle. Modified from Demmig-Adams *et al.* (2020). 32

Figure 9: The four main groups of specialized metabolites in plants and their biosynthetic pathways, modified from figures in Yadav *et al.* (2021). The underlined groups of compounds denote targeted/detected metabolites in the present thesis. Abbreviations are as follows: MEP, methylerythritol phosphate pathway; MVA, mevalonate pathway. 33

Figure 10: Plant cuticle structure. (a) Schematic representation of a leaf transversal cut showing the major structural features of the cuticle. Extracted from Yeats & Rose (2013). (b) Schematic model of triterpenoid localization. Triterpenoids (orange) form extended deposits within the cutin polymer (brown) which fixate the polymer strands. Extracted from Schuster *et al.* (2016). (c) Scanning electron microscopy (SEM) images of *Quercus pubescens* abaxial leaf surface. Extracted from Tschan & Denk (2012). 37

Figure 11: Schema representing the Growth-Differentiation-Balance (GDB) theory, modified from Herms & Mattson (1992). (1) Severe resource deficiency (severe stress) altering photosynthetic system and limiting the rate of CO_2 assimilation leading to both, low growth (central metabolism) and specialized defenses (specialized metabolism). (2) Moderate resource deficiency (moderate stress) does not alter net CO_2 assimilation while the growth rate is slowing, leading to a surplus of C in the plant which benefits specialized metabolism. (3) Optimal resource availability (no stress), growth is maximal favoring central metabolism at the expense of specialized metabolism. 39

Figure 12: Schema of the oxidative pressure hypothesis after Treutter (2006). Symbols indicate positive (+) or negative (-) effects. 40

Figure 13: Summary of the different chapters of this thesis. A_n, net CO_2 assimilation; g_s, stomatal conductance to water; SLA, Specific Leaf Area; WUE, water-use efficiency; Ψ_{md}, midday water potential; Ψ_{pd}, predawn water potential..... 43

Figure 14: EPR spectrometry study on *Q. pubescens* leaf thylakoids. (a) Spectrometer BRUKER EMX with light (blue and red) installation. (b) TEMPOL EPR signal variation before and after irradiation. (c) redox balance between TEMPOL and TEMPOL-H..... 47

Figure 15: Raman imaging and spectra on *Q. pubescens* leaf surface. (a) Experimental laser device. (b) Raman spectrum of metabolites of interest (chlorophyll *a*, phenylalanine, galic acid, quercetin-glucoside, β-carotene, kaempferol-glucoside, lutein, and lupeol). (c) Stimulated Raman Spectroscopy (SRS) microscopy imaging showing β-carotene (yellow), acid galic/quercetin-glucoside (purple) and fluorescence (blue)..... 49

Figure 16: Distribution of *Quercus pubescens* Willd. in Europe from Wellstein *et al.,* (2017) 51

Figure 17: Experimental site at the Oak Observatory at Observatoire de Haute Provence (O_3HP). Photo of the experimental site at the O_3HP with the exclusion device (a) opened and (b) closed. (c) Scheme of the experimental site showing the distribution of the 20 sampled trees. Trees under natural drought (ND) are shown in light grey and under amplified drought (AD) in dark grey. 53

Figure 18: Ombrothermic diagrams for natural (light gray) and amplified (dark gray) drought plots on the experimental site O_3HP (Oak Observatory at Observatoire de Haute Provence) from 2014 to 2022. Bars represent monthly cumulative precipitation (P, mm) and curves represent mean monthly temperature (T, °C) with P = 2 T. When temperature curves are above precipitation bars, it corresponds to dry periods indicated by red horizontal arrows. 55

Figure 19: Structure and classification of flavonoids. The main subclasses of major flavonols are circled in blue. The difference between flavonoid groups depends on the chemical structure, the degree of oxidation, and the unsaturation of the linking chain (C3).

Flavonols differ from each other in the number and position of the hydroxyl groups (-OH). The *ortho*-dihydroxy structure of quercetin circled in orange..... 65

Figure 20: Biosynthesis and subcellular localization of flavonols in leave tissues. Flavonols are synthesized in the cytoplasm, on the cytosolic face of the endoplasmic reticulum (ER) (right picture). The different enzymes involved in their biosynthesis (left box) are shown in blue and flavonols are indicated and framed by different colors. The pathway shown represents the general pathway found in model plants such as Arabidopsis thaliana. The first step begins with the synthesis of phenylalanine in the chloroplasts which is then transported to the cytosol via the phenylalanine plasticial cationic amino acid transporter (PhpCAT), identified in petunia. Abbreviations are as follows: C4H, cinnamate 4-hydroxylase; CHI, chalcone isomerase; CHS, naringenin-chalcone synthase; DFR, bifunctional dihydroflavonol 4 reductase/flavanone 4-reductase; F3H, flavanone 3-hydroxylase; F3′H, flavonoid 3′-hydroxylase; F3′5′H, flavonoid 3′5′-hydroxylase; FLS, flavonol synthase; LDOX, leucoanthocyanidin dioxygenase; PAL, phenylalanine ammonia-lyase; Phe, phenylalanine; UGT, UDP-dependent glucosyl transferase. Once synthetized, flavonols can be subjected to various modifications (glycosylation, methylation, etc.) and be stocked into vacuoles. They are transported into different compartments and through cells by MATE (multidrug and toxic compound extrusion) and ABC (ATP binding cassette) transporters families. In nucleus, vacuole, and chloroplast, flavonols will inhibit ROS accumulation..... 71

Figure 21: Plant responses to abiotic stress. The colored boxes summarize the four abiotic stresses referred to in this review and their main consequences for plant physiology. Flavonols' role as ROS scavengers and their interaction with the phytohormones ABA in leaves and auxin in roots is shown in black boxes. In leaves, the opening of stomata is allowed by the binding of ABA to membrane receptors resulting in an efflux of ions and therefore an efflux of water leading to stomata closure. ABA act on the R2R3-MYB gene by enhancing its expression thus stimulating flavonol biosynthesis. It also triggers a signaling cascade leading to ROS production. In roots, flavonols inhibit auxin transport leading to auxin accumulation and root elongation. ABA is a phytohormone considered as a plant..... 82

Figure 22: Climatic conditions on the experimental site in 2021. (a) Ombrothermic diagram for natural (light gray) and amplified (dark gray) drought plots where bars represent monthly cumulative precipitation (P, mm) and curves represent mean monthly temperature (T, °C) with P = 2 T. When temperature curves are above precipitation bars, it corresponds to dry periods indicated by red horizontal arrows. Vertical black arrows indicate field campaigns in May (spring), July (summer), and October (autumn). (b) Cumulative precipitation for natural (light gray) and amplified (dark gray) drought plots. The dotted red line represents the annual mean precipitation calculated for the period 1967–2000 (830 mm). (c) Sum of precipitation during the 30 days preceding each sampling campaign in spring (green), summer (pink), and autumn (yellow) under amplified drought (AD) and natural drought (ND). (d) Density of temperature values for each season where the mean temperature during the 30 days preceding each sampling campaign is highlighted in the corresponding color. 90

Figure 23: Physiological (a–f) and physical (g, h) leaf traits through seasons (spring, summer, and autumn) and drought conditions (natural drought (ND) in light gray and amplified drought (AD) in dark gray). When interaction between season and drought was not significant (a–d, g), significant differences across seasons and drought conditions are noted on separate graphs. When significant interactions occurred (e, f, and h), differences are highlighted in a single graph. Significant differences are denoted using letters (a > b > c) for the seasons and asterisks for drought condition: (*): 0.05 < *P* < 0.1, *: 0.01 < *P* < 0 0.05, **: 0.001 < *P* < 0.01, and ***$P < 0.001$. Ns is for non-significant results. The horizontal black lines inside the boxes are the medians and the horizontal red dashed lines are the means (n = 7). A_n, assimilation; C_i, internal CO_2 concentration; g_s, stomatal conductance, WUE, water-use efficiency; Ψ_{md}, midday water potential; Ψ_{pd}, predawn water potential; LS, leaf surface; and SLA, specific leaf area..... 95

Figure 24: Principal component analysis (PCA) for the first two PCA axes of (a) the metabolite groups and subgroups, and (b) the 30 most contributive single metabolites (among the 57 single metabolites analyzed). Metabolite groups (photosynthetic pigments, plastoquinones, tocochromanols, phenolic compounds, and cuticular waxes) are indicated with arrows in different colors. Seasons are represented in green (spring), pink (summer), and yellow (autumn). Drought conditions are represented in light (ND) and dark circled colors (AD), with n = 7 for each condition..... 97

Figure 25: Overall conclusion of the main chemical trait responses of *Q. pubescens* leaves through (a) seasonality where the most concentrated groups (or subgroups) within each season are represented with their main function and (b) amplified drought (AD) where green arrows indicate a significant increase and orange arrows a significant decrease in single metabolites in comparison with natural drought (ND). PQ, Plastoquinones; PC-OH: Hydroxy plastochromanol; PC- 8, Plastochromanol-8. See **Table 6** for bibliographic references regarding metabolite functions. 101

Figure 26: Climatic conditions at O_3HP. (a) Cumulative precipitation in the natural (ND, light grey) and amplified (AD, dark grey) drought plots in 2020. The dotted red line represents the annual mean precipitation calculated for the period 1967-2000 (830 mm). (b) Cumulative precipitation under ND and AD plots in 2021 (from January to July). (c) Ombrothermic diagram under natural ND and AD plots in 2020 and 2021 (until July) where bars represent monthly cumulative precipitation (P, mm) and curves represent mean monthly temperature (T, °C) with P=2T. When temperature curves are above precipitation bars (indicated by red horizontal arrows) it corresponds to dry periods. 113

Figure 27: Principal component analysis (PCA) for the first two PCA axes including all physiological and morpho-anatomical traits measured in this study. Color scale indicate the contribution of each variable with red indicating high contribution and blue low contribution. Drought conditions are represented in light grey (ND) and dark grey (AD), with n=10 for each condition and differences were tested with a PERMANOVA (permutational multivariate ANOVA). Ab. ep, abaxial epidermis; Ad. ep, adaxial epidermis; A_n, net CO_2 assimilation; E, transpiration; GTD, glandular trichome density; g_s, stomatal conductance to water; NGTD, non-glandular trichome density; SD stomatal density; SLA,

specific leaf area; SS, stomatal size; Thickness, total leaf thickness; WUE, water use efficiency. 116

Figure 28: Leaf morphological traits of *Q. pubescens* including stomatal density and size on the abaxial leaf surface according to natural drought (ND) and amplified drought (AD) conditions. (a) Scanning electron microscopy (SEM) images of the abaxial leaf surface under ND (left) and AD (right). (b) Stomatal density (SD). (c) Stomatal size (SS). The horizontal black lines inside the boxes are the medians and the horizontal red dashed lines are the means (n=10 trees). Differences between ND and AD were tested with Student tests with asterisk denoting significant differences between conditions (**: 0.001 < *P* < 0.01; ns: not significant). 119

Figure 29: Leaf morphological traits of *Q. pubescens* including trichome density on the abaxial leaf surface under natural drought (ND) and amplified drought (AD) conditions. (a) Scanning electron microscopy (SEM) images of the abaxial leaf surface under ND (left) and AD (right). The arrows indicate non-glandular trichomes (NGT) and glandular trichomes (GT). (b) Non-glandular trichome density (NGTD). (c) Glandular trichome density (GTD). The horizontal black lines inside the boxes are the median and the horizontal red dashed lines are the mean (n=10 trees). Differences between ND and AD were tested with Student tests with asterisk denoting significant differences between conditions (*: 0.01 < *P* < 0 .05). 120

Figure 30: Linear Pearson correlations between leaf surface morphological traits. (a) Correlation between stomatal density (SD) and stomatal size (SS) under both drought conditions. (b) Correlation between glandular trichome density (GTD) and non-glandular trichome density (NGTD) under both drought conditions. In figure (b), solid light grey and dark grey lines represent the regression line for natural drought (ND) and amplified drought (AD), respectively. Pearson coefficient of determination (*r*) and P-values are indicated. Each point represents the means ± se (n=10 trees). 121

Figure 31: Leaf anatomical traits of *Q. pubescens* according to natural drought (ND) and amplified drought (AD). (a) Optical microscopy images of leaf cross sections under ND (left) and AD (right). Ad. Ep, adaxial epidermis; Ab. Ep, abaxial epidermis. (b) Leaf thickness of the different tissues. (c) Leaf surface. (d) Specific leaf area (SLA). The horizontal black lines inside the boxes represent the median and the horizontal red dashed lines represent the mean (n=10 trees). Differences between ND and AD were tested with Student tests. Asterisks denote significant differences between drought conditions (*: 0.01 < *P* < 0 .05, ***: *P* < 0.001; ns: not significant). 122

Figure 32: Linear Pearson correlations between physiological and morphological traits. A_n, net CO_2 assimilation; E, transpiration; g_s, stomatal conductance to water; NGTD, non-glandular trichome density; SD, stomatal density and WUE, water use efficiency. Solid light grey and dark grey lines represent the regression line for natural drought (ND) and amplified drought (AD), respectively. Pearson coefficient of determination (*r*) and *P*-values are indicated. Values are means ± se (n=10 trees)....123

Figure 33: Linear Pearson correlations between physiological and anatomical traits. A_n, net CO_2 assimilation; E, transpiration; g_s, stomatal conductance to water and WUE, water use efficiency. Solid light grey and dark grey lines represent the regression line for

natural drought (ND) and amplified drought (AD), respectively. Pearson coefficient of determination (*r*) and *P*-values are indicated. Values are means ± se (n=10 trees).....124

Figure 34: Linear Pearson correlations between water use efficiency (WUE) and leaf surface. Solid dark grey lines represent the regression line for amplified drought (AD). Pearson coefficient of determination (*r*) and *P*-values are indicated. Values are means ± se (n=10 trees).....125

Figure 35: Experimental site at the Oak Observatory at the Observatoire de Haute Provence (O_3HP). Photo of the experimental site at the O_3HP with the exclusion device (a) opened and (b) closed. (c) Photo on the footbridge. (d) Scheme of the experimental site showing the distribution of the seven sampled trees. Trees under natural drought (ND) are shown in light grey and trees under amplified drought (AD) in dark grey. Trees circled in yellow are additional trees monitored for physiological measurements (seven trees by drought condition) and those not circled were used for metabolite analysis (five trees by drought condition).....135

Figure 36: Climatic conditions on the experimental site from 2014 to 2022. (a) Annual cumulative precipitation for natural (ND, light gray) and amplified (AD, dark gray) drought plots for each year from 2014 to 2022. The dotted black line represents the annual mean precipitation calculated for the period 1993–2022 (784 mm). Under ND, when precipitation bars are below the 784 mm annual mean, the year is considered as "dry year" while when it is above the annual mean the year is considered as "wet year". (b) Density of temperature values for each year. The mean temperature for each year is represented by the dotted line and highlighted in the corresponding color. 138

Figure 37: Physiological leaf traits. (a) Net CO_2 assimilation (A_n), (b) stomatal conductance to water (g_s) and predawn water potential ($\Psi_{predawn}$) through years (2020, 2021 and 2022) and drought conditions (natural drought (ND) in light gray and amplified drought (AD) in dark gray). Differences are tested with a two-way ANOVA. Since interaction between year and drought was not significant, significant differences across years and drought conditions are noted on separate graphs. Significant differences are denoted using letters (a > b > c) for the years and asterisks for the drought condition: (*): $0.05 < P < 0.1$. Ns is for not significant results. The horizontal black lines inside the boxes are the medians and the horizontal red dashed lines are the means (n = 4-7 trees). 141

Figure 38: Principal component analysis (PCA) for the first two PCA axes of (a) individuals and (b) variables (metabolites and precipitation patterns), observed under natural drought (ND) and amplified drought (AD) from 2016 to 2022, with n = 5 for each condition. AZ / VAZ, de-epoxidation of violaxanthin to antheraxanthin and zeaxanthin; Chl. tot, total chlorophyll (chl. a + b); der., derivatives; Precip. growing season, precipitation during the growing season (from 15th March to harvest date); Precip jan. to march, precipitation from 1st January to 15th March of leaf harvest year; Total precip. y-1, Total annual precipitation 1-year before sampling; Total precip. y-2, Total annual precipitation 2-years before sampling.....143

Figure 39: Leaf concentrations of photosynthetic pigments (µg g_{DM}^{-1}) according to years (from 2016 to 2022) and drought conditions. (a) Total photosynthetic pigments (carotenoids and chlorophyll). (b) Total chlorophyll (Chlorophyll *a* and *b*). (c) Ratio of

chlorophyll *a* to *b* (Chl *a*/*b*). (d) Neoxanthin (carotenoid). (e) β-carotene (carotenoid). (f) Lutein (carotenoid). (g) Xanthophyll cycle (including three carotenoids: violaxanthin, antheraxanthin and zeaxanthin; VAZ). (h) De-epoxidation of violaxanthin to antheraxanthin and zeaxanthin (AZ/VAZ). Differences between years were tested with post hoc Tukey tests and are indicated with different letters (a > b > c > d). Differences between drought conditions were indicated by asterisks with **: 0.001 < *P* < 0.01 and ***: *P* < 0.001. Ns is for not significant results. Values are mean ± se (n =5 trees). 145

Figure 40: Leaf concentrations of flavonols (µg g_{DM}^{-1}) according to years (from 2016 to 2022) and drought conditions. (a) Quercetin derivatives. (b) Kaempferol derivatives. (c) Isorhamnetin derivatives. (d) Myricetin derivatives. Differences between years were tested with post hoc Tukey tests and are indicated with different letters (a > b > c > d). Differences between drought conditions were indicated by asterisks with ***: *P* < 0.001. Ns is for not significant results. Values are mean ± se (n =5 trees). 146

Figure 41: Linear Pearson correlation between total photosynthetic pigment and total flavonol concentrations (µg g_{DM}^{-1}). Solid line represents the regression line, both drought conditions pooled together with the shaded areas around the lines indicating the 95% of confidence interval. Pearson correlation coefficient (*r*) and *P*-values are indicated (n = 5 trees). 147

Figure 42: Linear Pearson correlations between the total annual precipitation 1 and 2-years before sampling and metabolite concentrations (µg g_{DM}^{-1}). Relationship between the total annual precipitation 2-years before sampling and (a) AZ / VAZ, (b) VAZ and (c) total flavonol concentrations, and between the total annual precipitation 1-year before sampling and (d) neoxanthin, (e) VAZ and (f) total flavonol concentrations. Solid line represents the regression line for both drought conditions pooled together with the shaded areas around the lines indicating the 95% of confidence intervals. Pearson correlation coefficient (*r*) and *P*-values are indicated. 148

Figure 43: concluding schema of the main results obtained in this thesis. Abbreviations are as follows: e^-, electron; Chl, chlorophylls (*a* and *b*); GTD, glandular trichome density; NGTD, non-glandular trichome density; PC, plastochromanol; PQ, plastoquinones; ROS, reactive oxygen species; SD, stomatal density; VAZ, xanthophyll cycle (violaxanthin, antheraxanthin, zeaxanthin). 164

List of tables

Table 1: The ten types of trichomes found in *Quercus* species as described by Hardin (1976). 25

Table 2: Summary of studies on the impact of short and mild-term amplified drought *in natura* (at O_3HP) on physiological, metabolic and growth traits of *Quercus pubescens.* The three cited studies were performed on the same experimental forest (*in natura*)... 41

Table 3: Climatic data (cumulative annual precipitation and annual mean temperature) for 2014-2022 period. Cumulative annual precipitation is presented under natural drought (ND) and amplified drought (AD). 54

Table 4: Comparative physico-chemical properties of some of the main flavonols, flavones and flavanones. The higher the number of hydroxyl groups, the higher the antioxidant activity. An exception is made for quercetin for which the higher antioxidant activity is due to the *ortho*-dihydroxy structure in the B ring (see **Figure 19**). 67

Table 5: Increasing of flavonol concentration under different abiotic stresses reported in literature for different species and experimental conditions. All studies are performed on harvested leaves or roots. 74

Table 6: Metabolite groups and subgroups targeted in this study and belonging to central and specialized metabolism in the whole leaf and leaf surface (cuticular waxes), biosynthetic pathways, main functions, and references. 99

Table 7: Results of two-way ANOVA performed on metabolite subgroup concentrations ($\mu g\ g^{-1}_{DM}$) according to season and drought conditions (n = 7). 100

Table 8: Physiological leaf traits measured in July 2021 under natural drought (ND) and amplified drought (AD). Significant differences are tested with Student tests and are denoted using asterisks (***: $P < 0.001$). Ns: not significant. Values are mean ± se (n=10). 118

Table 9: Precipitation during both, the period from 1st January to 15th March and during the growing season (i.e. from 15th March to harvest date), and mean temperature during the growing season for 2014-2022 period. 139

A. Supplementary information for analyses of chapter IV

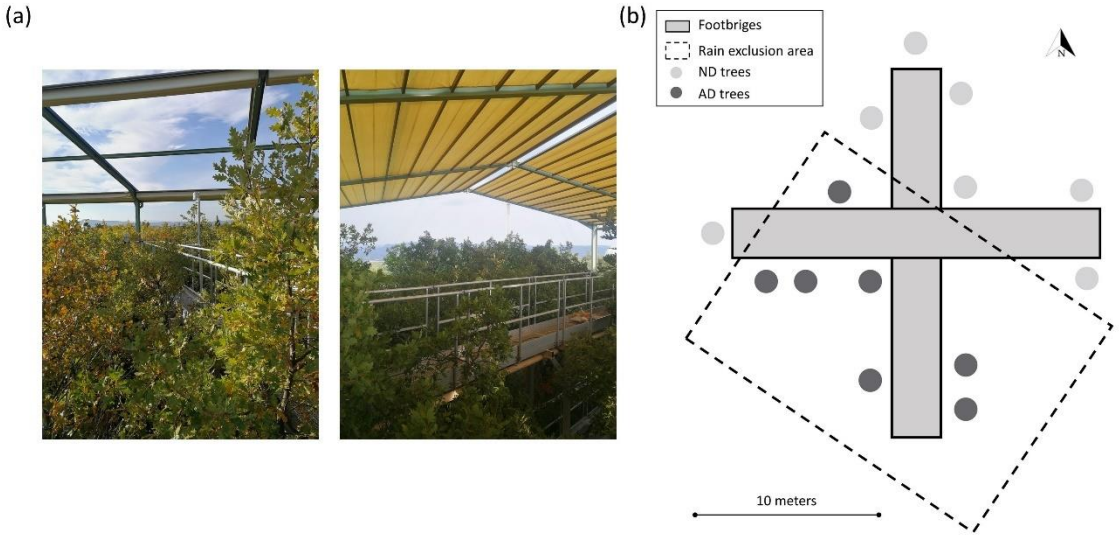

Figure S1: Experimental site and sampling plan. (a) Photo of the experimental site at the Oak Observatory at Observatoire de Haute-Provence (O_3HP) taken in 2021 with the exclusion device opened (left) and closed (right). (b) Schema of the experimental site showing the repartition of the 14 sampled trees. Trees under natural drought (ND) are shown in light grey and under amplified drought (AD) in dark grey.

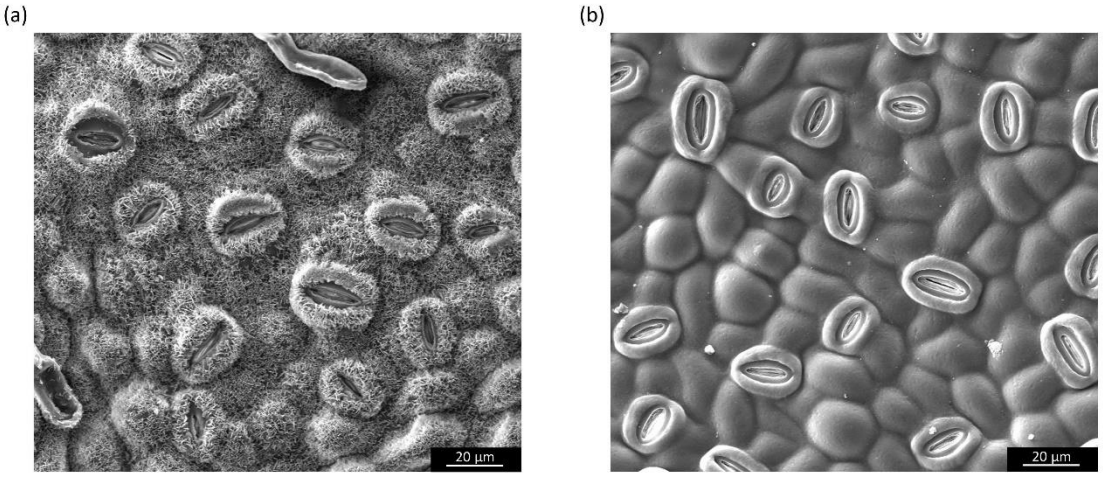

Figure S2: Scanning electron microscopy (SEM) images of the leaf abaxial surface of *Q. pubescens*. (a) before and (b) after cuticular wax removal.

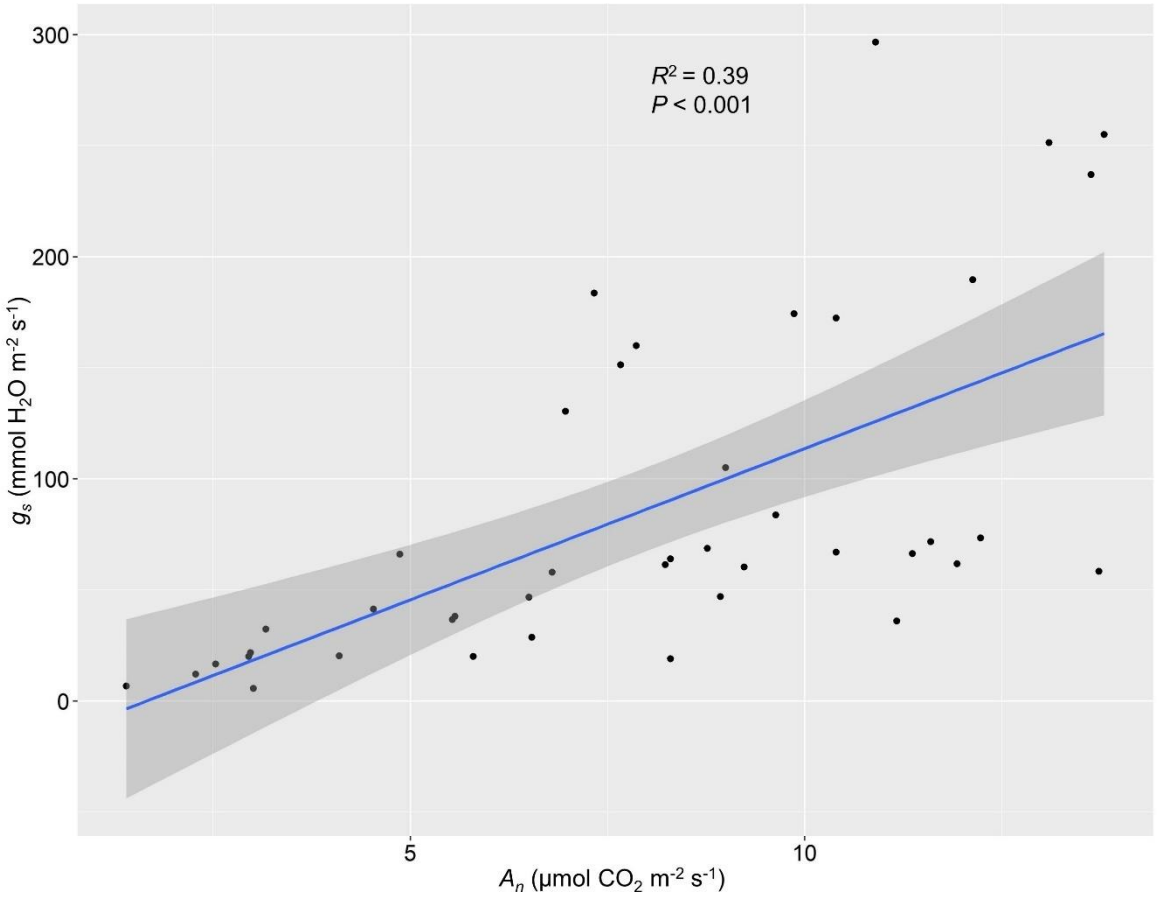

Figure S3: Correlation between stomatal conductance (g_s) and net CO_2 assimilation (A_n) with data from all seasons and drought conditions. Regression line (blue), 95% confidence intervals (grey), R^2 and *P*-value are shown.

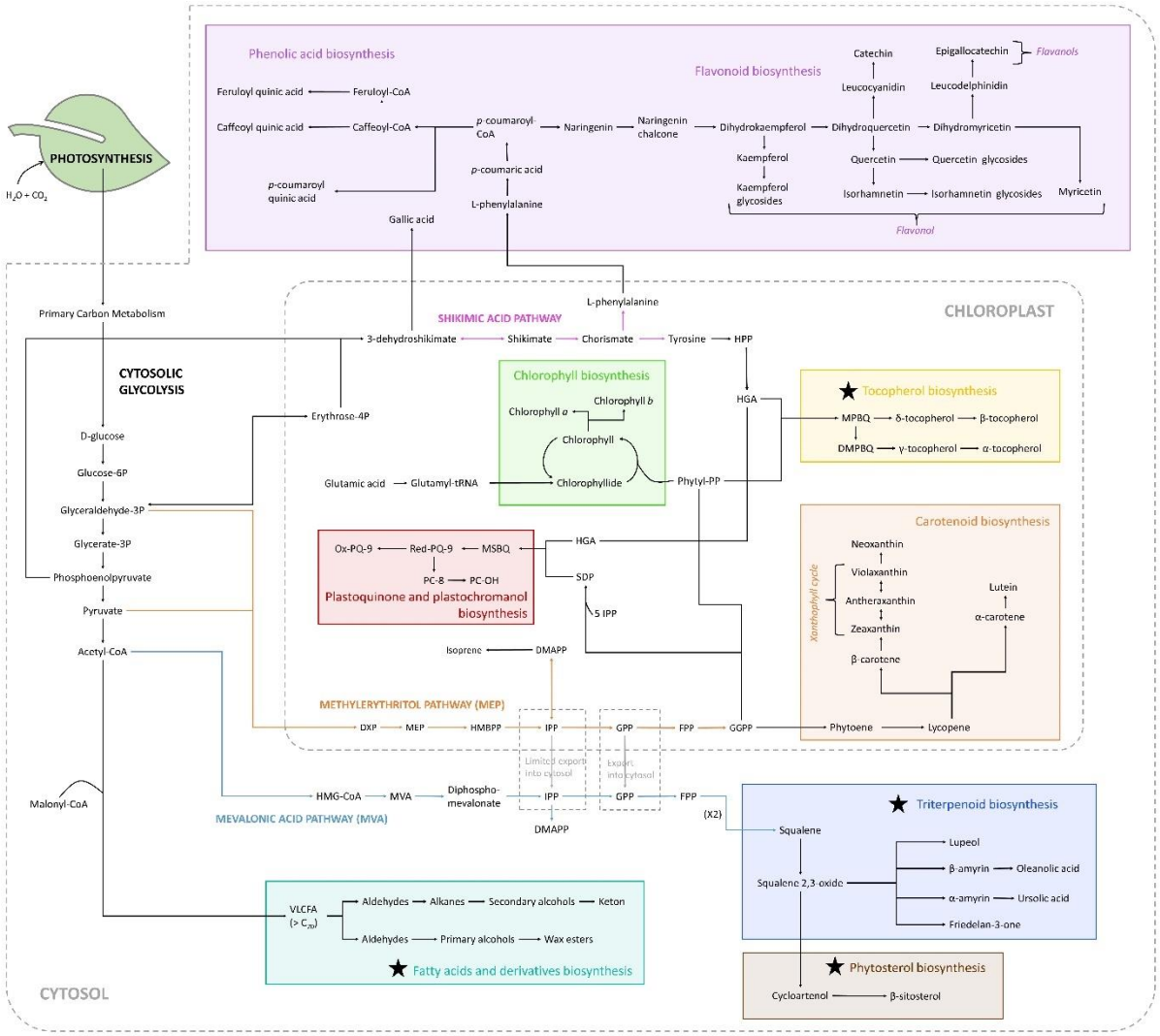

Figure S4: Biosynthetic pathways of metabolites targeted in this study. Each metabolite is assigned to a group and a subgroup as referred in **Table 6**. Photosynthetic pigments including chlorophylls and carotenoids are represented in green and orange boxes, respectively. Plastoquinones and plastochromanols are represented in the red box. Phenolics compounds including phenolic acids, flavonols and flavanols are represented in the purple box. Cuticular waxes encompassed fatty acids and derivatives, phytosterol, triterpenoids and tocopherols are represented in turquoise blue, brown, blue and yellow boxes, respectively and are indicated with a star. The MEP (or the methylerythritol phosphate) pathway is represented with orange lines, the MVA (or mevalonate) pathway with blue lines and the shikimate pathway with pink lines. Abbreviations are as follows: 5 IPP, 5 Isopentenyl diphosphate; CoA, coenzyme A; DMAPP, dimethylallyl-diphosphate; DMPBQ, dimethylphytylbenzoquinol; DXP, 1-deoxy-D-xylulose-5-phosphate; FPP, farnesyl pyrophosphate; GGPP, geranylgeranyl pyrophosphate; GPP, Geranyl pyrophosphate; HGA, Homogentisic acid ou homogentisate (phenolic acid); HMG-CoA, β-Hydroxy β-methylglutaryl-CoA; HMBPP, 1-hydroxy-2-methyl-2-(E)-butenyl 4-diphosphate; HPP, hydroxyphenylpyruvate; IPP, isopentenyl diphosphate; MEP, 2-C-methyl-D-Erythritol-4-phosphate; MPBQ, methylphytylbenzoquinol; MVA, (R)-mevalonate; Ox. PQ-9, oxidised plastoquinone; Phytyl-PP, phytyl-diphosphate; MSBQ, methyl-solanesyl-enzoquinone; SDP, solanesyl diphosphate; PC-8, plastochromanol-8; PC-OH, hydroxy-plastochromanol; Red-PQ-9, reduced plastoquinone or plastoquinol.

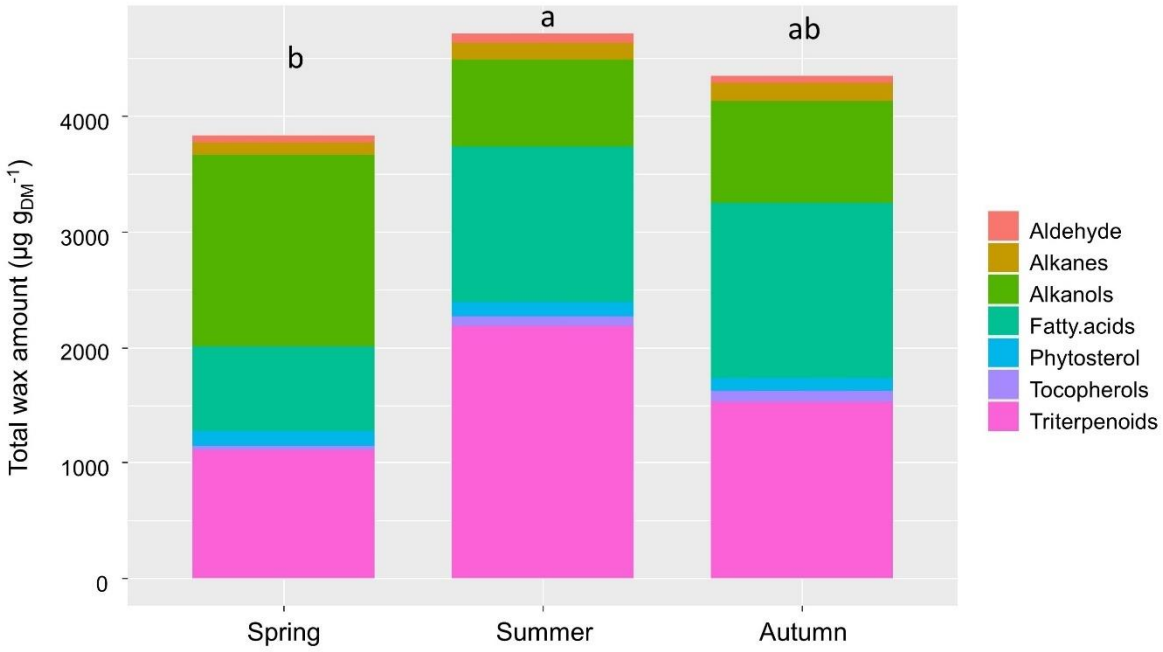

Figure S5: Seasonal variation of cuticular waxes (divided in subgroups) of *Q. pubescens* leaves with drought condition pooled. Values represent the mean value of each metabolite subgroup (n=7). Letters denote significant differences in total wax amount between seasons tested with two-way ANOVA (a > b).

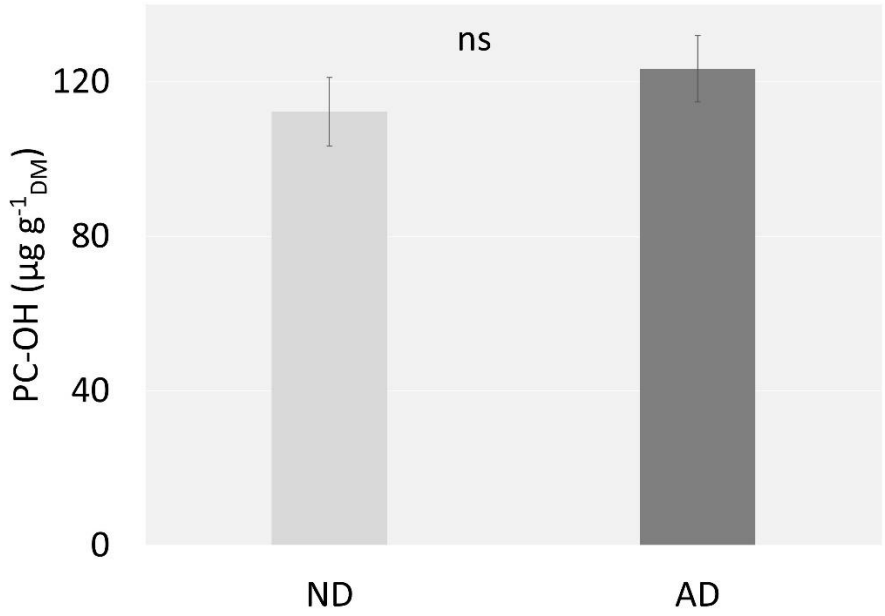

Figure S6: Concentration of plastochromanol-OH (PC-OH) in summer 2015. Values are mean ± se (n=7). Differences between ND and AD were tested with Student tests (ns is for not significant).

Table S1: Results of two-way ANOVA performed on metabolite group concentrations (µg g^{-1}_{DM}) according to season and drought conditions (n=7). P-values are indicated by (*) 0.05 < *P* < 0.1, *0.01 < *P* < 0.05, **0.001 < *P* < 0.01, *** *P* < 0.001. Lower case letters denote the significant differences between seasons ordered as follows in the parenthesis: (spring, summer, autumn), with a > b > c. Upper-case letters denote the significant differences between drought conditions ordered as follows in the parenthesis: (ND, AD), with A > B.

	Spring (Sp)		**Summer (Su)**		**Autumn (Au)**		**Two-way ANOVA**		
Compound group	**ND**	**AD**	**ND**	**AD**	**ND**	**AD**	**Season (Sp, Su, Au)**	**Drought (ND, AD)**	**S x D**
Photosynthetic pigments	4925.81 ± 247.10	5430.04 ± 212.42	4011.74 ± 215.12	4734.82 ± 265.35	3219.54 ± 133.24	3230.33 ± 412.09	***** (a, b, c)**	**(*) (B,A)**	ns
Plastoquinones	192.58 ± 26.80	195.17 ± 11.22	713.50 ± 45.29	727.99 ± 35.37	1819.21 ± 170.61	1909.93 ± 213.64	***** (c, b, a)**	ns	ns
Tocochromanols	78.73 ± 6.22	86.17 ± 5.79	318.38 ± 54.77	251.27 ± 12.94	627.40 ± 22.44	671.44 ± 77.64	***** (c, b, a)**	ns	ns
Phenolic compounds	10297.31 ± 372.00	9930.92 ± 725.24	8580.29 ± 555.46	9051.14 ± 640.99	8521.38 ± 699.39	8476.51 ± 572.00	**** (a, b, b)**	ns	ns
Cuticular waxes	3541.51 ± 264.77	4120.96 ± 498.94	4822.75 ± 599.31	4627.00 ± 376.11	4335.01 ± 350.92	4367.46 ± 179.54	*** (b, a, ab)**	ns	ns

Table S2: Results of two-way ANOVA performed on single metabolite concentrations (µg g^{-1}_{DM}) according to season and drought conditions (n=7). *P*-values are indicated by (*) 0.05 < *P* < 0.1, *0.01 < *P* < 0.05, **0.001 < *P* < 0.01, *** *P* < 0.001. Lower case letters denote the significant differences between seasons ordered as follows in the parenthesis: (spring, summer, autumn), with a > b > c. Upper-case letters denote the significant differences between drought conditions ordered as follows in the parenthesis: (ND, AD), with A > B. For plastochromanol-8 the interaction between season and drought was significant and differences between ND and AD are indicated for each season separately.

			Spring (Sp)				Summer (Su)				Autumn (Au)				Two-way ANOVA		
Metabolite group	**Metabolite subgrou**	**Single metabolite**	**ND**		**AD**		**ND**		**AD**		**ND**		**AD**		**Season (Sp, Su, Au)**	**Drought (ND, AD)**	**S x D**
Photosynthetic pigments	Carotenoids	Neoxanthin	67.25	± 2.65	78.03	± 3.62	54.39	± 3.35	65.96	± 4.73	46.99	± 2.60	51.14	± 6.20	*** **(a, b, c)**	* **(B, A)**	ns
		VAZ	311.17	± 10.93	297.94	± 15.64	182.91	± 8.94	166.02	± 9.34	161.61	± 7.54	130.55	± 6.39	*** **(a,b,c)**	* **(A,B)**	ns
		Lutein	301.81	± 14.17	332.67	± 11.82	231.01	± 11.29	273.12	± 15.10	190.13	± 8.22	194.33	± 22.74	*** **(a, b, c)**	* **(B, A)**	ns
		β-Carotene	213.15	± 11.27	228.00	± 9.78	176.96	± 10.73	195.08	± 12.54	127.05	± 2.95	121.45	± 19.82	*** **(a, b, c)**	ns	ns
	Chlorophylls	Chlorophyll *b*	463.88	± 29.07	518.87	± 22.05	398.98	± 25.98	492.33	± 32.20	293.60	± 16.40	309.62	± 43.06	*** **(a, a, b)**	* **(B, A)**	ns
		Chlorophyll *a*	3568.55	± 192.69	3974.52	± 167.41	2967.49	± 167.99	3542.31	± 201.80	2400.16	± 104.72	2423.24	± 319.18	*** **(a, b, c)**	(*) **(B, A)**	ns
		Chl a/b	7.72	± 0.09	7.67	± 0.10	7.49	± 0.21	7.22	± 0.11	8.21	± 0.13	7.88	± 0.22	*** **(ab,b,a)**	**ns**	ns
Plastoquinone	Plastoquinones	Plastoquinone	193.69	± 27.16	195.17	± 11.22	705.12	± 51.80	740.40	± 38.35	1812.05	± 171.10	1896.95	± 184.38	*** **(c, b, a)**	ns	ns
Tocochromanols	Plastochromanols	Hydroxy-plastochromanol	2.86	± 0.33	3.61	± 0.41	8.77	± 0.59	11.81	± 0.26	42.41	± 2.18	42.49	± 4.86	*** **(c, b, a)**	* **(B, A)**	ns
		Plastochromanol-8	0.37	± 0.05**d**	0.40	± 0.035**d**	0.97	± 0.22**c**	1.96	± 0.15**b**	4.34	± 0.56**a**	4.06	± 0.42**a**	*** **(c, b, a)**	* **(B, A)**	**
	Tocopherol	α-Tocopherol	75.50	± 5.92	82.16	± 5.48	308.64	± 54.88	237.51	± 13.08	580.64	± 20.57	624.90	± 73.31	*** **(c, b, a)**	**ns**	ns
Phenolic compounds	Flavonols	Myricitrin	0.00	± 0.00	0.00	± 0.00	107.69	± 10.71	73.26	± 13.59	296.64	± 32.23	202.76	± 46.28	*** **(c, b, a)**	** **(A, B)**	ns
		Quercetin galloyl glucose	239.41	± 51.02	157.77	± 12.10	663.52	± 109.95	520.67	± 41.61	782.94	± 169.95	623.82	± 69.00	*** **(b, a, a)**	* **(A, B)**	ns
		Quercetin hexose	1136.91	± 134.44	1086.25	± 174.28	652.68	± 86.08	651.12	± 108.82	555.57	± 94.09	597.37	± 111.98	*** **(a, b, b)**	ns	ns
		Quercetin-3-*O*-glucose	1684.97	± 220.35	1529.20	± 195.51	1241.42	± 211.16	1333.93	± 190.28	1133.87	± 220.28	1309.31	± 169.80	ns	ns	ns
		Quercetin pentose	361.60	± 56.50	352.04	± 115.11	272.88	± 42.86	249.09	± 38.03	277.09	± 51.67	248.87	± 37.19	ns	ns	ns
		Kaempferol-3-glucose	2490.38	± 231.84	2186.39	± 369.03	762.13	± 151.15	973.34	± 170.10	779.36	± 79.28	905.09	± 161.72	*** **(a, b, b)**	ns	ns
		Kaempferol hexose	30.01	± 18.20	46.89	± 32.50	168.88	± 53.19	213.72	± 49.57	240.91	± 58.64	312.96	± 99.01	*** **(b, a, a)**	ns	ns
		Isorhamnetin-3-*O*-glucoside	1174.52	± 223.81	1257.99	± 322.31	1141.76	± 202.32	1512.71	± 444.26	1087.16	± 232.45	1385.90	± 362.48	ns	ns	ns
		Isorhamnetin-3-glucuronide	517.51	± 106.30	463.57	± 45.44	376.34	± 78.94	385.28	± 53.89	336.41	± 69.62	356.41	± 40.81	ns	ns	ns
	Flavanols	Catechin	377.34	± 55.60	426.52	± 54.32	791.37	± 179.59	931.56	± 124.51	1607.32	± 318.41	1300.87	± 181.16	*** **(c, b, a)**	ns	ns
		Epigallocatechin caffeate	418.65	± 73.81	337.65	± 32.04	567.50	± 94.22	441.18	± 60.36	339.41	± 91.85	263.52	± 59.43	* **(ab, a, b)**	ns	ns
	Phenolic acids	Gallic acid conjugate	878.79	± 139.24	1217.31	± 122.65	835.77	± 85.37	886.15	± 106.07	418.97	± 44.70	370.11	± 33.87	*** **(a, a, b)**	ns	ns
		p- coumaroyl quinic acid	0.00	± 0.00	0.00	± 0.00	0.00	± 0.00	0.00	± 0.00	22.55	± 10.98	11.74	± 6.01	*** **(b, b, a)**	ns	ns
		Feruloyl quinic acid	364.28	± 57.46	375.56	± 38.89	221.93	± 23.84	166.92	± 11.16	71.54	± 7.99	61.39	± 6.09	*** **(a, b, c)**	ns	ns
		p- coumaric acid glycosylated derivative 1	426.59	± 24.22	332.74	± 30.52	543.13	± 28.72	489.30	± 42.94	403.01	± 18.21	360.97	± 14.99	*** **(b, a, b)**	** **(A, B)**	ns
		p-coumaric acid glycosylated derivative 2	196.34	± 9.11	161.04	± 12.21	233.27	± 8.46	222.90	± 16.34	168.63	± 6.18	165.41	± 6.92	*** **(b, a, b)**	(*) **(A, B)**	ns

Table S2: *continued*

			Spring (Sp)				Summer (Su)				Autumn (Au)				Two-way ANOVA		
Metabolite group	**Metabolite subgrou**	**Single metabolite**	**ND**		**AD**		**ND**		**AD**		**ND**		**AD**		**Season (Sp, Su, Au)**	**Drought (ND, AD)**	**S x D**
Cuticular waxes	Alkanes	Docosane	6.13	± 0.21	12.12	± 4.09	9.28	± 1.60	8.03	± 0.71	7.79	± 0.55	7.38	± 0.26	ns	ns	(*)
		Tricosane	19.83	± 2.85	21.48	± 3.10	15.65	± 1.61	17.65	± 1.22	14.77	± 1.86	15.54	± 1.37	*** (a, ab, b)**	ns	ns
		Tetracosane	5.49	± 0.43	5.73	± 0.38	8.38	± 0.59	8.30	± 0.60	11.41	± 1.42	11.76	± 1.41	***** (c, b, a)**	ns	ns
		Pentacosane	16.90	± 2.14	17.90	± 2.67	37.28	± 3.22	34.79	± 4.55	44.92	± 6.65	44.07	± 7.30	***** (b, b, a)**	ns	ns
		Heptacosane	25.82	± 2.74	30.48	± 4.82	36.54	± 3.62	39.06	± 5.76	43.35	± 6.15	46.98	± 7.05	**** (b, ab, a)**	ns	ns
		Octacosane	3.60	± 0.27	3.19	± 0.33	3.56	± 0.37	3.48	± 0.31	5.16	± 0.74	5.09	± 0.69	**** (b, b, a)**	ns	ns
		Nonacosane	27.14	± 3.63	22.43	± 4.73	21.00	± 3.46	23.85	± 4.29	28.38	± 3.65	33.09	± 6.43	ns	ns	ns
		Untriacontane	4.20	± 0.86	3.38	± 0.50	7.03	± 4.37	2.72	± 0.46	3.24	± 0.51	2.21	± 0.30	ns	ns	ns
	Alkanols	Octadecanol	14.35	± 0.61	16.49	± 1.01	14.56	± 1.79	11.87	± 0.38	12.47	± 0.71	13.82	± 0.99	*** (a, b, b)**	ns	(*)
		Docosanol	167.04	± 33.48	203.16	± 27.32	48.60	± 9.87	67.67	± 3.07	51.98	± 8.13	72.19	± 6.67	***** (a, b, b)**	**** (B, A)**	ns
		Tetracosanol	1450.96	± 193.21	1460.19	± 165.16	661.68	± 48.65	704.23	± 63.80	781.30	± 82.34	834.39	± 33.87	***** (a, b, b)**	ns	ns
	Aldehyde	Octacosanal	56.35	± 9.08	44.23	± 8.70	104.12	± 9.84	71.58	± 8.39	57.92	± 5.91	53.43	± 7.02	***** (b, a, b)**	*** (A, B)**	ns
	Fatty acids	Hexadecanoic acid	97.01	± 6.81	189.62	± 66.25	102.74	± 9.86	95.63	± 8.38	127.25	± 11.58	107.49	± 6.92	ns	ns	(*)
		Octadecanoic acid	104.84	± 5.22	212.72	± 74.32	85.35	± 13.19	78.80	± 6.07	104.63	± 11.06	87.59	± 5.94	***** (a, b, ab)**	ns	(*)
		Icosanoic acid	26.00	± 2.33	32.76	± 3.28	72.93	± 39.16	48.99	± 9.99	26.61	± 4.55	44.20	± 7.93	**(*) (b, a, b)**	ns	ns
		Docosanoic acid	47.97	± 5.09	58.48	± 6.59	42.90	± 7.00	48.03	± 4.28	38.65	± 6.31	50.90	± 2.63	ns	*** (B, A)**	ns
		Tetracosanoic acid	101.39	± 10.58	104.01	± 11.18	202.56	± 28.14	153.80	± 22.27	117.14	± 20.59	143.67	± 15.31	**** (b, a, b)**	ns	ns
		Pentacosanoic acid	4.30	± 0.87	4.81	± 0.64	29.46	± 3.12	26.30	± 4.32	43.99	± 6.07	52.08	± 7.07	***** (c, b, a)**	ns	ns
		Hexacosanoic acid	116.48	± 11.45	120.87	± 6.78	571.78	± 64.62	436.89	± 72.46	576.04	± 58.05	611.51	± 94.15	***** (b, a, a)**	ns	ns
		Octacosanoic acid	112.83	± 11.09	121.25	± 11.96	385.61	± 19.59	334.35	± 36.37	423.99	± 37.58	479.04	± 44.31	***** (c, b, a)**	ns	ns
	Tocopherols	δ-Tocopherol	7.59	± 3.88	20.16	± 6.09	12.38	± 2.49	23.80	± 10.74	7.37	± 1.93	9.07	± 3.97	ns	**(*) (B, A)**	ns
		β-Tocopherol	7.01	± 2.02	11.02	± 2.43	22.95	± 5.93	35.24	± 10.79	15.48	± 4.81	13.29	± 2.08	**** (b, a, ab)**	ns	ns
		α-Tocopherol	7.92	± 0.94	10.04	± 1.32	43.28	± 2.11	32.62	± 3.05	75.18	± 4.95	65.58	± 4.49	***** (c, b, a)**	ns	ns
	Phytosterol	β-Sitosterol	124.31	± 12.07	157.04	± 26.99	131.30	± 8.04	106.71	± 5.48	111.93	± 7.49	111.13	± 7.20	ns	ns	ns
	Triterpenoids	Squalene	8.34	± 4.43	8.52	± 2.81	5.97	± 1.11	9.42	± 2.38	10.64	± 3.04	7.90	± 1.11	ns	ns	ns
		β-Amyrin	35.07	± 2.57	47.12	± 4.31	101.08	± 13.12	129.20	± 34.41	89.52	± 10.03	99.16	± 19.28	***** (b, a, a)**	ns	ns
		α-Amyrin	29.43	± 3.16	48.28	± 7.91	56.82	± 16.54	65.90	± 19.75	42.20	± 11.66	53.03	± 18.08	ns	ns	ns
		Lupeol	68.93	± 25.05	103.29	± 30.37	1381.18	± 296.05	1441.72	± 204.53	1177.19	± 215.03	1004.00	± 119.56	***** (b, a, a)**	ns	ns
		Friedelan-3-one	36.03	± 7.75	47.69	± 11.92	143.80	± 52.31	135.35	± 70.78	97.66	± 40.02	66.84	± 34.62	ns	ns	ns
		Oleanolic acid	428.85	± 30.50	511.08	± 67.38	279.61	± 84.20	245.58	± 16.19	106.99	± 10.83	120.11	± 16.77	***** (a, b, c)**	ns	ns
		Ursolic acid	379.39	± 34.39	471.43	± 64.81	183.37	± 42.33	185.44	± 19.04	79.85	± 10.40	100.89	± 12.65	***** (a, b, c)**	ns	ns

B. Supplementary information for analyses of chapter V

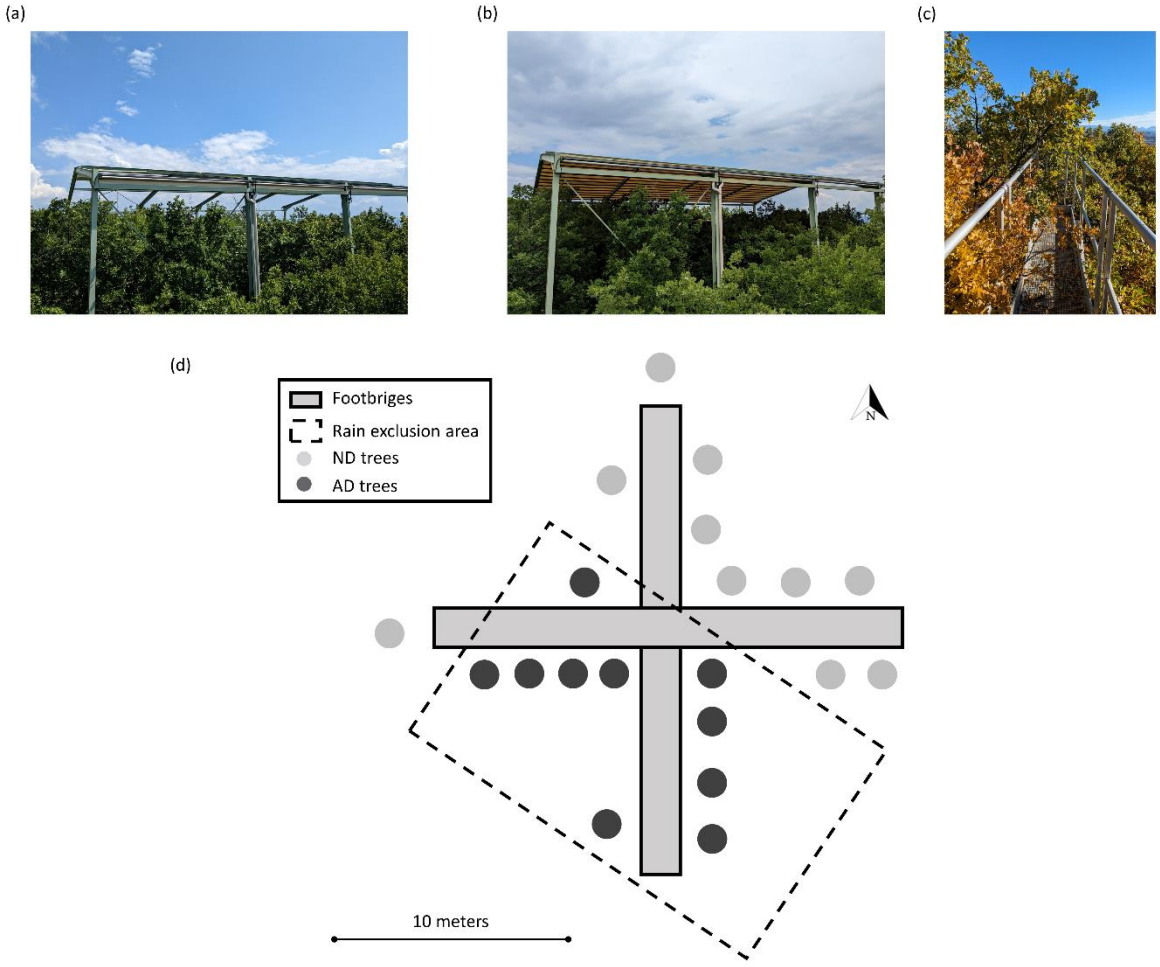

Figure S7: Experimental site at the Oak Observatory at Observatoire de Haute Provence (O_3HP). Photo of the experimental site at the O_3HP with the exclusion device (a) opened and (b) closed. (c) Scheme of the experimental site showing the distribution of the 20 sampled trees. Trees under natural drought (ND) are shown in light grey and under amplified drought (AD) in dark grey.

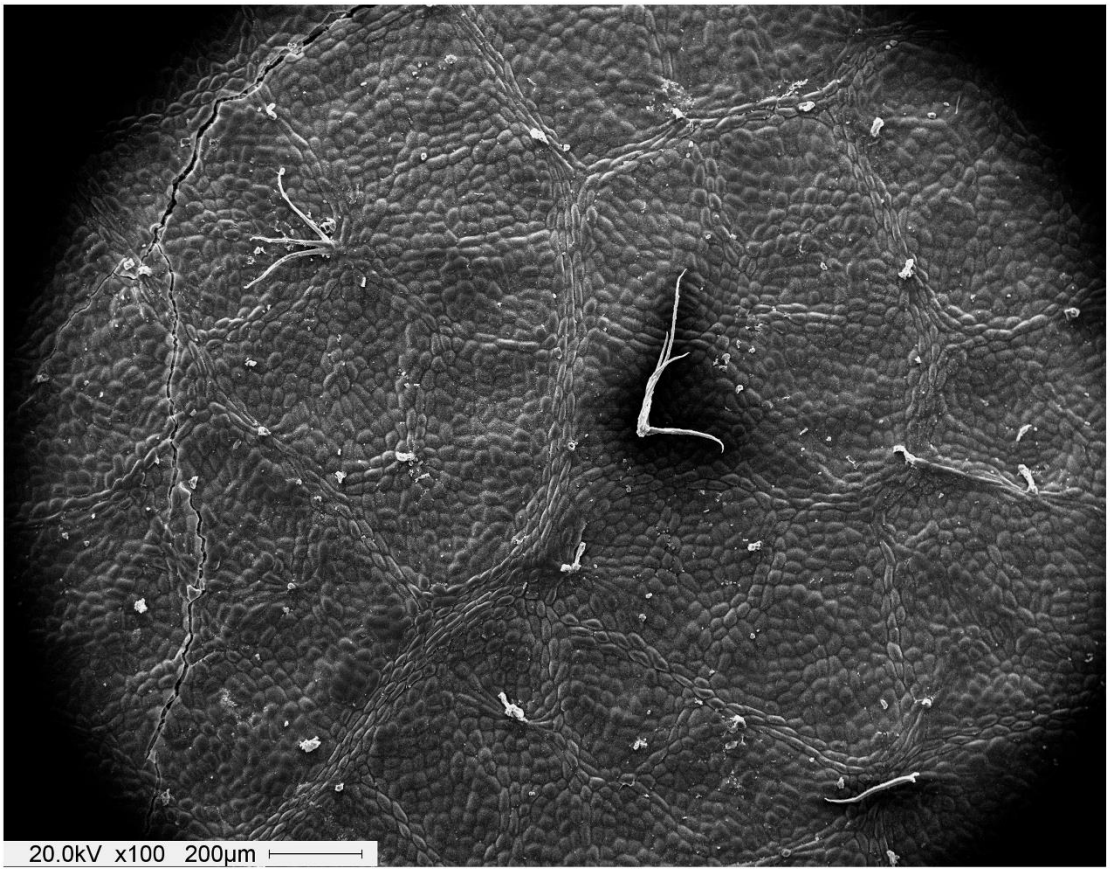

Figure S8: Scanning electron microscopy (SEM) images of the adaxial leaf surface of *Q. pubescens*.

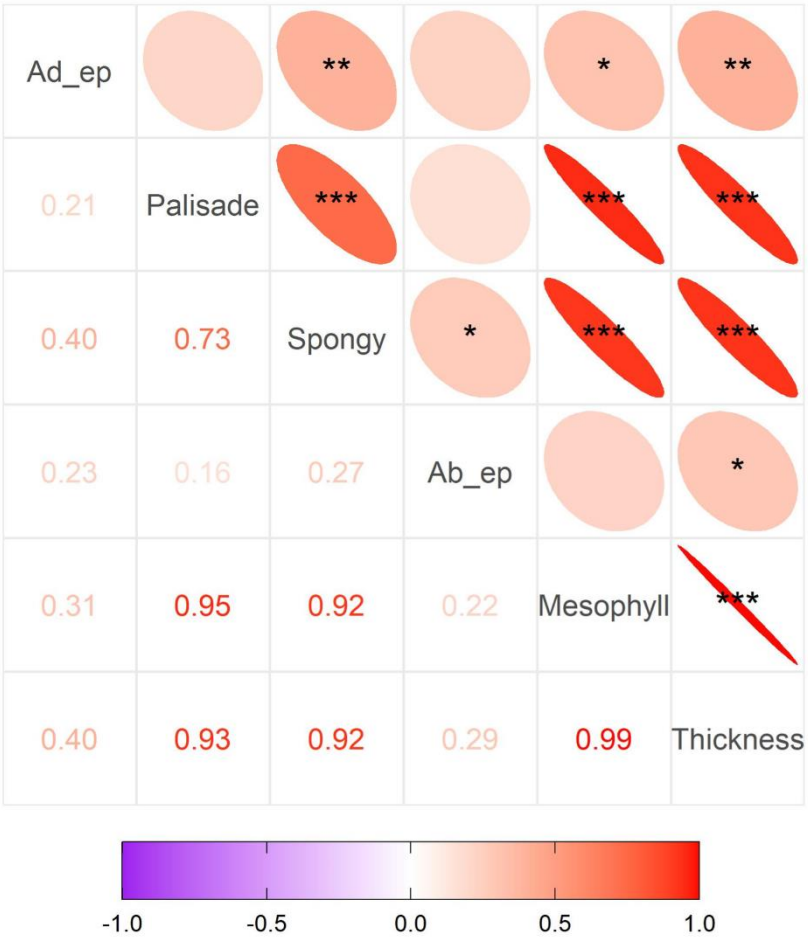

Figure S9: Correlation matrix for anatomical traits (Ad. Ep., palisade, spongy, Ab. Ep., mesophyll and leaf thickness). Pearson's correlation coefficient is shown within each cell. Color scale ranges from red (positive correlation) to purple (negative correlation). Pearson's correlation coefficients are shown at the bottom left and *P*-values at the top right with *: 0.01 < *P* < 0 .05, **: 0.001 < *P* < 0.01 and ***: *P* < 0.001. Ad_ep, adaxial epidermis; Ab_ep, abaxial epidermis.

Table S3: Correlation coefficient of variables associated with PC1 and PC2.

Variables	PC1	*P*-value	PC2	*P*-value
Ab. ep	0.13	0.593	0.02	0.929
Ad. ep	0.20	0.399	**-0.48**	**0.032**
An	**0.55**	**0.013**	0.38	0.095
E	0.25	0.297	**0.84**	**< 0.001**
g_s	0.24	0.304	**0.85**	**< 0.001**
GTD	**0.55**	**0.012**	**-0.48**	**0.033**
Leaf surface	0.42	0.062	-0.31	0.182
Mesophyll	**0.89**	**< 0.001**	0.11	0.656
NGTD	**-0.69**	**0.001**	0.14	0.544
Palisade	**0.79**	**< 0.001**	0.10	0.666
SD	**0.72**	**< 0.001**	0.07	0.764
SLA	**-0.73**	**< 0.001**	0.22	0.348
Spongy	**0.90**	**< 0.001**	0.10	0.685
SS	-0.23	0.333	0.29	0.216
Thickness	**0.91**	**< 0.001**	0.06	0.793
WUE	0.24	0.316	**-0.75**	**< 0.001**

Ab. Ep, abaxial epidermis; Ad. Ep, adaxial epidermis; A_n, net CO_2 assimilation; E, transpiration; GTD, glandular trichome density; g_s, stomatal conductance to water; NGTD, non-glandular trichome density; SD, stomatal density; SLA, specific leaf area; SS, stomatal size; Thickness, total leaf thickness and WUE, water use efficiency.

C. Supplementary information for analyses of chapter VI

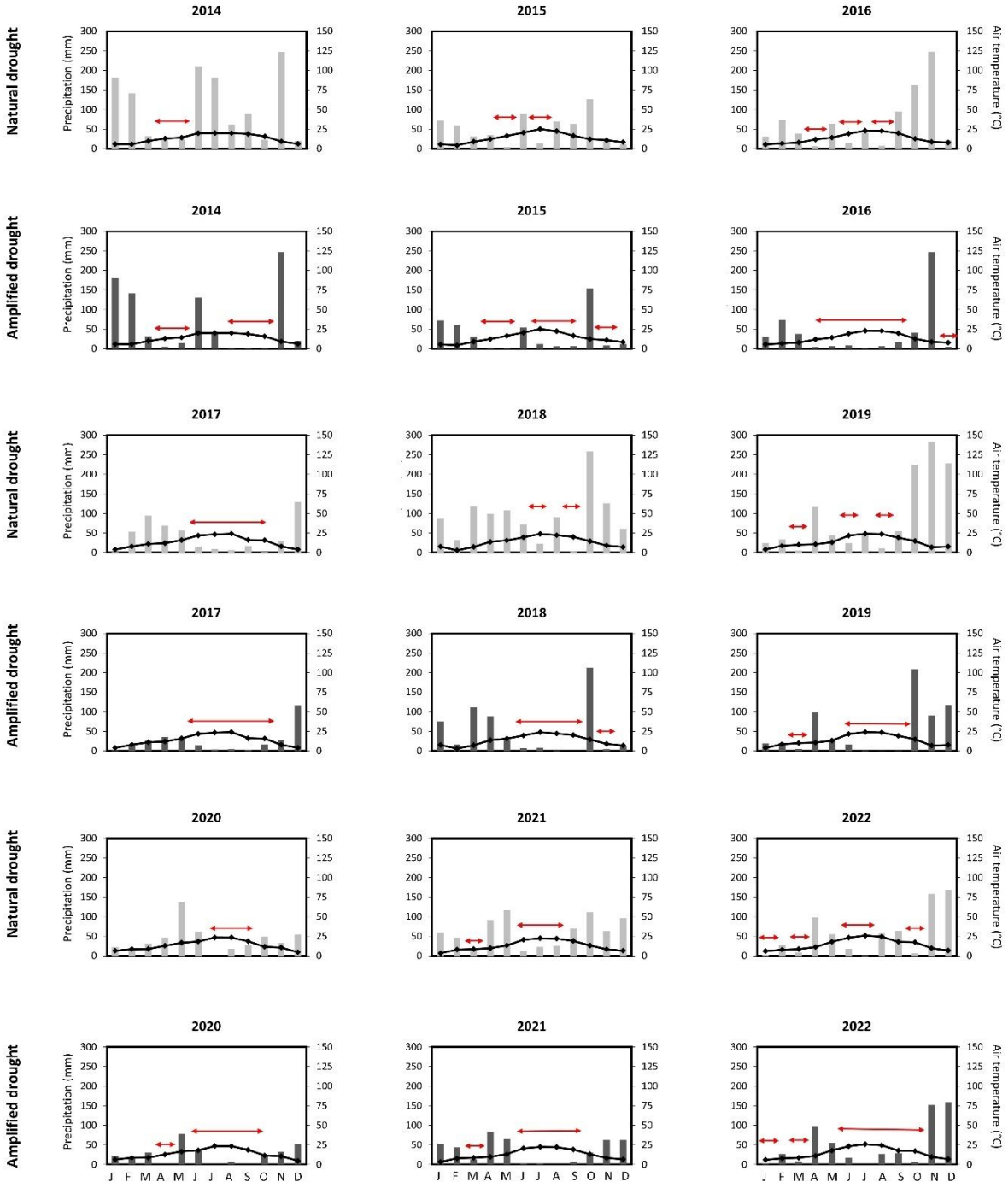

Figure S10: Ombrothermic diagram for natural (light gray) and amplified (dark gray) drought plots on the experimental site O_3HP (the Oak Observatory at the Observatoire de Haute Provence) for the years 2014 to 2022. Bars represent monthly cumulative precipitation (P, mm) and curves represent mean monthly temperature (T, °C) with P = 2 T. When temperature curves are above precipitation bars, it corresponds to dry periods indicated by red horizontal arrows.

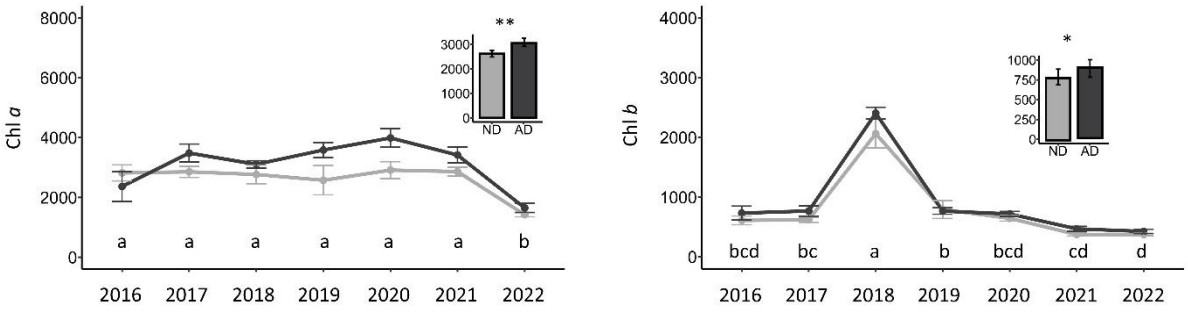

Figure S11: Leaf concentrations of chlorophyll a and b (µg g_{DM}^{-1}) according to years (from 2016 to 2022) and drought conditions. Differences between years were tested with post hoc Tukey tests and are indicated with different letters (a > b > c > d). Differences between drought conditions were indicated by asterisks with *: 0.01 < *P* < 0.05 and **: 0.001 < *P* < 0.01 and represented in a separate graph at the top right. Values are mean ± se (n =5 trees).

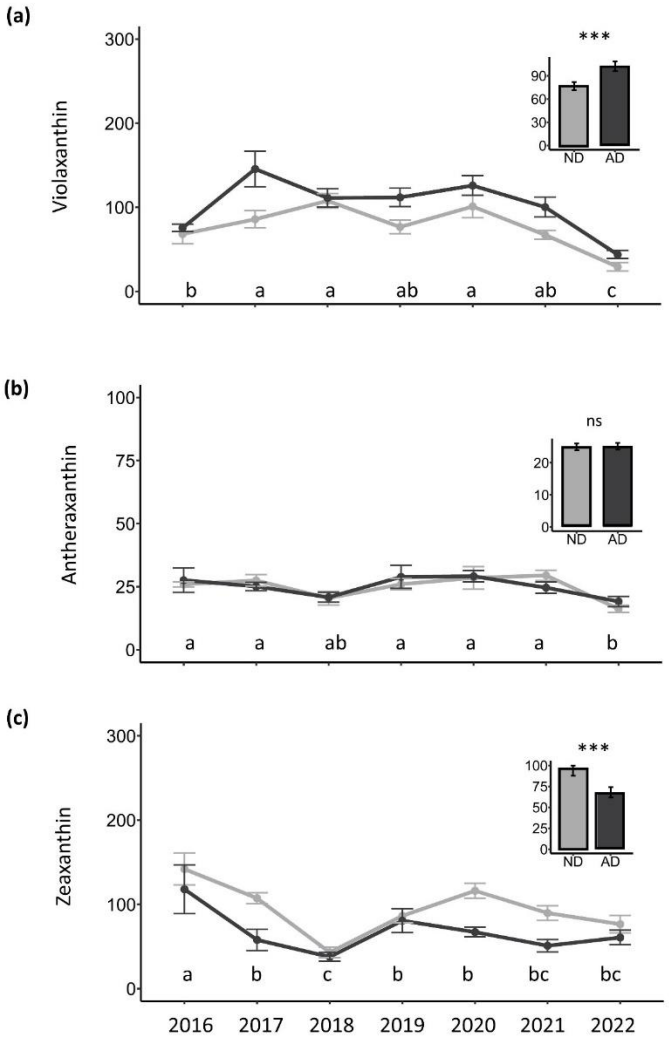

Figure S12: Leaf concentrations of carotenoids from the xanthophyll cycle (VAZ) (µg g_{DM}^{-1}) according to years (from 2016 to 2022) and drought conditions. (a) Violaxanthin. (b) Antheraxanthin and (c) Zeaxanthin. Differences between years were tested with post hoc Tukey tests and are indicated with different letters (a > b > c). Differences between drought conditions were indicated by asterisks with ***: $P < 0.001$ and represented in a separate graph at the top right. Values are mean ± se (n =5 trees).

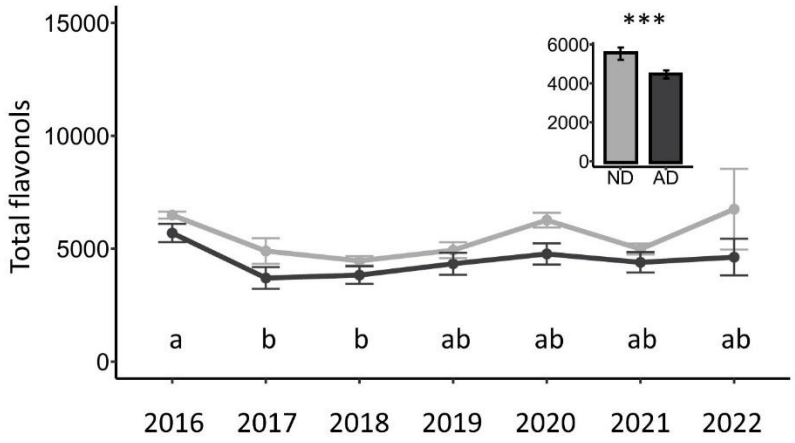

Figure S13: Leaf concentrations of total flavonols (µg g_{DM}^{-1}) according to years (from 2016 to 2022) and drought conditions. Differences between years were tested with post hoc Tukey tests and are indicated with different letters (a > b). Differences between drought conditions were indicated by asterisks with ***: $P < 0.001$ and represented in a separate graph at the top right. Values are mean ± se (n =5 trees).

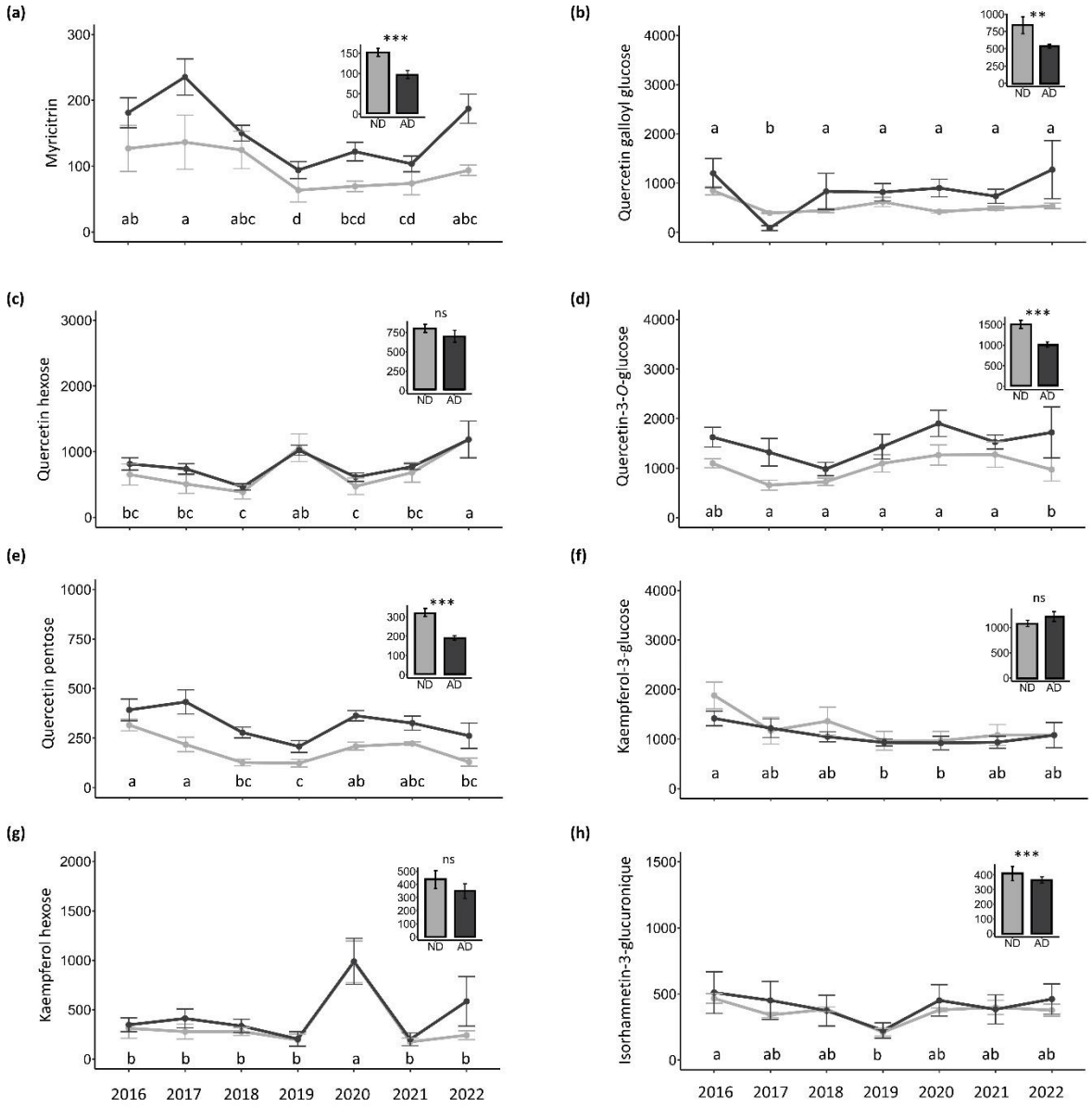

Figure S14: Leaf concentrations of flavonols (µg g_{DM}^{-1}) according to years (from 2016 to 2022) and drought conditions. Differences between years were tested with post hoc Tukey tests and are indicated with different letters (a > b > c > d). Differences between drought conditions were indicated by asterisks with ***: $P < 0.001$ and **: $0.001 < P < 0.01$ and represented in a separate graph at the top right. Ns is for not significant results. Values are mean ± se (n =5 trees).